

**Cycloadditions for the Formation of Functionalized  
Biorelevant *N*-Heterocycles**

Anna Elizabeth Davis  
Pittsburgh, Pennsylvania

B. Sc. Chemistry, University of Louisville, 2019

A Dissertation presented to the Graduate Faculty  
of the University of Virginia in Partial Fulfillment for the  
Degree of Doctor of Philosophy

Department of Chemistry

April 2024

# COPYRIGHT INFORMATION

The following chapters contain data and experiments from previously published works:

**Chapter 2:** Davis, A. E.; Lowe, J. M.; Hilinski, M. K.; *Chem. Sci.* **2021**, *12*, 15947-15952.

# ABSTRACT

Nitrogen heterocycles constitute a class of highly privileged motifs in complex molecule synthesis. Specifically, cyclic compounds with a nitrogen atom in their ring structure constitute most FDA-approved drugs, pharmaceutical leads, and natural products. For this reason, synthetic chemists have sought out strategies to efficiently assemble complex molecular frameworks containing *N*-heterocycles for nearly as long as synthetic chemistry has been studied. Among these strategies, cycloaddition reactions have continuously been established as a highly effectual method for the rapid and atom-economical formation of molecular complexity with a high degree of chemo-, regio-, and stereoselectivity. Herein we report three novel cycloadditions for the incorporation and formation of *N*-heterocycles in biorelevant structures: the vinylazaarene Diels-Alder [4+2], the organocatalytic aza-Pauson-Khand formal [2+2+1], and the pyridyl vinylcyclopropane [5+1] using a nitrene source as a one-atom component.

Cyclohexyl azaarenes constitute a biorelevant motif present in a variety of FDA-approved drugs and several more pharmaceutical candidates. Six-membered carbon rings are common retrans for the Diels-Alder reaction, however, very few examples exist of vinylazaarenes being employed as dienophiles, whether thermally or promoted by Lewis acids. Our work addresses this deficiency in the literature, utilizing the same chemical principles that govern increased yields, regioselectivity, and diastereoselectivity under Lewis acid-catalysis of  $\alpha,\beta$ -unsaturated carbonyl dienophiles compared to their thermal counterparts. The scope of this reaction includes unactivated dienes, scalability up to 10 grams, and access to biorelevant scaffolds. The presence of a highly Lewis basic lone pair in conjugation with a dienophilic olefin

opens the established vinylazaarene scope to additional means of Lewis acid catalysis, including enantioselective methods.

Five-membered *N*-heterocycles such as pyrroles and pyrrolidines are also highly prominent in drug discovery. Organocatalysis is an attractive option for the syntheses of druglike molecules owing to cost-efficacy over many metal catalysts and non-toxicity in the body. We have expanded upon previously established reactivity and mechanistic understanding of the Hilinski iminium organocatalyst to establish a formal [2+2+1] reaction for the diastereo- and regioselective formation of pyrrolines: synthetic precursors to both aromatic and aliphatic five-membered *N*-heterocycles and biorelevant motifs of rising prominence themselves. In this work, the iminium catalyst cyclizes a nitrene precursor, a styrene, and an alkyne in a stepwise fashion similar to the metal-catalyzed Pauson-Khand reaction to furnish a partially saturated ring. This reaction represents an unprecedented chemical transformation in its own right, as no metal-catalyzed approaches to the same three-component formal cycloaddition have been identified.

# ACKNOWLEDGMENTS

This section easily warrants its own chapter. This Ph.D. has taken an army. I'm so unspeakably thankful for everyone who has passed through my life these past five years, and I am certain I wouldn't have made it to this point without every single one of them. I hope I never win an academy award. My acceptance speech would be 4 hours long.

To my advisor, Prof. Mike Hilinski, you've been a confidante, a friend, an advocate, and a weird family member (said with kindness) on top of being my advisor. I came to UVA solely to work with you and it's a decision that shaped the rest of my life for the better. I'm so incredibly grateful for the opportunity to have learned from you these past five years. It's been a difficult journey, but I couldn't have done it without you as an ally. I owe so much good in my grad career and everything that will come of it to you being unflinchingly in my corner.

To my committee: Profs. Charlie Machan, Dean Harman, Lin Pu, Lindsay Bazydlo, and Jetze Tepe (kinda): thank you all so much for your support, kindness, and wisdom over the course of my grad school career. Charlie, it has been an honor, and even more importantly, a BLAST working with you in SciComm and collaborating on the ORR project. I look back on every time we both came in wearing Hawaiian shirts with pride. Dean, thank you for your kindness and support throughout this time, both in apologizing over email for kicking my butt in candidacy and being so gracious and communicative during combiflashgate 2023. Lin, I love that you were always so available to offer extra support in office hours, both for classes and for milestones in my Ph.D. I know I came in constantly and asked a litany of stupid questions, but your patience and knowledge meant the world to me. Lindsay, thank you for coming into an organic chemist's defense despite being outside of your specialty. You've been kicking my butt on Tuesday mornings for five years now and I've loved every second. Jetze, thank you for coming in to be my backup committee member in the eleventh hour. I hope you have a fulfilling and incredibly fun time at UVA. It's so cool to finally have another hardcore organic chemist in our department.

To my labmates, past and present: I love you all so, so much. Thank you so much to the fourth-year cohort when I joined the lab for making me feel welcome and at home as soon as I came in, and the early lab members who helped me hit my stride in research. Philip, you were the real adult that held the lab together. Thank you so much for the humor, advice, stability, and snazzy purple outfits you were always ready to provide. Rob, I am so grateful for the friendship we've maintained and that you did so much to take care of me when I was dead set on joining the lab *and* trying every beer at Draft during visitation weekend. Carrick, thank you for the COVID-time lab life chats and letting me stay on your couch during my two weeks of homelessness. I'm so happy we became friends in the time we overlapped in the lab. Jared, coauthoring the Diels-Alder paper with you was one of the highlights of grad school. I learned so much from you (from DFT to "don't throw away other people's vials") and always knew I had someone to stroll across the hall and gossip with when I needed a break.

Julie, you were the first friend I made in the lab and one of the people I've deeply connected with the fastest. I'm so proud of you for everything you've done in your career despite incredibly difficult circumstances and I'm so grateful for the love and positivity you've always been willing to give me. Grilled cheese nights forever!

Freddie, if I think too hard about how many times you've passively suggested I visit you in Boston that led to me dropping everything and buying plane tickets, I'll probably get self-conscious. Thank you for the friendship, guidance, Firefly Place wine nights, dope lizards, and mushroom hunting expeditions. You've been a source of stability for my meltdowns since I started.

To my cohort, whether still in the lab or not: we've been through the gamut together and I'm so glad I've maintained my relationship with all of you no matter where we've ended up. Amber, it's been an honor being your friend, getting to see your relationship with Jordan develop, and meet your beautiful boy Daniel. Ethan, despite the ups and downs, your loyalty and dedication to our friendship has been constant, and I so deeply appreciate that. Thank you for being the world's worst covid bubble buddy. I wish I could go back and tell first year Anna that you make a 3200 mile round trip to see me defend. She'd lose her mind. Yubo, I love being in the lab with you and rooting for you. Your kindness and sense of humor has been a constant high point in my experience here. You're up next, buddy. I'm so excited to see what you do.

To Kevin, nothing in any future lab of mine will compare to Thursday morning crosswords, gabbing sessions, and weird movie nights. You're the cool big brother I never knew I needed. Thank you for constantly lending humor and perspective when I'm acting insane.

To Ian, you've stood by me through every up and down I've been through since you joined the lab. Tuesday nights at Durty's have been my anchor to sanity for as long as you've been around. Your constant compassion, understanding, and willingness to listen to me vent have been imperative to my graduate experience. You were right there with me for hours on end during all the upheaval I went through in my penultimate semester, and I will always cherish that. You're one of Gwen's favorite friends of mine, and Gwen has excellent taste.

To the second years, I can rest easy knowing this lab has a wonderful future in your hands. Alex, I know you were set on our lab from the beginning, and I hope you feel you ended up in the right place. I also hope you finish out grad school without any more candle-related injuries. Lauren, thank god I have someone I can talk to about Gilmore Girls. Thank you for reaching out and remaining in my corner in a very turbulent time of my graduate career. Jacque Moon, I can yap with you for hours, to the detriment of my productivity. I am so happy I got to connect with a fellow artist and former weird Warrior Cats stan.

To my mentees, it's been an honor teaching you, working with you, and learning from you. Erika, you were my gateway drug into having 900 undergrads. Your taste in lab jams is untouchable. Thanks for making my first experience having an undergrad so fantastic. Lauren, how insane has it been to go from horse girl internet friends to labmates? Thank you so much for balancing out Serena's and my crazy. I am so grateful for the work you have done on this project and the wonderful friend you've become. Serena, I'm typing this sitting next to you at Jack

Brown's, and I'm not sure which "section" of the acknowledgements you belong in since you've become so much to me. I'm a strong believer in platonic soulmates, and I feel like you came into my life right when I needed you. You're an incredible scientist and an incredible person, and you don't give yourself enough credit for either. There's no one I'd have rather spent this year joined at the hip with. Sjlmmfr.

To my friends in the department, past and present, thank you so much for making every party, department retreat, social event, and mandatory annual safety meeting so much fun. I'm so grateful for the coffee walks, weeknight happy hours, hallway chats, and office gossip sessions, and so lucky to have a collection of memories with some wonderful people to take with me wherever I end up. Hannah, I always know I have someone to go into a corner at a party with when I want to talk about horses. Kaeleigh, our weekend mimosas and late-night life chats helped support me through a very tough time in grad school, and I'm so incredibly grateful for that. Emma, working on the collaboration with you was such a cool experience. Thank you so much for always being around to answer my dumb questions or commiserate about the fifth-year trudge. Julissa, I love how close we've gotten and I wish you could come with me to every horse show ever. Megan (M.), I've loved our time watching movies and getting cute little drinks and hanging out with Kitty. He is truly the ideal man. Mason, you literally dunking on me the first time we hung out set the tone for our friendship, and I'm so happy to have had you around in my final stretch of grad school. Karl, you've been one of the most consistent presences in my life these past five years, and I am so grateful to have kept up such a fantastic long-distance friendship. Thank you for the constant sanity checks and hours of wandering around Boston.

To #ChemTwitter, I expected to become a lot of things in grad school, but a niche internet microcelebrity was not one of them. Social media can be heavy sometimes, but the amazing scientists I've met and real-life friends I've made in this community will hopefully stay with me forever. I hope I've brought some joy and humor into chemistry for all of you, because you've absolutely done so for me.

To the twitter group chat, you get your own paragraph. I keep forgetting that we all live so far away from each other because of how connected and supported the three of you have made me feel every day. Nick, I have learned more chemistry from you than from a lot of classes I've taken. I never know if seeing your name pop up on my screen portends a sweet paper, great advice, fanfic cultural deep cuts, or hockey. (All are welcome and appreciated.) KC, I am constantly amazed by your resilience and positivity, especially in difficult times. Your penchant for kindness, joy, and exuberance in everything you do has been inspirational and aspirational for me. Noah, Mr. Science, Mr. Future Leader: you simultaneously uplift me and challenge me, and if you are what the next generation of big-name professors looks like, then I think we're in good hands.

To my fellow horse girls and every friend I've made through riding, thank you for keeping me sane and making sure I have a personality outside of science. Everyone at Grayson, Wheatland, and Whitehall has played an enormous role in making Charlottesville feel more like home and my time outside of lab more fun. I'm better for having known all of you. Kim, Hannah, Rachel, Sarah, and Peyton: thank you so much for all the wisdom and training you've imparted to me and

Violet, and the friendship you've given beyond that. You've helped us both grow in more ways than you know. Kelsey, thank you for taking such wonderful care of ~~Violence~~ Violet despite her "personality quirks," letting me steal your truck all the time, and wonderful late-night chats about horses we've loved. Clark, you're an honorary horse girl and I've loved chatting chemistry and life with you. Jennifer, I live for our summer field trips and can't wait for more without a defense looming over me. Rhia, thank you for being my first-line riding buddy, trivia host, and the last person at lunch with me at Mount Ida. Rachel, our friendship extends far beyond horses, and I'm so lucky to have you as a riding trainer, perpetual lunch date, and the big sister. I'm so glad to have learned so much from my randomly assigned peer "mentee."

To the Louisville crew, thank you for the continued friendship even though I'm far away. Diana, Aspen, Caroline, Ali, Reid, Troy, and all the old 422 gals: it takes a lot of conscious effort to maintain the level of communication we still have, and I am thrilled to still occupy a corner of your mind, no matter how small. Dr. Grapperhaus and Dr. Rich, thank you for the foundation you both gave me going into grad school. This dissertation is thanks to your guidance and mentorship too. And to my labmates and honorary labmates: Caleb, Nick, Kritika, Faye, and Justin: you all somehow sold me the grad school dream. Thank you for the best parties I went to in undergrad (that ended at 9pm), banger weddings, girls' nights, boys' nights, and utter annihilation in uno. You all showed me what I could be as a scientist, and more importantly, what I could be besides a scientist.

To everyone on my medical care team: my gratitude goes out deeply and profoundly to Chapin, Deepti, Kristen, Dr. Buni, and Dr. Lewis. Thank you for the mental and physical stability, listening ears, irrelevant life chats, and Paxlovid. Grad school is hell on the body and the mind, and all of you held me together with duct tape, ingenuity, great advice, and (legal, prescribed) drugs.

To the JB's crew: beertenders, fellow notchers, and everyone who sat next to me at the bar and peered over my shoulder to ask what all those hexagons were. 90% of this thesis was brought to life over a stiff IPA and a lot of community support. I've loved bringing you along on my writing journey, and you've made me feel loved, supported, and full of carbs every time I've walked through the door. Thank you for making me (and Levi) feel so at home for these past five years.

To my friends that feel more like family now: I can't believe we've made it this far. Megan (E.), you will eternally have a monopoly on Wednesday nights. Thank you for giving me something to look forward to, whether it be gossip, support, life chats, or good old fashioned complaining every week for four years. Jeremy, the summer of 2021 bound us for life. Thank you for your constant friendship, dinner outings, jazz concerts, equally messed up sense of humor. You've always managed to make me feel seen, supported, and cared for in a way that doesn't make me feel self-conscious. Haley, I wish I could have told first-year Anna that the super cool girl she skipped TA training with would end up as a long-time roommate and lifelong friend. Grad school has been a jarring ride, but I wouldn't have made it through without your voracious loyalty, empathy, and righteous fury. You're ALWAYS invited home for Thanksgiving. Levi, I have so much I could say to you, but words can't do justice to the rock you've been throughout grad school. You've been so much to me: best friend, confidante, family, partner in mess, and husband

(for tax reasons). I love you so much. Wild Jan, I'm your Crazy Dave forever. You're living proof that a lifelong friendship can start in a single waitress shift. It's so much of a joy to have been a part of your life and know that this is just the beginning.

To my four-legged thesis coauthors, Violet, Marcy, Archie, and Timmy. I have a kiss ready and waiting for the top of all your heads. I'm forever an animal person, and I can't wait to take on whatever is next with you. Thank you for bringing joy, happiness, and compound clavicle fractures into my life.

To my family, you're my foundation and my bones and you always have been. To the extended relatives, thank you for making every party and trip home so full of laughter and wonderful memories. Cheri, you have singlehandedly been my kit kat dealer for 9 years now. I'll miss the care packages, but I'll always get to look forward to the golden retriever Christmas cards. Jeff, you truly know what it means to PARTY. I've loved every family gathering where we ended up singing at the Scolettis' piano and over the bar, wherever that may be. Matthew, I look forward to your relentless positivity and talking fitness every time I see you. Christopher, I would have -11 dollars to my name if it weren't for your support, wisdom, and knowledge of how stocks and taxes work.

Aunt Diane and Uncle Mike, I can't stress enough how much I cherish the time I spend with you both and the opportunity to have become so close with you throughout. I feel like I've brought you both along on so many of the ups and downs that grad school and my 20s have had to offer, it's so easy to forget you live far away. Our Taipei Tokyo dinner outings are always such a highlight of visiting home. I always feel so heard and seen and loved when I talk to either of you. I am so, so grateful for the relationship I have with both of you.

Aunt Joanie and Uncle Al, family gatherings haven't been the same without you. I miss you both horribly and am so grateful for the love I've gotten to share with you both, even before grad school. I hope you're proud of me. I think of you both so often and I like to think you'll be looking down on me at my defense and in whatever comes after.

Aunt Kirstie, you give the best hugs in the game. Thank you for being a master bartender, one of the funniest people I know, my constant fellow O.S. enthusiast, and the daintiest beer shotgunner I've ever seen. Uncle Greg, I can't articulate how much of this thesis and this degree I owe to you. You got me through one of the hardest things I've ever experienced with grace and humor. I will never take the love you have shown me and the rock you've been for granted.

To "The Girls": you've been smiling down on me from the pictures at my desk and my workspace for 5 years now. Caroline, your wit and perspective have kept me reasonable and more importantly, kept me hip. Juice (Jocelyn. Fine.), it's been so wonderful to go through the whole science thing with you. I always know I can go to you for empathy and perspective and commiseration. Gillian, I love hiding in the bathroom and gossiping with you at parties. Your kindness and your unflinching care for others inspire me every day. Mary, you get me. I've been so happy to have gotten closer these past five years and I'm so excited to see what direction your life takes from Saint Mary's and beyond.

Nana, thank you so much for always being an incredible listening ear, not just in grad school but throughout my entire life. Your love for sharing and taking in stories has always made me feel close to you. You're one of those people I can talk to for hours and never get bored. Grandpa, thank you for holiday break downtime in the family room talking about life and politics and current events. Your cinnamon toast rocks my world and I love our mornings reading the newspaper together. It's almost enough to forgive you for always beating me at card games and chess.

Dad, when we were watching *The Last Ship* when I was in middle school, you turned to me during a commercial break and said, "you should get a Ph.D.," to which I (already vaguely committed to becoming a "scientist") responded "sure, why not?" I also have a specific memory of you mentioning offhand that the hardest part of getting into med school was passing organic chemistry, which prompted me (at age fifteen) to take an orgo class out of spite. I inadvertently fell in love in that classroom and the rest was history. One of my favorite books has a line that says something to the effect of, "there are days you'll remember for the rest of your life, and there are days you *think* you'll remember for the rest of your life. They're very rarely the same days." Those tiny exchanges altered my trajectory. I've heard a lot of passionate, deeply rooted reasons to go to grad school in my time, but none better than "my dad passively suggested it once when I was twelve and I said, 'sure, why not?'" Thank you for always checking in and checking up on me. I am so grateful for the trajectory our relationship has taken in the past few years and your constant willingness to listen and understand me. You're the only person I'd deliberately travel to Texas in the summer to see (although the pool fountain helps). I love you.

Mom, of course I saved the best for last. Six more pages of acknowledgements just for you wouldn't even scratch the surface of everything you've done for me. There's a post-it note on my desk that just says "sad? call ur mom." It's been a packed five years. The covid holidays, Katie visits, six-month-apart beach trips of 2022, horse show photographer stints, dozens of hour-long phone calls, Gilmore Girls marathons, and the fact that you drive eight hours to visit me every year on YOUR birthday weekend have been persistent points of light and peace in an otherwise wildly tumultuous section of my life. Thank you for every road trip playing the "thinking game" or listening while I go off for the millionth time trying to explain what it is I've been doing all this time. Thank you for always being there to cheer me up when I'm upset. Thank you for always inherently sensing through our weird twin telepathy when I'm upset and reaching out before I even think to. You're an incredible example of the human capacity to adapt, evolve, and grow even after you're a "real adult." It gives me much-needed hope for a career largely built on delayed gratification and a difficult world beyond that. I love you.

# DEDICATION

This thesis is dedicated to Mr. Racchini and Mrs. Shank, my eighth and ninth grade science teachers. It's been half my lifetime since I had the privilege of learning from both of you, but you instilled in me the love of chemistry and science that has been a constant driver throughout this Ph.D. Through my most frustrating seasons of work, remembering and emulating the joy, fascination, and hunger for discovery I felt as a teenager in your classes has carried me. I wouldn't have finished this degree without the veritable mob in the acknowledgements, but I wouldn't have even started it without the two of you.

# TABLE OF CONTENTS

COPYRIGHT INFORMATION.....	ii
ABSTRACT.....	iii
ACKNOWLEDGMENTS .....	v
DEDICATION.....	xi
TABLE OF CONTENTS.....	xii
LIST OF ABBREVIATIONS.....	xvi
LIST OF FIGURES.....	xviii
LIST OF SCHEMES.....	xix
CHAPTER ONE: [4+2] Cycloadditions for the Construction of <i>N</i> <sup>2</sup>	
Heterocycles in Total Synthesis.....	1
1.1 Introduction.....	2
1.2 Intramolecular [4+2] Cycloadditions .....	4
1.2.1 Carbocyclic [4+2] Cycloadditions .....	4
1.2.2 Nitrogen-Containing Dienophiles .....	7
1.2.3 Nitrogen-Containing Dienes .....	12
1.3 Intermolecular [4+2] Cycloadditions .....	19
1.3.1 Carbocyclic [4+2] Cycloadditions .....	20
1.3.2 Nitrogen-Containing Dienophiles .....	25
1.3.3 Nitrogen-Containing Dienes .....	26

1.4	Dearomative [4+2] Cycloadditions.....	31
1.4.1	Dearomatization of Vinylindole .....	31
1.4.2	Dearomatization of Indole .....	35
1.5	Inverse Demand [4+2] Cycloadditions.....	37
1.5	Conclusions.....	40
1.7	References .....	41
CHAPTER TWO: Lewis Acid-Promoted Diels-Alder Reactions		
	With Vinylazaarene Dienophiles .....	44
2.1	Introduction.....	44
2.1.1	Relevance of cyclohexyl-functionalized azaarenes.....	44
2.1.2	$\alpha,\beta$ -unsaturated carbonyls as dienophiles .....	45
2.1.3	<i>In situ</i> formation of $\alpha,\beta$ -unsaturated iminium dienophiles	46
2.2	Overview of prior work on vinylazaarene dienophiles .....	47
2.2.1	Thermal cycloadditions.....	47
2.2.2	Lewis acid-catalyzed cycloadditions .....	48
2.3	Optimization and controls .....	49
2.3.1	Initial investigation .....	49
2.3.2	Lewis acid screening.....	50
2.3.3	Reaction condition screening .....	51
2.3.4	Control reactions .....	54
2.4	Scope.....	55
2.4.1	Diene scope .....	56
2.4.2	Dienophile scope .....	57
2.4.3	Limitations to scope.....	58
2.4.4	Pharmaceutical relevance.....	60
2.5	Mechanistic insight .....	61

2.5.1 DFT stepwise energy level calculation .....	62
2.5.2 DFT transition state geometry optimization .....	63
2.6 Conclusions.....	64
2.7 References .....	65
<b>CHAPTER THREE: Development of the Organocatalytic Formal</b>	
<b>Aza-Pauson-Khand Reaction .....</b>	<b>67</b>
3.1 Introduction.....	67
3.1.1 Relevance of 5-membered <i>N</i> -heterocycles.....	68
3.1.2 The Pauson-Khand reaction .....	69
3.2 Prior transition metal-catalyzed formal [2+2+1] work.....	70
3.3.1 Diaziridinium active species for nitrene transfer .....	76
3.3.2 Nitrene-transfer aziridination of styrenes.....	77
3.3.3 Aziridine/alkyne formal [3+2] .....	80
3.4 Optimization and controls .....	81
3.4.2 Initial intermolecular catalyst screenings .....	83
3.4.3 Organocatalytic reaction condition screening.....	84
3.4.4 Nitrene source optimization .....	87
3.5 Reaction scope .....	90
3.5.1 Alkene scope .....	90
3.5.2 Alkyne scope .....	93
3.5.3 Intramolecular entry .....	95
3.5.4 Limitations to scope.....	96
3.5.5 Pharmaceutical relevance.....	98
3.6 Conclusions.....	99
3.7 References .....	100
<b>APPENDIX .....</b>	<b>103</b>

Appendix 1: Chapter 2 Experimental Data.....	104
A.1 General methods .....	104
A.2 Screening and reaction optimization .....	105
A.3 General Diels-Alder procedure.....	105
A.4 Starting material and substrate synthesis .....	106
A.5 Characterization of Diels-Alder reactions.....	109
A.6 References .....	133
A.7 NMR Spectra.....	134
B – Appendix 2: Chapter 3 Experimental Data .....	160
B.1 General methods .....	160
B.2 Screening and Reaction Optimization .....	161
B.3 Reagent and Substrate Synthesis.....	163
B.4 Nitrene Precursor Synthesis.....	165
B.5 General [2+2+1] reaction procedure.....	171
B.6 Characterization of [2+2+1] Products .....	171
B.7 Computational details.....	189
B.8 Crystallographic Data.....	193
B.9 References .....	210

# LIST OF ABBREVIATIONS

br	Broad
Bs	Brosyl
d	Doublet
DCE	Dichloroethane
DCM	Dichloromethane
DFT	Density functional theory
DIBAL	Diisobutylaluminum hydride
DIPEA	Diisopropylethylamine
DMF	N,N-Dimethylformamide
EtOAc	Ethyl acetate
GC	Gas Chromatography
HFIP	1,1,1,3,3,3-hexafluoroisopropan-2-ol
<i>i</i> Pr	Isopropyl
m	Multiplet
MS	Mass Spectrometry
<i>m</i> -CPBA	<i>meta</i> -Chloroperbenzoic acid
Me	Methyl
MeCN	Acetonitrile
MeOH	Methanol
<i>n</i> -Bu	<i>n</i> -Butyl

NMR	Nuclear Magnetic Resonance
<i>n</i> -Pr	<i>n</i> -Propyl
[N]	Nitrene source
[O]	Oxidant
OAc	Acetate
OBz	Benzoate
OTf	Triflate
OTs	Tosylate
Ph	Phenyl
Py	Pyridine
q	quartet
Rh <sub>2</sub> (esp) <sub>2</sub>	Bis[rhodium( <i>α,α,α',α'</i> -tetramethyl-1,3-benzenedipropionic acid)]
Rh <sub>2</sub> (espn)Cl	Bis[rhodium( <i>α,α,α',α'</i> -tetramethyl-1,3-benzenepropanamidate)]
s	singlet
t	triplet
<i>t</i> -Bu	<i>tert</i> -butyl
TFA	Trifluoroacetic acid
TFAA	Trifluoroacetic anhydride
TfOH	Trifluoromethanesulfonic acid
THF	Tetrahydrofuran
TMS	Trimethylsilyl
Ts	Tosyl

# LIST OF FIGURES

- 1.1 Examples of biorelevant alkaloids.
- 1.2 *N*-acyl nitroso resonance hybrid contributors.
- 1.3 Rubrulone and rubrulone aglycon structure.
- 1.4 Product mixture from the final S<sub>N</sub>2 reaction of starting material **1.48**.
- 1.5 Structures of securamine alkaloids.
- 2.1 *N*-heteroarenes functionalized with cyclohexyl groups.
- 2.2 Route of dienophile activation by MacMillan's chiral amine catalysts.
- 2.3 Diene scope of the vinylazaarene Diels-Alder reaction.
- 2.4 Dienophile scope of the vinylazaarene Diels-Alder reaction.
- 2.5 Limitations to diene scope.
- 2.6 Limitations to dienophile scope.
- 2.7 Free energy diagram of Lewis acid-promoted and thermal *endo* cycloadditions of 2-vinylpyridine and 1-phenylbutadiene to form the major regioisomers. Energies in kcal/mol.
- 2.8 Free energy diagram of Lewis acid-promoted and thermal *endo* cycloadditions of 2-vinylpyridine and 1-phenylbutadiene to form the minor regioisomers. Energies in kcal/mol.
- 2.9 Comparison of thermal and Lewis acid-promoted transition states. Bond distances in angstroms.
- 3.1 Structures of FDA-approved drugs and drug leads containing a 5-membered *N*-heterocycle.
- 3.2 Model intramolecular Pauson-Khand substrate.
- 3.3 Evaluated nitrene sources for stabilization of the rate-determining transition state.
- 3.4 Organocatalytic aza-Pauson-Khand alkene scope.
- 3.5 Crystal structure of pyrroline product **3.11**.
- 3.6 Alkyne scope of the organocatalytic aza-Pauson-Khand reaction.
- 3.7 Limitations to alkene scope.
- 3.8 Limitations to alkyne scope.

# LIST OF SCHEMES

- 1.1 Oppolzer's routes to chelidonine, norchelidonine, and their derivatives.
- 1.2 Retro-Diels-Alder/Diels-Alder/elimination/Diels-Alder sequence to form psuedotabernine.
- 1.3 Rawal's use of the Diels-Alder cycloaddition to form strychnine's B and D rings.
- 1.4 Kibayashi's divergent syntheses of fascicularin and lepadiformine.
- 1.5 Kibayashi's abridged synthesis of (–)-lepadin B.
- 1.6 Abbreviated steps and stereochemical rationalization in Danheiser's enantioselective synthesis of **1.22**.
- 1.7 Heathcock's synthesis of daphniphyllates, featuring a one-pot double cyclization.
- 1.8 [4+2] cycloaddition of oxime followed by aromatization to pyrrole.
- 1.9 *In situ* cycloaddition cascade to form anhydrocorinone (**1.37**) from intramolecular cycloaddition of **1.35**.
- 1.10 Williams' syntheses of both versicolamide enantiomers.
- 1.11 Formal Kondrat'eva reaction by Wipf and coworkers toward marinoquinoline A.
- 1.12 Maeng and Funk's route to racemic fascicularin.
- 1.13 Rawal's diastereoselective route to tabersonine.
- 1.14 Takayama's initial Diels-Alder for enantiomeric formation of voacangalactone.
- 1.15 Jiang's syntheses of (+)-dehydroaspidospermidine and related alkaloids.
- 1.16 Gin's use of two hetero-Diels-Alder reactions to convergently form batzelladine A.
- 1.17 Formal Povarov reaction towards the tricyclic structure of martinelline by the Batey group.
- 1.18 Scheerer's intermolecular approach to [2.2.2] diazabicycle brevianamide B.
- 1.19 Singlet oxygen [4+2] to build the cyclic urea of securamines C, D, G, and I.
- 1.20 Ricci's general organocatalytic asymmetric vinylindole [4+2].
- 1.21 Ricci's short formal synthesis of tubifulodine.
- 1.22 Key asymmetric Diels-Alder in MacMillan's nine-step synthesis of minifiensine.
- 1.23 Key asymmetric Diels-Alder in MacMillan's nine-step synthesis of vincorine.

- 1.24 Complexity-generating Diels-Alder cyclization cascade by the Cossy group.
- 1.25 Vanderwal's strychnine synthesis with a Zincke aldehyde precursor.
- 1.26 Boger's route to streptonigrin through two inverse-demand Diels-Alder reactions.
- 1.27 Boger's early use of an inverse-demand Diels-Alder for the synthesis of phomazarin.
- 1.28 Total synthesis of *ent*-(--)-roseophilin.
- 2.1 Lewis acid activation of  $\alpha,\beta$ -unsaturated carbonyl dienophiles.
- 2.2 Thermal Diels-Alder of 2-vinylpyridine and isoprene.
- 2.3 Lewis acid-catalyzed Diels-Alder of 4-vinylpyridine and isoprene.
- 2.4 Lewis acid-catalyzed Diels-Alder of 2-vinylpyridine and pentamethylcyclopentadiene.
- 2.5 Control reaction.
- 2.6 Scale-up of the Diels-Alder reaction between 2-vinylpyridine and 1-acetoxybutadiene.
- 2.7 Concise synthesis of a Linrodostat fragment.
- 3.1 Overview of the Pauson-Khand reaction.
- 3.2 Pauson-Khand reaction mechanism.
- 3.3. Overview of the Tonks group's work on Ti-catalyzed formal [2+2+1] reactions for the formation of pyrroles.
- 3.4 General mechanism of the Tonks group's Ti-catalyzed formal [2+2+1] reactions.
- 3.5 Vanadium-catalyzed formal [2+2+1] to form azadiphospholes from phosphalkynes and diazoarenes.
- 3.6 Ruthenium-catalyzed formal [2+2+1]
- 3.7 Established applications of the Hilinski iminium organocatalyst.
- 3.8 Mechanistic evaluation of C—H amination with organocatalyst **3.1**.
- 3.9 Formal [2+1] reaction of styrenes.
- 3.10 Experimental mechanistic probes for iminium-catalyzed aziridination.
- 3.11 Experimental kinetic investigation for iminium-catalyzed aziridination.
- 3.12 Mechanism of iminium-catalyzed aziridination of styrenes.
- 3.13 Wender's formal [3+2] cycloaddition to form pyrrolines.
- 3.14 Preliminary intermolecular aza-Pauson-Khand study.

- 3.15 Rate-determining step of organocatalytic nitrene transfer reactions.
- 3.16 Effect of TMI-NBs (**3.19**) on formal [2+2+1] yield.
- 3.17 General scope evaluation.
- 3.18 Proposed organocatalytic aza-Pauson-Khand mechanism.
- 3.19 Intramolecular aza-Pauson-Khand and future directions within similar substrates.
- 3.20 Diversification of pyrroline adducts.
- 3.21 Synthesis of the carbon framework of atrasentan.

# LIST OF TABLES

- 2.1 Initial azaarene Diels-Alder reaction condition screening.
- 2.2 Azaarene Diels-Alder Lewis acid screening.
- 2.3 Azaarene Diels-Alder Stoichiometry screening.
- 2.4 Azaarene Diels-Alder Solvent screening.
- 2.5 Azaarene Diels-Alder Temperature screening.
- 2.6 Azaarene Diels-Alder Reaction time screening.
- 3.1 Initial aza-Pauson-Khand screenings.
- 3.2 Initial intermolecular aza-Pauson-Khand screenings.
- 3.3 Organocatalytic aza-Pauson-Khand stoichiometry screening.
- 3.4 Organocatalytic aza-Pauson-Khand solvent screening.
- 3.5 Organocatalytic aza-Pauson-Khand reaction temperature screening.
- 3.6 Organocatalytic aza-Pauson-Khand reaction time screening.
- 3.7 Organocatalytic aza-Pauson-Khand nitrene source screening.

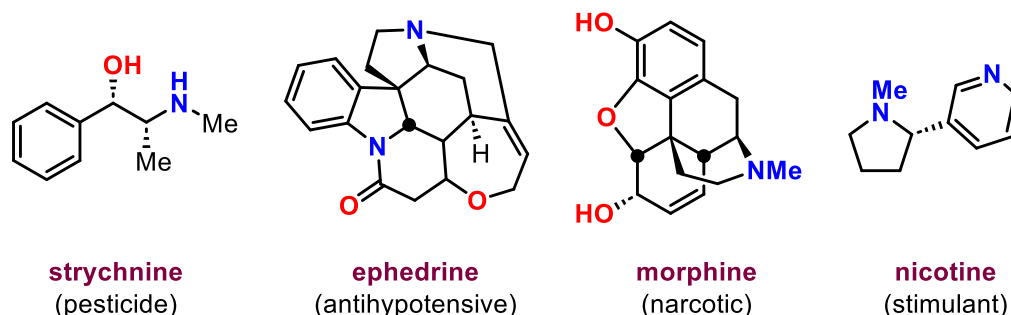
# CHAPTER ONE: [4+2] Cycloadditions for the Construction of *N*-Heterocycles in Total Synthesis

## 1.1 Introduction

There is no synthetic chemical subfield more demonstrative of the power and utility of current methods than total synthesis. The pursuit of synthetic access to complex molecular structures has defined organic chemistry as a field and put its most cutting-edge methods to the test of their true utility. Among the most popular and challenging synthetic targets are alkaloids, natural products containing one or more nitrogen atom. Among these, the “true alkaloids” are structures bearing *N*-heterocyclic frameworks deriving from enzymatic pathways that link amino acids together in natural systems (Figure 1.1).

---

**Figure 1.1.** Examples of biorelevant alkaloids.



Benefitting from nitrogen's ubiquitous chemical reactivity in the body, alkaloids are inherently bioactive compounds synthesized by organisms for defense against predators or disease. This property necessarily leads to a host of desirable pharmacological effects in humans, from anti-inflammatory to chemotherapeutic. These wide applications, in addition to their synthetically challenging polycyclic carbon skeletons, make them highly sought-after total synthetic targets.

The Diels-Alder [4+2] cycloaddition is, for good reason, the first example of a pericyclic reaction that undergraduate organic chemistry students learn. Forming two new sigma bonds with perfect atom economy and predictable regio- and diastereoselectivity, this reaction forms synthetically ubiquitous six-membered rings and has been universally applied to total syntheses with commonality that has inspired many comprehensive reviews.<sup>1-3</sup> Extending beyond carbocycles and into *N*- and *O*-heterocyclic formation, the hetero-Diels-Alder reaction has found comparable utility in total synthesis as well, establishing the highly robust nature of this cycloaddition in the face of various steric and electronic conditions.

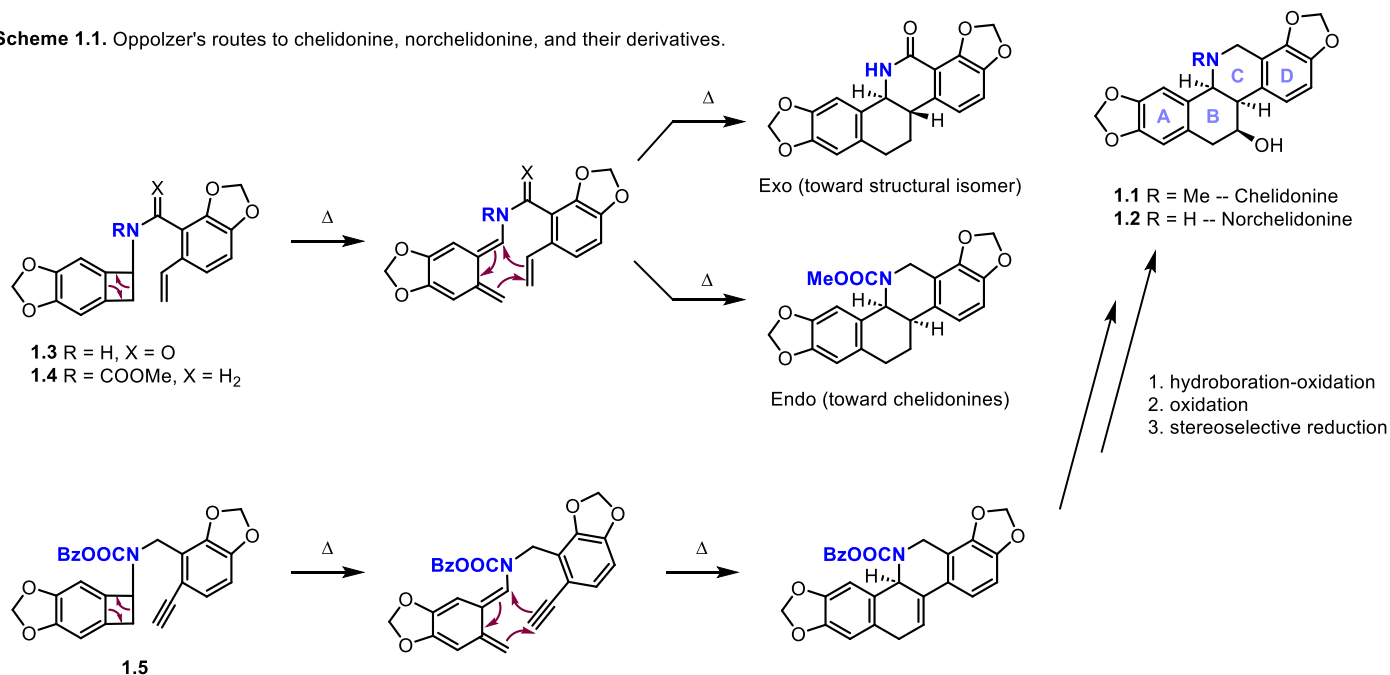
Herein we examine the total synthetic applications to *N*-heterocycle formation that have employed the Diels-Alder for the formation of alkaloid moieties: both in carbocyclic Diels-Alders, where *N*-heterocycles are secondarily formed by the reaction of carbon-containing dienes and dienophiles, and in hetero-Diels-Alders wherein nitrogen atoms constitute parts of the dienophile or diene. Examples are considered of both intra- and intermolecular instances for the formation of natural products, as well as dearomative cycloadditions and inverse demand Diels-Alders, heavily favored in many total syntheses by the Boger group.

# 1.2 Intramolecular [4+2] Cycloadditions

Intramolecular examples of this reaction take advantage of the entropic favor inherent in tethering dienes and dienophiles. Strategic architecture of starting materials also allows for a greater degree of stereocontrol than intermolecular counterparts: up to total determination of regioselectivity and even diastereoselectivity, given appropriately restricted conformational freedom. These methods to favor formation of a desired product have been heavily employed toward the synthesis of natural products, as low yields or poor selectivity on long linear sequences have an exponential effect on synthetic outcomes.

## 1.2.1 Carbocyclic [4+2] Cycloadditions

Scheme 1.1. Oppolzer's routes to chelidonine, norchelidonine, and their derivatives.



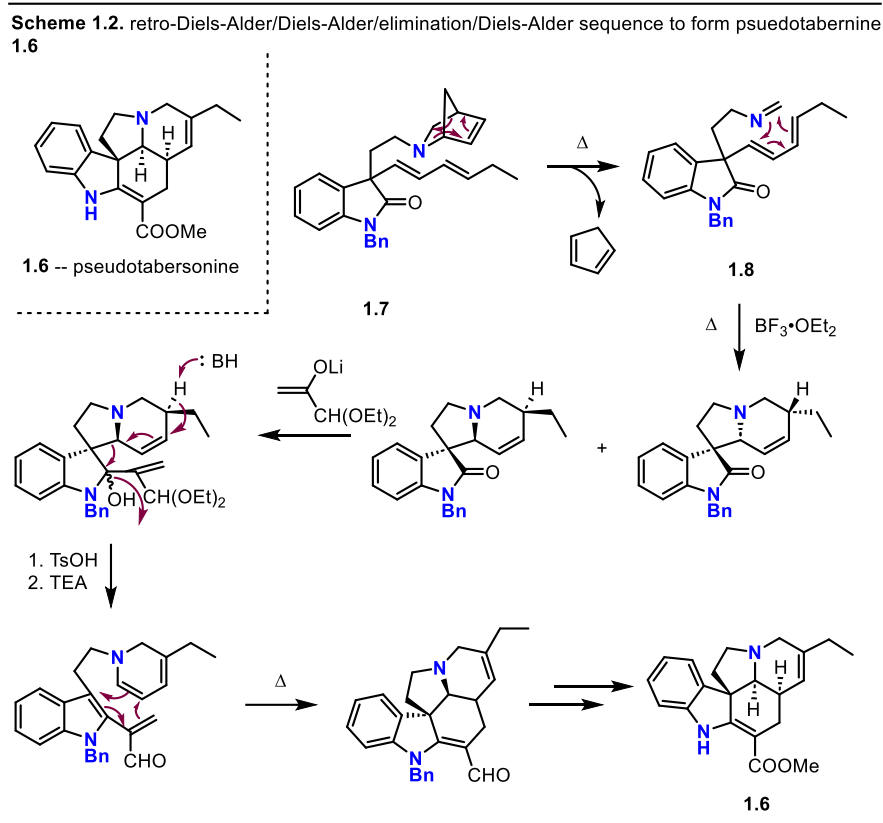
In 1983, Oppolzer and coworkers employed an intramolecular Diels-Alder cycloaddition in their racemic total synthesis of Chelidonine (**1.1**) and Norchelidonine (**1.2**), establishing the precedent for formation of *N*-heterocycles using this method. This transformation simultaneously

formed the carbocyclic B-ring and tetrahydropyridine C-ring of its hexacyclic structure.<sup>4</sup> This group first attempted the intramolecular cycloaddition of precursor **1.3**, which gave the *trans* stereochemistry about the ring fusion. Upon strategic variation of the electronic properties of the precursor, they postulated **1.4**, which preestablished *cis* ring fusion analogous to that of **1.1** and **1.2** by engineering orbital overlap of an extended  $\pi$ -system in the diene to interact favorably with that of the dienophile.

To establish facile formation of the desired ring fusion and hydroxylation diastereochemistry, **1.5** was synthesized in preparation for a hydroboration-oxidation/oxidation/stereoselective reduction cascade, which led to ready formation of the desired stereochemistry in products **1.1** and **1.2** (Scheme 1.1). Although these transformations were purely carbocyclic, they concomitantly formed the *N*-heterocyclic C ring as the desired diastereomer.

A series of similar transformations was employed by Carroll and Grieco eight years later in their synthesis of racemic pseudotabernine (**1.6**).<sup>5</sup> This synthesis set a basis for the further

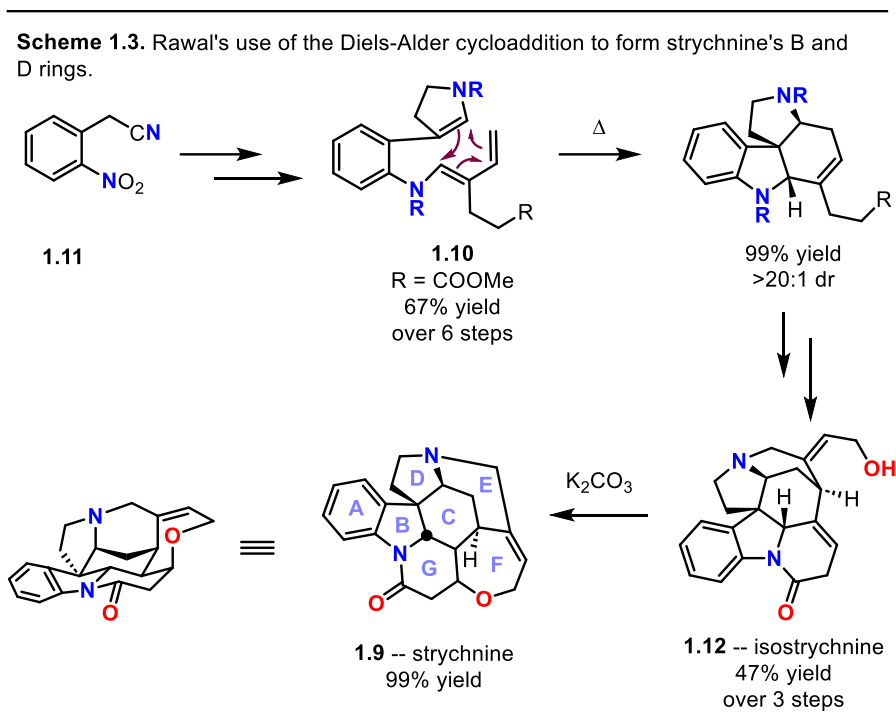
development of *Aspidosperma* alkaloids, utilizing an intramolecular Diels-Alder to form two of



the structures' five rings: a carbocyclic retro-Diels-Alder of **1.7** followed by the analogous [4+2] cycloaddition of resultant **1.8** with the N-containing dienophile to form the D-ring of the five-membered *N*-heterocyclic moiety of **1.6** after elimination of an alcohol group. Though this was a more complex transformation involving a step that included an *N*-heterodienophile in one of the Diels-Alder reactions, the final [4+2] carried out in the cascade was a carbocyclic cycloaddition that secondarily formed the *N*-heterocyclic D ring (Scheme 1.2). Through careful manipulation of cycloaddition diastereoselectivity and prediction of inherent regioselectivity, the Grieco group was able to selectively form their desired product with its correct stereochemistry.

In a more straightforward transformation to conquer the complex skeleton of Strychnine (**1.9**), the Rawal group took advantage of a carbamate-protected pyrrolines to draw electron density away from the intended dienophilic olefin.<sup>6</sup> Their facile thermal cycloaddition (185°C,

benzene, 4h) of **1.10**, prepared in 6 steps in 67% yield from commercially available precursor **1.11**, proceeded stereoselectively in quantitative yield. This transformation concomitantly formed the



partially saturated indoline B ring, along with stereoselectively saturating the pyrroline dienophile precursor to strychnine's pyrrolidine ring D (Scheme 1.3).

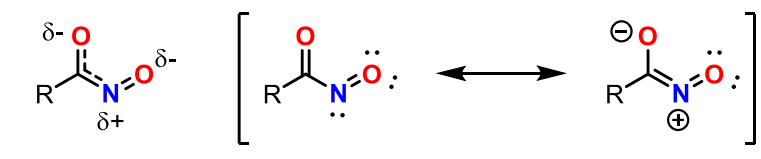
The use of the Diels-Alder cycloaddition in this synthesis also provided a functionalization handle in the carbocyclic C ring. This alkene was later isomerized to isostrychnine (**1.12**) and again isomerized *in situ* to a Michael acceptor that then underwent a base-catalyzed cyclization to the established heptacyclic structure of **1.9** based on literature precedent.<sup>7</sup>

## 1.2.2 Nitrogen-Containing Dienophiles

In a more direct route to formation of *N*-heterocycles, many total syntheses carry out hetero-Diels-Alder reactions with nitrogen-containing dienes or dienophiles. To establish

electronic conditions that circumvent the “inverse-demand Diels-Alder” label (*vide infra*), nitrogen-containing dienophiles must be functionalized so that nitrogen's characteristic electron richness is directed elsewhere, either through inductive effects or resonance. Because of this, two of three entries in this section utilize acyl nitroso groups (RCON=O) as  $2\pi$  components. The polar double bond between oxygen and nitrogen concentrates negative charge on the more electronegative oxygen center, and the same direct  $\pi$ -bond between the two formally uncharged  $\pi$ -donors precludes them from resonating into one another. The *N*-acyl group acts as an electron sink for  $N_{LP}$  resonance as well, further drawing electron density from the nitrogen center.

**Figure 1.2.** *N*-acyl nitroso resonance hybrid contributors.



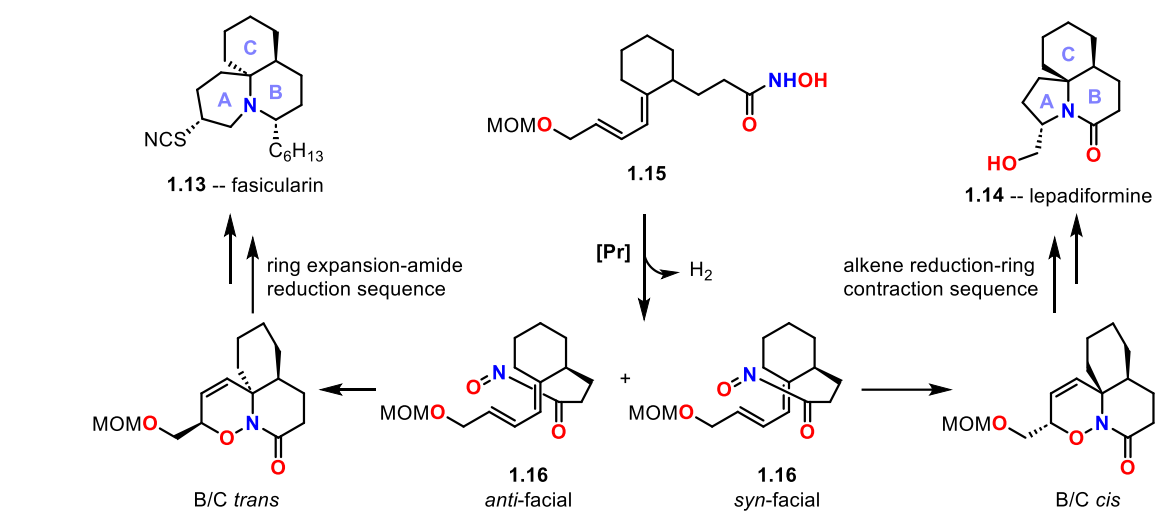
In tandem, these groups establish a formal partial positive charge on the nitrogen (Figure 1.2), which lends itself toward faster reaction rates and increased regio- and diastereoselectivity. The third and most recent literature example of *N*-centered dienophile makes use of an  $\alpha$ -cyano imine in place of the *N*-acyl nitroso group. This functional group choice establishes the desired reactivity as well as providing a functionalization handle for further derivatization of intermediates to the desired target.

The Kibayashi group's 1999 racemic syntheses of fascicularin (**1.13**) and lepadiformine (**1.14**) took advantage of *N*-acyl nitroso dienophiles to construct both natural products' tricyclic structures. Each of these targets stems from a different diastereomer of the observed [4+2] products.<sup>8</sup>

Starting from **1.15**, a precursor derived in 9 steps from a commercially available starting material, the *N*-acyl nitroso compound **1.16** was formed upon praseodymium-mediated oxidation

of the hydroxylamine to its nitroso analog. As the geometry of this intermediate allowed for two different facial diastereoselectivities of [4+2] cycloaddition, two stereoisomers were formed, with the B/C-*cis* mildly predominating (Scheme 1.4). As each target was accessible via a separate diastereomer, Kibayashi and coworkers embarked on the divergent syntheses of two natural products from these separable intermediates.

**Scheme 1.4.** Kibayashi's divergent syntheses of fascicularin and lepadiformine.

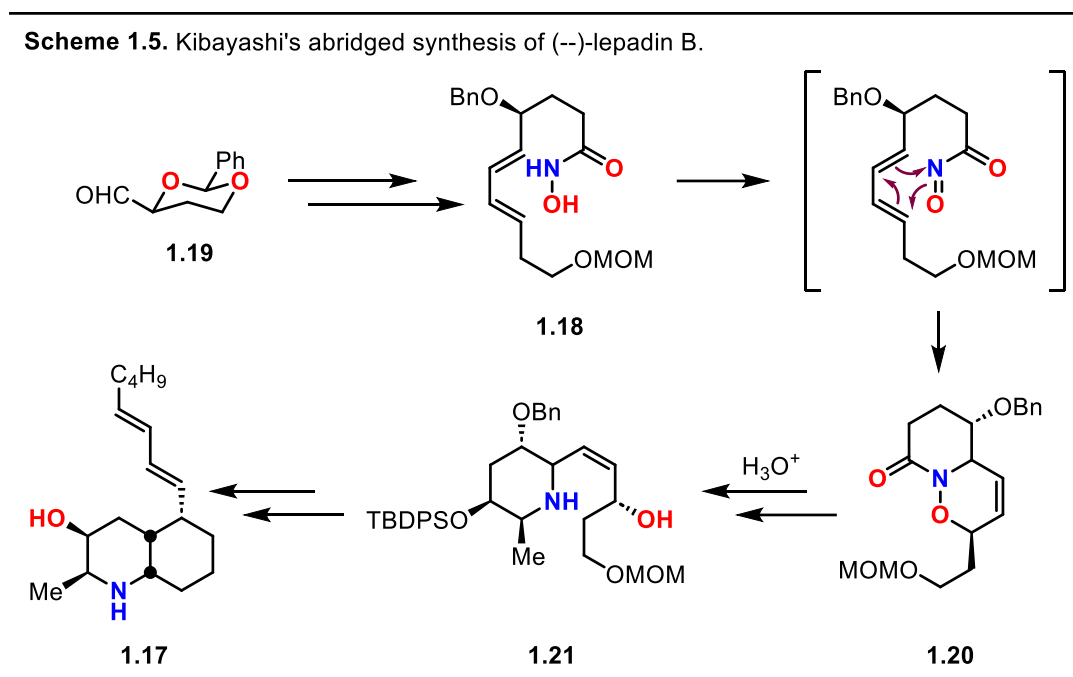


The minor product B/C-*trans* isomer (stemming from *anti*-facial **1.16**) was first isomerized through a ring expansion, mediated through opening of the 1,2-oxazidine ring, protecting group manipulations, and subsequent reformation of six-membered *N*-heterocycle at the newly established electrophilic carbon. This step was followed by amide alkylation and reduction of the amide and alkene to form **1.13**.

The major stereoisomer B/C-*cis* (product of *syn*-facial attack of **1.16**) followed similar stepwise redox adjustments to form **1.14**. Pd-mediated reduction of the resultant alkene followed by ring opening, epoxidation, and entropically favored selective five-membered ring formation readily gave way to lepadiformine. Both structures were confirmed against natural product <sup>1</sup>H

and  $^{13}\text{C}$  NMR standards as well as via X-ray crystallography. Despite subsequent skeletal edits to ring C of both targets, the *N*-acyl nitroso dienophile directly formed both B rings.

Working from their previously developed expertise in dienophiles of this nature, Kibayashi and coworkers returned to their total synthetic work the following year with an asymmetric synthesis of (–)-lepadin B (**1.17**).<sup>9</sup> Starting from **1.18**, formed in 8 steps from commercially available enantiopure **1.19**, intermediate **1.20** was diastereoselectively produced via the same Pr-mediated oxidation followed by *in situ* cycloaddition this group had employed the previous year (Scheme 1.5).

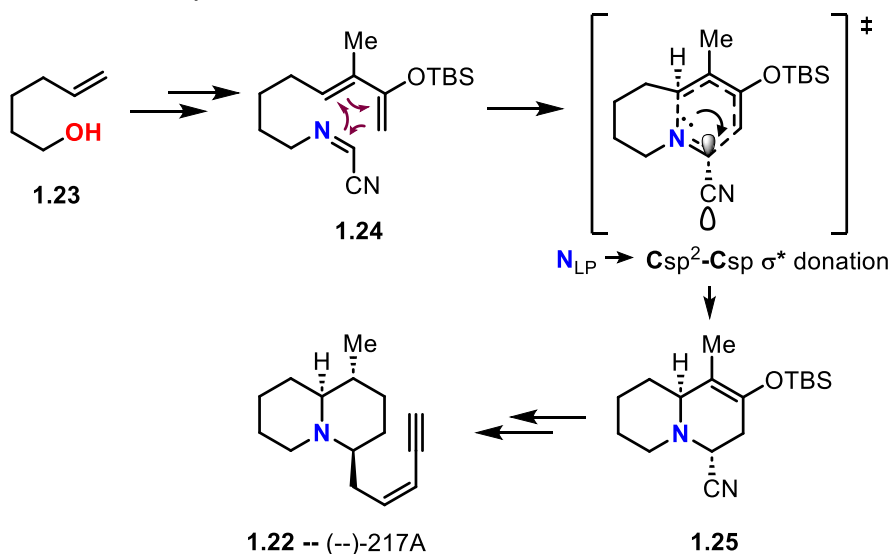


Separating **1.20** from its minor (6.6:1 dr) diastereomer, the intermediate was carried forward in a series of redox and protecting group adjustment steps toward **1.17**. However, as one of the two six-membered rings formed by the Diels-Alder was a 1,2-oxazidine not native to the natural product, a ring opening—ring closing sequence to isomerize to the desired *N*-heterocycle was required. Following the acid-catalyzed ring cleavage to corresponding  $\delta$ -amino alcohol

**1.21**, an deprotection-oxidation-aldol addition sequence was employed to cyclize to a **1.17** precursor with the desired stereochemistry. After a series of further redox adjustments, protecting group manipulations, and alkylation steps, (–)-lepadin **1.17** was stereoselectively formed. Despite the cumbersome nature of this twenty-six-step linear sequence, the N-heterocyclic ring B of this alkaloid was formed in good yield and diastereoselectivity in the key [4+2] cycloaddition step. This transformation is the third example by the Kibayashi group of N-acyl nitroso groups as  $2\pi$  components in a hetero-Diels-Alder, which irrefutably asserts its utility as a transformation in total synthesis.

In 2005, the Danheiser group employed an  $\alpha$ -imino nitrile as a  $2\pi$  component in their Diels-Alder to form quinolizidine alkaloid (–)-217A (**1.22**). In a simple linear sequence,  $\delta$ -enol **1.23** was converted in a series of high-yielding steps to cycloaddition precursor **1.24**. This highly electron-deficient imine underwent thermal addition to the intramolecular diene to form cycloadduct **1.25** as the sole diastereomer in 59% yield.<sup>10</sup>

**Scheme 1.6.** Abbreviated steps and stereochemical rationalization in Danheiser's enantioselective synthesis of **1.22**.



Curiously, this diastereomer was formed from the *exo* transition state, normally disfavored for extended dienophile  $\pi$ -systems due to constructive secondary orbital interactions. Danheiser and coworkers postulated that this was due to the anomeric effect of the nitrogen lone pair favoring pseudo-axial orientation of the nitrile as the six-membered ring formed (Scheme 1.6). Such cases of this geometry have previously been documented in  $\alpha$ -amino nitriles. With this exclusive geometry in hand, **1.25** was further alkylated and reduced to asymmetrically form **1.22** in a linear 14 steps, its six-membered B ring directly formed by cycloaddition of **1.24**.

### 1.2.3 Nitrogen-Containing Dienes

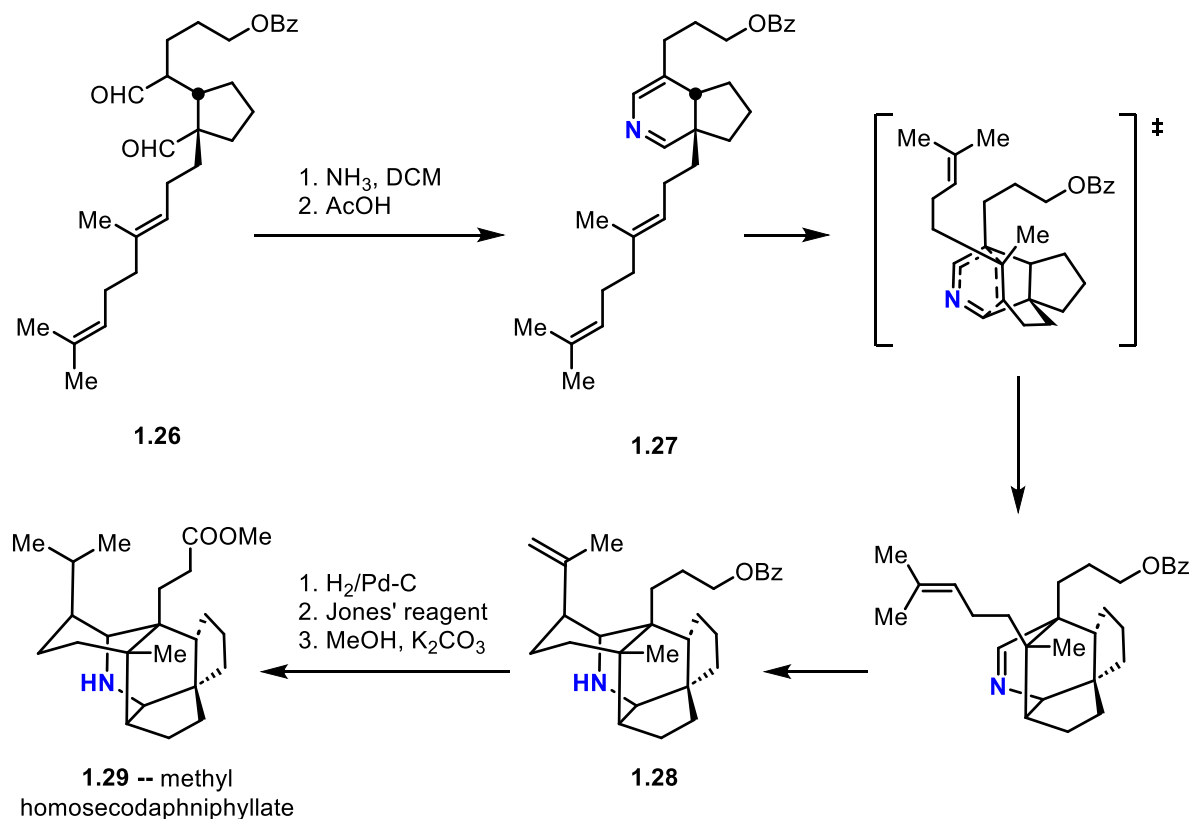
By far the most common method of directly incorporating nitrogen atoms into heterocyclic structures via Diels-Alder is by using nitrogen-containing dienes. As previously stated, formally uncharged trivalent nitrogen atoms are  $\pi$ -donors through resonance and are comparatively electropositive as heteroatoms. These characteristics lend themselves well to the electron-richness required of dienes in regular-electron-demand [4+2] cycloadditions.

To our knowledge, the first documented use of *N*-heterodienes as intramolecular  $4\pi$  components was in 1988 by Heathcock and Ruggeri. Formed through a modular sequence of enolate additions from commercially available starting materials, dialdehyde intermediate **1.26** was condensed to *N*-alkenyl imine **1.27**, which was then doubly cyclized in a Diels-Alder-iminium-addition sequence to yield tetracyclic structure **1.28**. This intermediate was then reduced at the isopropene, deprotected, oxidized at the free alcohol, and esterified to the desired synthetic target, methyl ester **1.29** (Scheme 1.7).

The Diels-Alder step was notably fully diastereoselective from its less sterically constrained transition state (in the absence of secondary orbital interactions) and entirely

chemoselective for the proximal olefin. This selectivity allowed for smooth transition into the second cyclization step, the addition of the distal isopropenyl olefin to the iminium formed *in situ*.

**Scheme 1.7.** Heathcock's synthesis of daphniphyllates, featuring a one-pot double cyclization.

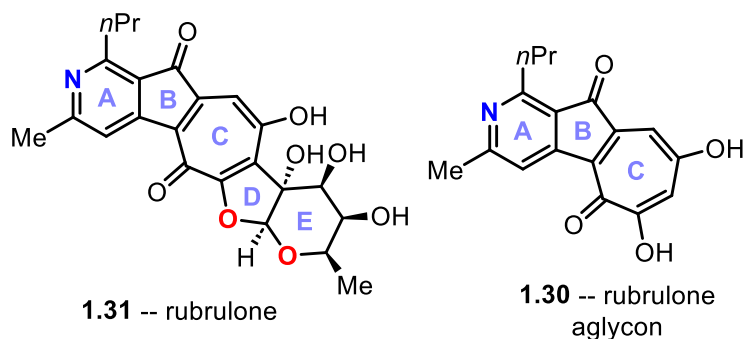


With only straightforward redox adjustments and a single deprotection remaining, the final three steps established **1.29** in 44% yield over an impressively concise 9-step sequence. This synthesis unlocked the skeletal structure of multiple daphniphyllates up to the gram scale, their varying redox features accessible through the modular triple condensation of starting materials or redox edits throughout the established methodology.

Representing the first contribution to this chapter by the Boger group but far from the last, their 2000 synthesis of the rubrulone aglycon (**1.30**) also took advantage of a nitrogen-containing diene. This pathway forgoes the functionalization of rubrulone (**1.31**) at rings D and E

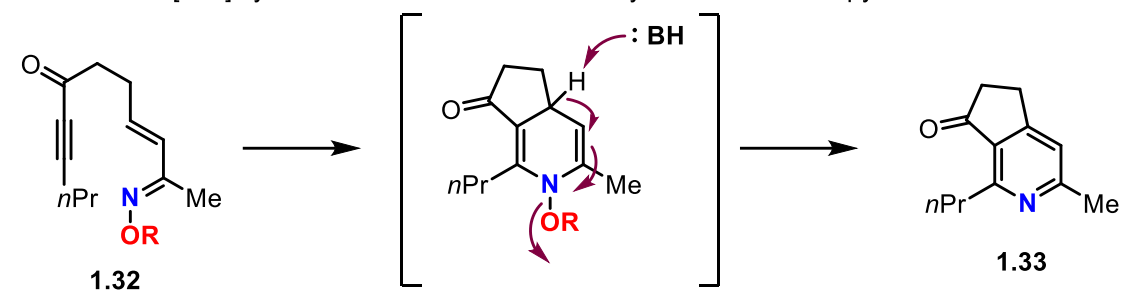
with furanose and pyranose sugars, respectively, for ease of synthetic access and demonstration of their facile methodology to access the A, B, and C rings, which are common functionalities across related alkaloids (Figure 1.3). The syntheses uses two [4+2] cycloadditions for the formation of the tricyclic structure, but only the first employs a nitrogen dienophile towards an *N*-heterocycle: pyridyl ring A.<sup>11</sup>

**Figure 1.3.** Rubrulone and rubrulone aglycon structures.



Following a linear sequence of well-established C—C bond-forming reactions, oxime intermediate **1.32** was produced in anticipation of its intramolecular thermal cycloaddition. The specific conditions of this reaction underwent a short optimization, selecting for solvent, reaction time, temperature, and oxime R group. Optimal conditions (triisopropylbenzene, 175 – 185°C, 36h, no preference on –OR identity) smoothly formed **1.33** in 70% yield after aromatization *in situ* via the initial cycloadduct (Scheme 1.8). This formal oxidation to the corresponding pyridine proceeded through net loss of methanol or benzyl alcohol, installing the *n*-propyl and methyl substituents on the pyridine with total regiocontrol. **1.33** was then carried into several C-C bond-forming and protection steps to a highly activated diene precursor. This 4 $\pi$  component underwent a second thermal [4+2] cycloaddition with a cyclopropenone acetal, followed by eventual ring expansion and deprotection to tropone ring C.

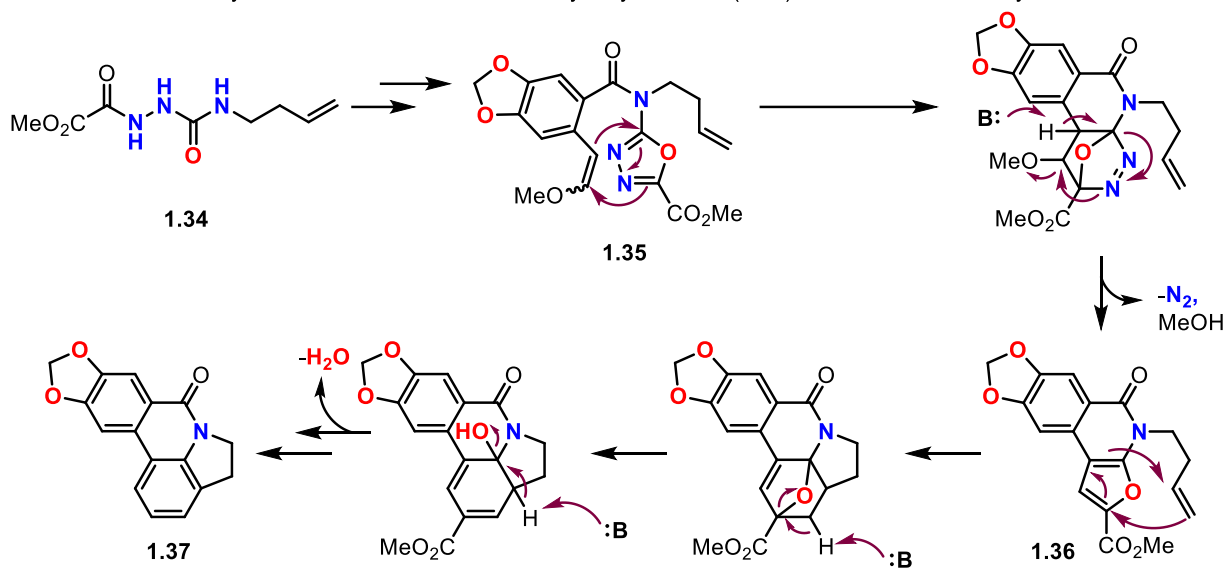
**Scheme 1.8.** [4+2] cycloaddition of oxime followed by aromatization to pyrrole.



The next entry by the Boger group was published two years later and employed a [4+2] to form an *N*-heterocycle at a site other than that of the cycloaddition. However, this transformation still took advantage of 1,3,4-oxadiazole as a nitrogen-containing diene, performing an intermediate that would undergo several subsequent eliminations and an additional [4+2] cycloaddition to form the desired product.<sup>12</sup>

Linear precursor **1.34** was sequentially synthesized and cyclized to form the intramolecular starting material oxadiazole **1.35**. This oxygen-rich aromatic diene underwent cycloaddition with the more kinetically accessible dienophile to form a bridged intermediate. The oxygen richness of the 1,3,4-oxadiazole ring was sufficient to overcome the comparably electron-rich nature of the closer tethered dienophile under thermal conditions, entirely kinetically selecting the more accessible  $2\pi$  system prefunctionalized with a leaving group rather than the more electron-deficient one. Through formal elimination of methanol and thermodynamically favored expulsion of  $N_2$ , furan intermediate **1.36** was produced. Acting as a diene with the remaining tethered dienophile, a second Diels-Alder reaction occurred to produce a bridged ether. After two sequential protonation-elimination steps, the bridging oxygen was lost as water and the remaining six-membered ring was aromatized to the phenyl D ring of anhydrolycorinone **1.37** (Scheme 1.9).

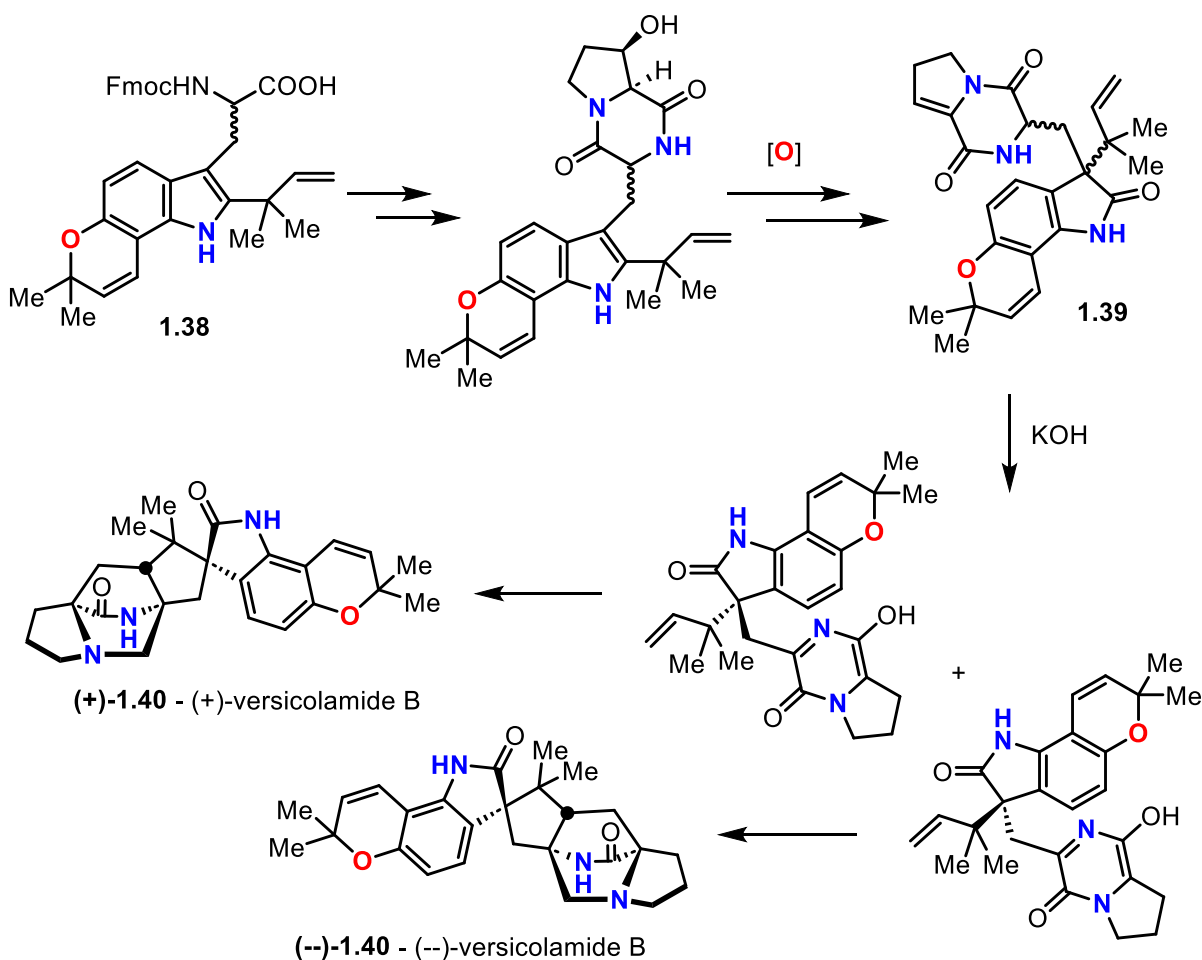
**Scheme 1.9.** *In situ* cycloaddition cascade to form anhydrolycorinione (**1.37**) from intramolecular cycloaddition of **1.35**.



Although the nitrogen atoms in the diene of this cycloaddition did not end up being incorporated into the structural skeleton of **1.37**, this work by Boger and coworkers still secondarily formed an *N*-heterocycle through their use of a nitrogen-containing diene in their Diels-Alder.

The Williams group's synthesis of enantiopure (–)- and (+)-versicolamide B took advantage of a more direct hetero-Diels-Alder in their synthesis, employing it as the ultimate step in their concise synthesis of both versicolamide enantiomers.<sup>13</sup> Starting from commercially available racemic amino acid **1.38**, a non-diastereoselective bond-forming step produced a 1:1 diastereomeric ratio of **1.39** precursors. These precursors were chromatographically separated and each diastereomer was further functionalized in separate reaction vessels. Sequential oxidation and pinacol rearrangement of each stereoisomer yielded four diastereomers of **1.39**, which underwent base-catalyzed elimination to afford tethered nitrogen-containing dienes and dienophiles (Scheme 1.10).

**Scheme 1.10.** Williams' syntheses of both versicolamide enantiomers.

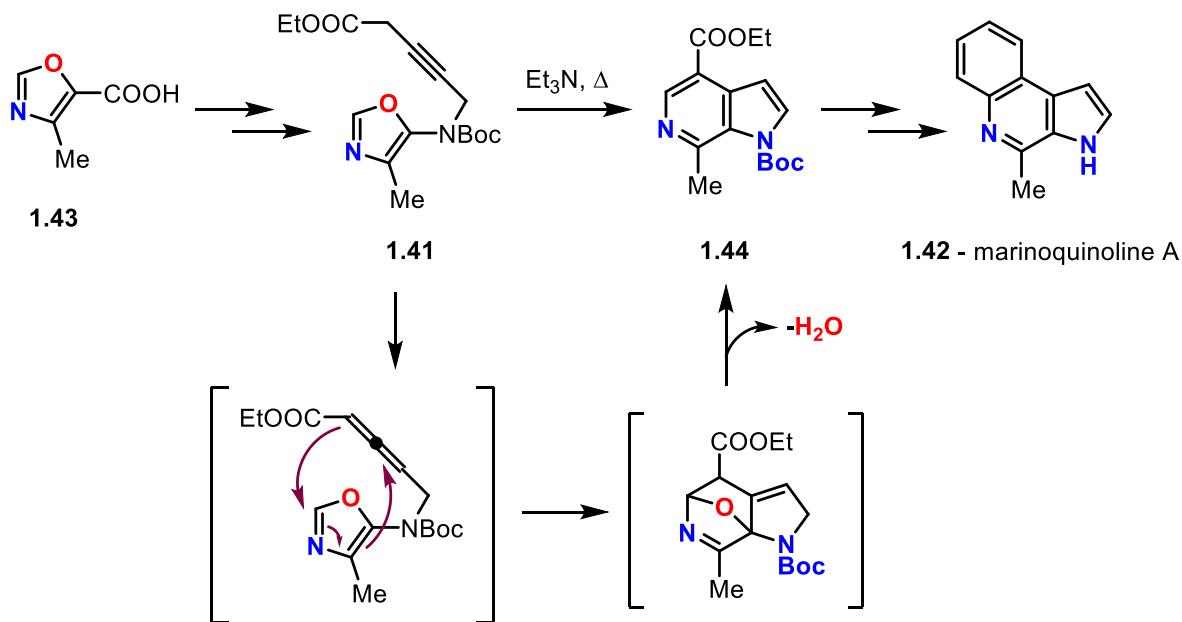


This transformation also eliminated a chiral center, once again producing just two diastereomers of Diels-Alder precursors. Each diastereomer spontaneously underwent [4+2] cycloaddition at room temperature to yield both versicolamide enantiomers **(-)-1.40** and **(+)-1.40**. Due to the lack of secondary orbital interactions to stabilize the *endo* transition state, the less sterically congested (albeit desired) *exo* products prevailed in a 1.4:1 ratio. Overall, this synthesis took advantage of a commercially available racemic amino acid and several nontrivial diastereomeric separations to synthesize separate enantiomers of versicolamide in only five steps. The late-stage convergence of the synthesis allowed the Williams group to carry forward

all products of two non-diastereoselective bond-forming steps, only sacrificing yield to the unwanted diastereomer in the final Diels-Alder.

The most recent example of *N*-heterocycle formation via intramolecular heterodienophile Diels-Alder was carried out by Wipf and coworkers. Their strategy developed a [4+2] with oxazoles as 4 $\pi$  components, functionalized at the C5 position with a  $\beta$ -amino allene (via the corresponding alkyne) as the 2 $\pi$  component (intermediate **1.41**). This method's synthetic utility was then demonstrated in a short formal synthesis of marinoquinoline A (**1.42**).<sup>14</sup> Like the Boger group's second sequential [4+2] reaction in their synthesis of anhydrolycorinone, formal loss of water *in situ* from the bridged ether resulted in irreversible aromatization of the 6-membered cycloadduct. In instances where this aromatative loss of water forms a pyridine, the [4+2]-aromatization sequence constitutes a Kondrat'eva pyridine synthesis.<sup>15</sup>

**Scheme 1.11.** Formal Kondrat'eva reaction by Wipf and coworkers toward marinoquinoline A



Once the [4+2] had been optimized for yield and functional group tolerance where additional functionalities were required for the total synthesis, the Wipf group carried out the

synthesis of **1.42** in 10 steps from commercially available starting material **1.43** (Scheme 1.11). Centering around their use of this cycloaddition, intermediate **1.41** was subjected to base-catalyzed allene isomerization. From the allene, the Kondrat'eva synthesis occurred *in situ* through the bridged ether, which underwent elimination of water to the desired 6-azaindole **1.44**. Through a series of well-established C-C bond-forming steps and protecting group adjustments, **1.42** was produced in over 11% overall yield.

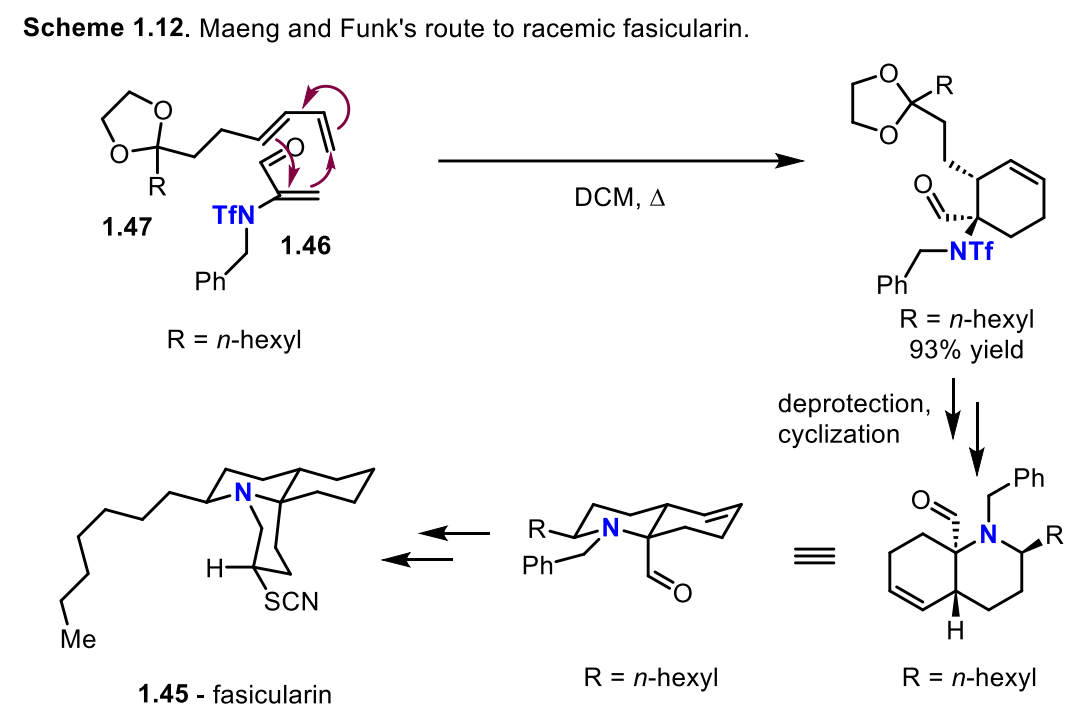
## 1.3 Intermolecular [4+2] Cycloadditions

Offering complementarity to intramolecular methods, the use of intermolecular [4+2] cycloadditions has also been extensively documented in total synthesis. While intramolecular reactions may offer greater selectivity, intermolecular variants allow greater freedom in retrosynthetic analysis. More possible disconnections and an inherently modular approach to the construction of complex targets are highly valued in the preparation of drug lead analogs, a staple operation of structure-activity relationship (SAR) studies. Extremely high to total regio- and diastereoselectivity can also be engineered in reaction conditions through careful selection of starting material electronics.

Intermolecular Diels-Alders in total synthesis have been greatly dominated by carbocyclic cycloadditions. As with the previous section, [4+2] routes to *N*-heterocycles will be classified into those that secondarily form azacycles or preestablish their functionality before a subsequent cyclization, and those using nitrogen-containing dienes or dienophiles. Several examples exist of dearomative cycloaddition of one or both starting materials that fall under one of these categories. However, those will be discussed in section 1.4.

### 1.3.1 Carbocyclic [4+2] Cycloadditions

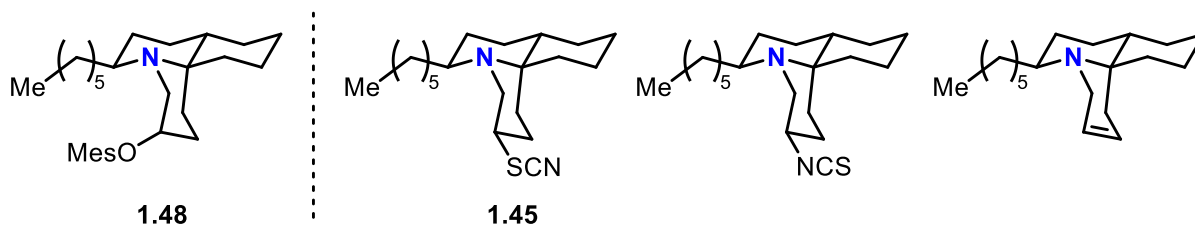
In 2001, Maeng and Funk carried out the racemic synthesis of fascicularin (**1.45**), initiating their work with an intermolecular Diels-Alder. This cycloaddition combined a readily prepared acrolein derivative dienophile (**1.46**) and a diene containing a masked ketone (**1.47**) for a subsequent cyclization to form the six-membered precursor to the tricyclic structure (Scheme 1.12).



Thermal cycloaddition in DCM yielded the desired cycloadduct in 93% and total regio- and *endo* diastereoselectivity, facilitated by constructive orbital overlap by the dienophile's extended  $\pi$ -system. This six-membered ring preestablished the nitrogen-atom conformation before subsequent structural edits: nitrogen protecting group and acetal cleavage, which spontaneously underwent intramolecular condensation to the iminium, followed by reduction for a net reductive amination. Having formed two of the three rings of fascicularin, subsequent

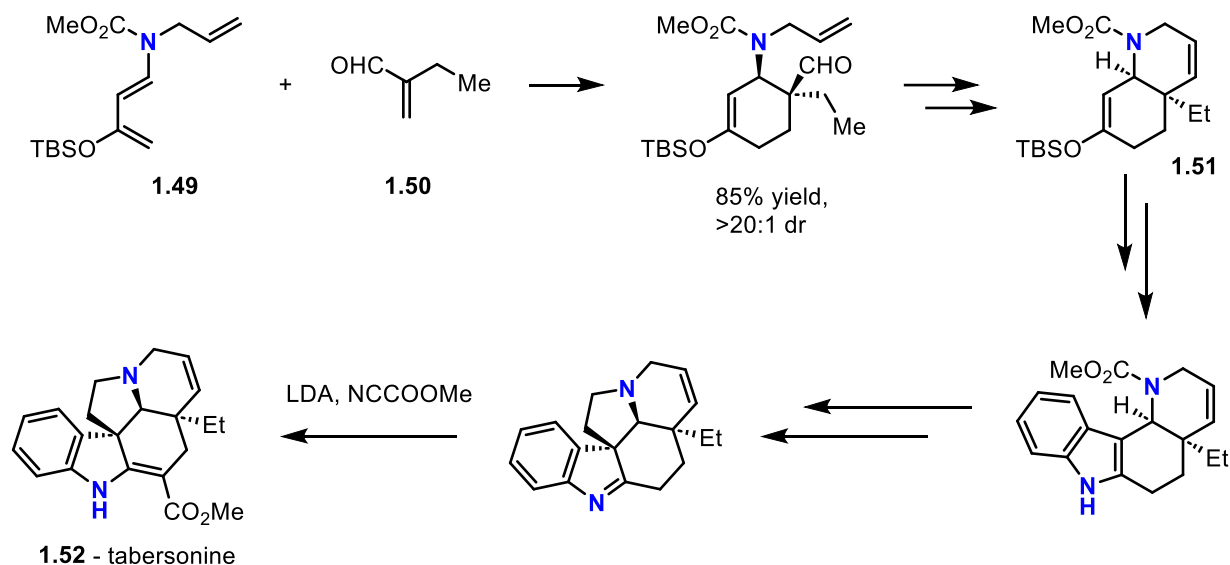
carbon-carbon bond-forming reactions and functional group manipulations produced **1.45** in a total of 16 steps. However, the final  $S_N2$  step yielded a mixture of products, including differing nucleophilic attack by the nitrogen to form an isothiocyanate and competing E2 reaction (Figure 1.4).<sup>16</sup>

**Figure 1.4.** Product mixture from the final  $S_N2$  reaction of starting material **1.48**.



Later that same year, the Rawal group employed a similar strategy to preform an *N*-heterocycle precursor with a Diels-Alder reaction. Utilizing the placement of a nitrogen on the diene to lend electron density, starting materials **1.49** and **1.50** were subjected to heat in toluene. This cycloaddition resulted in total regioselectivity, almost complete *endo* selectivity, and 85% isolated yield. These sole diastereomers were readily subjected to an olefination at the aldehyde moiety followed by a ring-closing metathesis reaction to starting material **1.51**, now functionalized with the six-membered *N*-heterocycle of tabersonine (**1.52**, Scheme 1.13).<sup>17</sup>

**Scheme 1.13.** Rawal's diastereoselective route to tabersonine.



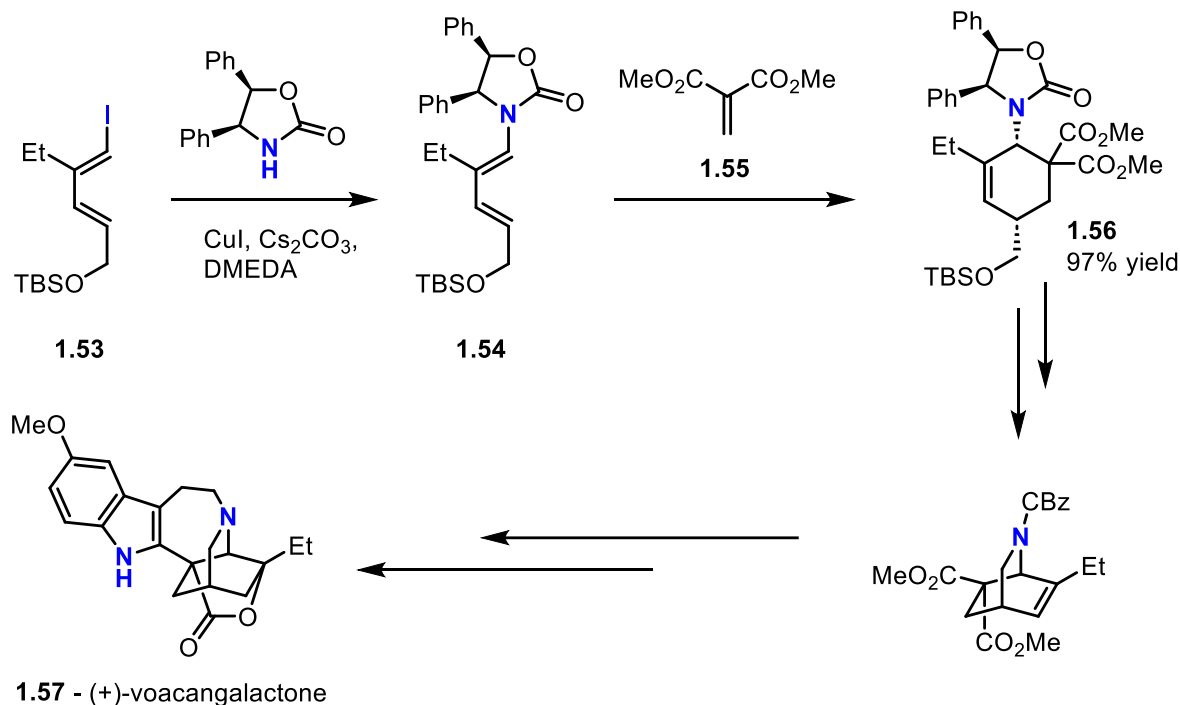
**1.51** underwent indole formation at the masked ketone moiety, followed by installation of ethyl iodide at the nitrogen center. Upon subjection to *t*BuOK, nucleophilic indole C3 cyclized to form the other fused *N*-heterocycle of **1.52**. The pentacyclic imine intermediate that resulted from this reaction was then deprotonated at the imine  $\alpha$ -position and functionalized with an ester to form racemic tabersonine.

In their 2012 asymmetric synthesis of voacangalactone, the Takayama group also used an intermolecular Diels-Alder as an early step to form molecular complexity towards their target. Like the previous two entries, this cycloaddition established the correct diastereochemistry of the nitrogen atom, which underwent cyclization in a later step.<sup>18</sup>

To establish asymmetry in their synthesis, diene **1.53** was formed from condensation of the corresponding alkyl iodide with chiral auxiliary **1.54**. This material underwent cycloaddition with commercially available diester dienophile **1.55** to yield cycloadduct **1.56** as the sole regio- and stereoisomer in quantitative yield. This complete selectivity owes to the symmetry of the

dienophile as well as steric influence from the chiral auxiliary toward approaching a singular face of the diene (Scheme 1.14).

**Scheme 1.14.** Takayama's initial Diels-Alder for enantiomeric formation of voacangalactone.



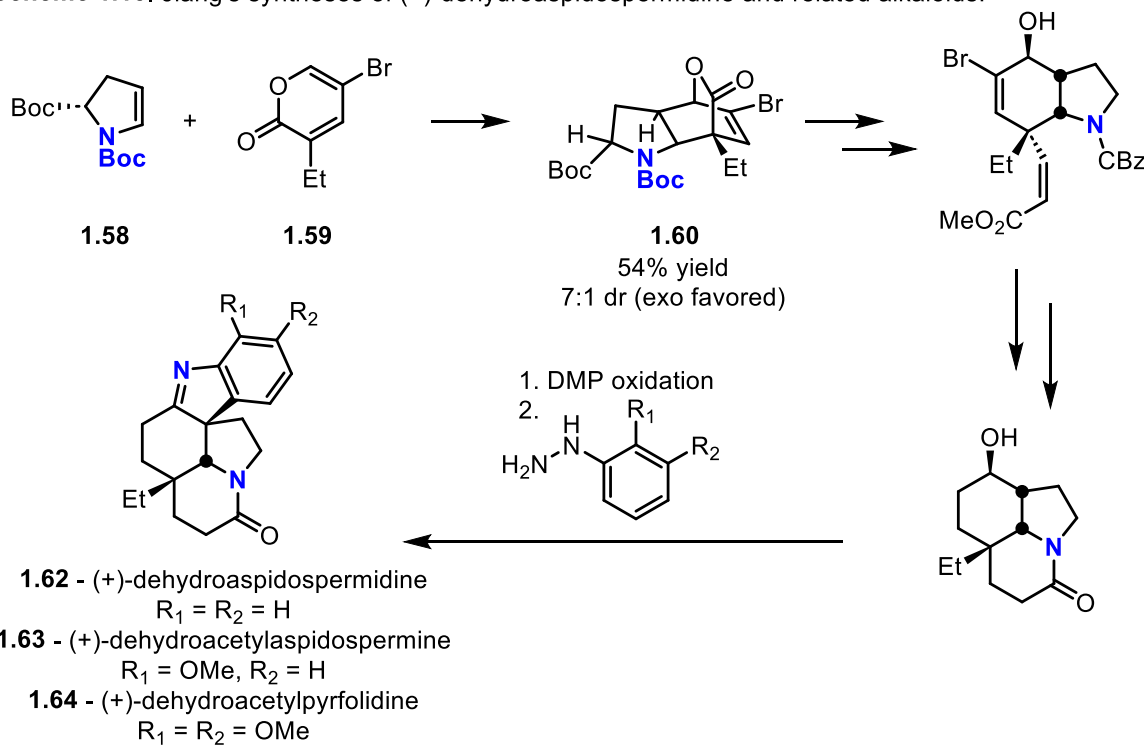
This cycloadduct established the *syn* stereochemistry needed to cyclize the nitrogen substituent with the protected methylene alcohol to form the bridged precursor to **1.57**. Upon cleavage of the chiral auxiliary, reductive desilylation of the –OTBS group, and re-protection via mesylation, the product was refluxed in DMF in the presence of a weak base to undergo the nucleophilic substitution that led to cyclization.

Further derivatizations of this precursor including lactone formation, indolization, and *N*-alkylation, were employed toward the final enantioselective formation of (+)-voacangalactone. This total synthesis took place over 22 steps, with the [4+2] cycloaddition as a key early step toward forming structural complexity that laid the foundation for the stereochemistry of the desired target.

The most recent example of *N*-heterocycle formation through a carbocyclic Diels-Alder was by the Jiang group in 2017. This final example is the only entry in this section that directly forms an *N*-heterocycle within the cycloaddition, not just establishing nitrogen stereochemistry for a later cyclization.

Like previous examples, however, Jiang and coworkers take advantage of the perfect atom economy inherent in cycloaddition reactions to rapidly assemble molecular complexity early on in their synthetic route. From commercially available pyrroline **1.58** and readily prepared pyrone **1.59**, their thermal cycloaddition proceeds in moderate yield with good *exo* selectivity (Scheme 1.15). This counterintuitive diastereoselectivity likely owes to the steric considerations of a cyclic diene, combined with the lack of an extended  $\pi$ -system in the dienophile to maximize constructive orbital overlap in the transition state.<sup>19</sup>

**Scheme 1.15.** Jiang's syntheses of (+)-dehydroaspidospermidine and related alkaloids.



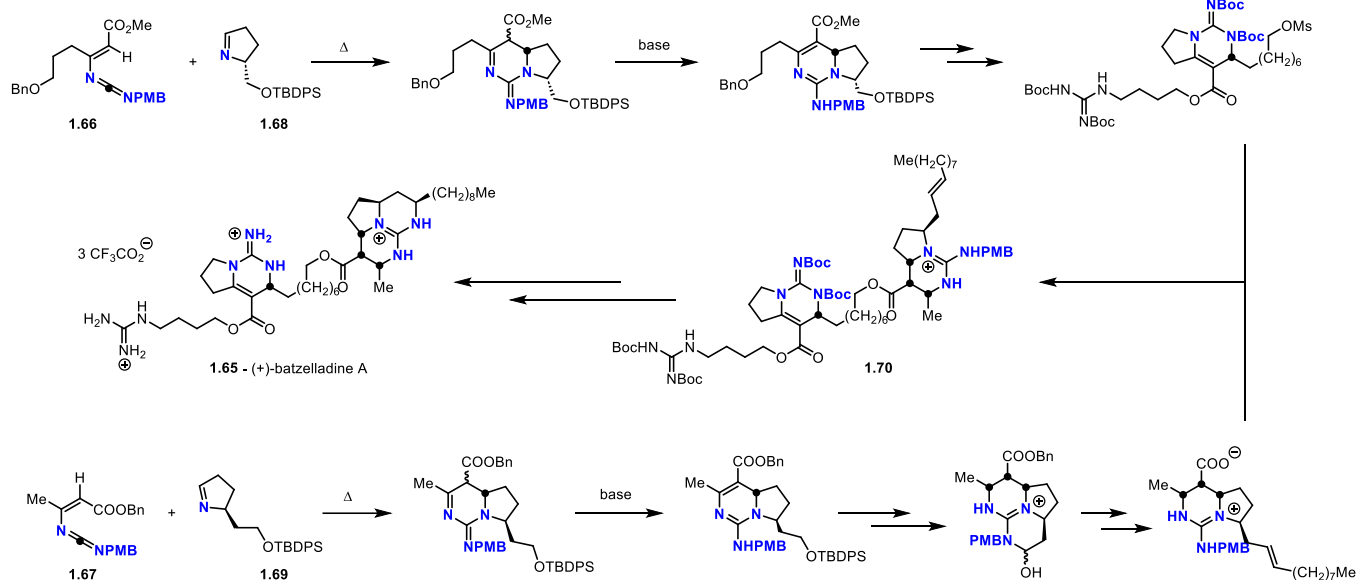
Intermediate cycloadduct **1.60** was then subjected to reduction, ring opening, and olefination to afford a bicyclic intermediate. Deprotection of the nitrogen followed by amidation afforded tricyclic intermediate **1.61**, which was subjected to Fischer indolization under a variety of starting materials to afford three separate natural products: dehydroaspidospermidine (**1.62**), dehydroacetylaspidospermidine (**1.63**), and dehydroacetylpyrrolidine (**1.64**).

### 1.3.2 Nitrogen-Containing Dienophiles

To our knowledge, only one example exists of an intermolecular Diels-Alder toward an *N*-heterocycle using a nitrogen-containing dienophile. This example is the Gin group's asymmetric total synthesis of (+)-batzelladine A (**1.65**), which utilizes both a heterodiene and a heterodienophile in two distinct [4+2] reactions to form two different azacycles in the target structure. These separate structures are further functionalized and convergently combined towards the end of the synthetic route to form the complex structure of **1.65**.<sup>20</sup>

Allenyl dienes **1.66** and **1.67** were assembled from simple starting materials through a sequence of well-known carbon-carbon bond-forming reactions and redox adjustments. Pyrrolines **1.68** and **1.69** were protected and reduced from their corresponding enantiopure  $\delta$ -lactams, which were also commercially available. The thermal Diels-Alder products of each diene-dienophile pair were attained at room temperature with total regioselectivity. While the *endo* adducts were lightly favored, the following base-catalyzed isomerization rendered the poor diastereoselectivity irrelevant when the thermodynamic conjugated  $\pi$ -systems were established in each intermediate (Scheme 1.16).

**Scheme 1.16.** Gin's use of two hetero-Diels-Alder reactions to convergently form batzelladine A.



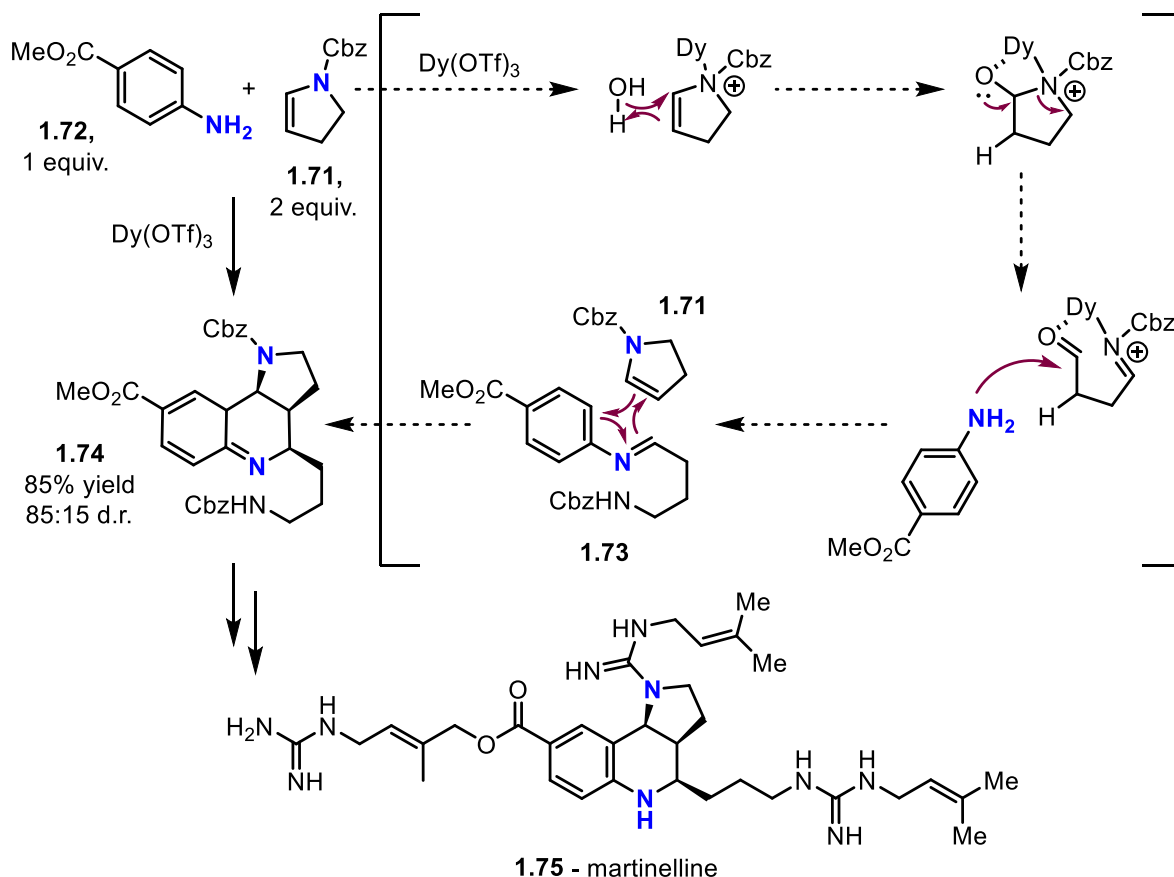
Both bicyclic systems were further functionalized toward the desired connectivity of their respective fragment. Once the desired structures were achieved, the “western” mesylate fragment was combined at room temperature with the “eastern” carboxylate, which smoothly underwent S<sub>N</sub>2 condensation to batzelladine precursor **1.70**. Once again, several bond-forming steps and redox adjustments were made to this structure to asymmetrically form target structure **1.65**, (+)-batzelladine A. The longest linear sequence of this highly convergent synthesis was 15 steps, capitalizing on two high-yielding [4+2] cycloadditions as early transformations for two structurally similar heterocyclic motifs of **1.65**.

### 1.3.3 Nitrogen-Containing Dienes

In 2002, the Batey group invoked a Povarov reaction in their synthesis of racemic martinelline. This reaction proceeds via an aldehyde-aniline condensation to form an *N*-aryl iminium diene that condenses with a dienophile in a Diels-Alder second step. In a strategic use of carbamate-protected pyrroline **1.71** as both an aldehyde source and a dienophile, subjection of

aniline **1.72** to two equivalents of **1.71** under dysprosium (III) Lewis acid-catalysis facilitates the Povarov reaction in its entirety.<sup>21</sup>

**Scheme 1.17.** Formal Povarov reaction towards the tricyclic structure of martinelline by the Batey group.

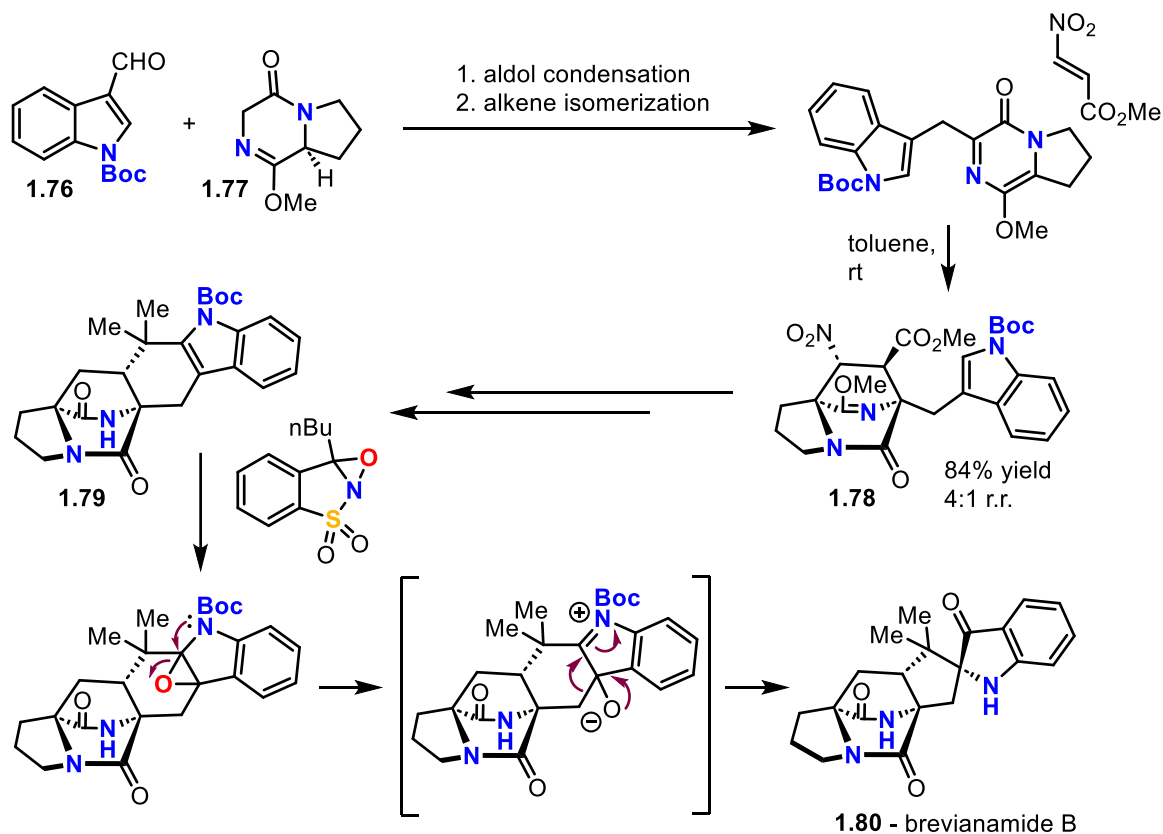


Ring-opening of one equivalent of pyrroline occurs first, upon association of the dysprosium (III) cation with the Lewis basic nitrogen lone pair. A formal hydration occurs across the C2-C3 double bond, leading to cleavage of the hemiaminal to its corresponding  $\delta$ -acyl iminium. This aldehyde, still coordinated to the Lewis acid, quickly condenses with aniline **1.72** to form *N*-aryl imine intermediate **1.73**, which undergoes a Diels-Alder reaction with a second equivalent of **1.71**. Previous transformations of this nature with ring-opening of pyrrolines, dihydrofurans, and other monounsaturated heterocycles have been extensively established in the

literature.<sup>22–24</sup> With 85% yield and 85:15 *endo* selectivity, tetrahydroquinoline **1.74** is furnished at room temperature. Although this cycloaddition is formally dearomative, the intermediate is rearomatized *in situ* before separation from the unwanted diastereomer. The aromatic product is then functionalized at the aryl ester and both protected amines with the necessary pendent alkyl guanidines of product **1.75**, racemic martinelline (Scheme 1.17).

Targeting a similar [2.2.2] diazabicyclic structure to Williams' syntheses of both versicolamide enantiomers, the Scheerer group undertook the total synthesis of brevianamide B in 2016. Commercially available starting materials **1.76** and **1.77** were condensed via aldol and isomerized to a diene conjugated with the amide carbonyl. The diene was then condensed with a highly electron-deficient  $\alpha,\beta$ -unsaturated ester in a Diels-Alder at room temperature to yield an inseparable 4:1 mixture of regioisomers at 84% yield (**1.78**, Scheme 1.18).<sup>25</sup>

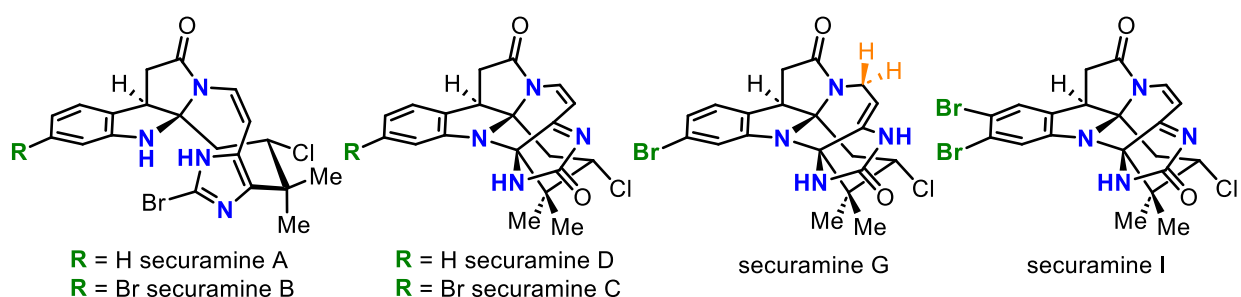
**Scheme 1.18.** Scheerer's intermolecular approach to [2.2.2] diazabicyclic brevianamide B.



This mixture was subjected to a subsequent reductive denitration step, after which the regioisomers were separable by chromatography. Following various connectivity and redox adjustments, intermediate **1.79** was produced over six steps. This compound is a known precursor to racemic brevianamide B (**1.80**) as per the past work of the Williams group towards the same target.<sup>26</sup> Proceeding through oxidation of the indole, the **1.79** epoxide ring opens to an alkoxide intermediate and undergoes a ring contraction to furnish **1.80** in a single step.

Our final example of an intermolecular, regular-demand Diels-Alder for the construction of an *N*-heterocycle is in the very recent work by the Herzon group, published in February 2024. In their impressive syntheses of six securamine alkaloids (Figure 1.5), the cyclic urea structure of securamines C, D, G, and I, are accessed through a late-stage photocatalytic [4+2] cycloaddition of singlet dioxygen to the bromoimidazole of securamines A and B.

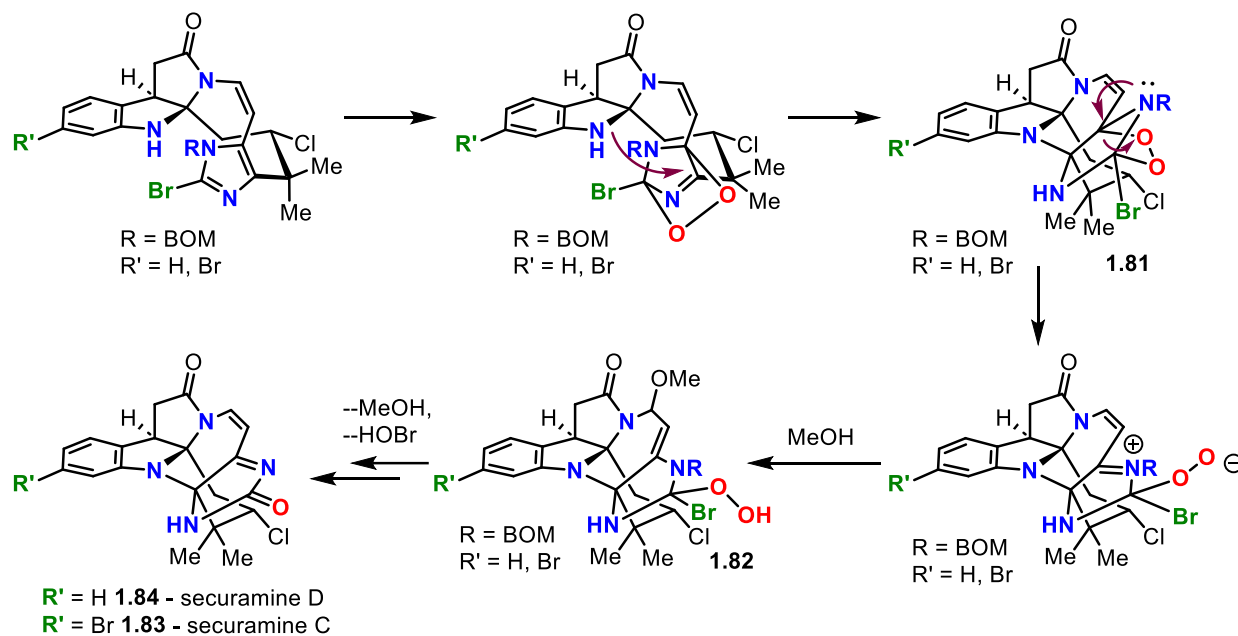
**Figure 1.5.** Structures of securamine alkaloids.



After syntheses of securamines A and B were established, each target was BOM-protected at imidazole- $N^5$  and subjected to rose bengal and visible light under positive pressure of oxygen gas. The bridged cycloadduct established an electrophilic site at carbon 3 of the imidazole, which was attacked by indole  $N^1$  to form polycyclic intermediate **1.81**. This intermediate underwent ring opening to the corresponding peroxide, which in solution in methanol gave the Michael addition product **1.82**. After formal loss of HOBr and methyl ether cleavage to the corresponding alcohol, base-catalyzed elimination yielded the desired cyclic

ureas of the oxidized securamines. Subjecting these structures to a Lewis acid BOM-protected both to yield securamine C (**1.83**) and securamine D (**1.84**, Scheme 1.19). Securamine C could also, even in its unprotected form, be converted to securamine G via reduction with borohydride or radical bromination of the indolyl phenyl ring with NBS to securamine I.

**Scheme 1.19.** Singlet oxygen [4+2] to build the cyclic urea of securamines C, D, G, and I.



The Herzon group's total syntheses of these six alkaloids are the first of their kind. Overall isolated yields range from 1.4% - 3.5%. Additionally, the longest linear sequence toward any of their structures is 18 steps with no more than 12 purifications. Oxidative access to securamines C, D, G, and I was entirely enabled by the singlet oxygen [4+2] cycloaddition, a unique and strategic entry to end discussion of regular-demand Diels-Alder reactions to form *N*-heterocycles in total synthesis.

## 1.4 Dearomative [4+2] Cycloadditions

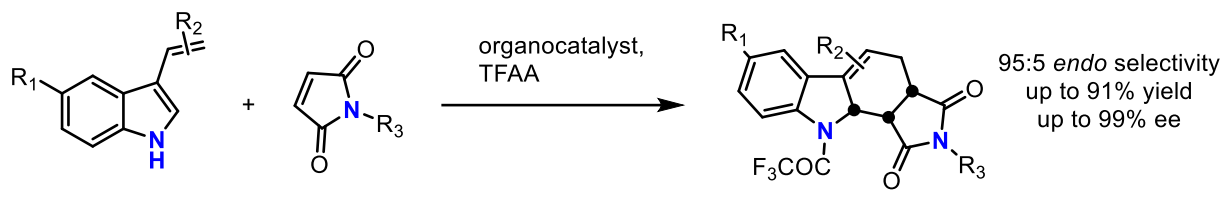
Several examples, both intra- and intermolecular, exist of Diels-Alder reactions that form azacycles via dearomatization of one or both reactants. Owing to the electron-rich nature of vinylindoles and more reactive, less aromatically delocalized nature of the C2 – C3 double bond, these compounds are commonly employed as dienes. Variation of where the vinyl functionality exists on the indole allows for precise incorporation of an indolyl moiety into a natural product. Even if indole-N<sup>1</sup> is not directly involved in the [4+2], formation of a functionalized indoline does establish an *N*-heterocycle.

Less commonly, functionalized indoles are employed as dienophiles. These discussed examples are both inverse electronic demand due to indole's electron richness, one of them taking advantage of an intramolecular cycloaddition to entropically favor cyclization as well. Similar to the employment of the less resonance-delocalized C2 – C3  $\pi$ -bond as part of a diene, its more weakly aromatic nature makes it a viable  $2\pi$ -component in the Diels-Alder and other cycloadditions, despite electronic constraints.

### 1.4.1 Dearomatization of Vinylindole

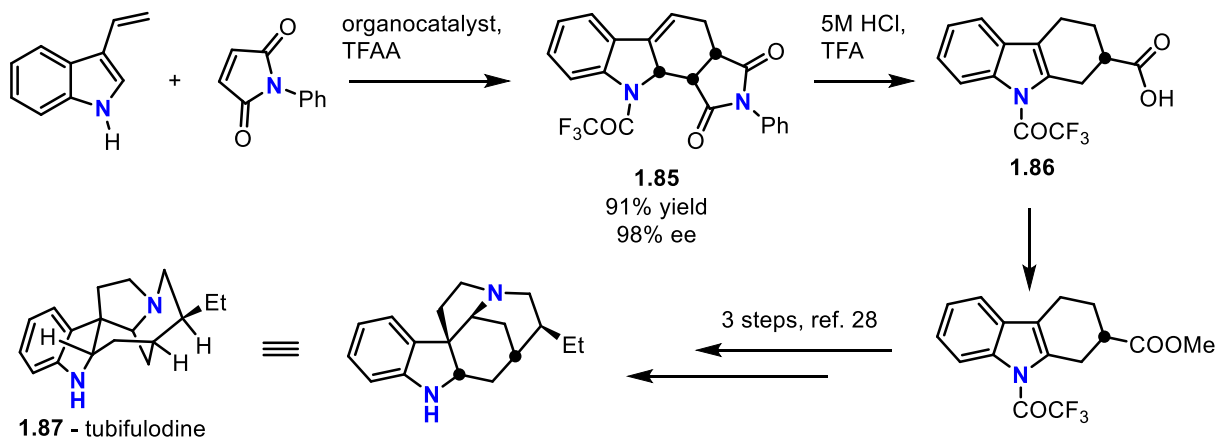
To demonstrate the synthetic utility of their organocatalytic asymmetric vinylindole Diels-Alder, the Ricci group carried out a formal synthesis of tubifulodine, which contained the tricyclic indoline structure constructed by their cycloaddition (Scheme 1.20).<sup>27</sup> As one of their scope entries for this method could be readily transformed into a literature precursor, they embarked on their formal synthesis through construction of this precursor.<sup>28</sup>

**Scheme 1.20.** Ricci's general organocatalytic asymmetric vinylindole [4+2].



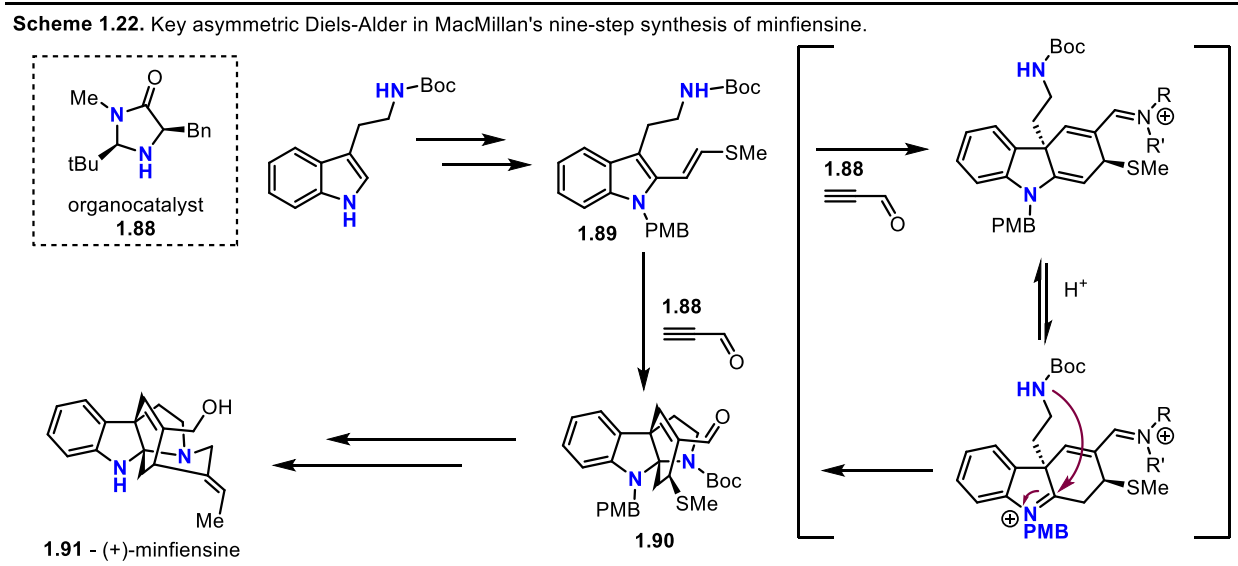
Starting with a high-yielding and very enantioselective cycloaddition of 3-vinylindole and *N*-phenylmaleimide with their optimized organocatalyst and a Bronsted acid, cycloadduct **1.85** was formed (Scheme 1.21). Strongly acidic conditions reductively cleaved the maleimide to acid **1.86**, which was readily converted to its corresponding methyl ester. Although the Ricci group stopped their synthesis at the formation of this ester, a known tubifulodine precursor, it could be further alkylated to an acyclic precursor, then subsequently cyclized and the indole deprotected to form natural product **1.87**, tubifulodine.

**Scheme 1.21.** Ricci's short formal asymmetric synthesis of tubifulodine.



The year after the Ricci group published their formal synthesis, the MacMillan group used their own chiral organocatalyst **1.88** to carry out a similar asymmetric Diels-Alder with a functionalized 2-vinylindole as a diene.<sup>29</sup> This cycloaddition was a key early step in their concise nine-step route to establish the chiral complexity and connectivity of minfiensine. To begin the

synthetic route, trans-thioether olefin **1.89** was installed on C2 of a commercially available alkylamino indole precursor over three steps. The thioether moiety provided further electron density to the diene as well as establishing a functionalization handle for a later radical cyclization. This diene was dearomatized via Diels-Alder with propynal, asymmetrically catalyzed by condensation of the aldehyde with **1.88**. Following the cycloaddition, an acid-catalyzed isomerization established an electrophilic site at indole C2, which was cyclized by the pendant amine to tetracyclic product **1.90** (Scheme 1.22). The organocatalyst was cleaved and went on to turn over its catalytic cycle *in situ*.



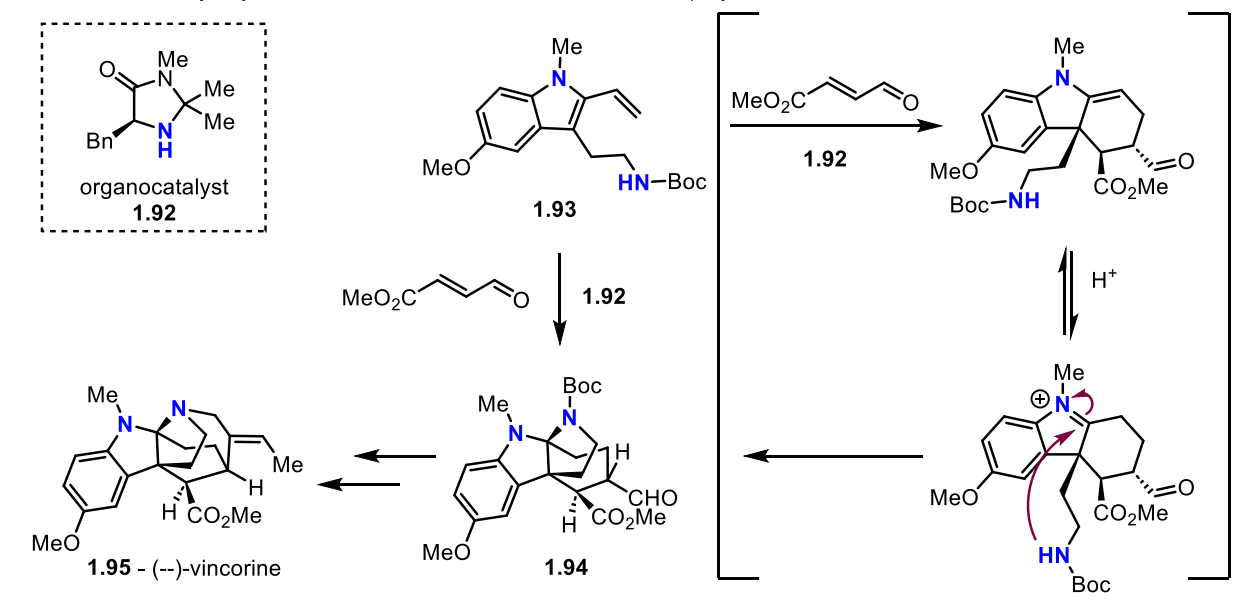
Five subsequent steps, namely *N*-alkylation of the pyrroloindoline, a 6-*exo*-dig radical cyclization, and three redox and protecting group adjustments, produced enantiopure (+)-minfiensine (**1.91**) in nine steps with an impressive 21% overall yield.

In a very similar synthetic pathway by the same research group a few years later, likely inspired by the minfiensine project, (–)-vincorine was also produced in nine steps.<sup>30</sup> Vincorine possesses a very similar pyrroloindoline moiety to minfiensine with the same bridged six-membered ring accessible through a Diels-Alder with 2-vinylindole as a diene. Aiming to obtain

the opposite bridged ring stereochemistry as their previous target, organocatalyst **1.92** was employed for the transformation.

From the same commercially available starting material used in the minfiensine synthesis, precursor **1.93** was produced in two steps. After undergoing the same diastereoselective asymmetric Diels-Alder as the previous work, acid-catalyzed isomerization of the newly formed indoline to its corresponding imine allowed the penultimate cyclization to take place (Scheme 1.23).

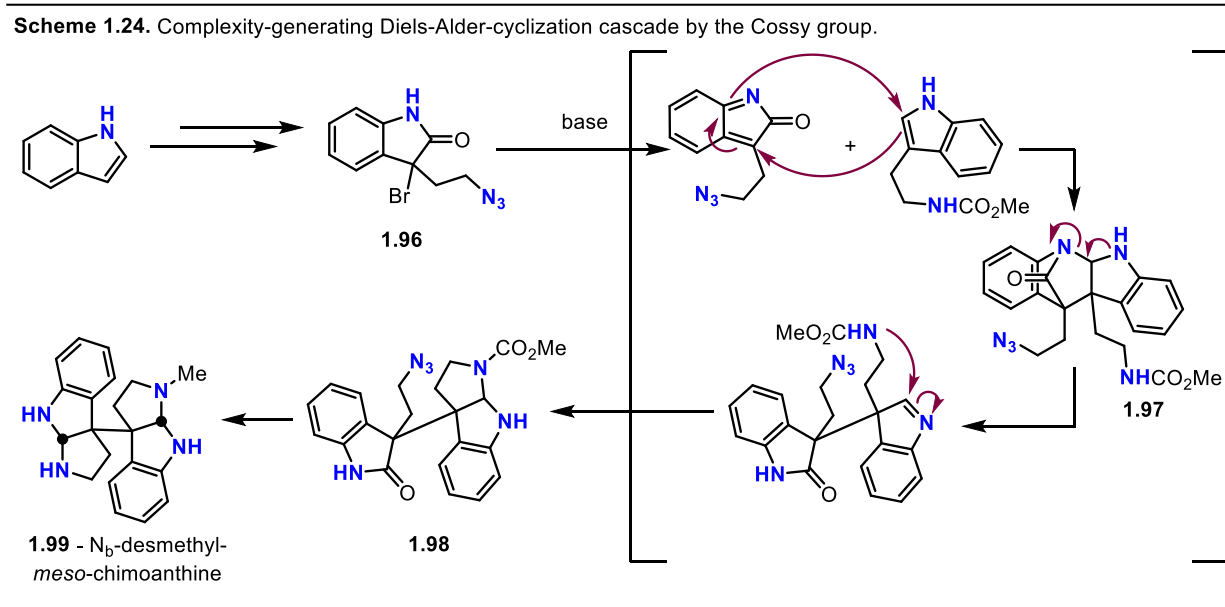
**Scheme 1.23.** Key asymmetric Diels-Alder in MacMillan's nine-step synthesis of vincorine.



Again, in an analogous series of structural edits to those of minfiensine, tetracyclic precursor **1.94** was alkylated at pyrroloindoline-N<sup>2</sup>, allowing the final bridged structure to be produced through a radical cyclization. Notably, this cyclization took place through an acyl telluride intermediate as a radical precursor. The final 7-*exo*-dig cyclization step proceeded smoothly in 51% yield where other, more common radical sources such as thiohydroxamic acid or an acyl selenide failed to produce isolable products. Thus, (-)-vincorine (**1.95**) was produced in nine steps with 9% overall yield.

## 1.4.2 Dearomatization of Indole

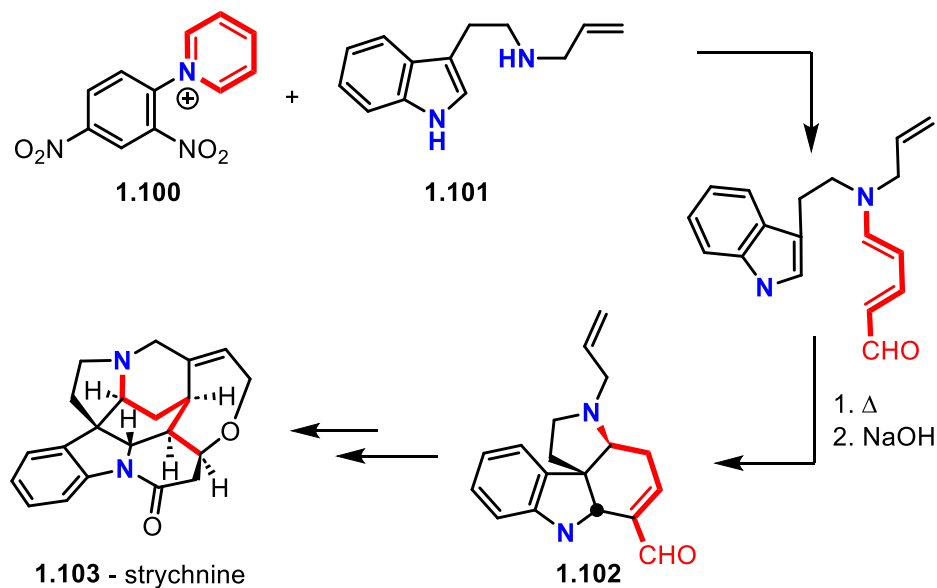
In their 2011 concise symmetric synthesis of  $N_b$ -desmethyl-*meso*-chimoanthine, Cossy and coworkers used indole derivatives for both diene and dienophile, although the diene fragment is not dearomatized within the cycloaddition.<sup>31</sup> In a five-step sequence, indole was functionalized to form diene precursor **1.96**, which was subjected to base *in situ* and underwent elimination to the desired reactant. This diene, sufficiently electron-deficient for the inverse-electronic-demand cycloaddition by means of its lactam functionality, was exposed to a 2-alkylamino indole, which underwent [4+2] cycloaddition to form a bridged pentacyclic intermediate **1.97** (Scheme 1.24).



After N – C bond cleavage to form two tethered bicycles, the weakly nucleophilic pendent carbamate cyclized to penultimate product **1.98**, which was then reduced and concomitantly cyclized in one pot to form **1.99**, racemic  $N_b$ -desmethyl-*meso*-chimoanthine. This sequence consisted of a brief seven steps that furnished the desired product in 22% overall yield.

The other example of an indole dearomatization that was maintained in the final target is the synthesis of strychnine by the Vanderwal group in 2011.<sup>32</sup> As their publication title boasts, the longest linear sequence in this total synthesis is only six steps and remains the shortest synthesis of strychnine to date. The convergent second step of two facile starting material syntheses from commercially available precursors involves formation of the Zincke aldehyde of pyridinium **1.100** with secondary amine **1.101** to directly form an intramolecular Diels-Alder precursor. This tethered diene and dienophile undergo a slightly inverse-demand cycloaddition under 80 °C heat between the relatively electron-rich indole and a dienal. The cycloadduct, furnished in 64% yield and total *endo* diastereoselectivity, was then subjected to base *in situ* and isomerized to conjugated enal **1.102**.

**Scheme 1.25.** Vanderwal's strychnine synthesis with a Zincke aldehyde precursor.



Tetracyclic **1.102** was subjected to a series of stereoselective bond-forming reactions and a Brook rearrangement to furnish the Wieland-Gumlich aldehyde, which is known in the literature to be converted to strychnine (**1.103**) in a single step. The Vanderwal group's use of the Diels-Alder from a Zincke aldehyde was pivotal in stereoselectively forming the central

framework of strychnine early in their sequence. Highlighted are the carbon centers originating from pyridinium salt **1.100**, showcasing their contribution to the core framework and the strategic disconnection that retrosynthetically provided an aromatic ring (Scheme 1.25).

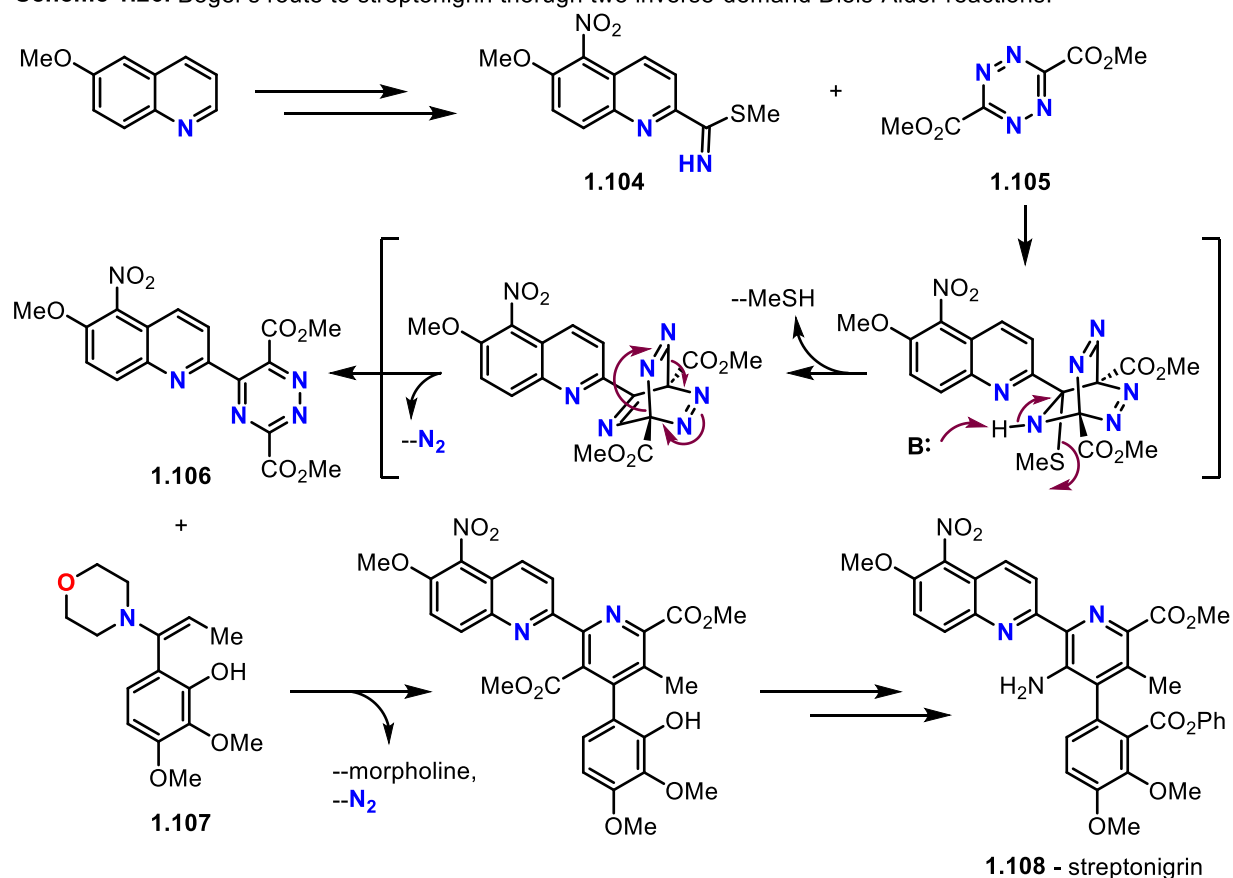
## 1.5 Inverse Demand [4+2]

### Cycloadditions

Three publications showcasing examples of inverse-electronic-demand Diels-Alder reactions will be discussed, all of which are invoked by Boger and coworkers over several decades' time. This group heavily favors inverse-demand [4+2] cycloadditions for the facile construction of aromatic polycyclic structures. All three total synthetic targets employ intermolecular Diels-Alder reactions, many with a formal loss of nitrogen gas and an elimination product from tri- or tetrazines.

The Boger group's first employment of inverse-demand Diels-Alder reactions utilized two consecutive cycloadditions in their concise route to streptonigrin in 1983, an achiral natural product that finds use as an antibiotic and antitumor agent. Their tetrazine diester starting material acts as an electron-poor diene that undergoes loss of nitrogen gas in each iteration of the [4+2], in the end only conserving its two carbons in the final structure (Scheme 1.26).<sup>33</sup>

**Scheme 1.26.** Boger's route to streptonigrin through two inverse-demand Diels-Alder reactions.

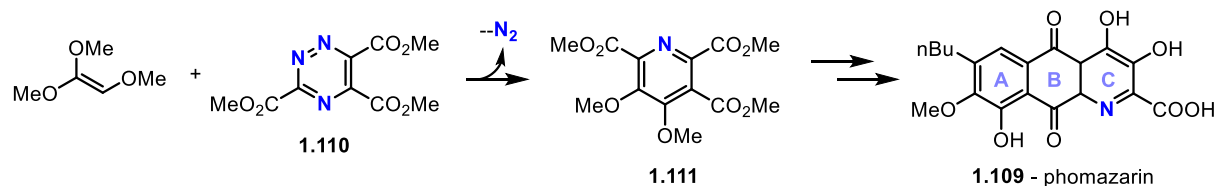


Despite this, imine dienophile **1.104** was readily synthesized from a commercially available methoxyquinoline, functionalizing it with a methyl thioester at the same carbon as the aromatic group. This fragment was subjected to the first inverse-demand [4+2] with tetrazine **1.105** to yield a bridged cycloadduct. This product underwent sequential elimination of methanethiol and then nitrogen gas and aromatized to triazine dienophile **1.106**. Still functionalized with electron-withdrawing esters, this structure underwent a second inverse-demand Diels-Alder with dienophile **1.107**, which was prepared from existing literature. Following an elimination of morpholine and  $\text{N}_2$  like the same transformation from the previous cycloaddition, the six-membered resultant heterocycle was aromatized to the central pyridine ring of streptonigrin. Following a sequence of minor functional group adjustments, streptonigrin

(**1.108**) was produced over ten steps. This was the first example of an inverse-demand Diels-Alder that underwent an elimination followed by extrusion of nitrogen gas to form an aromatic ring, a strategy heavily employed by the Boger group throughout this section.

Sixteen years after this initial use, a similar transformation was used toward the pyridyl C ring of phomazarin (**1.109**, Scheme 1.27).<sup>34</sup> Also an early transformation, the direct establishment of functionalization handles on this motif set the foundation for the further construction of the tricyclic structure. From 1,1,2-trimethoxyethene and triazine **1.110**, Diels-Alder followed by elimination of methanol and nitrogen gas yielded pyridine **1.111**.

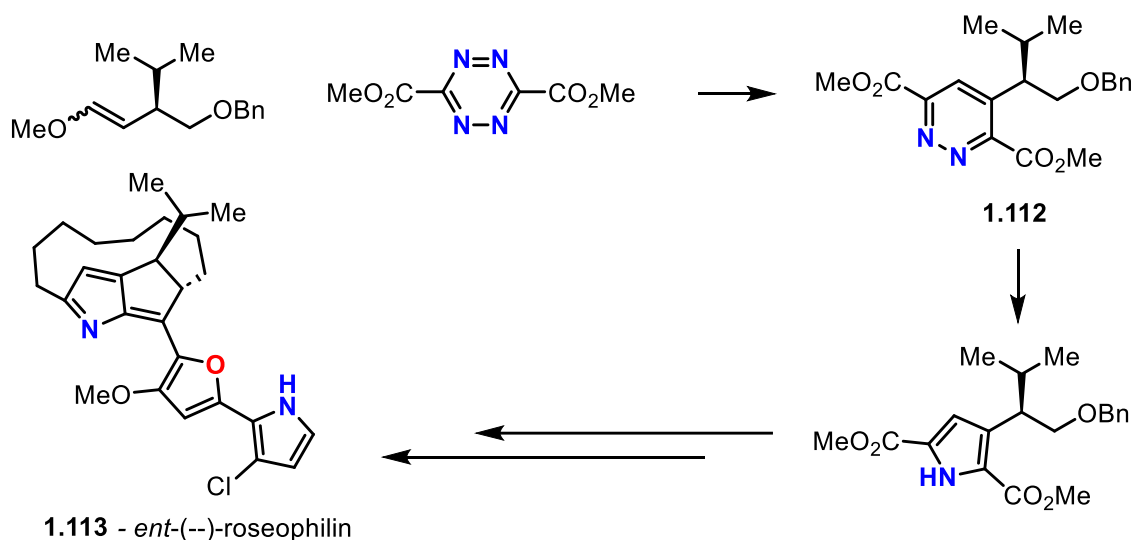
**Scheme 1.27.** Boger's early use of an inverse-demand Diels-Alder for the synthesis of phomazarin.



Through tethering a second functionalized phenyl ring to the two adjacent ester positions, the B ring was also able to be oxidized to the requisite quinone. The early establishment of the pyridyl C ring was pivotal to the following steps, which produced phomazarin in 23 steps.

A third example of a transformation in this family of cycloadditions is the Boger group's synthesis of *ent*-(--)-roseophilin. This synthesis took advantage of the same aromatization via elimination-nitrogen gas expulsion, with a subsequent ring contraction step to form the pyrrole instead of the pyridine or other *N*-heteroarene. A chiral methoxy dienophile was reacted with a similar diester tetrazine to that of the first example to provide diazine **1.112**. This intermediate underwent zinc-catalyzed ring contraction to the pyrrole, which was further functionalized with two other five-membered aromatic heterocycles and cyclized with a pendent alkyl group to produce *ent*-(--)-roseophilin (**1.113**).<sup>35</sup>

**Scheme 1.28.** Total synthesis of *ent*-(--)-roseophilin



## 1.5 Conclusions

The Diels-Alder [4+2] cycloaddition is one of, if not the most impactful transformations known to synthetic chemists, especially within total synthesis. It has been heavily employed to form *N*-heterocyclic structures, which are a defining attribute of alkaloids. As nitrogen constitutes the backbone of many amino acid sequences and therefore the primary structure of proteins, bodily metabolites and complex targets produced within biological organisms often contain nitrogen. The incorporation of nitrogen atoms into both dienes and dienophiles has allowed for great strides forward in the utility of the Diels-Alder in azacycle construction.

Intramolecular, intermolecular, dearomative, and inverse demand examples are well established tools in the utilization of [4+2] cycloadditions in total synthesis. Whether *N*-heterocycles are secondarily formed from a carbocyclic cycloaddition of this nature or directly by the condensation of one or more nitrogen-containing fragments, the use of the Diels-Alder reaction in total synthesis, especially for forming the *N*-heterocyclic structure of alkaloids, cannot be disputed.

# 1.6 References

- (1) Nicolaou, K. C.; Snyder, S. A.; Montagnon, T.; Vassilikogiannakis, G. The Diels-Alder Reaction in Total Synthesis. *Angew Chem Int Ed* **2002**, *41* (10) 1668–1698.
- (2) Houk, K. N.; Strozier, R. W. On Lewis Acid Catalysis of Diels-Alder Reactions. *J Am Chem Soc* **1973**, *95* (12), 4094–4096.
- (3) Ahrendt, K. A.; Borths, C. J.; MacMillan, D. W. C. New Strategies for Organic Catalysis: The First Highly Enantioselective Organocatalytic Diels - Alder Reaction. *J Am Chem Soc* **2000**, *122* (17), 4243–4244.
- (4) Oppolzer, W.; Robbiani, C. Highly Stereoselective Total Syntheses of (±)-Chelidonine and of (±)-Norchelidonine by an Intramolecular o-Quinodimethane/Nitrostyrene-Cycloaddition. *Helv Chim Acta* **1983**, *66* (4), 1119–1128.
- (5) Carroll, W. A.; Grieco, P. A. Biomimetic Total Synthesis of Pseudotabersonine: A Novel Oxindole-Based Approach to Construction of Aspidosperma Alkaloids. *J Am Chem Soc* **1993**, *115* (3), 1164–1165.
- (6) Rawal, V. H.; Iwasa, S. A Short, Stereocontrolled Synthesis of Strychnine. *J Org Chem* **1994**, *59* (10), 2685–2686.
- (7) Woodward, R. B.; Cava, M. P.; Ollis, W. D.; Hunger, A.; Daeniker, H. U.; Schenker, K. The Total Synthesis of Strychnine. *J Am Chem Soc* **1954**, *76* (18), 4749–4751.
- (8) Abe, H.; Aoyagi, S.; Kibayashi, C. First Total Synthesis of the Marine Alkaloids (±)-Fasicularin and (±)-Lepadiformine Based on Stereocontrolled Intramolecular Acylnitroso-Diels- Alder Reaction. *J Am Chem Soc* **2000**, *122* (19), 4583–4592.
- (9) Naruse, M.; Aoyagi, S.; Kibayashi, C.; Corcoran, R. C.; Thiam, M.; Slassi, A.; Chastrette, F. Total Synthesis of the Marine Alkaloid (-)-Lepadin B. *Org Lett* **2000**, *2* (19), 2955–2958.
- (10) Maloney, K. M.; Danheiser, R. L. Total Synthesis of Quinolizidine Alkaloid (-)-217A. Application of Iminoacetonitrile Cycloadditions in Organic Synthesis. *Org Lett* **2005**, *7* (14), 3115–3118.
- (11) Boger, D. L.; Ichikawa, S.; Jiang, H. Total Synthesis of the Rubrolone Aglycon. *J Am Chem Soc* **2000**, *122* (49), 12169–12173.
- (12) Wolkenberg, S. E.; Boger, D. L. Total Synthesis of Anhydrolycorinone Utilizing Sequential Intramolecular Diels-Alder Reactions of a 1,3,4-Oxadiazole. *J Org Chem* **2002**, *67* (21), 7361–7364.
- (13) Miller, K. A.; Tsukamoto, S.; Williams, R. M. Asymmetric Total Syntheses of (+)- and (-)-Versicolamide B and Biosynthetic Implications. *Nat Chem* **2009**, *1* (1), 63.

- (14) Osano, M.; Jhaveri, D. P.; Wipf, P. Formation of 6-Azaindoles by Intramolecular Diels-Alder Reaction of Oxazoles and Total Synthesis of Marinoquinoline A. *Org Lett* **2020**, *22* (6), 2215–2219.
- (15) Jouanno, L. A.; Chevalier, A.; Sekkat, N.; Perzo, N.; Castel, H.; Romieu, A.; Lange, N.; Sabot, C.; Renard, P. Y. Kondrat'eva Ligation: Diels-Alder-Based Irreversible Reaction for Bioconjugation. *J Org Chem* **2014**, *79* (21), 10353–10366.
- (16) Maeng, J. H.; Funk, R. L. Total Synthesis of (±)-Fasicularin via a 2-Amidoacrolein Cycloaddition. *Org Lett* **2002**, *4* (3), 331–333.
- (17) Kozmin, S. A.; Iwama, T.; Huang, Y.; Rawal, V. H. An Efficient Approach to Aspidosperma Alkaloids via [4 + 2] Cycloadditions of Aminosiloxydienes: Stereocontrolled Total Synthesis of (±)-Tabersonine. Gram-Scale Catalytic Asymmetric Syntheses of (+)-Tabersonine and (+)-16-Methoxytabersonine. Asymmetric Syntheses of (+)-Aspidospermidine and (-)-Quebrachamine. *J Am Chem Soc* **2002**, *124* (17), 4628–4641.
- (18) Harada, M.; Asaba, K. N.; Iwai, M.; Kogure, N.; Kitajima, M.; Takayama, H. Asymmetric Total Synthesis of an Iboga-Type Indole Alkaloid, Voacangalactone, Newly Isolated from Voacanga Africana. *Org Lett* **2012**, *14* (22), 5800–5803.
- (19) Wang, N.; Du, S.; Li, D.; Jiang, X. Divergent Asymmetric Total Synthesis of (+)-Vincadifformine, (-)-Quebrachamine, (+)-Aspidospermidine, (-)-Aspidospermine, (-)-Pyrifolidine, and Related Natural Products. *Org Lett* **2017**, *19* (12), 3167–3170.
- (20) Arnold, M. A.; Day, K. A.; Duró, S. G.; Gin, D. Y. Total Synthesis of (+)-Batzelladine A and (-)-Batzelladine D via [4 + 2]-Annulation of Vinyl Carbodiimides with N-Alkyl Imines. *J Am Chem Soc* **2006**, *128* (40), 13255–13260.
- (21) Powell, D. A.; Batey, R. A. Total Synthesis of the Alkaloids Martinelline and Martinellic Acid via a Hetero Diels-Alder Multicomponent Coupling Reaction. *Org Lett* **2002**, *4* (17), 2913–2916.
- (22) Batey, R. A.; Powell, D. A.; Acton, A.; Lough, A. J. Dysprosium(III) Catalyzed Formation of Hexahydrofuro[3,2-c]Quinolines via 2:1 Coupling of Dihydrofuran with Substituted Anilines. *Tetrahedron Lett* **2001**, *42* (45), 7935–7939.
- (23) Yadav, J. S.; Reddy, B. V. S.; Sadasiv, K.; Reddy, P. S. R. Montmorillonite Clay-Catalyzed [4+2] Cycloaddition Reactions: A Facile Synthesis of Pyrano- and Furanoquinolines. *Tetrahedron Lett* **2002**, *43* (21), 3853–3856.
- (24) Zhang, H.; Li, C. J. InCl<sub>3</sub>-Catalyzed Domino Reaction of Aromatic Amines with Cyclic Enol Ethers in Water: A Highly Efficient Synthesis of New 1,2,3,4-Tetrahydroquinoline Derivatives. *J Org Chem* **2002**, *67* (11), 3969–3971.
- (25) Robins, J. G.; Kim, K. J.; Chinn, A. J.; Woo, J. S.; Scheerer, J. R. Intermolecular Diels-Alder Cycloaddition for the Construction of Bicyclo[2.2.2]Diazaoctane Structures: Formal Synthesis of Brevianamide B and Premalbrancheamide. *J Org Chem* **2016**, *81* (6), 2293–2301.

- (26) Williams, R. M.; Kwast, E. Carbanion-Mediated Oxidative Deprotection of Non-Enolizable Benzylated Amides. *Tetrahedron Lett* **1989**, *30* (4), 451–454.
- (27) Gioia, C.; Hauville, A.; Bernardi, L.; Fini, F.; Ricci, A. Organocatalytic Asymmetric Diels-Alder Reactions of 3-Vinylindoles. *Angew Chem Int Ed* **2008**, *47* (48), 9236–9239.
- (28) Shimizu, S.; Ohori, K.; Arai, T.; Sasai, H.; Shibasaki, M. A Catalytic Asymmetric Synthesis of Tubifolidine. *J Org Chem* **1998**, *63* (21), 7547–7551.
- (29) Jones, S. B.; Simmons, B.; Macmillan, D. W. C. Nine-Step Enantioselective Total Synthesis of (+)-Minfiensine Enantioselective Catalytic Cascade Sequence to Core. *J Am Chem Soc* **2009**, *131*, 13606–13607.
- (30) Horning, B. D.; MacMillan, D. W. C. Nine-Step Enantioselective Total Synthesis of (-)-Vincorine. *J Am Chem Soc* **2013**, *135* (17), 6442–6445.
- (31) Menozzi, C.; Dalko, P. I.; Cossy, J. Concise Synthesis of the (+/-)-Nb-Desmethyl-Meso-Chimonanthine. *Chem Commun* **2006**, 4638–4640.
- (32) Martin, D. B. C.; Vanderwal, C. D. A Synthesis of Strychnine by a Longest Linear Sequence of Six Steps. *Chem Sci* **2011**, *2*, 649–651.
- (33) Boger, D. L.; Panek, J. S. Formal Total Synthesis of Streptonigrin. *J Org Chem* **1983**, *48* (4), 621–623.
- (34) Boger, D. L.; Hong, J.; Hikota, M.; Ishida, M. Total Synthesis of Phomazarin. *J Am Chem Soc* **1999**, *121* (11), 2471–2477.
- (35) Nakatani, S.; Kiriara, M.; Yamada, K.; Terashima, S. T.; Lett ; Kim, S. H.; Fuchs, P. L.; Fürstner, A.; Weintritt, H. J.; Kim, S. H.; Figuerosa, I.; Weintritt, H.; Luker, T.; Koot, W.-J.; Hiemstra, H.; Speckamp, W. N.; Mochizuki, T.; Itoh, E.; Shibata, N.; Katoh, T.; Terashima, S.; Gastner, T.; Robertson, J.; Hatley, R. J. D.; Harrington, P. E.; Tius, M. A.; Fagan, M. A.; Knight, D. W.; Bamford, S. J.; Doherty, G. A.; Watkin, D. J.; Nakamura, A.; Nagai, K.; Ando, K.; Tamura, G. J.; Antibiot ; Han, S. B.; Kim, H. M.; Kim, Y. H.; Lee, C. W. Asymmetric Total Synthesis of Ent(-)-Roseophilin: Assignment of Absolute Configuration. *J Am Chem Soc* **2001**, *123* (35), 8515–8519.

# CHAPTER TWO: Lewis Acid-Promoted Diels-Alder Reactions With Vinylazaarene Dienophiles

## 2.1 Introduction

As rigorously established in Chapter 1, the Diels-Alder reaction is fundamental to the synthesis of complex molecules and is frequently employed therein. Its predictable regio- and diastereoselectivity and perfect atom economy in the construction of complex frameworks renders it ubiquitous in every branch of synthetic chemistry.<sup>1,2</sup> From its simple foundation in 1928, its scope of viable dienes and dienophiles has been highly diversified and engineered for compatibility with various catalysts.<sup>3</sup>

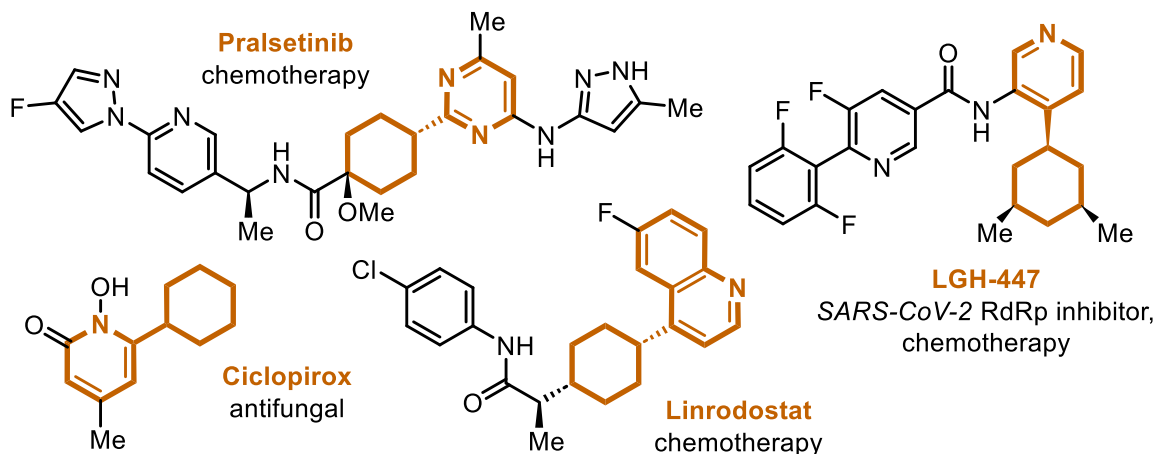
The biological importance of N-heterocycles has also been thoroughly stressed, and methods to form and functionalize these quintessential rings are highly valued in chemical synthesis. The Diels-Alder [4+2] has already emerged as a powerful means for their construction, but we identified a gap in the literature for dienophiles prefunctionalized with aromatic *N*-heterocycles. Owing to the weak electron-withdrawing effects of an aromatic ring, styrenes and their derivatives remain well-established as dienophiles.<sup>4,5</sup> We hypothesized that this utility could be extended to vinylazaarenes.

### 2.1.1 Relevance of cyclohexyl-functionalized azaarenes

Pyridine rings constitute the second-most common ring structure in FDA-approved drugs, cyclohexyl rings the fifth.<sup>6</sup> Biorelevant structures containing both moieties bonded to one another

are common across a wide variety of drug types and are therefore highly applicable to drug discovery. Notable among these examples is LGH-447, which has been demonstrated to have anticarcinogenic properties across various cancers but has recently found use as a treatment for COVID-19 as well.<sup>7,8</sup>

**Figure 2.1.** *N*-heteroarenes functionalized with cyclohexyl groups.



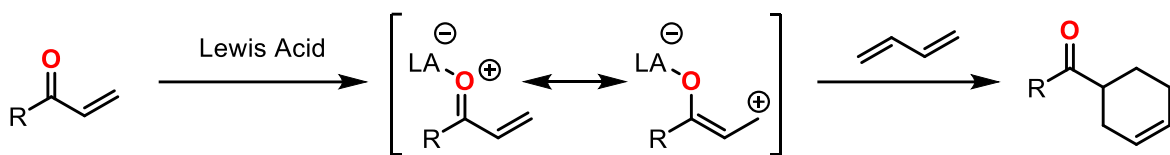
Current synthetic approaches to these compounds commonly include coupling reactions that require prefunctionalizations on one or both starting materials, as well as expensive transition metal catalysts and bespoke ligands. We envisioned an easier, more step-efficient route to these structures might come from viewing the cyclohexyl rings as Diels-Alder retrans. This alternative approach would widely expand accessibility to these structures as well as facilitate rapid, modular access to diverse medicinal analogs.

## 2.1.2 $\alpha,\beta$ -unsaturated carbonyls as dienophiles

Representing the most common method of dienophile activation is that of  $\alpha,\beta$ -unsaturated carbonyls. Owing to two Lewis basic lone pairs on the oxygen atom in conjugation with an olefin, complexation of a Lewis acid places a formal positive charge on the oxygen. This in turn favors a resonance structure in which a positive charge exists on a dienophilic carbon, lowering the LUMO

of the dienophile and accelerating the rate of reaction, as well as the regio- and diastereoselectivity (Figure 2.1).

**Scheme 2.1.** Lewis acid activation of  $\alpha,\beta$ -unsaturated carbonyl dienophiles.

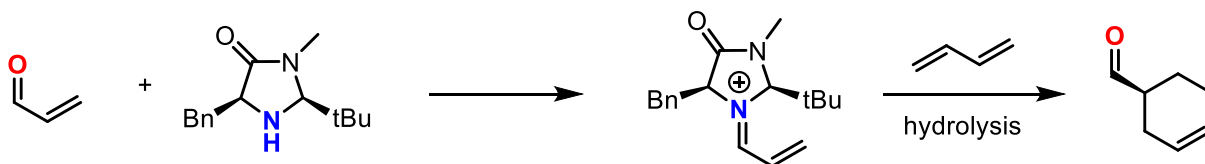


Myriad Lewis acids have been identified since the advent of this catalysis and used in synthetic methods and total synthesis.<sup>9,10</sup> This approach can affect enantioselectivity as well, opening the Diels-Alder reaction up to asymmetric variants.<sup>11</sup>

### 2.1.3 *In situ* formation of $\alpha,\beta$ -unsaturated iminium dienophiles

Amine catalysis of the Diels-Alder was quickly brought to prominence by MacMillan and coworkers for their chiral organocatalysts.<sup>11,12</sup> These pyrrolidine-derived structures readily condense with  $\alpha,\beta$ -unsaturated carbonyls to form  $\alpha,\beta$ -unsaturated iminium ions, which activate the dienophile in a similar fashion to Lewis acids.

**Figure 2.2.** Route of dienophile activation by MacMillan's chiral amine catalysts.



Bulky functionalities installed asymmetrically on these catalysts favor diene attack on a single face of the dienophile, enantioenriching the product. While this groundbreaking work won MacMillan the Nobel prize in 2021, we took particular note of the active dienophile species as well. If dienophile activation was not limited to formation of a formal oxonium ion in conjugation

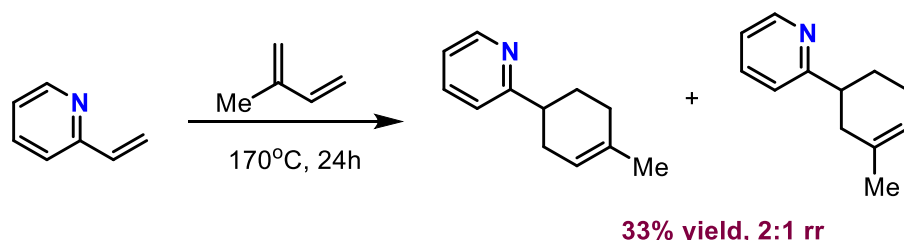
with the olefin, our theoretical foundation for catalysis of vinylpyridines and other vinylazaarenes was viable.

## 2.2 Overview of prior work on vinylazaarene dienophiles

### 2.2.1 Thermal cycloadditions

Existing literature on vinylpyridines as dienophiles was surprisingly stark. To our knowledge, very few thermal or Lewis acid-catalyzed examples existed of our desired transformation. Thermal entries demonstrated that vinylpyridines were in fact viable dienophiles that underwent Diels-Alder cycloaddition. Combining with unactivated dienes such as butadiene and isoprene at high temperatures, cycloadducts were produced, albeit in low yields and regioselectivity (Scheme 2.3).<sup>13,14</sup>

**Scheme 2.2.** Thermal Diels-Alder of 2-vinylpyridine and isoprene.

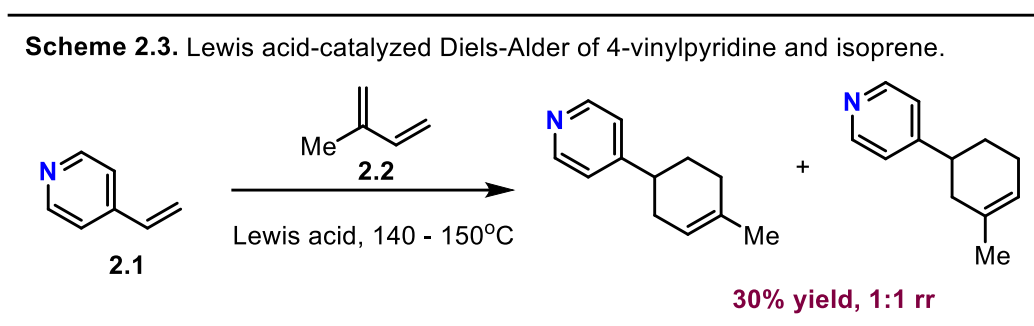


Under thermal conditions, this reaction is limited to the intrinsic HOMO-LUMO gap between a mildly electron-rich diene and a mildly electron-poor dienophile. Overcoming this significant kinetic barrier toward reaction required extensive heating for the observed poor yield and selectivity. In recreating this reaction, we observed the same 2:1 regioselectivity but were only able to isolate 9% expected product (Table 2.1, entries 1 and 2). Thus necessitated greater

reagent control of yield and selectivity, and investigation into the literature precedent of Lewis acid-catalyzed variants of this transformation.

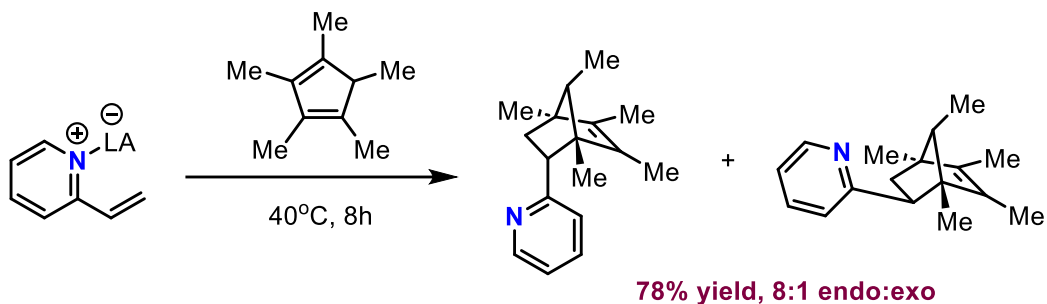
## 2.2.2 Lewis acid-catalyzed cycloadditions

We only identified a single dedicated example of dienophile activation via Lewis acid complexation to the pyridyl nitrogen atom. This cycloaddition between 4-vinylpyridine (**2.1**) and isoprene (**2.2**) was catalyzed by Ni(0) and Zr(IV) catalysts, resulting in poor yield and nonexistent regioselectivity (Scheme 2.4).<sup>15</sup> Requisite heating of the reaction vessel reached nearly the same temperature as the thermal cycloaddition, which in fact reported a higher yield than this example.



A more successful entry into our desired mode of catalysis was established as a side reaction in an unrelated study. Using  $\text{Zn}(\text{NO}_3)_2 \cdot 6\text{H}_2\text{O}$  as a Lewis acid to activate 2- and 4-vinylpyridine towards a different transformation, exposure to pentamethylcyclopentadiene and mild heat resulted in production of their cycloadduct (Scheme 2.5). Under these conditions, this adduct was formed in 78% yield and 8:1 diastereoselectivity, a noted improvement over the poor yields and selectivities that were observed in more dedicated studies despite constructive effects from a more reactive diene.

**Scheme 2.4.** Lewis acid-catalyzed Diels-Alder of 2-vinylpyridine and pentamethylcyclopentadiene.

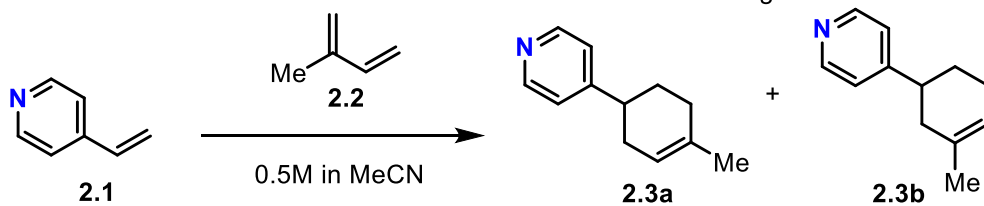


## 2.3 Optimization and controls

### 2.3.1 Initial investigation

Starting from the Zn(II) salt that saw success with a highly reactive diene, we attempted to extend the scope of this reactivity toward less electron-rich  $4\pi$  components. However, less reactive dienes such as dimethylbutadiene, isoprene, and cyclohexadiene failed to produce even trace cycloadduct. Increasing the molar loading of Lewis acid and the reaction temperature also failed to appreciably affect a desired outcome (Table 2.1).

**Table 2.1.** Initial azaarene Diels-Alder reaction condition screening.

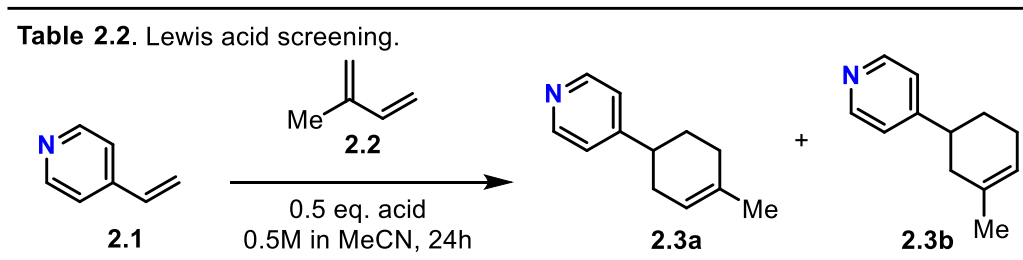


Entry	Temperature (oC)	Reaction time (h)	Lewis acid	GC yield (%)	2.3a : 2.3b
1	170	24	-	9	2:1
2	170	72	-	13	2:1
3	40	24	Zn(NO <sub>3</sub> ) <sub>2</sub> •6H <sub>2</sub> O	<1	-

4	82	24	Zn(NO <sub>3</sub> ) <sub>2</sub> •6H <sub>2</sub> O	<1	-
---	----	----	--	----	---

## 2.3.2 Lewis acid screening

It became clear that although Lewis acid catalysis was an effective way to improve yield and selectivity through greater polarization of the vinyl group, a different acid would be necessary to optimize the reaction. Sampling from simple and accessible acids, we focused our screening on boron- and aluminum-based catalysts as they are commonly employed for Diels-Alder reactions and can be functionalized with chiral auxiliaries. Two Brønsted acids with non-coordinating counterions were also screened but found to be less effective than Lewis acids. Overall yields were evaluated on a GC-FID instrument using dodecane as an internal standard.



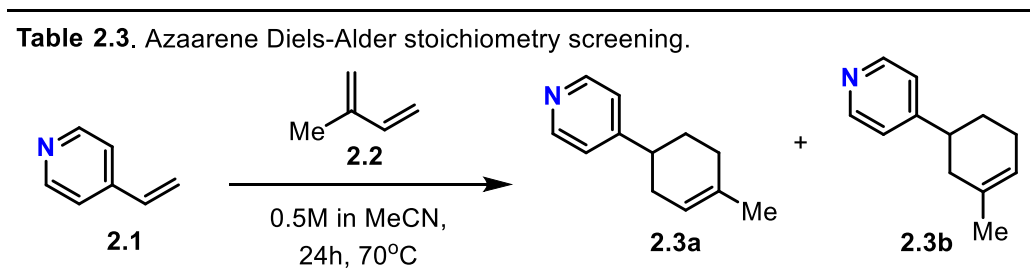
Entry	Lewis acid	GC Yield (%)	2.3a : 2.3b
1	Me <sub>3</sub> Al	3	4:1
2	BCl <sub>3</sub>	4	3:1
3	EtAlCl <sub>2</sub>	12	3:1
4	B(C <sub>6</sub> F <sub>5</sub> ) <sub>3</sub>	12	3:1
5	AlCl <sub>3</sub>	21	4:1
6	BF <sub>3</sub> ·MeCN	23	5:1
7	BF <sub>3</sub> ·OEt <sub>2</sub>	35	5:1
8	HBF <sub>4</sub>	15	4:1
9	TfOH	11	3:1

After thorough investigation, we found  $\text{BF}_3 \cdot \text{OEt}_2$  to be the most efficacious acid for the desired reaction, impacting both yield and regioselectivity the most. Notably, use of a Lewis acid improved regioselectivity over the thermal cycloaddition more than twofold (Table 2.1, entries 1 and 2; Table 2.2). In line with our expectations, this higher selectivity can be attributed to a more resonance-polarized dienophile.

This 35% yield result, although modest, was highly promising considering the model reaction. As isoprene's reactivity is only enhanced by the hyperconjugative effects of a methyl group and lacks resonance forms to greatly favor one regioisomers over another, we hypothesized that greater yields and selectivities could be observed with more electron-dense dienes. Additionally, we had already observed 2-vinylpyridine to be a more potent dienophile than its 4-vinyl isomer owing to greater resonance and inductive effects of Lewis acid complexation more proximal to the olefin.

### 2.3.3 Reaction condition screening

Upon establishment of our optimal Lewis acid, we continued toward reaction condition screening. Stoichiometry, solvent, reaction temperature, and reaction time were evaluated in succession toward a full set of optimized conditions.

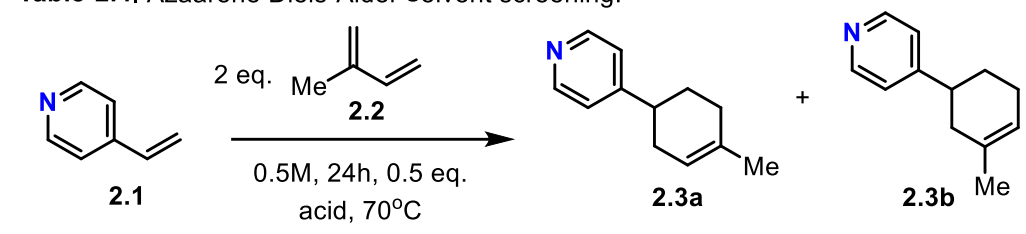


Entry	Equiv. Lewis acid	Equiv. 2.2	GC Yield (%)
1	0.5	3	37

2	0.5	2	35
3	0.5	1.5	22
4	0.5	1	18
5	0.4	2	12
6	1.0	2	25

Our first screening regarded optimum stoichiometric equivalents of the acid and diene. All regioselectivities in this screening remained at 5:1 **2.3a** : **2.3b**. While raising diene equivalents to 1.5 and then 2 substantially increased the yield, raising the excess further to 3 equivalents saw a plateau in efficacy. Carrying the screening forward with two equivalents of diene, we screened for optimum Lewis acid loading. While dropping the equivalents by just 10% loading showed a stark drop in yield, increasing them to one whole equivalent did as well. This was likely due to the stability of the BF<sub>3</sub>-bound complex of the cycloadduct, which is thermodynamically favorable to form as will be discussed in section 2.5.

**Table 2.4.** Azaarene Diels-Alder solvent screening.

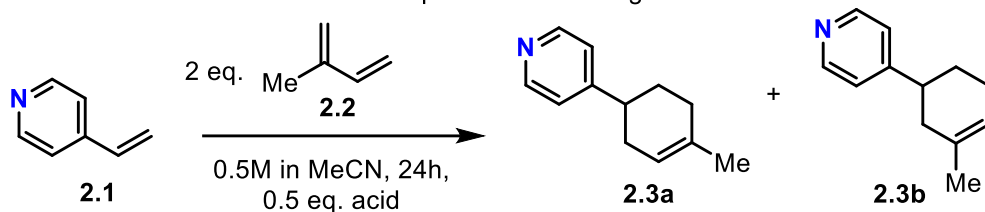


Entry	Solvent	GC Yield (%)	2.3a : 2.3b
1	MeCN	35	5:1
2	DMF	25	5:1
3	1:1 MeCN:DMF	32	4:1

While we evaluated the reaction in over a dozen solvents, only four particularly polar entries gave appreciable yield upon gas chromatography. Nonpolar, hydrocarbon solvents never

exceeded trace product yield, with DCM, chlorobenzene, and ethanol reaching single-digit results. The only solvent other than acetonitrile that facilitated production of the cycloadduct was DMF, suggesting necessity of a polar solvent to stabilize a more polar Lewis acid-base complex in the transition state. A 1:1 mixture of the two solvents provided a yield close to our optimum entry, but a decrease in regioselectivity.

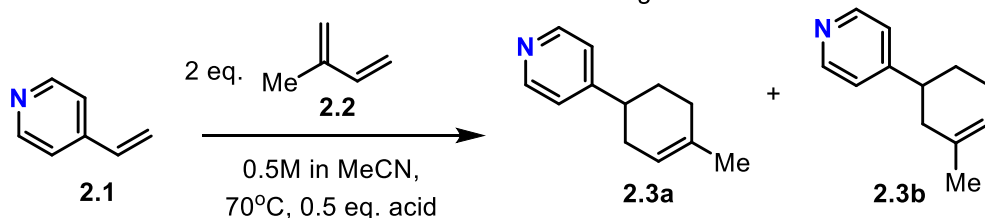
**Table 2.5.** Azaarene Diels-Alder temperature screening.



Entry	Temperature (°C)	GC Yield (%)	2.3a : 2.3b
1	50	3	6:1
2	60	16	5:1
3	70	35	5:1
4	80	18	5:1
5	100	16	5:1

Where temperature was concerned, there was a clear “sweet spot” at 70°C: warm enough to kinetically facilitate the reaction, but not so hot that side reactions or reactant degradation accelerated at the expense of the Diels-Alder. Higher temperatures did in fact tend to yield more separated products on the GC chromatogram where lower ones showed greater amounts of unreacted starting material.

**Table 2.6.** Azaarene Diels-Alder reaction time screening.



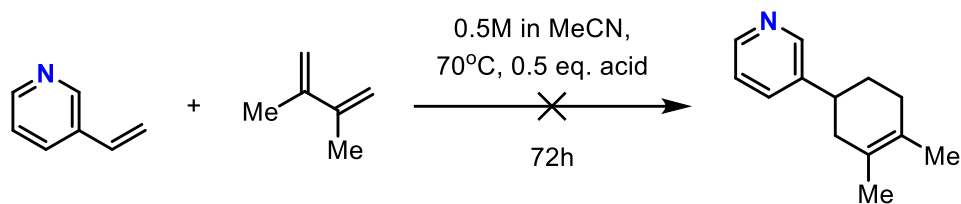
Entry	Time (h)	GC yield (%)	Isolated yield (%)
1	24	35	33
2	48	47	44
3	72	54	52

Finally, in evaluating reaction times after full optimization, we discovered that allowing the reaction to progress over 72 hours raised the yield of cycloadduct to 54% (Table 2.6, entry 3). While this measure was not necessary for all dienes, it opened the possibility that particularly unreactive diene-dienophile pairs such as the **2.1/2.2** combination could see very improved yields after a longer reaction time. Isolated yields of these reactions were also determined to verify accuracy of the GC yield metric.

### 2.3.4 Control reactions

As a mechanistic probe, 3-vinylpyridine was subjected to the optimum reaction conditions and a slightly more reactive diene, dimethylbutadiene. Under the same conditions that afforded 54% yield between 4-vinylpyridine and a less reactive diene, 3-vinylpyridine did not form the cycloadduct and instead resulted in complete recovery of starting materials. This supports the necessity of the Lewis acid to be in conjugation with the dienophilic alkene to facilitate the Diels-Alder. Simply the inductive effect of placing a formal positive charge on a slightly proximal nitrogen is not enough to promote the [4+2] (Scheme 2.7). Additionally, subjection of 4-vinylpyridine and isoprene to the reaction conditions without an acid present produces 0% yield as well.

**Scheme 2.5.** Azaarene Diels-Alder control reaction.



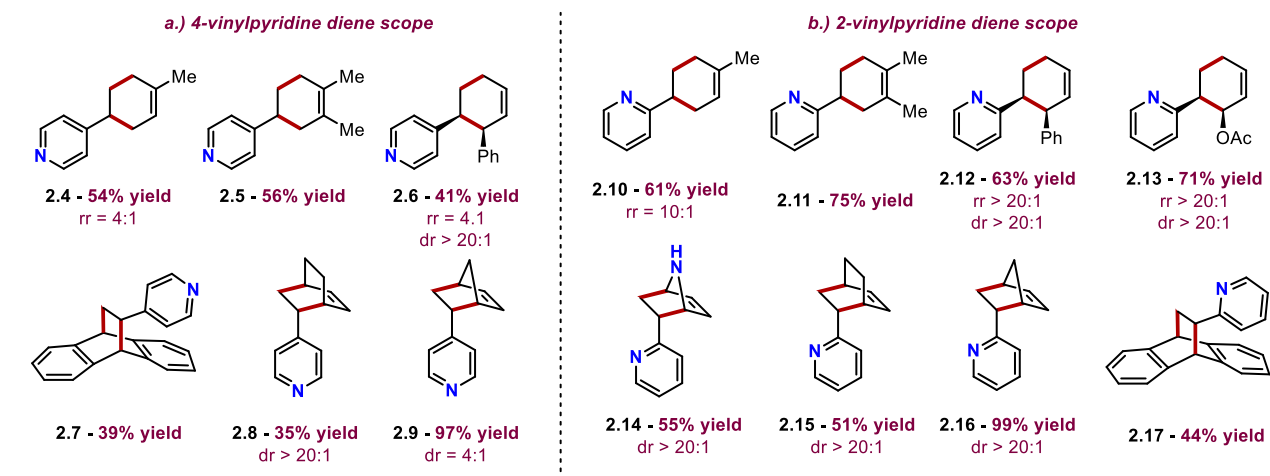
## 2.4 Scope

Optimized procedure in hand, we proceeded to establish a scope of both dienes and dienophiles within our reaction scheme. While optimum conditions were established on a low-yielding reactant pair, most scope entries readily met or exceeded the established yield in 24 hours. Selected dienes for the scope are commonly used in practical syntheses and provide the opportunity to showcase good to excellent diastereoselectivity, regioselectivity, or both.

All scope reactions were conducted on a 2 mmol scale for 24h unless otherwise noted. All yields are isolated and selectivities were determined through integration of  $^1\text{H}$  NMR spectra. Observed selectivities and yields are in keeping with expected trends based on steric and electronic properties of both dienes and dienophiles. For example, analogous cycloadditions of 4-vinylpyridine and 2-vinylpyridine with dimethylbutadiene (**2.5** and **2.11**, Figure 2.3) have a 20% difference in yield despite their only difference being the connectivity of the dienophile. Differences in reaction rate of dienes can be observed as well, illustrated by the nearly 15% yield disparity between cycloadditions of 2-vinylpyridine with isoprene (**2.10**) vs. dimethylbutadiene (**2.11**) with the simple addition of one methyl group. Cyclopentadiene adducts (**2.9** and **2.16**) demonstrated quantitative yield due to their electron richness and locked reactive conformation as planar conjugated dienes.

## 2.4.1 Diene scope2.9

Figure 2.3. Diene scope of the vinylazaarene Diels-Alder reaction.

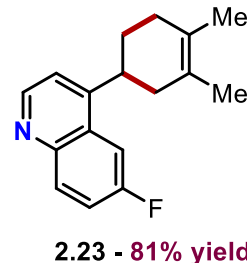
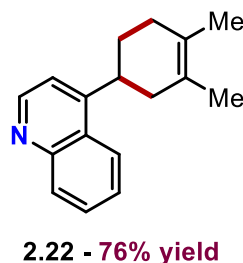
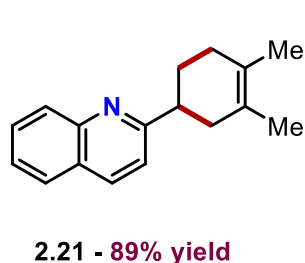
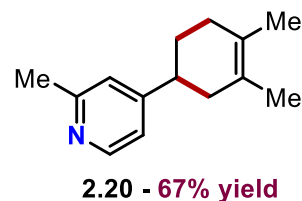
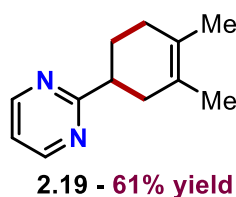
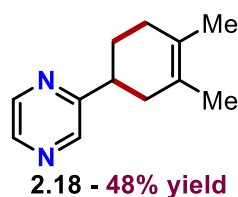


In the full collection of diene scope entries, we observe good to excellent diastereoselectivity, favoring the *endo* isomers more heavily than thermal counterparts due to increased polarization in the extended dienophile  $\pi$ -system. Regioselectivities also remain consistently high, more so than analogous thermal cycloadditions as can be seen in entries **2.4** and **2.10**. These reactions form up to three new stereocenters from achiral starting materials and constitute functional entries into cyclohexylazaarene moiety of various drugs and drug leads.

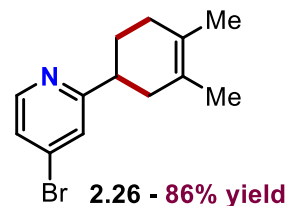
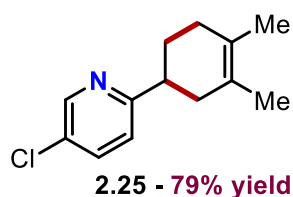
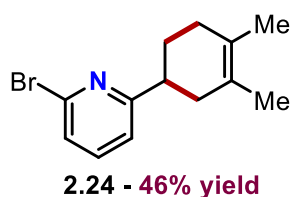
## 2.4.2 Dienophile scope

Figure 2.4. Dienophile scope of the vinylazaarene Diels-Alder reaction.

*monocyclic, bicyclic, and substituted vinylazaarenes*



*halogenated pyridines for further functionalization*



Upon evaluation of diene substrate tolerance, the scope was extended to include diverse vinylazaarenes as well. Diazines were well-tolerated, notably in the case of the pyrazine adduct (**2.18**, Figure 2.4) in which one nitrogen was out of conjugation with the dienophilic olefin. As expected, however, the vinylpyrimidine cycloadduct **2.19** with two Lewis basic sites in conjugation, was furnished in higher yield.

Quinolines were readily incorporated into the dienophile scope as well, even better tolerating activation at 2- and 4- vinyl substitutions than their pyridyl counterparts. Cyclohexyl azaarenes **2.19** and **2.23** can specifically be traced back to representative structures in Figure 2.1 –

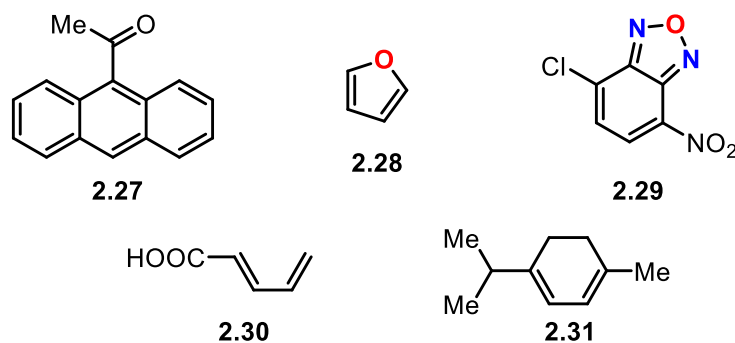
Pralsetinib and Linrodostat. The observed trends in yield are in line with expectation, as quinolines constitute more electron-withdrawing systems than pyridines.

Likewise, halogenation of the dienophile is also tolerated well. Fluorination of 4-vinylquinoline at C9 leads to a 5% increase in yield over its unfunctionalized counterpart, and chloro- and bromo- substituents are tolerated in good yields. Not only do entries **2.24** – **2.26** provide halogenated aryl frameworks for further skeletal diversification at the 2-, 3-, and 4-positions of the pyridine, but the 2-bromo substitution of **2.26** places a large, electronegative group proximal to the key Lewis basic lone pair. Although this functionalization results in a decrease in yield, the reaction still proceeds to form a synthetically useful amount of product.

### 2.4.3 Limitations to scope

While the vinylazaarene Diels-Alder demonstrated a robust scope in its optimized form, several limitations existed to its tolerance for both dienes and dienophiles. Electron-deficient and/or aromatic dienes such as **2.27**, **2.29**, and **2.30** failed to produce appreciable yield. Despite its high electron density, furan (**2.28**) also did not react (Figure 2.5). We postulate that this is likely due to the presence of a highly Lewis basic lone pair that competed with the azaarene nitrogen(s) for complexation with BF<sub>3</sub>. Not only would this lower the availability of catalyst in the reaction vessel, but it would lower the HOMO of furan through the same route that it lowers the dienophile LUMO. Despite electron-donating hyperconjugative effects from the methyl and isopropyl groups of  $\alpha$ -terpinene (**2.31**), steric bulk at the bond-forming carbons also destabilized the transition state enough to preclude its reaction.

**Figure 2.5.** Limitations to diene scope.

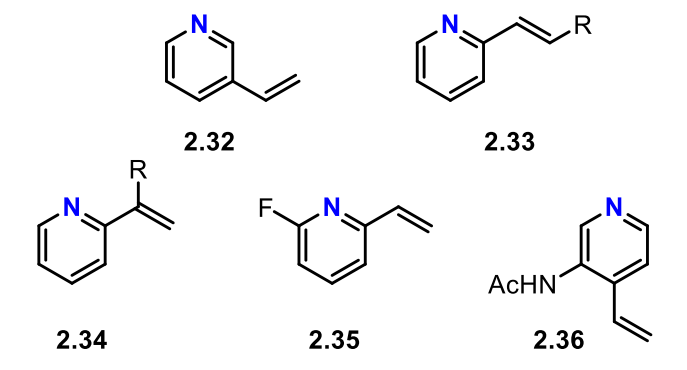


The range of dienophiles was, as previously mentioned, limited to vinyl groups in conjugation with the pyridyl nitrogen lone pair. Although 3-vinylpyridine (**2.32**) did not react in our optimized scheme, we found it to perform similarly to 2- and 4-vinylpyridine under uncatalyzed thermal conditions, providing further support for the efficacy of Lewis acid promotion (Figure 2.6). Substitution of the dienophilic olefin beyond a monosubstituted vinyl group was also not tolerated. 1,2- and 1,1-disubstitution (**2.33** and **2.34**) both failed to produce cycloadduct—this observation could be due to steric constraints of an additional group at a bond-forming carbon, or the enhanced stability of higher olefin substitutions leading to a higher activation energy barrier.

In a related observation to the diminished yield of 2-bromo-6-vinylpyridine (**2.24**, Figure 2.4) as a dienophile, 2-bromo-6-vinylpyridine (**2.35**) failed to react entirely. While fluorine possesses a much smaller atomic radius to bromine, its higher electronegativity diminished the Lewis basicity of its proximal nitrogen to the point where  $\text{BF}_3$ -coordination was insufficient to facilitate the reaction. This is supported by the visual observation of gas formation ( $\text{BF}_3 \cdot \text{H}_2\text{O}$ , water vapor) upon addition of Lewis acid to all successful dienophile entries in solution. No visible gas was formed upon addition of  $\text{BF}_3 \cdot \text{OEt}_2$  to **2.35** in solution. Much like the diene limitations, presence of a competing Lewis basic lone pair on the dienophile also precluded the reaction. Amide

**2.36** did not react, despite having a similar electron-donating effect to the successful methyl-substituted pyridine entry (**2.20**, Figure 4) based on Hammett parameter.<sup>16</sup>

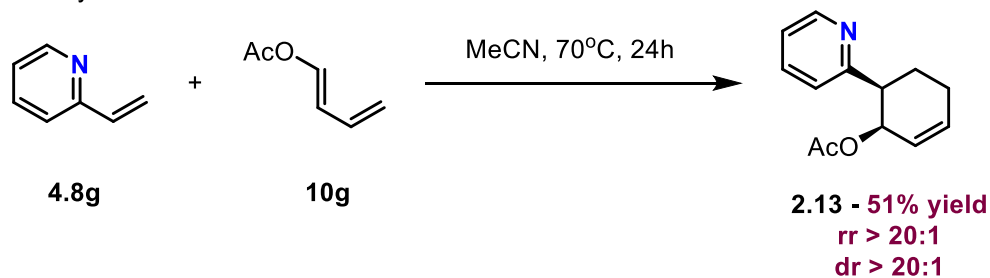
**Figure 2.6.** Limitations to dienophile scope.



## 2.4.4 Pharmaceutical relevance

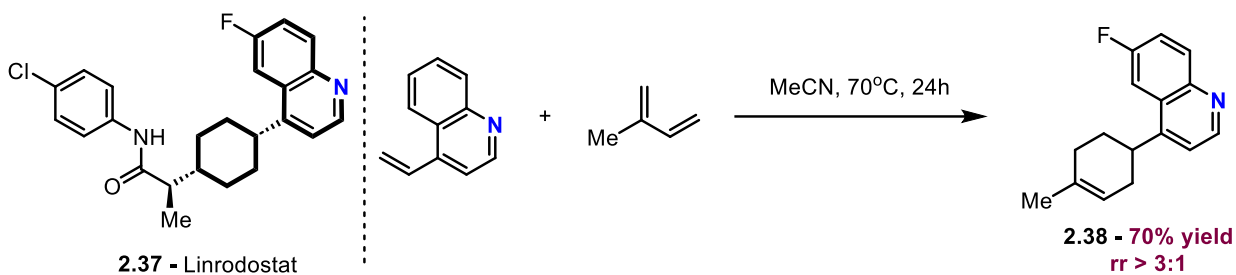
Beyond establishment of the scope, we also set out to demonstrate applicability to medicinal chemistry on a practical level. Without re-optimization, formation of cycloadduct **2.13** proceeded in 51% yield on the 10-gram scale with no adverse impact on the excellent diastereo- and regioselectivity (Scheme 2.8).

**Scheme 2.6.** Scale-up of the Diels-Alder between 2-vinylpyridine and 1-acetoxybutadiene



As shown in Figure 2.1, Linrodostat (**2.37**) is a chemotherapy lead in phase III trials for several cancers.<sup>17</sup> To demonstrate the utility of this Diels-Alder, we assembled fragment **2.38**, the 4-cyclohexylquinoline moiety of this small molecule, in a single step (Scheme 2.9).

**Scheme 2.7.** Concise synthesis of a Linrodostat fragment.

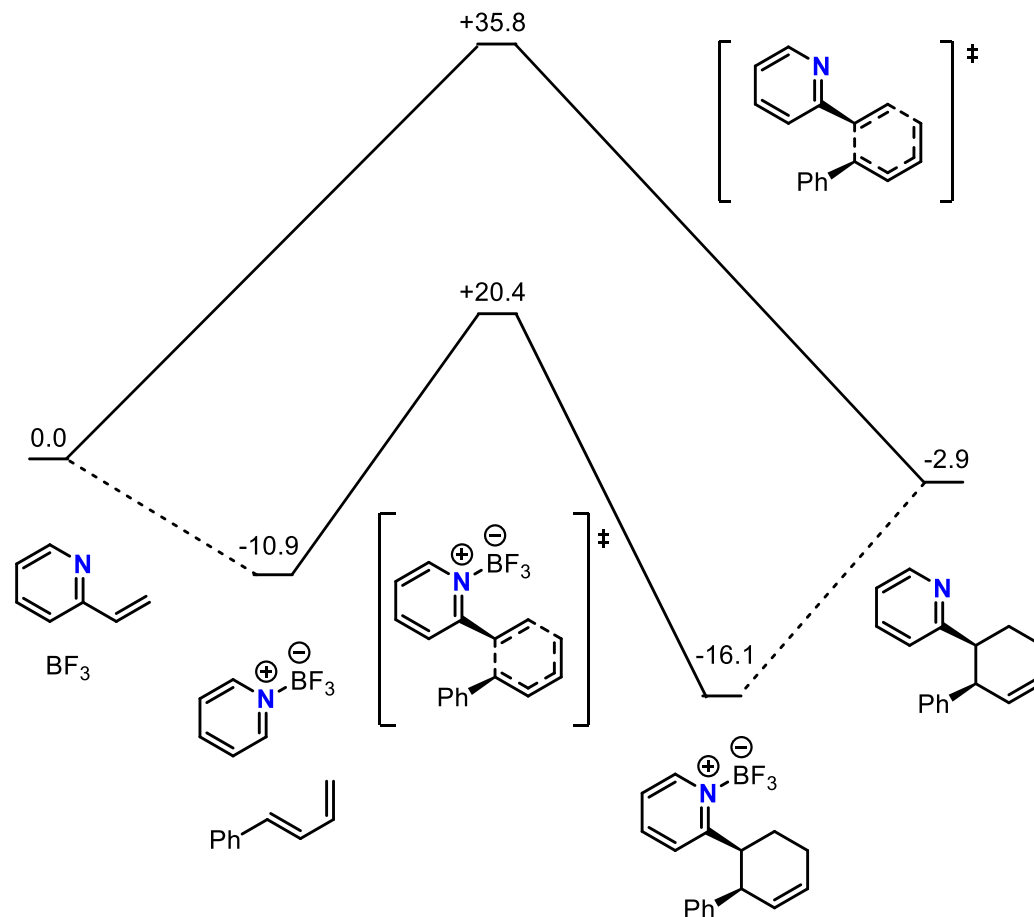


## 2.5 Mechanistic insight

To provide further support for our mechanistic postulations, DFT calculations were run on the cycloaddition between 2-vinylpyridine and *trans*-1-phenyl-1,3-butadiene, comparing the energetic profiles of  $\text{BF}_3$ -promoted and thermal pathways. Calculations were carried out using Gaussian 16, with the B3LYP functional and the 6-31+G(d) basis set levels of theory.

## 2.5.1 DFT stepwise energy level calculation

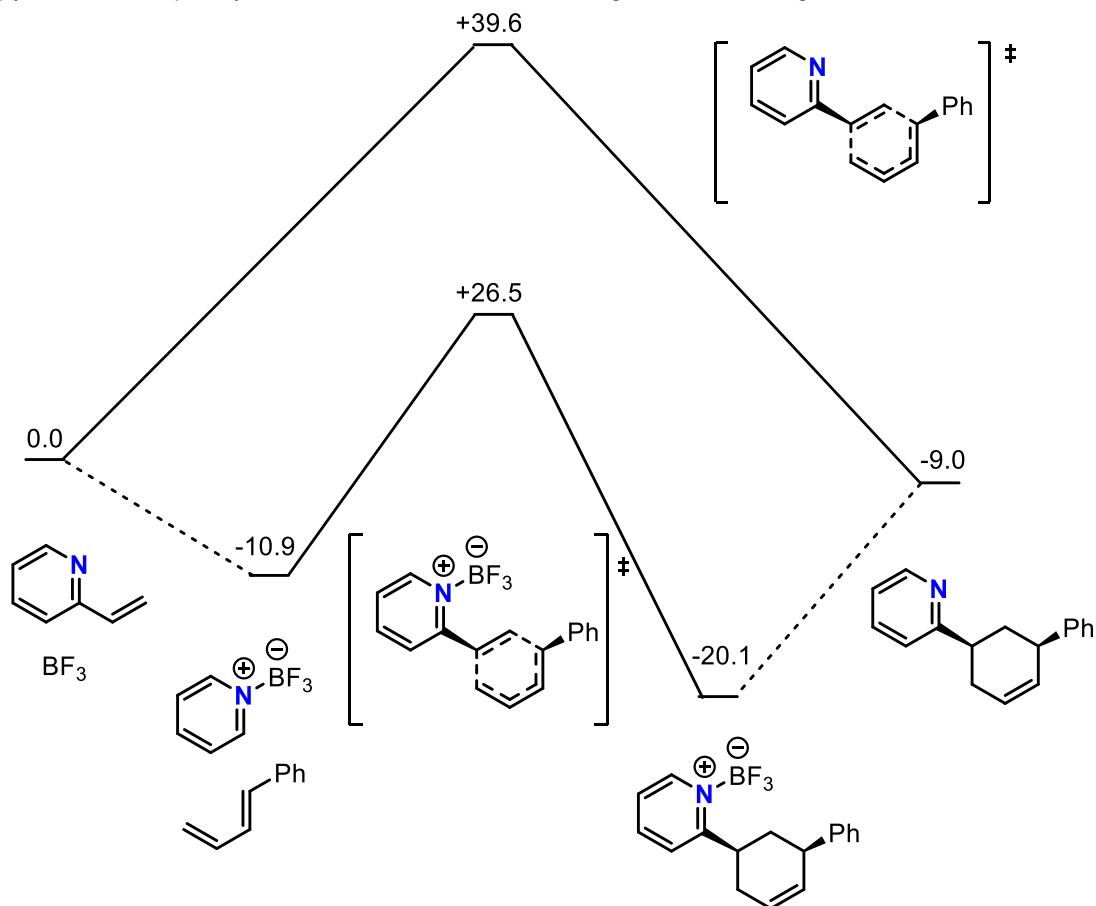
**Figure 2.7.** Free energy diagram of Lewis acid-promoted and thermal *endo* cycloadditions of 2-vinylpyridine and 1-phenylbutadiene to form the major regioisomer. Energies in kcal/mol.



In keeping with expectation, calculations supported a major disparity between the thermal and BF<sub>3</sub>-promoted product-forming transition states. The complexation of BF<sub>3</sub> with 2-vinylpyridine is thermodynamically favored and lowers the activation energy of the concerted cycloadditions from the thermal variants for both the major (Figure 2.7) and minor (Figure 2.8) regioisomers. The BF<sub>3</sub>-bound complexes of both major and minor cycloadducts are significantly thermodynamically favored. This observation provides insight into the optimum catalyst loading.

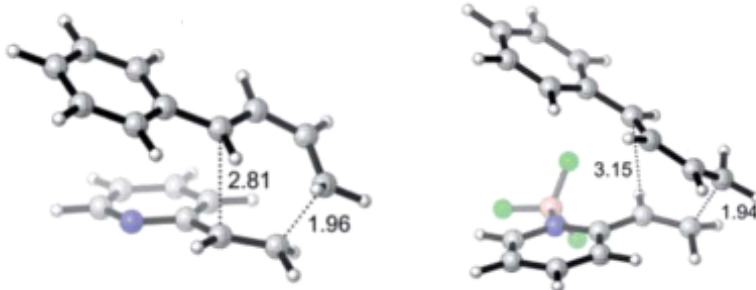
A steep decrease in isolated yield is observed at 0.4 molar equivalents of  $\text{BF}_3$  vs. 0.5 equivalents, which may be attributed to the thermodynamic sink of the cycloadduct- $\text{BF}_3$  complex.

**Figure 2.8.** Free energy diagram of Lewis acid-promoted and thermal *endo* cycloadditions of 2-vinylpyridine and 1-phenylbutadiene to form the minor regioisomer. Energies in kcal/mol.



## 2.5.2 DFT transition state geometry optimization

**Figure 2.9.** Comparison of thermal and Lewis acid-promoted transition states. Bond distances in anstroms.



In addition to energy calculations, transition state geometry for both thermal and Lewis acid-promoted reactions was optimized to provide insight into increased regioselectivity (Figure 2.9). While energy calculations showed a  $\Delta\Delta G^\ddagger$  between the thermal and  $\text{BF}_3$ -promoted transition state energies of 15.4 kcal/mol, optimized geometry showed a greater degree of geometrical asynchronicity to support this value. Thermally, the difference in bond distance between the two developing carbon-carbon bonds was 0.85 Å. Representing a small but significant difference in bond length disparity ( $\Delta\Delta_A$ ) of 0.36 Å, the more asynchronous  $\text{BF}_3$ -promoted transition state had a bond length difference of 1.21 Å.

## 2.6 Conclusions

Vinylazaarenes have been established as viable and synthetically useful dienophiles to undergo the Diels-Alder [4+2] with unactivated dienes. Lewis acid-promotion by 0.5 molar equivalents of  $\text{BF}_3\cdot\text{OEt}_2$  greatly diminishes the required reaction temperatures versus thermal cycloadditions, as well as consistently increasing the observed diastereoselectivity and regioselectivity of isolated products. Featuring a wide scope of dienes and various N-heteroarene dienophile scaffolds, as well as direct application to the synthesis of biologically relevant frameworks, we have taken advantage of the pyridyl nitrogen's Lewis basic lone pair for activation that renders these previously unreactive dienophiles synthetically useful.

Additionally, we have supported our experimental observations and expanded upon our mechanistic understanding of this transformation by carrying out a series of computational studies into its transition state energies and geometries. We have therefore provided a foundation for future studies and diversification of our methodology, including possible forays into enantioselective

catalysis, scope expansion into hetero-Diels-Alders or current limitations, and applications to the total synthesis of natural products.

## 2.7 References

- (1) Nicolaou, K. C.; Snyder, S. A.; Montagnon, T.; Vassilikogiannakis, G. The Diels-Alder Reaction in Total Synthesis. *Angew Chem Int Ed* **2002**, *41* (10), 1668–1698.
- (2) Gregoritz, M.; Brandl, F. P. The Diels–Alder Reaction: A Powerful Tool for the Design of Drug Delivery Systems and Biomaterials. *Eur J Pharm Biopharm* **2015**, *97*, 438–453.
- (3) Diels, O.; Alder, K. Synthesen in Der Hydroaromatischen Reihe. *Liebigs Ann Chem* **1928**, *460* (1), 98–122.
- (4) Andrus, M. B.; Saavedra, D. I. The Vinylarene Diels-Alder Reaction, Development and Potential. *Tetrahedron* **2019**, *75* (14), 2129–2142.
- (5) Jung, Y. G.; Kang, H. U.; Cho, H. K.; Cho, C. G.  $\beta$ -Silyl Styrene as a Dienophile in the Cycloaddition with 3,5-Dibromo-2-Pyrone for the Total Synthesis of ( $\pm$ )-Pancratistatin. *Org Lett* **2011**, *13* (21), 5890–5892.
- (6) Taylor, R. D.; Maccoss, M.; Lawson, A. D. G. Rings in Drugs. *J Med Chem* **2014**, *57* (14), 5845–5859.
- (7) Raab, M. S.; Thomas, S. K.; Ocio, E. M.; Guenther, A.; Goh, Y. T.; Talpaz, M.; Hohmann, N.; Zhao, S.; Xiang, F.; Simon, C.; Vanasse, K. G.; Kumar, S. K. The First-in-Human Study of the Pan-PIM Kinase Inhibitor PIM447 in Patients with Relapsed and/or Refractory Multiple Myeloma. *Leukemia* **2019**, *33* (12), 2924–2933.
- (8) Jang, W. D.; Jeon, S.; Kim, S.; Lee, S. Y. Drugs Repurposed for COVID-19 by Virtual Screening of 6,218 Drugs and Cell-Based Assay. *Proc Natl Acad Sci USA* **2021**, *118* (30), e2024302118.
- (9) Houk, K. N.; Strozier, R. W. On Lewis Acid Catalysis of Diels-Alder Reactions. *J Am Chem Soc* **1973**, *95* (12), 4094–4096.
- (10) Gelman, D. M.; Forsyth, C. M.; Perlmutter, P. Lewis Acid Catalyzed Diels-Alder Reactions of 1,2-Naphthoquinones. *Org Lett* **2009**, *11* (21), 4958–4960.
- (11) Northrup, A. B.; Macmillan, D. W. C. The First General Enantioselective Catalytic Diels-Alder Reaction with Simple Unsaturated Ketones. *J Am Chem Soc* **2002**, *124* (11), 2458–2460.
- (12) Ahrendt, K. A.; Borths, C. J.; MacMillan, D. W. C. New Strategies for Organic Catalysis: The First Highly Enantioselective Organocatalytic Diels - Alder Reaction. *J Am Chem Soc* **2000**, *122* (17), 4243–4244.

- (13) Meek, J. S.; Merrow, R. T.; Cristol, S. J. The Diels-Alder Reaction of Isoprene with Styrene and 2-Vinylpyridine. *J Am Chem Soc* **1952**, *74* (10), 2667–2668.
- (14) Doering, W. V. E.; Rhoads, S. J.; 2- and 3-Vinylpyridines as Dienophiles in the Diels-Alder Reaction. *J Am Chem Soc* **1953**, *75* (19), 4738–4740.
- (15) Ptashko, O. The  $[2\pi+4\pi]$ -Cyclocodimerization of Vinylpyridines with Cyclopentadiene and Its Derivatives Catalyzed by Ni and Zr Complexes. *Bashkirskii Khimicheskii Zhurnal* **2000**, *7* (6), 7–10.
- (16) Hammett, L. P. The Effect of Structure upon the Reactions of Organic Compounds. Benzene Derivatives. *J Am Chem Soc* **1937**, *59* (1), 96–103.
- (17) Balog, A.; Lin, T. A.; Maley, D.; Gullo-Brown, J.; Kandoussi, E. H.; Zeng, J.; Hunt, J. T. Preclinical Characterization of Linrodostat Mesylate, a Novel, Potent, and Selective Oral Indoleamine 2,3-Dioxygenase 1 Inhibitor. *Mol Cancer Ther* **2021**, *20* (3), 467–476.
- (18) Davis, A. E.; Lowe, J. M.; Hilinski, M. K. Vinylazaarenes as dienophiles in Lewis acid-promoted Diels–Alder reactions. *Chem Sci* **2021**, *12*, 15947–15952.

# CHAPTER THREE:

## Development of the Organocatalytic Formal Aza- Pauson-Khand Reaction

### 3.1 Introduction

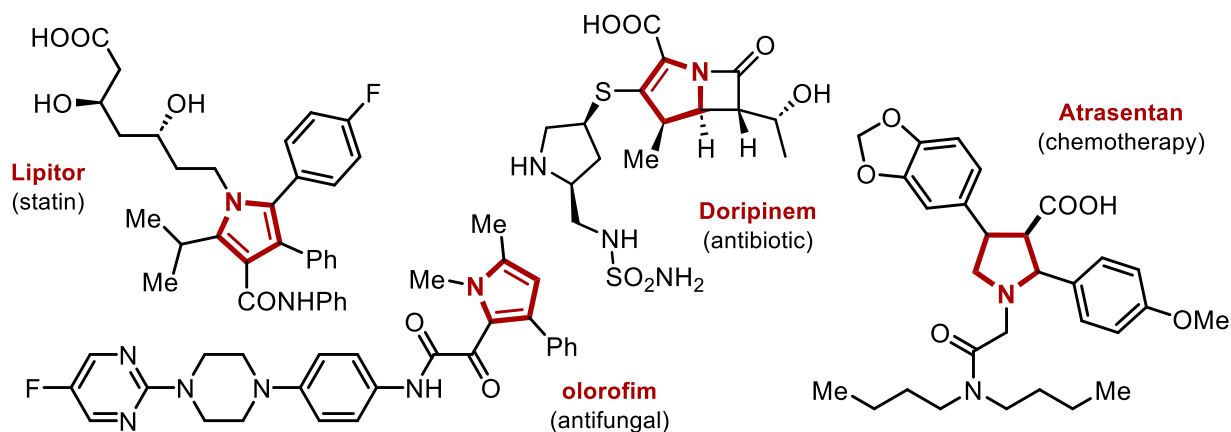
Although the Diels-Alder might be the most prevalent name in cycloadditions, it is by no means the only one. True cycloadditions, pericyclic reactions where the rearrangement of  $\pi$ -bonds gives way to a new cyclic structure with a net reduction in bond multiplicity, expand into complex assemblies of ring structures, from 3-membered to 10-membered.<sup>1</sup> Formal cycloadditions expand the possibilities of these transformations through stepwise mechanisms, often metal- or organocatalytic in nature, that proceed through radical or charged intermediates. Although not strictly pericyclic in nature, these reactions also furnish rings from  $\pi$ -bond-containing acyclic precursors.

Herein we report the first example of an organocatalytic formal [2+2+1] reaction, using nitrene surrogates as one-atom components. We have been inspired both by the state of the art in metal-catalyzed [2+2+1] reactions and mechanistic insight from our own previous work to devise this novel transformation. Having established optimum conditions as well as a scope including pharmaceutically relevant entries to demonstrate the broad applicability of this method, we have also engineered a nitrene source to specifically address mechanistic considerations towards a faster reaction rate in our scheme.

### 3.1.1 Relevance of 5-membered *N*-heterocycles

Pyrrolidines, fully saturated 5-membered *N*-heterocycles constitute the eighth most common ring structure in FDA-approved drugs.<sup>2</sup> Though less common, aromatic pyrroles are also a group of rising prominence in the drug discovery field. Both structures are accessible in one step through pyrrolines, a monounsaturated 5-membered nitrogen-containing ring. Whether FDA-approved or in clinical trials, all three of these motifs appear in drugs or drug leads (Figure 3.1).<sup>3-6</sup>

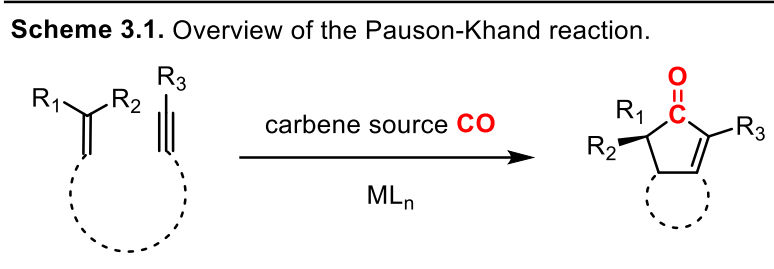
**Figure 3.1.** Structures of FDA-approved drugs and drug leads containing a 5-membered *N*-heterocycle.



As previously established, a facile and highly atom-economical route to *N*-heterocyclic structures such as these is through cycloadditions. Like the Diels-Alder, other true or formal cycloadditions proceed through well-documented mechanisms that lend themselves to predictable diastereo- or regioselectivity. Synthetic chemists have long leveraged these transformations toward the synthesis of complex targets, and further development of cycloaddition reactions lends a robust toolkit for the construction of such targets.

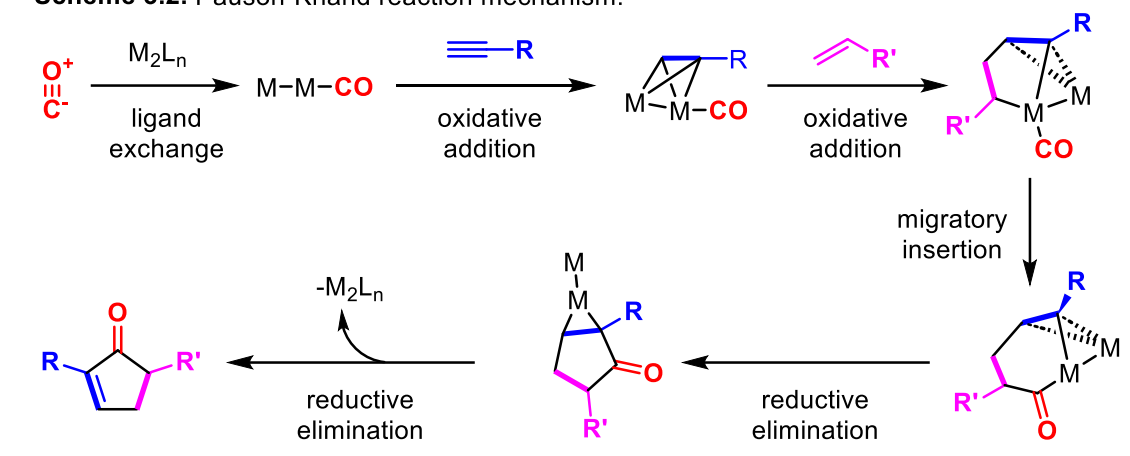
### 3.1.2 The Pauson-Khand reaction

Commonly employed in total synthesis and widely developed in the literature is the Pauson-Khand reaction, a transition-metal catalyzed formal [2+2+1] cycloaddition of an alkene, an alkyne, and carbon monoxide as a carbene source to form a cyclopentenone.<sup>7-9</sup> Not only does this reaction produce a five-membered carbocyclic ring in a single step, but also produces two inherent functionalization handles that lend themselves toward further diversification (Scheme 3.1).



This reaction proceeds through an organometallic mechanism that requires positive pressure of carbon monoxide and successive associations of all three Lewis basic components with a metal center (Scheme 3.2). Although cobalt polycarbonyls are the first and most prevalent examples of a metal catalyst in this reaction, palladium, titanium, ruthenium, iron, molybdenum, copper, and rhodium centers are also utilized for this transformation. Enantioselective variants as well as specially engineered conditions have been established for intra- and intermolecular substrates with varying functionalities. Specific ligands have also been produced to best accommodate the desired transformations.<sup>10,11</sup>

**Scheme 3.2.** Pauson-Khand reaction mechanism.



Our inspiration for this reaction stems ultimately from this transformation. Work in the Hilinski lab focuses heavily on nitrene chemistry, and substitution of a nitrene for a carbene in this scheme would represent an unprecedented and ubiquitous transformation. Predictable regio- and stereochemistry in the Pauson-Khand canon would theoretically be applicable to a nitrene variant as well.

## 3.2 Prior transition metal-catalyzed formal [2+2+1] work

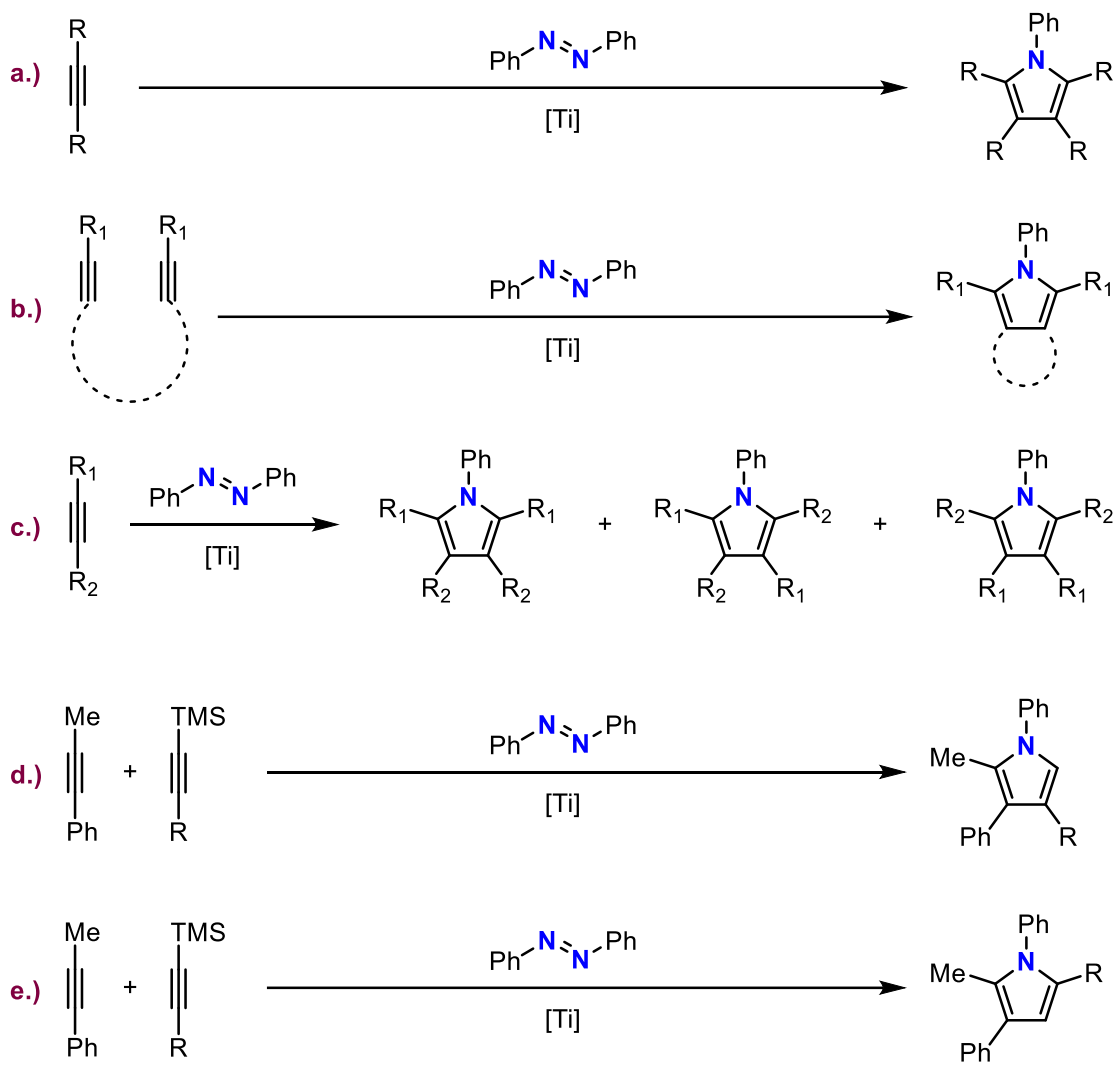
There is also a strong literature precedent for transition metal-catalyzed formal [2+2+1] reactions to form pyrroles in a similar scheme to the Pauson-Khand, yielding pyrroles instead of pyrrolines. Much work by the Tonks group centers around the formation of pyrroles by titanium complexes that combine two alkynes and a nitrene source, and examples exist of vanadium- and ruthenium-catalyzed variants of similar transformations.

### 3.2.1 Ti-catalyzed [2+2+1]

Spanning the past eleven years, works by the Tonks group have dominated the field of titanium-catalyzed formal [2+2+1] cycloadditions. In a robust series of publications, both inter- and intra-molecular examples have been established toward the formation of C<sub>2</sub>-symmetric and C<sub>2</sub>-asymmetric pyrroles. The scope of this group's preliminary publications included excess alkyne with respect to diazobenzene as a nitrene surrogate. Scope entries include symmetrical alkynes (Scheme 3.3a), tethered alkynes (Scheme 3.3b), and asymmetric alkynes that yielded a mixture of regioisomers (Scheme 3.3c).<sup>12,13</sup>

Subsequent studies focused on mechanistic understanding and allowed for further innovation in the field of C<sub>2</sub>-asymmetric formal cycloadditions with two different alkyne components in addition to the diazobenzene. TMS-substituted alkynes were deprotected *in situ* toward regioselective construction of trisubstituted pyrroles with regioselectivity for the R = H substituent both proximal and distal to the nitrogen (Scheme 3.3d and 3.3e).<sup>14,15</sup> While proximal-H iterations relied on the inherent anionic stabilization of the –TMS group, distal-H regioselective reactions utilized dative directing groups opposite the –TMS group: Lewis basic donor groups coordinating to the titanium center to influence the regioselectivity of the second alkyne addition.

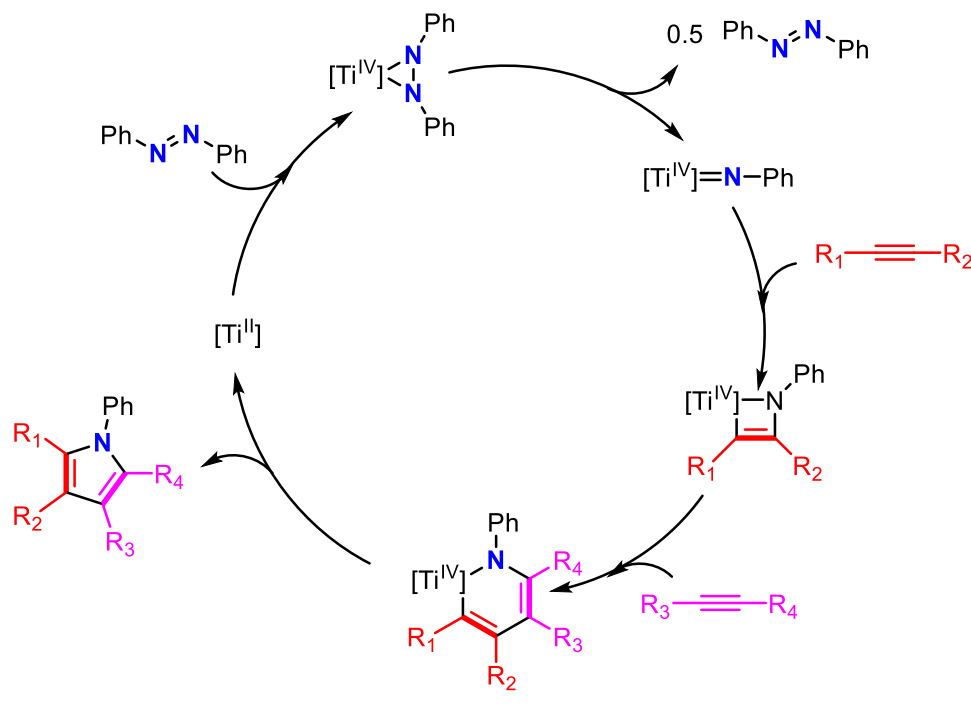
**Scheme 3.3.** Overview of the Tonks group's work on Ti-catalyzed formal [2+2+1] reactions for the formation of pyrroles.



Mechanistically, these formal cycloadditions followed the same general scheme, taking advantage of titanium's nitrene-philicity as an early transition metal. Undergoing oxidative addition with diazobenzene, a titanodiaziridine is formed, which quickly decomposes to the metal nitrene species. Successive oxidative additions of two alkynes form the six-membered titanacycle, which then undergoes reductive elimination to the corresponding pyrrole and regeneration of the catalyst (Scheme 3.4).<sup>16,17</sup> Inherent regioselectivity of this mechanism places the more electron-

rich carbon proximal to the highly Lewis acidic titanium, which is a common mechanistic quality in transformations of this nature and informed many subsequent formal [2+2+1] studies with different metal centers.

**Scheme 3.4.** General mechanism of the Tonks group's Ti-catalyzed formal [2+2+1] reactions.



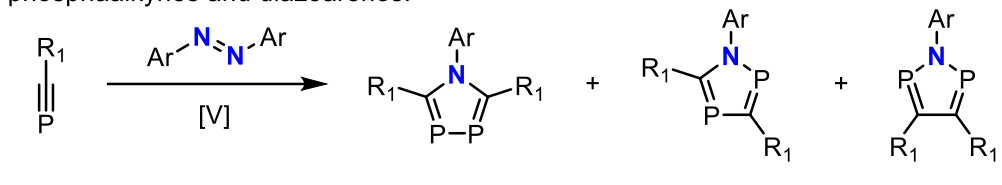
Similar cycloadditions using azides as nitrene sources in the place of diazobenzene have been established as well. These reactions follow a similar mechanism to Scheme 3.4, except with the thermodynamically favorable expulsion of nitrogen gas bridging the titanadiaziridine and metal nitrene species as opposed to the loss of one-half diazobenzene. They are also characterized by tolerance for terminal alkynes, regioselectively incorporating them into disubstituted pyrroles.<sup>18,19</sup>

### 3.2.2 V-catalyzed [2+2+1]

Though less thoroughly investigated than titanium-catalyzed reactions, vanadium centers have been studied to carry out similar transformations. Analogous reactions to that shown in

Scheme 3.3c, producing pyrroles regioselectively but not entirely so, from asymmetric alkynes specifically predominate. These formal cycloadditions follow a similar mechanism to their titanium analogs, the only notable difference being that the vanadium center maintains a higher valence than titanium throughout the organometallic cycle.<sup>20</sup>

**Scheme 3.5.** Vanadium-catalyzed formal [2+2+1] to form azadiphospholes from phosphalkynes and diazoarenes.

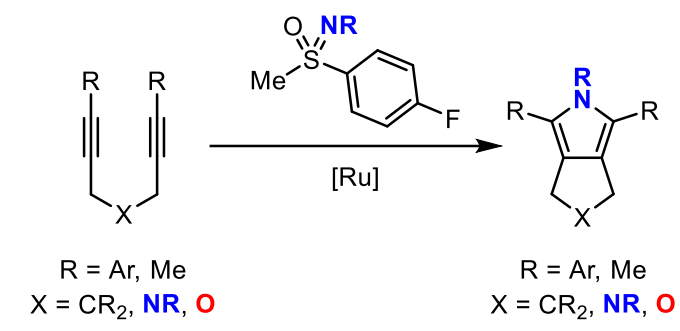


A distinct advantage that vanadium catalysis holds over titanium methods is compatibility with phosphalkynes (Scheme 3.5). A limited scope of azadiphospholes was produced with various regiochemical outcomes between aryl and adamantyl phosphalkynes and diazoarenes, which adds to the versatility of the formal [2+2+1] reaction.<sup>21</sup>

### 3.2.3 Ru-catalyzed [2+2+1]

A single example of a transition metal-catalyzed formal [2+2+1] reaction exists outside of titanium- and vanadium-based catalysts. These ruthenium-catalyzed reactions employ sulfoximines as nitrene source for the formation of pyrroles from tethered diynes (Scheme 3.6). While R groups were relegated to simple aryl and methyl groups, intramolecular tethers were varied between carbon- and nitrogen-centered groups with electron deficient functionalities and simple ethers, which expands the scope of the formal [2+2+1] further into various intramolecular substrates.<sup>22</sup>

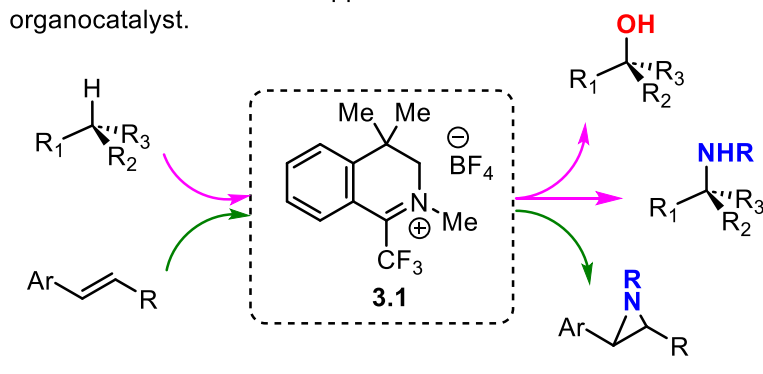
**Scheme 3.6.** Ruthenium-catalyzed formal [2+2+1].



### 3.3 Organocatalytic mechanistic insight from previous work

In addition to other groups' work on [2+2+1] chemistry, our development of the organocatalytic aza-Pauson-Khand drew broad inspiration from previous studies in our lab. Combining mechanistic knowledge from two separate publications, inception and optimization of the procedure was heavily based upon thorough investigation of our iminium organocatalyst's mechanism of action. Organocatalyst **3.1** has been established to carry out C—H oxidation, C—H amination, and aziridination of styrenes (Scheme 3.7).<sup>23–25</sup>

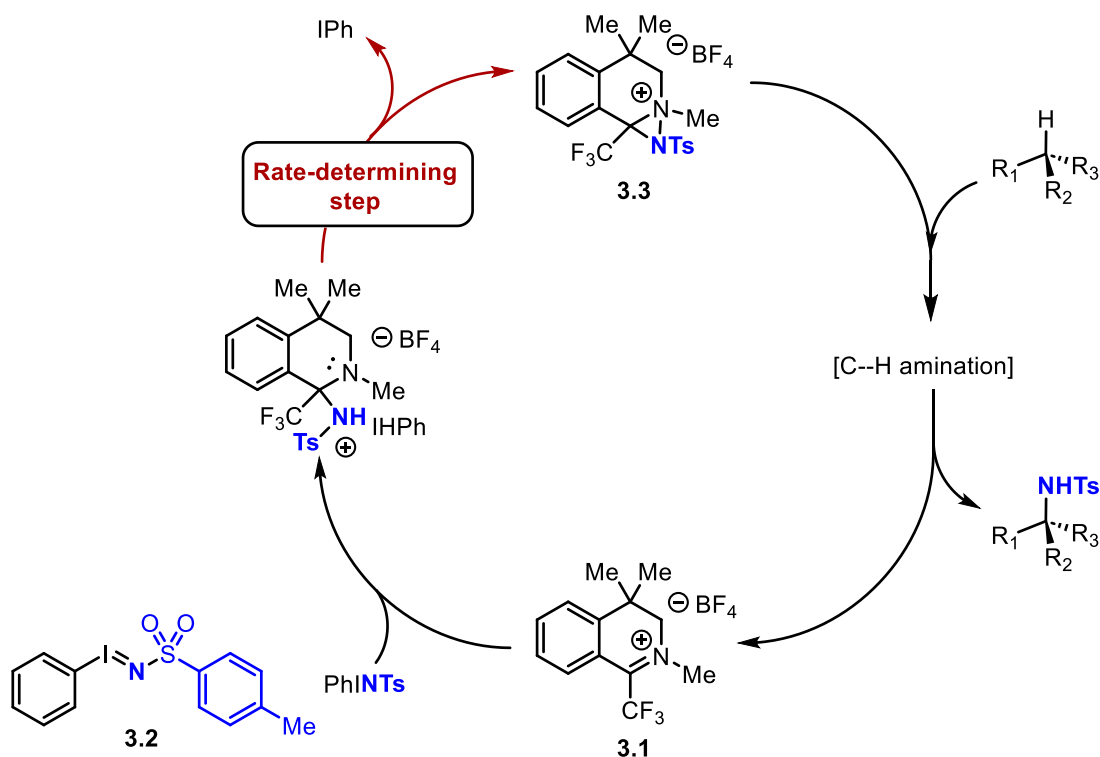
**Scheme 3.7.** Established applications of the Hilinski iminium organocatalyst.



### 3.3.1 Diaziridinium active species for nitrene transfer

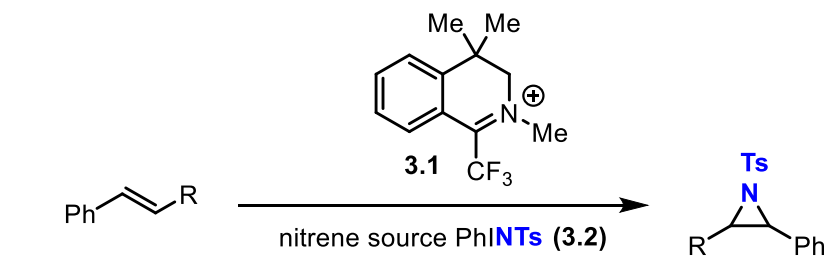
In 2019, the Hililnski group published a computational study evaluating the mechanism of benzylic C-H amination with **3.1** in collaboration with the Gutierrez group.<sup>26</sup> Although this study evaluated the nitrene-transfer amination mechanism, the rate-determining step was identified as the dissociation of the aryl iodide from the nitrene to form the active diaziridinium species (**3.3**, Scheme 3.8). Since the same nitrene source was utilized in aziridination (PhINTs, **3.2**), it followed that both mechanisms had the same active species and therefore the same rate-determining steps. This observation informed the mechanism of formal [2+1] aziridination of styrenes published the same year.

**Scheme 3.8.** Mechanistic evaluation of C-H amination with organocatalyst **3.1**.



### 3.3.2 Nitrene-transfer aziridination of styrenes

Scheme 3.9. Formal [2+1] aziridination of styrenes.

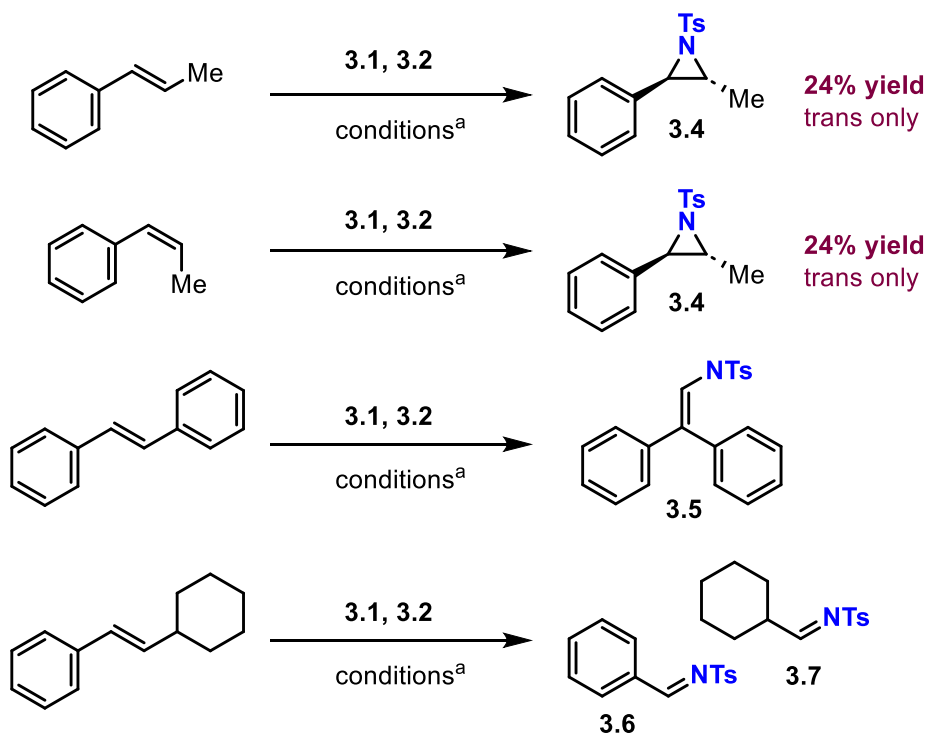


The first cycloaddition carried out by organocatalyst **3.1** was published in 2019: a formal [2+1] between a nitrene source and a styrene derivative to form a styrenyl aziridine with **3.2** as a nitrene surrogate (Scheme 3.9).<sup>23</sup> This transformation provided a basis for inception of the formal organocatalytic [2+2+1] based on mechanistic studies and familiarity with related transformations. The mechanism of aziridination following formation of active diaziridinium species **3.3** was discerned through a series of probing experiments that provided support for a key intermediate and the kinetics of the aziridine ring-closing step (Scheme 3.10).

Upon subjection of *trans*- $\beta$ -methylstyrene to the established reaction conditions, 24% of *trans* aziridine product **3.4** was isolated. Reaction of *cis*- $\beta$ -methylstyrene yielded the identical product **3.4**, demonstrating that stereochemistry about the styrene double bond was not conserved. Instead, isomerization to the more thermodynamically stable *trans* isomer in both aziridine products provided evidence for a ring-opened carbocationic intermediate through which the aziridine substitutions could rotate. Further evidence for this intermediate was gathered in the reaction of *trans*-stilbene, wherein 1,1-diphenyl substituted *N*-tosyl enamine **3.5** was produced as a side product. This likely resulted from a 1,2-phenyl shift to yield the more stable tertiary benzylic carbocation in the same intermediate, followed by tautomerization. A final mechanistic support came in the observation of an oxidative cleavage product, forming the *N*-tosylimines of both alkene

substitutions. To more readily identify these side products, *trans*-cyclohexylstyrene was subjected to the reaction conditions to produce benzylimine (**3.6**) and cyclohexylformimine (**3.7**), which were observable on NMR in 3% yield. Addition of a second equivalent of **3.2** to the proposed ring-opened carbocationic intermediate and subsequent reformation of the catalyst would mechanistically explain the formation of these two products.

**Scheme 3.10.** Experimental mechanistic probes for iminium-catalyzed aziridination.

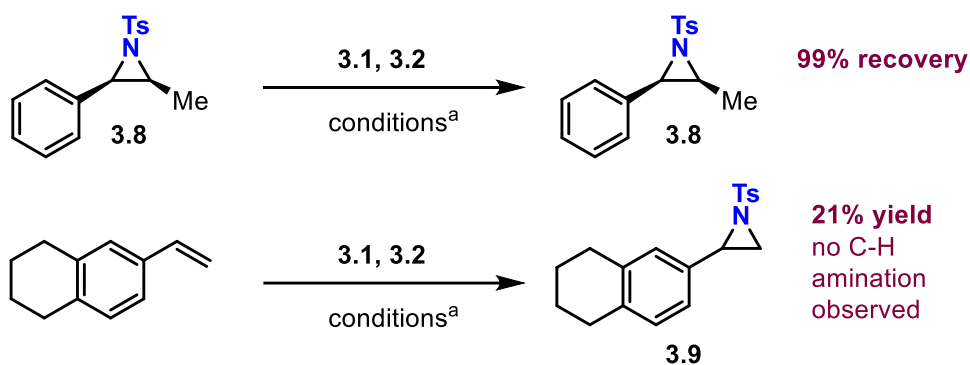


<sup>a</sup>Conditions: 2 equiv. PhINTs, 20 mol% **2**, 9:1 DCM:hexanes, rt, 20h

To examine the kinetics of the aziridination ring-closing step, two additional experiments were conducted (Scheme 3.11). The aziridine derivative of *cis*- $\beta$ -methylstyrene with conserved geometry was subjected to optimum conditions to probe for reversibility of ring opening. Under established conditions, the *cis*-2-phenyl-3-methyl aziridine **3.8** was quantitatively recovered with the same stereochemistry, suggesting irreversibility of the ring closing step. Of note, a chemoselectivity probe for C-H amination versus aziridination produced aziridine **3.9** as the sole

product, entirely outcompeting the benzylic amination that had been previously documented. While these relative rates are helpful to keep in mind for the establishment of related reactions, they also demonstrate the high relative speed of the irreversible aziridine ring-closing step.

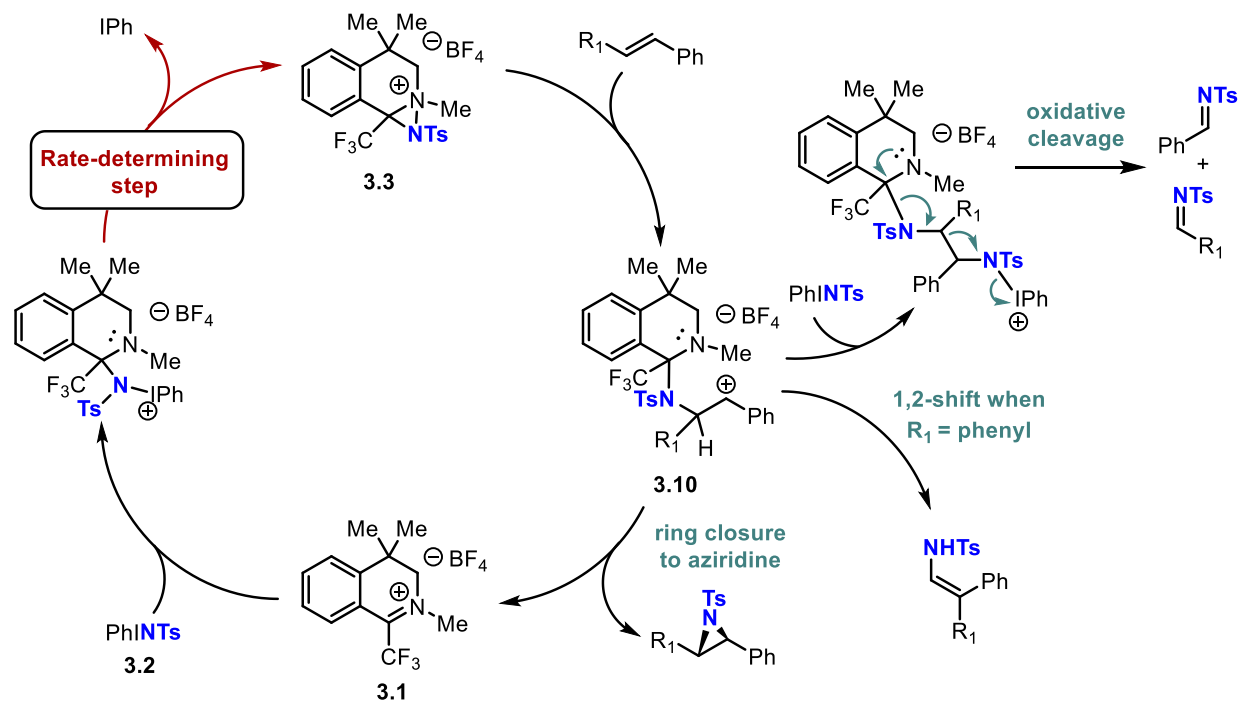
**Scheme 3.11.** Experimental kinetic investigation for iminium-catalyzed aziridination.



<sup>a</sup>Conditions: 2 equiv. PhINTs, 20 mol% **2**, 9:1 DCM:hexanes, rt, 20h

With strong experimental support of a ring-opened carbocationic intermediate, a full aziridination mechanism was proposed (Scheme 3.12). Following the attack of **3.2** on iminium **3.1**, the rate-determining step of phenyl iodide expulsion occurred to form active species **3.3**. Addition of one equivalent of styrene into this electrophilic nitrogen center resulted in carbocation **3.10**. From this intermediate, addition of a second equivalent of nitrene precursor led to oxidative cleavage, rearrangement and tautomerization of the stilbene-derived enamine, and fast, irreversible ring closure furnished the desired aziridine before reformation of **3.1**.

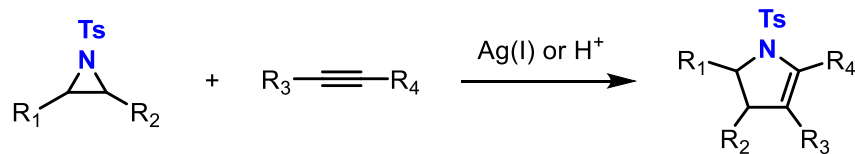
**Scheme 3.12.** Mechanism of iminium-catalyzed aziridination of styrenes.



### 3.3.3 Aziridine/alkyne formal [3+2]

Inspired by a 2009 publication by the Wender group that developed a formal [3+2] cycloaddition between aziridines and alkynes to form pyrrolines (Scheme 3.13), we hypothesized that addition of an alkyne into intermediate **3.10** could undergo a similar transformation. Although a carbocationic intermediate is not specifically invoked in this reaction, association of a Lewis or Brønsted acid with the aziridine nitrogen either promotes a ring opening places a partial positive charge on the carbon most equipped to stabilize it.<sup>27</sup>

**Scheme 3.13.** Wender's formal [3+2] cycloaddition to form pyrrolines.

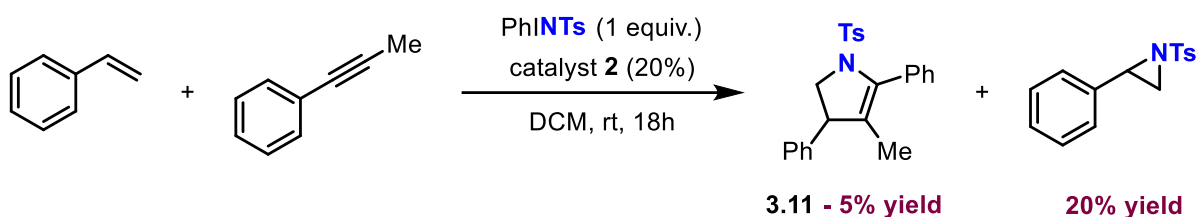


This formation of an electrophilic site leads to regioselective incorporation of the weakly nucleophilic alkyne component into a five-membered ring structure. The scope of this reaction is limited to aziridines functionalized at C2 with an aryl group, although it does tolerate 2,2- or 2,3-disubstitution. The alkyne scope also generally requires a positive charge-stabilizing group distant from the initial bond-forming carbon, but appears less limited to aryl groups: allyl and cyclopropyl substituents were also well tolerated. A superstoichiometric amount (10 eq.) of 3-hexyne also furnished the cycloadduct in 28% yield.

In 2023, a similar transformation promoted by a ruthenium catalyst and visible light was published by the Siddiqui group.<sup>28</sup> Though this transformation proceeds through a radical pathway, many electronic considerations remain consistent in implementation of regioselectivity. The mechanistic considerations of both works are applicable to our method as well.

## 3.4 Optimization and controls

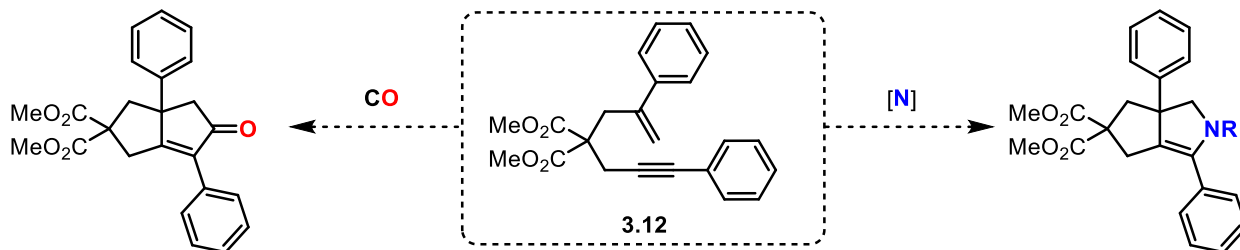
**Scheme 3.14.** Preliminary intermolecular aza-Pauson-Khand study.



With this theoretical framework in place, our hypothesis for the aza-Pauson-Khand was able to be implemented. Adding one equivalent of phenylpropyne, a common substrate for the formal [3+2] reactions, to the established aziridination conditions yielded trace pyrroline **3.11**. However, aziridine formation still predominated (Scheme 3.14). At this point, we turned our investigation toward tethered intramolecular substrates to give entropic advantage to our preliminary studies. Intramolecular substrates such as **3.12** (Figure 3.2) represent the earliest

scope entries in the Pauson-Khand canon due to their faster relative kinetics compared to intermolecular analogs.

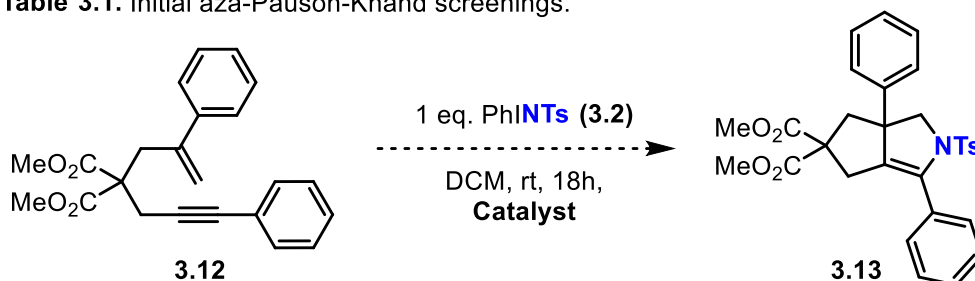
**Figure 3.2.** Model intramolecular Pauson-Khand substrate.



### 3.4.1 Initial intramolecular catalyst screenings

Our initial investigations did not relegate us to the organocatalyst; we screened a variety of metal centers known to facilitate nitrene chemistry. Not only did we find success in modest yields under organocatalysis of **3.1**, but a variety of metal catalysts known to be powerful and versatile nitrene mediators failed to produce product at all.

**Table 3.1.** Initial aza-Pauson-Khand screenings.



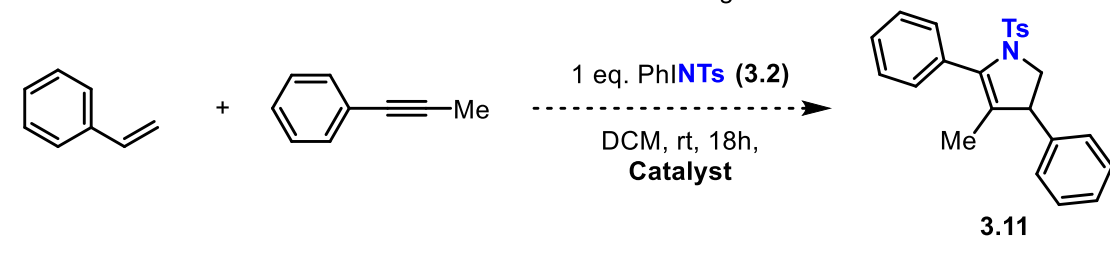
Entry	Catalyst	Loading (mol %)	Yield <b>3.13</b> (%)
1	[RhCl(CO)(PPh <sub>3</sub> ) <sub>2</sub> ]	2	0
2	Rh <sub>2</sub> esp <sub>2</sub>	2	0
3	Rh <sub>2</sub> espn <sub>2</sub> Cl	2	0
4	Rh <sub>2</sub> (OAc) <sub>2</sub>	2	0

5	Cu(OTf) <sub>2</sub>	5	0
6	AgSbF <sub>6</sub>	2	0
7	Cu(OTf) <sub>2</sub> + AgSbF <sub>6</sub>	5, 2	<1
8	Iminium <b>3.1</b>	20	11
9	Iminium <b>3.1</b> + AgSbF <sub>6</sub>	20, 2	13

### 3.4.2 Initial intermolecular catalyst screenings

Having had better luck and greater consistency of results isolating pyrroline product from the initial intermolecular reaction screening, we extended our catalyst studies to the styrene/phenylpropyne cycloaddition. We applied catalysts known to mediate aziridination, formal [3+2] of aziridines and alkynes, a combination thereof, and **3.1**. While the combination of known olefin aziridination catalyst Cu(OTf)<sub>2</sub> with formal [3+2] catalyst AgSbF<sub>6</sub> yielded the desired pyrroline (entry 3, table 3.2), this was simply a combination of two established methods into one pot at the detriment of combined yield. Formal yield for these substrate entries over two steps: Cu-catalyzed aziridination followed by the Ag-catalyzed [3+2], was roughly 85%<sup>27,29</sup> based on reported yields. Portionwise addition of catalysts after two hours under aziridination conditions yielded 57% (entry 4), but **3.1** demonstrated the potential to circumvent this unwieldy solution without the addition of AgSbF<sub>6</sub>.

**Table 3.2.** Initial intermolecular aza-Pauson-Khand screenings.

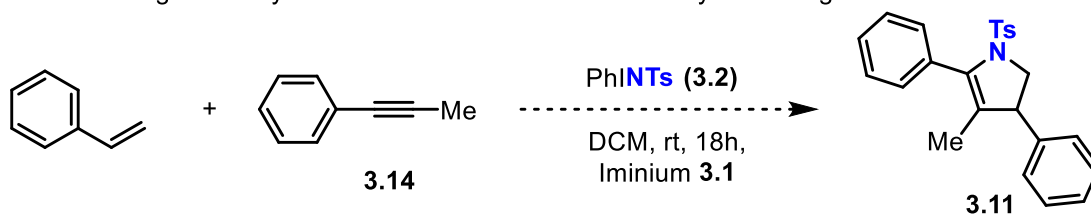


Entry	Catalyst	Loading (mol %)	Yield 3.11 (%)
1	Cu(OTf) <sub>2</sub>	5	0 (~60% aziridine)
2	AgSbF <sub>6</sub>	2	0
3	Cu(OTf) <sub>2</sub> + AgSbF <sub>6</sub>	5, 2	9
4	Cu(OTf) <sub>2</sub> + AgSbF <sub>6</sub> (Ag added portionwise after 2 hours)	5, 2	57
5	HBF <sub>4</sub>	5	0
6	Cu(OTf) <sub>2</sub> + HBF <sub>4</sub>	5, 5	0
7	Iminium <b>3.1</b>	20	5
8	Iminium <b>3.1</b> + AgSbF <sub>6</sub>	20, 2	8

### 3.4.3 Organocatalytic reaction condition screening

As the organocatalyst showed potential for pyrroline production despite poor yields, further optimization of reaction conditions was required before continuation of the study. Stoichiometry, solvent, reaction temperature, and reaction time were successively evaluated to establish optimized conditions.

**Table 3.3.** Organocatalytic aza-Pauson-Khand stoichiometry screening.

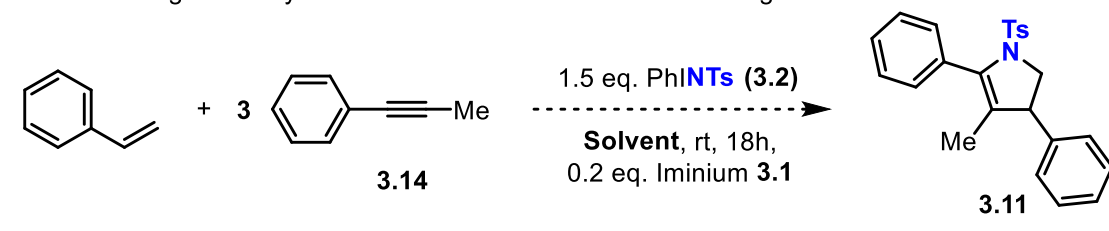


Entry	Eq. alkyne <b>3.14</b>	Eq. nitrene source <b>3.2</b>	Eq. iminium <b>3.1</b> (mol% loading)	Isolated yield <b>3.11</b> (%)
1	1	1	20	5

2	2	1	20	9
3	3	1	20	14
4	4	1	20	16
5	3	1.5	20	21
6	3	2	20	19
7	3	1.5	0	0
8	3	1.5	10	0
9	3	1.5	15	16
10	3	1.5	30	22

Stoichiometry was evaluated for alkyne **3.14**, nitrene source **3.2**, and catalyst **3.1** loading. While raising the alkyne equivalents to 3, our initial 5% yield was proportionally increased (entry 3, Table 3.3), with a plateau observed at 4 equivalents (entry 4). A similar plateau was observed with nitrene source equivalents between 1.5 and 2, solidifying the greatest efficiency and atom economy at 1.5 (entry 5). Lowering catalyst loading had an exponentially detrimental effect on yield, while raising it made no appreciable difference. Thus, further studies were carried out using 3 equivalents of **3.14** and 1.5 equivalents of **3.2** per mole of styrene with 20% loading of **3.1**.

**Table 3.4.** Organocatalytic aza-Pauson-Khand solvent screening.

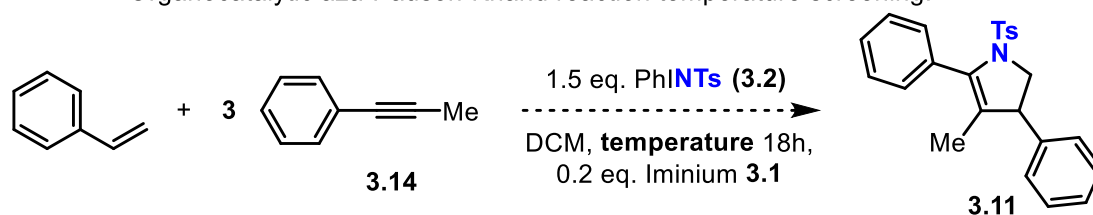


Entry	Solvent	Isolated yield <b>3.11</b> (%)
1	DCM	21
2	MeCN	20
3	DMF	3

4	DCE	5
5	THF	0
6	9:1 DCM:hexanes	9

A variety of polar aprotic solvents were evaluated for efficacy in this reaction. While MeCN gave excellent comparable yield to DCM (entry 2), later studies revealed that this solvent was not as versatile in the establishment of a substrate scope. While other solvents produced isolable product, DCM remained the most successful entry as well as the most adaptable to various conditions within the later-established scope.

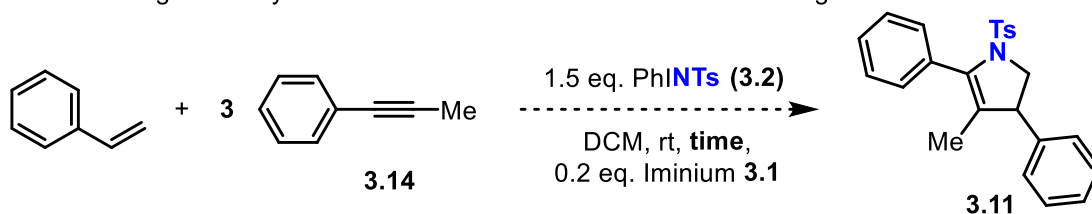
**Table 3.5.** Organocatalytic aza-Pauson-Khand reaction temperature screening.



Entry	Temperature (°C)	Isolated yield 3.11 (%)
1	4	0
2	23	21
3	30	8
4	40	0

The temperature screening was straightforward as PhINTs (3.2) is unstable above 40°C. Lower temperatures seemed to kinetically preclude the reaction from taking place (Table 3.5, entry 1), and higher temperatures showed partial or complete degradation of the nitrene source (entries 3 and 4). The reaction was therefore continued at room temperature.

**Table 3.6.** Organocatalytic aza-Pauson-Khand reaction time screening.



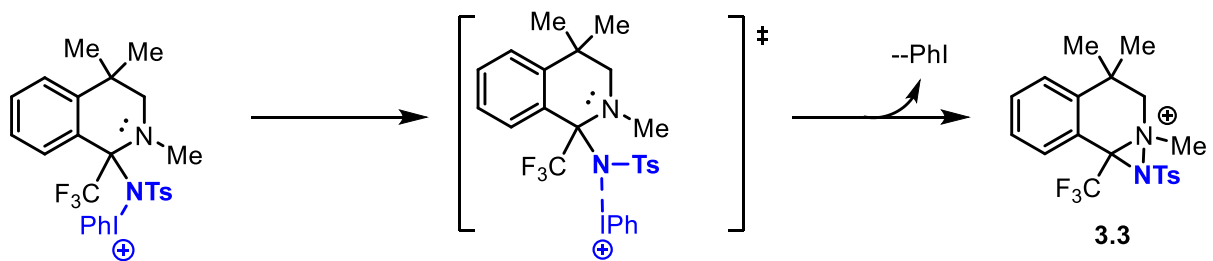
Entry	Time (h)	Isolated yield 3.11 (%)
1	18	21
2	24	30
3	30	19

The final evaluation of reaction time demonstrated that six more hours of reaction time than the established 18h “overnight” procedure made a drastic difference in yield (Table 3.6, entry 2). However, degradation of product into an inseparable mixture began to occur after longer reaction times.

### 3.4.4 Nitrene source optimization

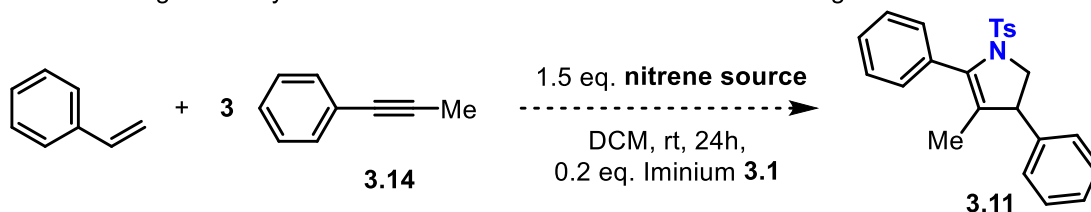
Our mechanistic knowledge greatly informed our next optimization: insight into the rate-determining step of the organocatalytic aza-Pauson-Khand prompted us to engineer the structure of the nitrene source. As the rate-determining transition state involved dissociation of phenyl iodide from the tethered *N*-tosylate, we hypothesized that decreasing the order of the N-I bond in the initial nitrene precursor would lead to more facile cleavage of the leaving group and subsequently accelerate the reaction (Scheme 3.15).

**Scheme 3.15.** Rate-determining step of organocatalytic nitrene transfer reactions.



Capitalizing upon this insight, we designed a series of nitrene precursors with structures analogous to the well-established PhINTs (**3.2**) and tested them in the context of our nitrene transfer reactions. As part of the optimization procedure, we subjected these nitrene sources to our optimum reaction conditions to compare their suitability for this work (Table 3.7).

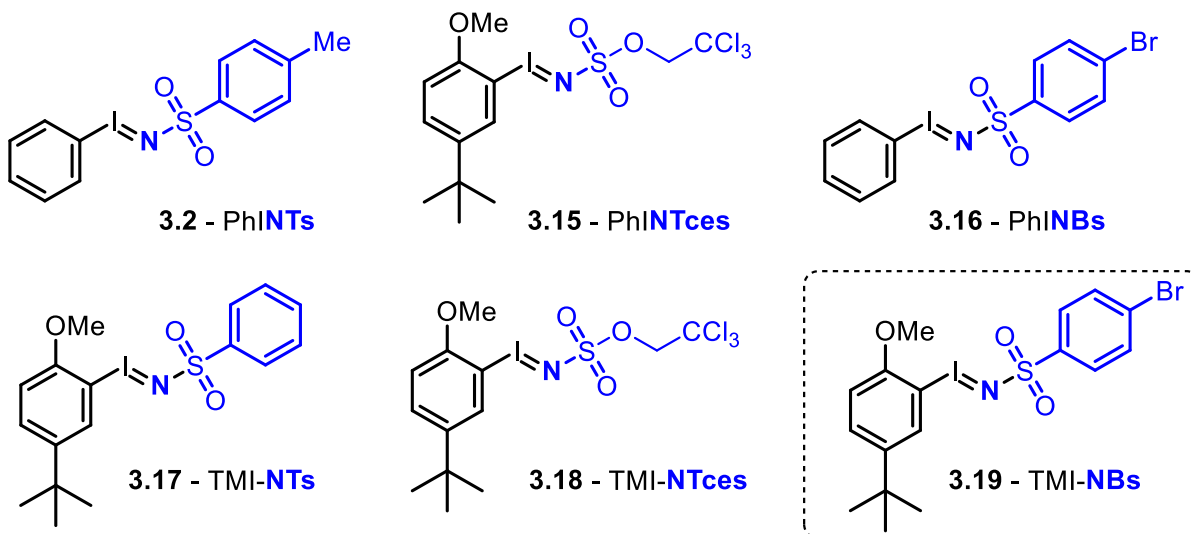
**Table 3.7.** Organocatalytic aza-Pauson-Khand nitrene source screening.



Entry	Nitrene (Figure 3.3)	Isolated yield 3.11 (%)
1	PhINTs ( <b>3.2</b> )	30
2	PhINTces ( <b>3.15</b> )	15
3	PhINBs ( <b>3.16</b> )	3
4	TMI-NTs ( <b>3.17</b> )	11
5	TMI-NTces ( <b>3.18</b> )	16
6	TMI-NBs ( <b>3.19</b> )	62

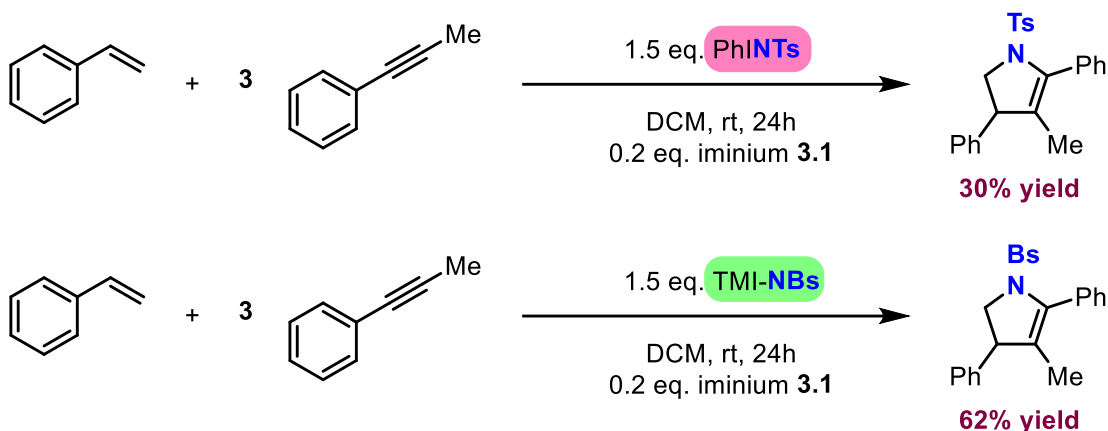
Substituting a brominesulfonamide (brosyl) group for the PhINTs tosyl and functionalizing the aryl iodide with tert-butyl and methoxy groups proved the most effective in the [2+2+1] paradigm by stabilizing the critical transition state (Figure 3.3). Thus, TMI-NBs (**3.19**) found the most success in abetting the formal [2+2+1].

**Figure 3.3.** Evaluated nitrene sources for stabilization of the rate-determining transition state.



While the brosyl group likely stabilizes the negative charge on the nitrogen in the ylide resonance form, we hypothesize that the methoxy group serves the dual purpose of stabilizing the positive charge through resonance and via proximal  $\sigma$ -donation to the iodonium. The tert-butyl group acts to hyperconjugatively donate electron density to the phenyl iodide ring, but also contributes to the solubility of the nitrene source in DCM, thermodynamically and kinetically contributing to the progress of the reaction. **3.19** was incorporated into the optimization study and resulted in over a twofold increase in 2-pyrroline yield (Scheme 3.16).

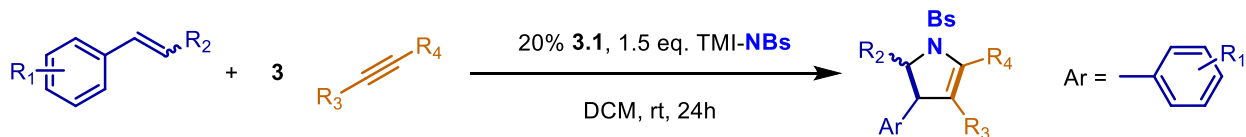
**Scheme 3.16.** Effect of TMI-NBs (3.19) on formal [2+2+1] yield.



## 3.5 Reaction scope

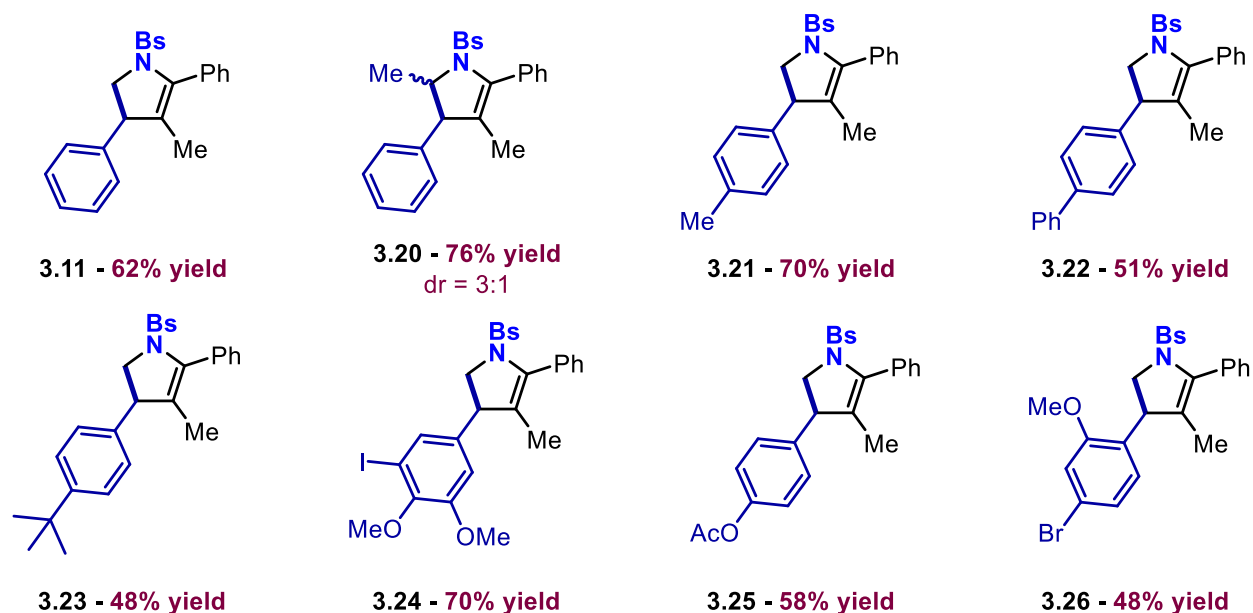
### 3.5.1 Alkene scope

**Scheme 3.17.** General scope evaluation.



Optimized conditions in hand, we embarked on establishing a substrate scope to evaluate the limits of our novel reaction and gain further mechanistic insight (Scheme 3.17). Much like our aziridination work, only styrenes were tolerated within the bounds of our alkenes, providing further evidence for the proposed mechanistic carbocation intermediate. While groups with a more weakly carbocation-stabilizing effect than aryl rings were tested in the reaction scheme (cyclopropyl, allyl, heteroaryl, etc.), functionalized phenyl rings were the only entries that gave way to discernible product.

**Figure 3.4.** Organocatalytic aza-Pauson-Khand alkene scope.



In general, aromatic rings with a moderate to slightly high level of activation were tolerated (Figure 3.4). Total regioselectivity was observed in all products and no homo-cycloaddition product was isolated. Yields tended to reflect relative phenyl electron density in the styrene. Aziridination was observed in some entries as a competing side reaction but never outpaced pyrroline formation in the presence of three equivalents of alkyne. Scope trials generally saw total consumption of starting material, with remaining starting material mass balance attributed to aziridination or other competing side reactions that failed to yield isolable product.

Entries include aryl and alkyl functionalizations of the phenyl ring, as well as a protected phenol. Halogenated compounds which could serve as downstream coupling partners were tolerated, provided sufficient ring activation by the presence of electron-donating methoxy groups. 1,2-disubstitution about the styrenyl olefin in  $\beta$ -methylstyrene proceeded to form a tetrasubstituted pyrroline in 3:1 diastereoselectivity (**3.20**) favoring the more sterically favored trans isomer. While the formation of **3.20** indeed showed selectivity, it was not produced as a sole diastereomer as

opposed to the mechanistic probe experiments on earlier aziridination work. This suggests a steric and electronic influence from the approaching alkyne in the product-determining transition state. While the *trans* geometry about the C4 – C5 bond was mostly conserved in a 3:1 ratio, some *cis* isomerization was observed.

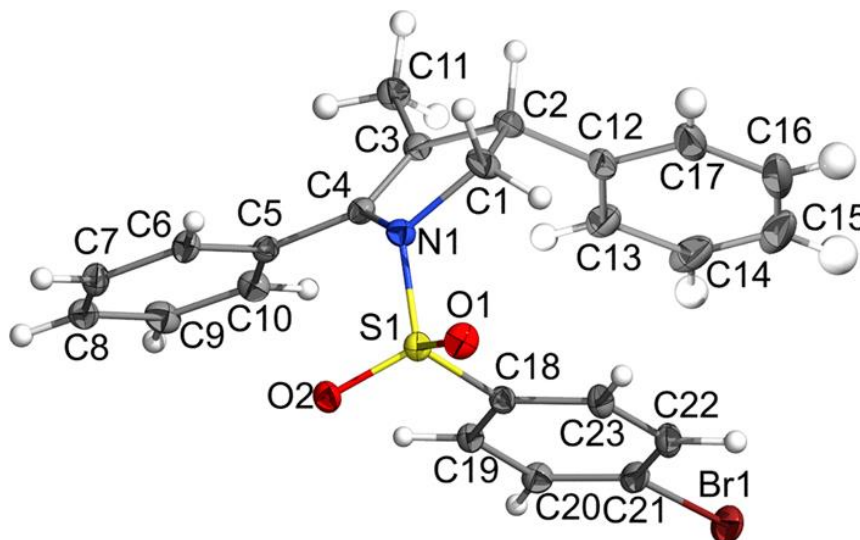
More heavily substituted alkenes were not tolerated, including 1,1-disubstitution and 1,2-disubstitution with sterically bulky groups such as in stilbene. Notably, both *trans* and *cis* stilbene under the optimized conditions formed the *trans* isomer of the 2,3-diphenylaziridine, however, approach of the alkyne for further cyclization was likely sterically prohibited.

While moderately activated arenes proceeded in good yields, highly electron-rich and highly electron-poor rings failed to undergo cycloaddition. To hypothesize from our proposed mechanism, electron-poor rings likely destabilized the carbocationic intermediate to kinetically favor aziridine ring-closing. Aziridination of all deactivated styrene entries was observed in modest yields. Conversely, highly electron-rich arenes might invite undesirable side reactions through prolonging the lifetime of the carbocation in the presence of multiple nucleophilic species in the reaction mixture. These scope attempts often yielded complex, inseparable mixtures of products.

Separation of these compounds was nontrivial. Carbocyclic entries such as **3.11** and **3.20** – **3.23** proved easier entries to purify via column chromatography, but heteroatom-containing entries such as **3.24** – **3.26** were subjected to at least one column followed by up to three iterations of preparatory TLC. High silica or alumina mesh and deactivation of acidic solid phase chromatography media was essential for the publication-quality isolation of these products.

To establish our product formation more rigorously, crystals of our optimization substrate were grown in a DCM/methanol mixture. Using X-ray diffraction, a crystal structure of **3.11** was produced (Figure 3.5).

**Figure 3.5.** Crystal structure of pyrroline product **3.11**.

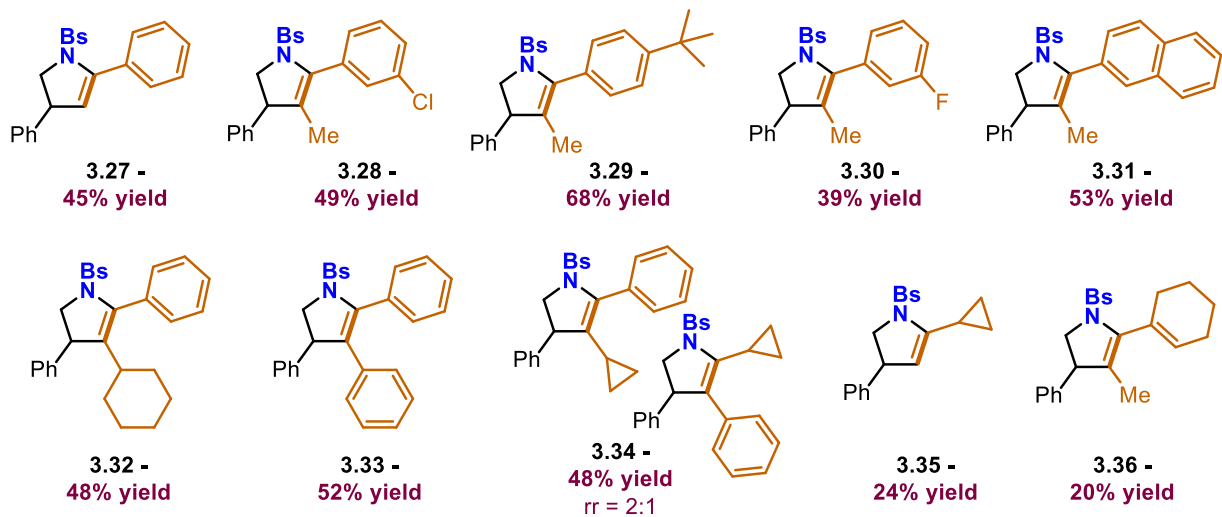


### 3.5.2 Alkyne scope

The scope of alkynes tolerated by this reaction was more robust. Disubstitution (even with bulky substituents), wider ranges of ring activation and deactivation, and non-aryl C -  $\delta^+$  stabilizing groups proceeded within our optimum conditions. Halogenated rings such as **3.28** are viable coupling partners for further product diversification, and fluorinated structures such as **3.30** are highly relevant to drug discovery for their ability to increase drug bioavailability in the body. **3.35** and **3.36** constitute possible precursors for further cyclizations: vinylcyclopropane [5+2] reactions in the case of **3.35** and a Diels-Alder-compatible diene in **3.36**.

A regioselectivity probe was synthesized to compare relative carbocation-stabilizing effects of different alkyne substituents. Phenyl and cyclopropyl alkyne termini featured in the formation of **3.34**, yielding 2:1 regioselectivity favoring the phenyl ring proximal to the pyrroline-N1. This observation supported our assertion of a  $\delta^+$  charge on the intermediate, as a phenyl group has a greater positive charge-stabilizing capacity than a cyclopropyl. However, both are viable within this reaction scheme and can be kinetically compared through their respective product distribution. This selectivity is also roughly reflected in yields of phenylacetylene and cyclopropylacetylene entries (**3.27**, **3.36**) over 24h. All products other than **3.34** proceeded with total regioselectivity.

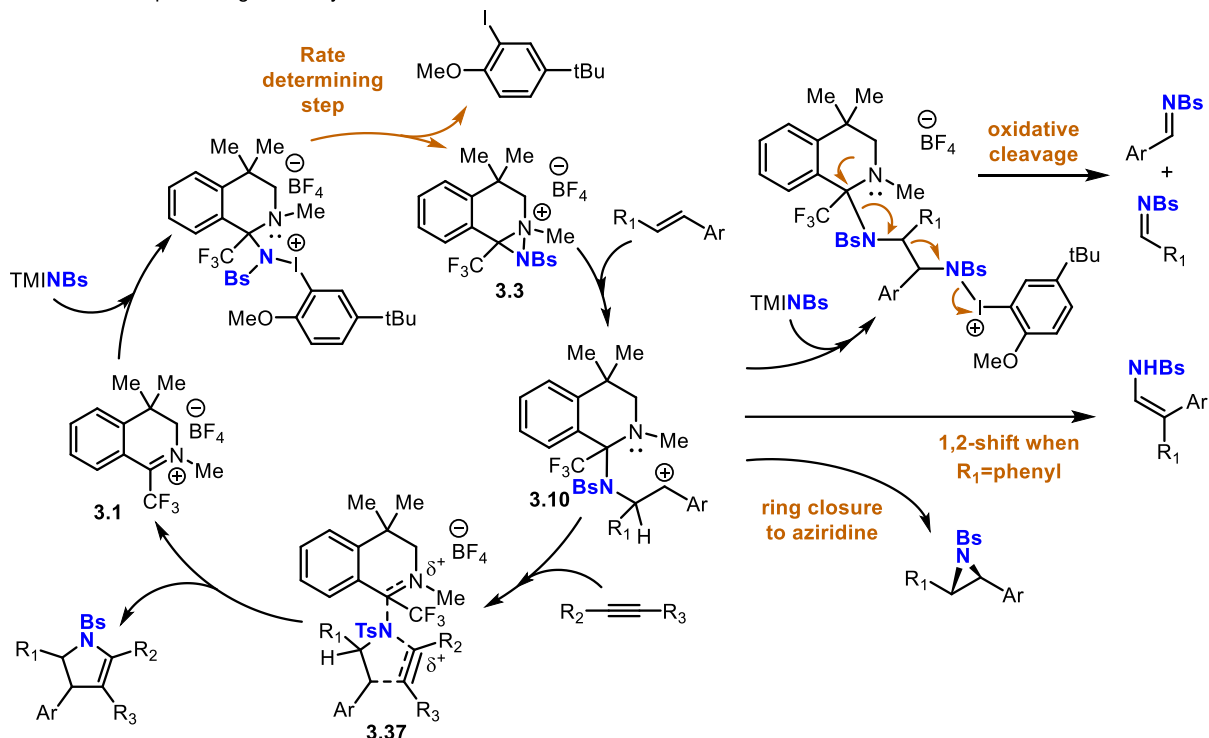
**Figure 3.6.** Alkyne scope of the organocatalytic aza-Pauson-Khand reaction.



Provided the alkyne scope's tolerance for non-aromatic carbocation-stabilizing groups, the full formation of a carbocationic intermediate after the alkyne addition step is unlikely. Evidence within the substrate scope suggests that this second addition is concerted rather than fully stepwise like that of the alkene. Stemming from carbocationic intermediate **3.10**, concerted addition of the alkyne proceeds through intermediate **3.37**, which in this case resembles a transition state rather than a proper intermediate. Subsequent reformation of iminium **3.1** drives

dissociation of the 5-membered *N*-heterocycle, regioselectively assembled to a single pyrroline structure (Scheme 3.18).

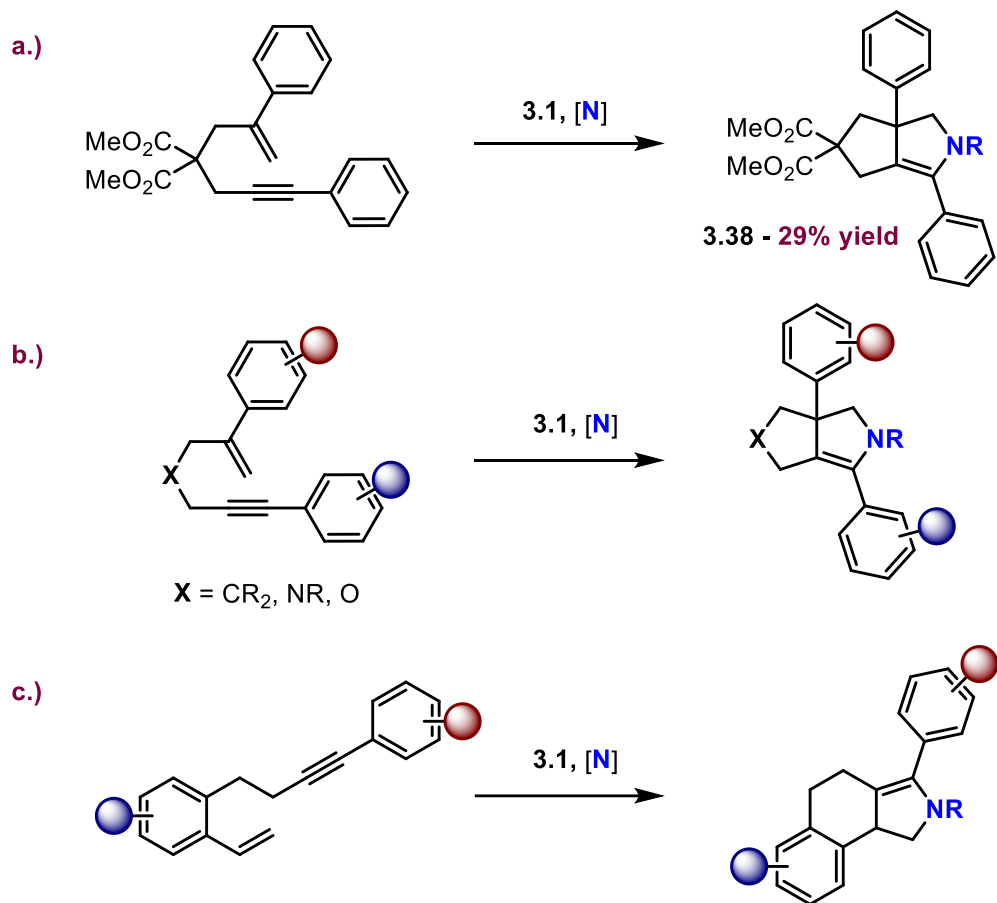
**Scheme 3.18.** Proposed organocatalytic aza-Pauson-Khand mechanism.



### 3.5.3 Intramolecular entry

Although this study was optimized toward the intermolecular reaction, the improvement in yield that TMI-NBs facilitated was readily applied to the tethered enyne we used to establish this branch of our work. Furnishing a modest yield of 29%, further optimization is clearly required to establish a robust intramolecular procedure. However, further intramolecular entries such as diversely functionalized aromatic frameworks and variation of the electron-deficient molecular tether at the “X” position (Scheme 3.19b) may provide entries into higher yields when the mechanistic pathway is further examined. Additionally, inherent aryl functionalizations where a positive charge must be stabilized can be leveraged toward highly bridged ring structures (Scheme 3.19c).

**Scheme 3.19.** Intramolecular aza-Pauson-Khand and future directions within similar substrates.

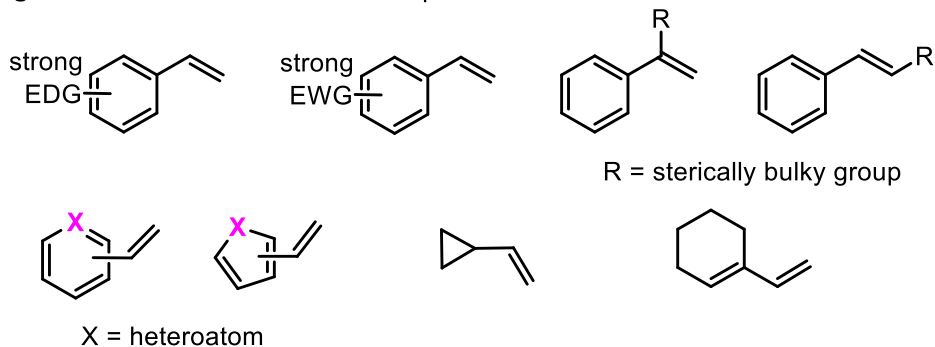


### 3.5.4 Limitations to scope

Limitations to scope are fairly straightforward: operating within a narrower steric, electronic, and functional parameter, alkenes are limited mostly to monosubstituted, moderately activated aryl rings. Other aromatic heterocycles such as pyridines, furans, and thiophenes are also not tolerated, likely due to their Lewis basic nature that can complex with the highly electrophilic carbon of **3.1** (Figure 3.8). As mentioned, cyclopropyl and allyl groups are not tolerated as their carbocation-stabilizing capabilities are insufficient for the fully positively charged intermediate **3.10**. 1,1-disubstitution of alkenes or 1,2-disubstitution with a functionality bulkier than a methyl group also arrest the reaction. Though these substrates are feasible in the

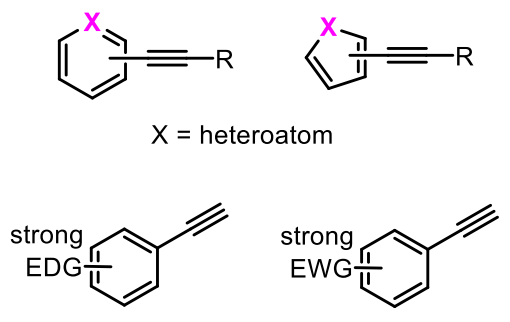
aziridination regime, there is likely a steric consideration in the subsequent approach of the alkyne in the following step.

**Figure 3.8.** Limitations to alkene scope.



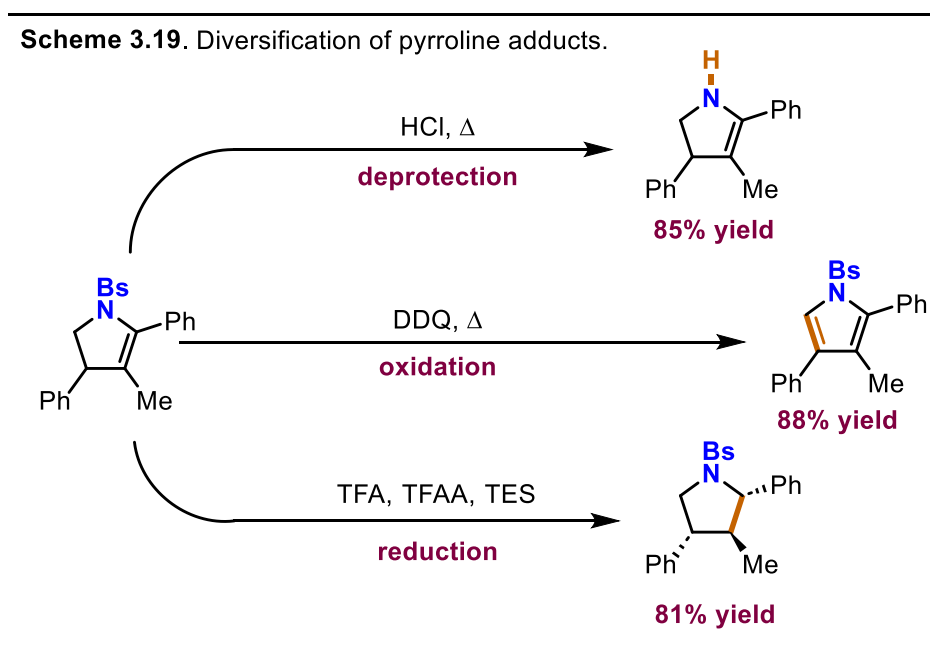
The most apparent limitation to the alkyne scope was the inclusion of heteroatoms. Even pyridyl alkynes with steric or electronic mitigation of the nitrogen lone pair's Lewis basicity (such as fluoropyridines and lutidine) were not tolerated by the reaction conditions (Figure 3.9). Electron-donating and electron-withdrawing groups were tolerated more than those of alkenes, but a sufficiently electron-deficient ring center tended to fail to react with carbocationic intermediate **3.10**, and an overly electron-dense ring caused a variety of undesired side reactions with the iminium catalyst.

**Figure 3.9.** Limitations to alkyne scope.



### 3.5.5 Pharmaceutical relevance

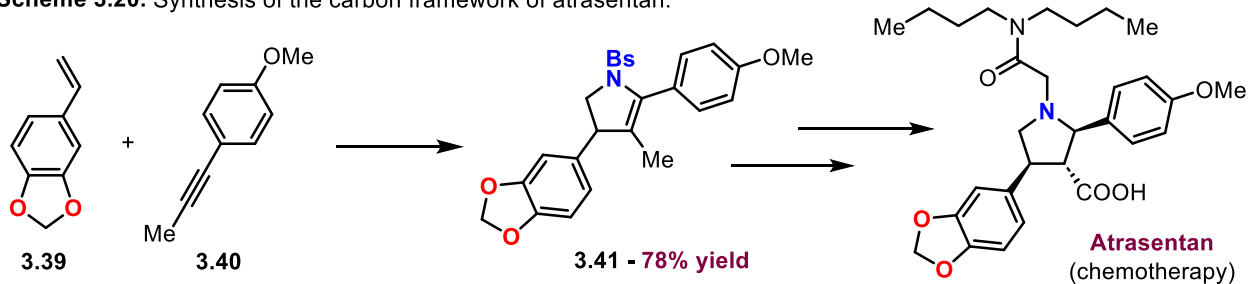
Much like the vinylazaarene Diels-Alder, this reaction finds wide applicability to the field of medicinal chemistry. The formal [2+2+1] cycloaddition between styrene, phenylpropyne, and TMI-NBs has been carried out on the multigram scale with no appreciable drop in isolated yield. Additionally, we have demonstrated our claim that pyrrolines represent one-step precursors to medicinally relevant structures pyrroles and pyrrolidines. Deprotection, oxidation to the corresponding pyrrole, and diastereoselective reduction to a pyrrolidine have been carried out in excellent yields (Scheme 3.19).



The proposed utility of this reaction was also demonstrated through the rapid construction of the *N*-heterocyclic core of atrasentan, an endothelin receptor agonist and chemotherapy lead currently in phase II trials for treatment of various cancers. With reactivity measured against styrene, 4-methoxyphenylpropyne was isolated in very modest yield and highly inconsistent results. However, when paired with a highly activated styrene, relative reaction rates are likely better matched, furnishing the framework of atrasentan in 78% yield. While piperonal-derived

olefin **3.39** relegates carbocationic intermediate **3.10** to be longer-lived, the stronger nucleophilicity of **3.40** and likely outcompetes other undesired side reactions to form **3.41** in good yield.

**Scheme 3.20.** Synthesis of the carbon framework of atrasentan.



## 3.6 Conclusions

In summary, we have established the first example of an intermolecular aza-Pauson-Khand reaction. This reaction represents an unprecedented chemical transformation, as no metal-catalyzed approaches to the same three-component formal cycloaddition have been identified, nor have intermolecular analogs. Drawing heavily from the literature and our previous work, we have rigorously established the theoretical basis behind this work.

Having developed optimum conditions, a reaction scope, and a rigorous purification procedure, we are confident that this reaction will find wide utility in the realms of medicinal chemistry and complex molecule synthesis. We have demonstrated its applicability to these fields through scalability to a multigram order of magnitude and the facile formation of the carbon core of a chemotherapy lead, as well as through rapid and high-yielding redox adjustments to the product structures.

## 3.7 References

- (1) Cycloaddition. *The IUPAC Compendium of Chemical Terminology* **2008**.  
<https://doi.org/10.1351/GOLDBOOK.C01496>.
- (2) Taylor, R. D.; Maccoss, M.; Lawson, A. D. G. Rings in Drugs. *J Med Chem* **2014**, *57* (14), 5845–5859.
- (3) Neoh, C. F.; Jeong, W.; Kong, D. C. M.; Slavin, M. A. The Antifungal Pipeline for Invasive Fungal Diseases: What Does the Future Hold? *Expert Rev Anti Infect Ther* **2023**, *21* (6), 577–594.
- (4) Chiappori, A. A.; Haura, E.; Rodriguez, F. A.; Boulware, D.; Kapoor, R.; Neuger, A. M.; Lush, R.; Padilla, B.; Burton, M.; Williams, C.; Simon, G.; Antonia, S.; Sullivan, D. M.; Bepler, G. Phase I/II Study of Atrasentan, an Endothelin A Receptor Antagonist, in Combination with Paclitaxel and Carboplatin as First-Line Therapy in Advanced Non-Small Cell Lung Cancer. *Clin Cancer Res* **2008**, *14* (5), 1464–1469.
- (5) Mazzei, T. The Pharmacokinetics and Pharmacodynamics of the Carbapenems: Focus on Doripenem. *J Chemotherapy* **2010**, *22* (4), 219–225.
- (6) McCrindle, B. W.; Ose, L.; Marais, A. D. Efficacy and Safety of Atorvastatin in Children and Adolescents with Familial Hypercholesterolemia or Severe Hyperlipidemia: A Multicenter, Randomized, Placebo-Controlled Trial. *J Pediatrics* **2003**, *143* (1), 74–80.
- (7) Khand, L. U.; Knox, G. R.; Pauson, P. L.; Watts, W. E. 977 Organocobalt Complexes. Part II. Reaction of Acetylenehexacarbonyl-Dicobalt Complexes, (R<sub>1</sub>C<sub>2</sub>R<sub>a</sub>)Co<sub>2</sub>(CO)<sub>4</sub>, with Norbornene and Its Derivatives. *J Chem Soc, Perkin Trans.* **1973**, *1*, 977–981.
- (8) Yang, Z.; Zhang, •; Zhao, Z.-C. ; Zhang, D.-D. ; Tan, Z.-C. ; Gong, X.-Y. ; Fu, J.-X. ; Yang, J.-K. ; Navigating the Pauson–Khand Reaction in Total Syntheses of Complex Natural Products Synthesis of 4-Desmethyl-Rippertenol and 7-Epi-Rippertenol via Photo-Induced. *Acc Chem Res* **2021**, *54* (3), 556–568.
- (9) Heravi, M. M.; Mohammadi, L. Application of Pauson–Khand Reaction in the Total Synthesis of Terpenes. *RSC Adv* **2021**, *11* (61), 38325–38373.
- (10) Ricker, J. D.; Geary, L. M. Recent Advances in the Pauson–Khand Reaction. *Top Catal* **2017**, *60* (8), 609.
- (11) Urgoiti, J. B.; Añorbe, L.; Serrano, L. P.; Domínguez, G.; Pérez-Castells, J. The Pauson–Khand Reaction, a Powerful Synthetic Tool for the Synthesis of Complex Molecules. *Chem Soc Rev* **2004**, *33* (1), 32–42.
- (12) Tonks, I. A.; Meier, J. C.; Bercaw, J. E. Alkyne Hydroamination and Trimerization with Titanium Bis(Phenolate) Pyridine Complexes: Evidence for Low-Valent Titanium Intermediates and Synthesis of an Ethylene Adduct of Titanium(II). *Organometallics* **2013**, *32* (12), 3451–3457.

- (13) Davis-Gilbert, Z. W.; Yao, L. J.; Tonks, I. A. Ti-Catalyzed Multicomponent Oxidative Carboamination of Alkynes with Alkenes and Diazenes. *J Am Chem Soc* **2016**, *138* (44), 14570–14573.
- (14) Chiu, H. C.; Tonks, I. A. Trimethylsilyl-Protected Alkynes as Selective Cross-Coupling Partners in Titanium-Catalyzed [2+2+1] Pyrrole Synthesis. *Angew Chem Int Ed* **2018**, *57* (21), 6090–6094.
- (15) Chiu, H. C.; See, X. Y.; Tonks, I. A. Dative Directing Group Effects in Ti-Catalyzed [2+2+1] Pyrrole Synthesis: Chemo- and Regioselective Alkyne Heterocoupling. *ACS Catal* **2019**, *9* (1), 216.
- (16) Davis-Gilbert, Z. W.; Wen, X.; Goodpaster, J. D.; Tonks, I. A. Mechanism of Ti-Catalyzed Oxidative Nitrene Transfer in [2 + 2 + 1] Pyrrole Synthesis from Alkynes and Azobenzene. *J Am Chem Soc* **2018**, *140* (23), 7267–7281.
- (17) Pearce, A. J.; See, X. Y.; Tonks, I. A. Oxidative Nitrene Transfer from Azides to Alkynes via Ti(II)/Ti(IV) Redox Catalysis: Formal [2+2+1] Synthesis of Pyrroles. *Chemical Communications* **2018**, *54* (50), 6891–6894.
- (18) Harman, W. H.; Lichterman, M. F.; Piro, N. A.; Chang, C. J. Well-Defined Vanadium Organoazide Complexes and Their Conversion to Terminal Vanadium Imides: Structural Snapshots and Evidence for a Nitrene Capture Mechanism. *Inorg Chem* **2012**, *51* (18), 10037–10042.
- (19) Liang, W.; Nakajima, K.; Nishibayashi, Y. Synthesis of 1,2,4-Azadiphosphole Derivatives Based on Vanadium-Catalyzed [2+2+1] Cycloaddition Reactions of Azobenzenes with Phosphaalkynes. *RSC Adv* **2020**, *10* (22), 12730–12733.
- (20) Matsui, K.; Shibuya, M.; Yamamoto, Y. Synthesis of Pyrroles via Ruthenium-Catalyzed Nitrogen-Transfer [2 + 2 + 1] Cycloaddition of  $\alpha,\omega$ -Diyne Using Sulfoximines as Nitrene Surrogates. *Commun Chem* **2018**, *1* (21).
- (21) Johnson, S. L.; Hilinski, M. K. Organocatalytic Olefin Aziridination via Iminium-Catalyzed Nitrene Transfer: Scope, Limitations, and Mechanistic Insight. *J Org Chem* **2019**, *84* (13), 8589–8595.
- (22) Combee, L. A.; Raya, B.; Wang, D.; Hilinski, M. K. Organocatalytic Nitrenoid Transfer: Metal-Free Selective Intermolecular C(Sp<sup>3</sup>)-H Amination Catalyzed by an Iminium Salt. *Chem Sci* **2018**, *9* (4), 935–939.
- (23) Wang, D.; Shuler, W. G.; Pierce, C. J.; Hilinski, M. K. An Iminium Salt Organocatalyst for Selective Aliphatic C-H Hydroxylation. *Org Lett* **2016**, *18* (15), 3826–3829.
- (24) Rotella, M. E.; Dyer, R. M. B.; Hilinski, M. K.; Gutierrez, O. Mechanism of Iminium Salt-Catalyzed c(Sp<sup>3</sup>)-h Amination: Factors Controlling Hydride Transfer versus h-Atom Abstraction. *ACS Catal* **2020**, *10* (1), 897–906.

- (25) Wender, P. A.; Strand, D. Cyclocarboamination of Alkynes with Aziridines: Synthesis of 2,3-Dihydropyrroles by a Catalyzed Formal [3 + 2] Cycloaddition. *J Am Chem Soc* **2009**, *131* (22), 7528–7529.
- (26) Kapoor, R.; Kapoor, R.; Chawla, R.; Verma Twinkle Keshari R Siddiqui, A. I.; Authors Ts R, C. N. Visible-Light-Promoted Click [3+2] Cycloaddition of Aziridine with Alkyne: An Efficient Synthesis of Dihydropyrrolidine R 4 Ru(II)/Blue LED. *Synlett* **2023**, *34* (13), 1621-1625.
- (27) Evans, D. A.; Faul, M. M.; Bilodeau, M. T. Copper-Catalyzed Aziridination of Olefins by (N-(p-Toluenesulfonyl)Imino)Phenyliodinane. *J Org Chem* **1991**, *56* (24), 6744–6746.

# APPENDIX

# Appendix 1:

## Chapter 2 Experimental Data

### A.1 General methods

All reagents were obtained commercially in the highest available purity and used without further purification unless otherwise mentioned. Anhydrous solvents were obtained from a solvent purification system utilizing activated alumina columns under a positive pressure of argon. Reactions carried out at temperatures above room temperature (23 °C) were conducted in a pre-heated oil bath. Diels-Alder reactions were performed in 15 mL pressure tubes under magnetic stirring unless otherwise noted. Flash column chromatography was performed using silica or basic alumina gel (230 - 400 mesh) purchased from Silicycle (Siliaflash P60). Elution of compounds was monitored by UV and vanillin stain on TLC.

**Instrumentation:** <sup>1</sup>H and <sup>13</sup>C NMR spectra were measured on a Varian Inova 600 (600 MHz), Bruker Avance DRX 600 (600 MHz), or Bruker Avance III 800 (800 MHz) spectrometer and acquired at 300 K. Chemical shifts are reported in parts per million (ppm  $\delta$ ) referenced to the residual <sup>1</sup>H or <sup>13</sup>C resonance of the solvent. The following abbreviations are used singularly or in combination to indicate the multiplicity of signals: s - singlet, d - doublet, t - triplet, q - quartet, m - multiplet, br - broad, and ap - apparent. High-resolution mass spectrometry was obtained using an Agilent Q-TOF ESI spectrometer.

## A.2 Screening and reaction optimization

Optimization Reaction conditions were screened with the Diels-Alder reaction of 4-vinylpyridine and isoprene using the following general procedure: To a 15 mL pressure tube equipped with a PTFE stir bar and charged with 4-vinylpyridine (213  $\mu$ L, 2 mmol, 1 equiv) in the indicated solvent (4 mL) was added the specified Lewis acid (0 to 1.0 equiv) and isoprene (1-5 equiv). The vial was placed in an oil bath pre-heated to the specified temperature and allowed to stir for 24-72 hours. Upon reaction completion, the mixture was cooled to room temperature. Dodecane (0.25 mmol, 57  $\mu$ L) was added as an internal standard and reaction was sampled and analyzed on GC-FID. Mixtures of an authentic sample of 3 with dodecane were analyzed by GC to determine burn ratio of 1.29 for 3 for use in obtaining corrected GC yields. Authentic samples of starting material: 4-vinylpyridine were analyzed by GC to determine retention times. Regioselectivity is reported as a simple signal ratio between substituent peaks of 3.

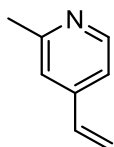
## A.3 General Diels-Alder procedure

To a 15 mL pressure tube equipped with a PTFE stir bar and charged with dienophile (2 mmol, 1 equiv) in acetonitrile (4 mL) was added boron trifluoride diethyl etherate (132  $\mu$ L, 1 mmol, 0.5 equiv) and diene (4 mmol, 2 equiv). The vial was placed in a 70 °C oil bath and allowed to stir for 24-72 hours as noted. Upon reaction completion, the mixture was cooled to room temperature and quenched with brine (15 mL). The biphasic mixture was separated in a separatory funnel, and the aqueous layer was extracted 3 additional times with diethyl ether (20 mL). The combined organic layers were washed once more with brine and dried over  $MgSO_4$ , then concentrated in vacuo. The crude mixture was then purified by silica or alumina flash chromatography as noted.

## A.4 Starting material and substrate synthesis

Substrates **A.1** – **A.7** were prepared according to literature procedure.

### 2-methyl-4-vinylpyridine (A.1)

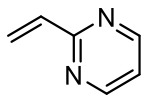


**<sup>1</sup>H NMR** (800 MHz, CDCl<sub>3</sub>): δ 8.38 (d, J = 5.3 Hz, 1H), 7.06 (s, 1H), 7.03 – 7.00 (m, 1H), 5.87 (d, J = 17.6 Hz, 1H), 5.38 (d, J = 10.9 Hz, 1H), 2.41 (s, 3H).

**<sup>13</sup>C NMR** (201 MHz, CDCl<sub>3</sub>): δ 158.8, 149.4, 145.0, 135.0, 120.4, 118.2, 117.8, 24.4.

NMR spectra are consistent with literature reports.<sup>1</sup>

### 2-vinylpyrimidine (A.2)

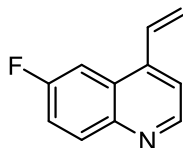


**<sup>1</sup>H NMR** (800 MHz, CDCl<sub>3</sub>): δ 7.10 (t, J = 4.9 Hz, 1H), 6.85 (dd, J = 17.3, 10.6 Hz, 1H), 6.60 (dd, J = 17.3, 1.6 Hz, 1H), 5.71 (dd, J = 10.6, 1.6 Hz, 1H).

**<sup>13</sup>C NMR** (201 MHz, CDCl<sub>3</sub>): δ 164.4, 157.0, 136.6, 123.9, 119.2.

NMR spectra are consistent with literature reports.<sup>2</sup>

### 6-fluoro-4-vinylquinoline (A.3)

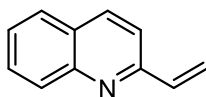


**<sup>1</sup>H NMR** (800 MHz, CDCl<sub>3</sub>): δ 8.84 (d, J = 4.5 Hz, 1H), 8.11 (dd, J = 9.2, 5.6 Hz, 1H), 7.68 (dd, J = 10.0, 2.7 Hz, 1H), 7.48 (dd, J = 9.7, 6.7 Hz, 2H), 7.28 (dd, J = 17.3, 11.0 Hz, 1H), 5.98 (d, J = 17.3 Hz, 1H), 5.68 (d, J = 11.0 Hz, 1H).

**<sup>13</sup>C NMR** (201 MHz, CDCl<sub>3</sub>): δ 161.3, 160.0, 149.6, 149.6, 145.8, 143.2, 143.1, 132.6, 132.6, 131.8, 127.1, 127.0, 121.3, 119.7, 119.6, 118.1, 107.4, 107.2.

NMR spectra are consistent with literature reports.<sup>3</sup>

#### 2-vinylquinoline (A.4)

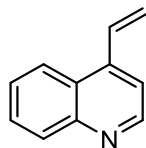


**<sup>1</sup>H NMR** (600 MHz, CDCl<sub>3</sub>): δ 8.07 – 8.00 (m, 2H), 7.74 – 7.70 (m, 1H), 7.66 (dddd, J = 8.4, 6.9, 2.7, 1.4 Hz, 1H), 7.54 (dd, J = 8.5, 3.8 Hz, 1H), 7.02 (dd, J = 17.7, 10.9 Hz, 1H), 6.25 (d, J = 17.6 Hz, 1H), 5.63 (d, J = 10.9 Hz, 1H).

**<sup>13</sup>C NMR** (600 MHz, CDCl<sub>3</sub>): δ 156.0, 148.0, 138.0, 136.3, 129.6, 129.4, 127.5, 126.3, 119.8, 118.3.

NMR spectra are consistent with literature reports.<sup>4</sup>

#### 4-vinylquinoline (A.5)

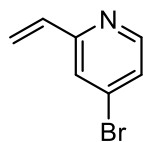


**<sup>1</sup>H NMR** (800 MHz, CDCl<sub>3</sub>): δ 8.84 (d, J = 4.6 Hz, 1H), 8.09 (d, J = 8.5 Hz, 1H), 8.04 (d, J = 8.5 Hz, 1H), 7.67 (t, J = 7.5 Hz, 1H), 7.51 (t, J = 7.5 Hz, 1H), 7.41 (d, J = 4.6 Hz, 1H), 7.37 (dd, J = 17.4, 11.0 Hz, 1H), 5.93 (d, J = 17.4 Hz, 1H), 5.61 (d, J = 11.0 Hz, 1H).

**<sup>13</sup>C NMR** (201 MHz, CDCl<sub>3</sub>): δ 150.3, 148.5, 143.4, 132.0, 130.0, 129.3, 126.5, 126.2, 123.5, 120.7, 117.4.

NMR spectra are consistent with literature reports.<sup>5</sup>

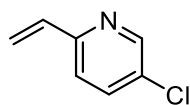
#### 4-bromo-2-vinylpyridine (A.6)



**<sup>1</sup>H NMR** (800 MHz, CDCl<sub>3</sub>): δ 8.38 – 8.32 (m, 1H), 7.46 (d, J = 2.0 Hz, 1H), 7.28 (dd, J = 5.3, 1.9 Hz, 1H), 6.71 (dd, J = 17.4, 10.8 Hz, 1H), 6.19 (dd, J = 17.4, 1.1 Hz, 1H), 5.50 (dd, J = 10.8, 1.1 Hz, 1H).

**<sup>13</sup>C NMR** (201 MHz, CDCl<sub>3</sub>): δ 157.1, 150.2, 135.8, 133.2, 125.6, 124.5, 119.9.

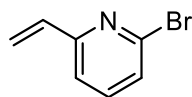
#### 5-chloro-2-vinylpyridine (A.7)



**<sup>1</sup>H NMR** (600 MHz, CDCl<sub>3</sub>): δ 8.48 (dd, J = 2.5, 0.7 Hz, 1H), 7.56 (dd, J = 8.4, 2.5 Hz, 1H), 7.23 (dd, J = 8.4, 0.7 Hz, 1H), 6.74 (dd, J = 17.4, 10.8 Hz, 1H), 6.15 (dd, J = 17.5, 1.1 Hz, 1H), 5.46 (dd, J = 10.8, 1.1 Hz, 1H).

**<sup>13</sup>C NMR** (201 MHz, CDCl<sub>3</sub>): δ 153.9, 148.4, 136.1, 135.8, 130.6, 121.8, 119.0.

### 6-bromo-2-vinylpyridine (A.8)



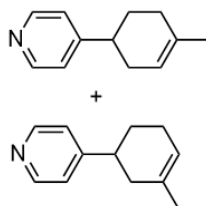
**<sup>1</sup>H NMR** (600 MHz, CDCl<sub>3</sub>): δ 7.49 – 7.45 (t, J = 7.8 Hz, 1H), 7.31 (dd, J = 7.8, 0.8 Hz, 1H), 7.28 – 7.22 (dd, J = 7.8, 0.8 Hz, 1H), 6.71 (dd, J = 17.4, 10.8 Hz, 1H), 6.22 (dd, J = 17.4, 1.0 Hz, 1H), 5.50 (dd, J = 10.8, 1.0 Hz, 1H).

**<sup>13</sup>C NMR** (201 MHz, CDCl<sub>3</sub>): δ 157.0, 142.0, 138.8, 135.4, 127.1, 126.7, 120.0.

NMR spectra are consistent with literature reports.<sup>6</sup>

## A.5 Characterization of Diels-Alder reactions

4-(4-methylcyclohex-3-en-1-yl)pyridine (2.4a) and 4-(3-methylcyclohex-3-en-1-yl)pyridine (2.4b)



4-(4-methylcyclohex-3-en-1-yl) pyridine and 4-(3-methylcyclohex-3-en-1-yl) pyridine were prepared according to the general Diels-Alder procedure using 4-vinylpyridine (213  $\mu\text{L}$ , 2 mmol, 1 equiv),  $\text{BF}_3 \cdot \text{OEt}_2$  (132  $\mu\text{L}$ , 1 mmol, 0.5 equiv), and isoprene (398  $\mu\text{L}$ , 4 mmol, 2 equiv) in acetonitrile (4 mL). The resulting mixture was stirred at 70  $^\circ\text{C}$  for 72 hr. After workup, the reaction mixture was purified on an alumina flash column (5% to 15% EtOAc/hexanes) to give products **2.4a** and **2.4b** as a yellow solid (93.5 mg, 1.08 mmol, 54% yield). Regioselectivity determined as 5:1 based on NMR integration of **2.4a**:**2.4b**.

**TLC** (Vanillin, 25% EtOAc/Hexanes)  $R_f = 0.40$ .

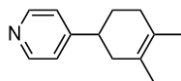
**$^1\text{H}$  NMR (2.4a)** (600 MHz,  $\text{CDCl}_3$ ):  $\delta$  8.72 (d,  $J = 5.3$  Hz, 2H), 7.76 (d,  $J = 5.3$  Hz, 2H), 5.48 (s, 1H), 3.04 (d,  $J = 11.6$  Hz, 1H), 2.37 (d,  $J = 8.2$  Hz, 1H), 2.16 (d,  $J = 8.2$  Hz, 2H), 2.05 – 1.95 (m, 2H), 1.88 – 1.79 (m, 1H), 1.70 (s, 3H).

**$^1\text{H}$  NMR (2.4b)** (600 MHz,  $\text{CDCl}_3$ ):  $\delta$  8.72 (d,  $J = 5.3$  Hz, 2H), 7.76 (d,  $J = 4.0$  Hz, 2H), 5.51 (s, 1H), 3.13 (s, 1H), 2.26 (d,  $J = 13.5$  Hz, 1H), 2.19 – 2.12 (m, 2H), 2.05 – 1.95 (m, 2H), 1.88 – 1.79 (m, 1H), 1.71 (s, 3H).

**$^{13}\text{C}$  NMR (2.4a and 2.4b)**  $\delta$  156.4, 156.3, 149.3, 134.2, 133.0, 122.6, 121.0, 120.0, 39.8, 39.3, 37.0, 32.4, 30.1, 29.1, 28.6, 25.2, 23.5, 23.4.

**HRMS** (EI/QTOF)  $m/z$ :  $[\text{M}]^+$  Calcd for  $\text{C}_{12}\text{H}_{15}\text{N}$  174.1283, found 174.1278.

#### 4-(3,4-dimethylcyclohex-3-en-1-yl)pyridine (2.5)



4-(3,4-dimethylcyclohex-3-en-1-yl)pyridine was prepared according to the general Diels-Alder procedure using 4-vinylpyridine (213  $\mu\text{L}$ , 2 mmol, 1 equiv),  $\text{BF}_3\cdot\text{OEt}_2$  (132  $\mu\text{L}$ , 1 mmol, 0.5 equiv), and 2,3-dimethylbutadiene (458  $\mu\text{L}$ , 4 mmol, 2 equiv) in acetonitrile (4 mL). The resulting mixture was stirred at 70  $^\circ\text{C}$  for 24 hr. After workup, the reaction mixture was purified on a silica flash column (5% to 15% EtOAc/hexanes) to give product **2.5** as a yellow oil (207.9 mg, 1.11 mmol, 56% yield).

**TLC** (Vanillin, 25% EtOAc/Hexanes)  $R_f = 0.34$ .

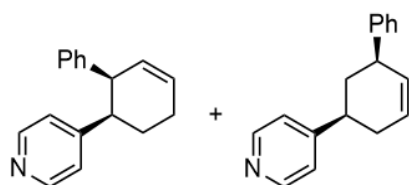
**$^1\text{H NMR}$**  (600 MHz,  $\text{CDCl}_3$ ):  $\delta$  8.50 (s, 2H), 7.15 (s, 2H), 2.78 (ddd,  $J = 11.5, 5.4, 2.9$  Hz, 1H), 2.19 – 2.08 (m, 3H), 1.99 – 2.02 (m, 1H), 1.94 – 1.87 (m, 1H), 1.73 – 1.66 (m, 1H), 1.65 (s, 6H).

**$^{13}\text{C NMR}$**  (151 MHz,  $\text{CDCl}_3$ ):  $\delta$  156.2, 149.5, 125.7, 124.7, 122.5, 40.2, 38.8, 31.7, 29.4, 19.0, 18.8.

**HRMS** (EI/QTOF)  $m/z$ :  $[\text{M}]^+$  Calcd for  $\text{C}_{13}\text{H}_{17}\text{N}$  188.1440, found 188.1453.

**4-((1S,2R)-1,2,3,4-tetrahydro-[1,1'-biphenyl]-2-yl)pyridine (2.6a) and**

**4-((1R,3R)-1,2,3,4-tetrahydro-[1,1'-biphenyl]-3-yl)pyridine (2.6b)**



4-((1S,2R)-1,2,3,4-tetrahydro-[1,1'-biphenyl]-2-yl)pyridine and 4-((1R,3R)-1,2,3,4-tetrahydro-[1,1'-biphenyl]-3-yl)pyridine were prepared according to the general Diels-Alder procedure using 4-vinylpyridine (213  $\mu\text{L}$ , 2 mmol, 1 equiv),  $\text{BF}_3\cdot\text{OEt}_2$  (132  $\mu\text{L}$ , 1 mmol, 0.5 equiv), and *trans*-1-phenyl-1,3-butadiene (559  $\mu\text{L}$ , 4 mmol, 2 equiv) in acetonitrile (4 mL). The resulting mixture was

stirred at 70 °C for 24 hr. After workup, the reaction mixture was purified on an alumina flash column (5% to 15% EtOAc/hexanes) to give products **2.6a** and **2.6b** as yellow oil (193.1 mg, 0.82 mmol, 41% yield). Regioselectivity determined as 4:1 based on NMR integration of **5a:5b**. Diastereoselectivity determined as >99:1 based on the absence of diastereomeric peaks on NMR.

**TLC** (Vanillin, 25% EtOAc/Hexanes)  $R_f = 0.49$ .

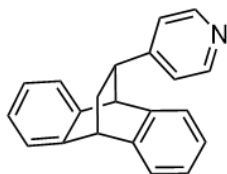
**$^1\text{H NMR}$  (2.6a)** (600 MHz,  $\text{CDCl}_3$ ):  $\delta$  8.34 – 8.28 (m, 2H), 7.08 (dd,  $J = 7.0, 1.5$  Hz, 3H), 6.77 – 6.71 (m, 2H), 6.68 – 6.62 (m, 2H), 6.03 – 6.05 (m, 1H), 5.86 (d,  $J = 10.0$  Hz, 1H), 3.61 (d,  $J = 5.5$  Hz, 1H), 3.23 (ddd,  $J = 13.1, 5.5, 2.1$  Hz, 1H), 2.42 – 2.35 (m, 1H), 2.34 – 2.29 (m, 1H), 2.02 (dd,  $J = 13.1, 6.7$  Hz, 1H), 1.71 – 1.63 (m, 1H).

**$^1\text{H NMR}$  (2.6b)** (600 MHz,  $\text{CDCl}_3$ ):  $\delta$  8.40 – 8.35 (m, 2H), 7.19 – 7.11 (m, 3H), 6.94 – 6.91 (m, 2H), 6.90 – 6.86 (m, 2H), 5.98 – 5.91 (m, 1H), 5.74 (dd,  $J = 10.0, 2.3$  Hz, 1H), 3.47 – 3.42 (m, 1H), 2.73 (ddd,  $J = 12.0, 9.5, 3.2$  Hz, 1H), 2.40 – 2.38 (m, 1H), 2.25 – 2.18 (m, 1H), 1.99 – 1.96 (m, 1H), 1.95 – 1.90 (m, 1H).

**$^{13}\text{C NMR}$  (2.6a and 2.6b)** (151 MHz,  $\text{CDCl}_3$ ):  $\delta$  153.3, 149.5, 149.0, 143.7, 139.2, 130.4, 130.1, 128.9, 128.2, 128.1, 128.0, 127.6, 127.4, 126.5, 126.4, 123.5, 123.1, 49.1, 48.8, 46.8, 44.5, 29, 25.8, 25.2, 21.4.

**HRMS** (EI/QTOF)  $m/z$ :  $[\text{M}]^+$  Calcd for  $\text{C}_{17}\text{H}_{17}\text{N}$  236.1440, found 236.1435.

### 2-((9S,10S,12R)-9,10-dihydro-9,10-ethanoanthracen-12-yl)pyridine (2.7)



2-((9S,10S,12R)-9,10-dihydro-9,10-ethanoanthracen-12-yl)pyridine was prepared according to the general Diels-Alder procedure using **4** (213  $\mu$ L, 2 mmol, 1 equiv),  $\text{BF}_3 \cdot \text{OEt}_2$  (132  $\mu$ L, 1 mmol, 0.5 equiv), and anthracene (713 mg, 4 mmol, 2 equiv) in acetonitrile (4 mL). The resulting mixture was stirred at 70  $^\circ\text{C}$  for 72 hr. After workup, the reaction mixture was purified on a silica flash column (5% to 15% EtOAc/hexanes) to give product **2.7** as a colorless oil (218.9 mg, 0.78 mmol, 39% yield).

**TLC** (Vanillin, 25% EtOAc/Hexanes)  $R_f = 0.60$ .

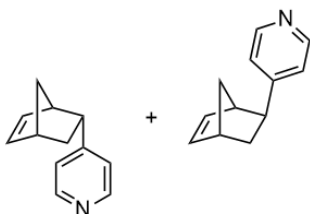
**$^1\text{H NMR}$**  (600 MHz,  $\text{CDCl}_3$ ):  $\delta$  8.33 (d,  $J = 5.1$  Hz, 2H), 7.37 (d,  $J = 7.3$  Hz, 1H), 7.32 (dd,  $J = 9.7, 4.3$  Hz, 2H), 7.19 (dd,  $J = 7.3, 5.1$  Hz, 1H), 7.15 (dd,  $J = 5.1, 1.4$  Hz, 2H), 7.08 – 7.02 (m, 1H), 6.92 (d,  $J = 7.2$  Hz, 1H), 6.51 (d,  $J = 7.2$  Hz, 2H), 4.45 (s, 1H), 4.18 (s, 1H), 3.25 – 3.16 (m, 1H), 2.36 – 2.26 (m, 1H), 1.82 – 1.72 (m, 1H).

**$^{13}\text{C NMR}$**  (151 MHz,  $\text{CDCl}_3$ ):  $\delta$  154.6, 148.5, 144.1, 143.4, 143.1, 139.2, 126.5, 126.2, 126.1, 125.9, 125.7, 123.7, 123.5, 123.4, 123.1, 51.2, 44.6, 44.2, 35.6.

**HRMS** (EI/QTOF)  $m/z$ :  $[\text{M}]^+$  Calcd for  $\text{C}_{21}\text{H}_{17}\text{N}$  284.1440, found 288.1437.

**4-((1R,2R,4R)-bicyclo[2.2.1]hept-5-en-2-yl)pyridine (2.8a) and**

**4-((1R,2S,4R)-bicyclo[2.2.1]hept-5-en-2-yl)pyridine (2.8b)**



4-((1R,2R,4R)-bicyclo[2.2.1]hept-5-en-2-yl)pyridine and 4-((1R,2S,4R)-bicyclo[2.2.1]hept-5-en-2-yl)pyridine were prepared according to the general Diels-Alder procedure using 4-vinylpyridine

(213  $\mu\text{L}$ , 2 mmol, 1 equiv),  $\text{BF}_3\cdot\text{OEt}_2$  (132  $\mu\text{L}$ , 1 mmol, 0.5 equiv), and freshly distilled cyclopentadiene (264  $\mu\text{L}$ , 4 mmol, 2 equiv) in acetonitrile (4 mL). The resulting mixture was stirred at 70  $^\circ\text{C}$  for 24 hr. After workup, the reaction mixture was purified on an alumina flash column (5% to 15% EtOAc/hexanes) to give products **2.8a** and **2.8b** as a brown oil (329.4 mg, 1.93 mmol, 97% yield). Diastereoselectivity determined as 4:1 based on NMR integration of **2.8a:2.8b**.

**TLC** (Vanillin, 25% EtOAc/Hexanes)  $R_f = 0.35$ .

**$^1\text{H}$  NMR (2.8a)** (600 MHz,  $\text{CDCl}_3$ ):  $\delta$  8.38 (d,  $J = 4.6$  Hz, 2H), 7.01 (d,  $J = 4.6$  Hz, 2H), 6.26 – 6.20 (m, 1H), 5.76 – 5.68 (m, 1H), 3.35 – 3.27 (m, 1H), 3.07 (s, 1H), 2.95 (s, 1H), 2.16 (ddd,  $J = 11.3, 3.9, 1.7$  Hz, 1H), 1.51 – 1.41 (m, 2H), 1.27 (dt,  $J = 11.3, 1.7$  Hz, 1H).

**$^1\text{H}$  NMR (2.8b)** (600 MHz,  $\text{CDCl}_3$ ):  $\delta$  8.45 (d,  $J = 4.5$  Hz, 2H), 7.15 (d,  $J = 4.5$  Hz, 2H), 6.21 (d,  $J = 3.1$  Hz, 1H), 6.18 – 6.12 (m, 1H), 3.21 – 3.23 (m, 1H), 2.90 (s, 1H), 2.63 (dd,  $J = 8.9, 5.0$  Hz, 1H), 1.71 – 1.60 (m, 2H), 1.41 – 1.43 (m, 1H).

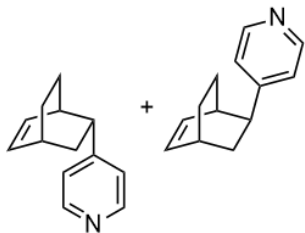
**$^{13}\text{C}$  NMR (2.8a)** (151 MHz,  $\text{CDCl}_3$ ):  $\delta$  146.5, 135.1, 129.7, 121.0, 47.7, 45.8, 45.0, 40.7, 40.6.

**$^{13}\text{C}$  NMR (2.8b)** (151 MHz,  $\text{CDCl}_3$ ):  $\delta$  151.6, 147.0, 134.3, 120.5, 43.2, 39.7, 30.8, 29.8, 29.7.

**HRMS** (EI/QTOF)  $m/z$ :  $[\text{M}]^+$  Calcd for  $\text{C}_{12}\text{H}_{13}\text{N}$  172.1127, found 172.1135.

**4-((1R,2R,4R)-bicyclo[2.2.2]oct-5-en-2-yl)pyridine (2.9a) and**

**4-((1R,2S,4R)-bicyclo[2.2.2]oct-5-en-2-yl)pyridine (2.9b)**



4-((1R,2R,4R)-bicyclo[2.2.2]oct-5-en-2-yl)pyridine and 4-((1R,2S,4R)-bicyclo[2.2.2]oct-5-en-2-yl)pyridine were prepared according to the general Diels-Alder procedure using 4-vinylpyridine (213  $\mu$ L, 2 mmol, 1 equiv),  $\text{BF}_3 \cdot \text{OEt}_2$  (132  $\mu$ L, 1 mmol, 0.5 equiv), and 1,3-cyclohexadiene (380  $\mu$ L 4 mmol, 2 equiv) in acetonitrile (4 mL). The resulting mixture was stirred at 70  $^\circ\text{C}$  for 48 hr. After workup, the reaction mixture was purified on a silica flash column (5% to 15% EtOAc/hexanes) to give products **2.9a** and **2.9b** as a white solid (131.2 mg, 0.70 mmol, 35% yield). Diastereoselectivity determined as 5:1 based on NMR integration of **2.9a**:**2.9b**.

**TLC** (Vanillin, 25% EtOAc/Hexanes)  $R_f = 0.35$ .

**$^1\text{H NMR}$  (2.9a)** (600 MHz,  $\text{CDCl}_3$ ):  $\delta$  8.44 – 8.37 (m, 2H), 7.09 – 7.04 (m, 2H), 6.41 (dd,  $J = 8.1$ , 6.5 Hz, 1H), 6.13 (dd,  $J = 8.1$ , 6.5 Hz, 1H), 2.92 (ddd,  $J = 10.1$ , 5.7, 1.9 Hz, 1H), 2.68 – 2.63 (m, 1H), 2.60 (td,  $J = 5.7$ , 1.9 Hz, 1H), 2.06 (td,  $J = 10.0$ , 2.8 Hz, 1H), 1.72 – 1.67 (m, 1H), 1.59 – 1.54 (m, 1H), 1.46 – 1.41 (m, 1H), 1.34 – 1.26 (m, 2H).

**$^1\text{H NMR}$  (2.9b)** (600 MHz,  $\text{CDCl}_3$ ):  $\delta$  8.50 (dd,  $J = 4.4$ , 1.9 Hz, 2H), 7.22 – 7.17 (m, 2H), 6.49 (t,  $J = 7.5$  Hz, 1H), 6.33 (t,  $J = 7.5$  Hz, 1H), 3.13 (dd,  $J = 10.1$ , 5.7 Hz, 1H), 2.84 – 2.76 (m, 1H), 2.75 – 2.69 (m, 1H), 2.48 (d,  $J = 3.3$  Hz, 1H), 2.14 (ddd,  $J = 12.9$ , 10.1, 2.0 Hz, 1H), 1.74 – 1.72 (m, 1H), 1.63 – 1.59 (m, 1H), 1.38 (dt,  $J = 11.4$ , 3.3 Hz, 1H), 1.08 – 0.98 (m, 1H).

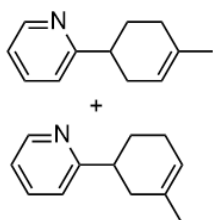
**$^{13}\text{C NMR}$  (2.9a)** (151 MHz,  $\text{CDCl}_3$ ):  $\delta$  157.5, 148.8, 135.6, 131.6, 43.2, 36.2, 35.4, 30.3, 30.0, 27.1, 24.0.

$^{13}\text{C}$  NMR (**2.9b**) (151 MHz,  $\text{CDCl}_3$ ):  $\delta$  149.1, 135.2, 134.4, 125.5, 42.5, 35.8, 30.5, 29.8, 26.0, 24.4, 8.9.

HRMS (EI/QTOF)  $m/z$ :  $[\text{M}]^+$  Calcd for  $\text{C}_{13}\text{H}_{15}\text{N}$  186.1283, found 186.1279.

### 2-(4-methylcyclohex-3-en-1-yl)pyridine (**2.10a**) and

### 2-(3-methylcyclohex-3-en-1-yl)pyridine (**2.10b**)



2-(4-methylcyclohex-3-en-1-yl) pyridine and 2-(3-methylcyclohex-3-en-1-yl) pyridine were prepared according to the general Diels-Alder procedure using 2-vinylpyridine (215  $\mu\text{L}$ , 2 mmol, 1 equiv),  $\text{BF}_3 \cdot \text{OEt}_2$  (132  $\mu\text{L}$ , 1 mmol, 0.5 equiv), and isoprene (398  $\mu\text{L}$ , 4 mmol, 2 equiv) in acetonitrile (4 mL). The resulting mixture was stirred at 70  $^\circ\text{C}$  for 24 hr. After workup, the reaction mixture was purified on an alumina flash column (5% to 15% EtOAc/hexanes) to give products **2.10a** and **2.10b** as a colorless oil (212.9 mg, 1.23 mmol, 61% yield). Regioselectivity determined as 10:1 based on NMR integration of **2.10a**:**2.10b**.

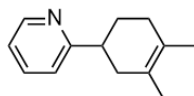
TLC (Vanillin, 25% EtOAc/Hexanes)  $R_f$  = 0.62.

$^1\text{H}$  NMR (**2.10a**) (600 MHz,  $\text{CDCl}_3$ ):  $\delta$  8.52 (s, 1H), 7.62 – 7.54 (m, 1H), 7.15 (d,  $J$  = 7.8 Hz, 1H), 7.09 – 7.04 (m, 1H), 5.57 – 5.38 (m, 1H), 2.90 (dd,  $J$  = 12.1, 5.7, Hz, 1H), 2.34 – 2.22 (m, 2H), 2.21 – 2.07 (m, 2H), 2.04 – 1.92 (m, 2H), 1.87 – 1.74 (m, 1H), 1.68 (s, 3H).

**<sup>13</sup>C NMR (2.10a and 2.10b)** (151 MHz, CDCl<sub>3</sub>): δ 165.9, 149.1, 136.3, 133.9, 133.4, 121.2, 121.0, 120.7, 120.4, 42.6, 42.1, 36.3, 31.6, 30.4, 29.0, 28.4, 25.6, 23.6, 23.5.

**HRMS** (EI/QTOF) m/z: [M]<sup>+</sup> Calcd for C<sub>12</sub>H<sub>15</sub>N 174.1283, found 174.1279

### **2-(3,4-dimethylcyclohex-3-en-1-yl)pyridine (2.11)**



2-(3,4-dimethylcyclohex-3-en-1-yl)pyridine was prepared according to the general Diels-Alder procedure using 2-vinylpyridine (215 μL, 2 mmol, 1 equiv), BF<sub>3</sub>·OEt<sub>2</sub> (132 μL, 1 mmol, 0.5 equiv), and 2,3-dimethylbutadiene (458 μL, 4 mmol, 2 equiv) in acetonitrile (4 mL). The resulting mixture was stirred at 70 °C for 24 hr. After workup, the reaction mixture was purified on a silica flash column (5% to 15% EtOAc/hexanes) to give product **2.11** as a yellow oil (282.1 mg, 1.51 mmol, 75% yield).

**TLC** (Vanillin, 25% EtOAc/Hexanes) R<sub>f</sub> = 0.66.

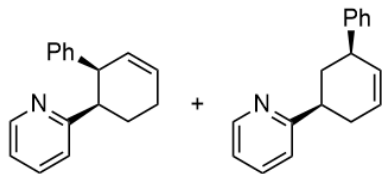
**<sup>1</sup>H NMR** (600 MHz, CDCl<sub>3</sub>): δ 8.52 (dt, J = 4.9, 1.4 Hz, 1H), 7.57 (td, J = 7.6, 1.4 Hz, 1H), 7.14 (d, J = 7.6 Hz, 1H), 7.05 – 7.07 (dd, J = 7.6, 4.9 Hz, 1H), 2.96 – 2.90 (m, 1H), 2.29 – 2.21 (m, 1H), 2.18 (m, 2H), 2.02 – 1.93 (m, 2H), 1.81 – 1.73 (m, 1H), 1.63 (s, 6H).

**<sup>13</sup>C NMR** (151 MHz, CDCl<sub>3</sub>): δ 165.9, 149.1, 136.3, 125.3, 125.0, 121.1, 121.0, 43.0, 38.0, 32.1, 29.3, 19.0.

**HRMS** (EI/QTOF) m/z: [M]<sup>+</sup> Calcd for C<sub>13</sub>H<sub>17</sub>N 188.1440, found 188.1450.

### **2-((1S,2R)-1,2,3,4-tetrahydro-[1,1'-biphenyl]-2-yl)pyridine (2.12a) and**

**2-((1R,3R)-1,2,3,4-tetrahydro-[1,1'-biphenyl]-3-yl)pyridine (2.12b)**



2-((1S,2R)-1,2,3,4-tetrahydro-[1,1'-biphenyl]-2-yl)pyridine and 2-((1R,3R)-1,2,3,4-tetrahydro-[1,1'-biphenyl]-3-yl)pyridine were prepared according to the general Diels-Alder procedure using 2-vinylpyridine (215  $\mu$ L, 2 mmol, 1 equiv),  $\text{BF}_3 \cdot \text{OEt}_2$  (132  $\mu$ L, 1 mmol, 0.5 equiv), and *trans*-1-phenyl-1,3-butadiene (559  $\mu$ L, 4 mmol, 2 equiv) in acetonitrile (4 mL). The resulting mixture was stirred at 70  $^\circ\text{C}$  for 24 hr. After workup, the reaction mixture was purified on an alumina flash column (5% to 15% EtOAc/hexanes) to give products **2.12a** and **2.12b** as a yellow oil (296.8 mg, 1.26 mmol, 63% yield). Regioselectivity determined as >20:1 based on NMR integration of **2.12a:2.12b**. Diastereoselectivity determined as >99:1 based on the absence of diastereomeric peaks on NMR.

**TLC** (Vanillin, 25% EtOAc/Hexanes)  $R_f = 0.59$ .

**$^1\text{H NMR}$  (2.12a)** (600 MHz,  $\text{CDCl}_3$ ):  $\delta$  8.48 (dd,  $J = 4.9, 1.9$  Hz, 1H), 7.27 (td,  $J = 7.7, 1.9$  Hz, 1H), 7.04 – 6.94 (m, 4H), 6.74 – 6.68 (m, 2H), 6.39 (dt,  $J = 7.7, 1.0$  Hz, 1H), 6.06 – 5.99 (m, 1H), 5.85 (dd,  $J = 9.7, 5.0$ , Hz, 1H), 3.94 – 3.89 (m, 1H), 3.47 (ddd,  $J = 13.3, 5.0, 2.5$  Hz, 1H), 2.41 – 2.26 (m, 2H), 2.00 (ddd,  $J = 13.3, 11.0, 6.1$  Hz, 1H), 1.79 – 1.70 (m, 1H).

**$^1\text{H NMR}$  (2.12b)** (600 MHz,  $\text{CDCl}_3$ ):  $\delta$  8.52 (dd,  $J = 4.9, 1.9$  Hz, 1H), 7.35 (td,  $J = 7.6, 1.9$  Hz, 1H), 7.13 – 7.07 (m, 2H), 6.98 – 6.92 (m, 5H), 5.89 – 5.93 (m, 1H), 5.75 (dd,  $J = 9.8, 2.9$  Hz, 1H), 3.83 (ddd,  $J = 9.8, 4.3, 2.9$  Hz, 1H), 2.88 (td,  $J = 12.6, 2.9$  Hz, 1H), 2.26 – 2.18 (m, 2H), 2.11 – 2.13 (m, 1H), 1.96 – 1.90 (m, 1H).

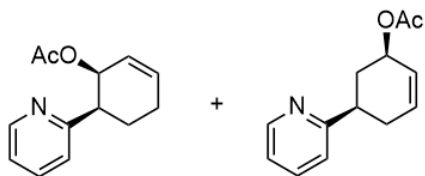
<sup>13</sup>C NMR (**2.12a**) (151 MHz, CDCl<sub>3</sub>): δ 163.6, 148.5, 148.4, 140.2, 135.6, 129.8, 129.1, 128, 127.2, 126.1, 121.8, 121.0, 46.9, 46.1, 26.0, 26.0, 21.0.

HRMS (EI/QTOF) m/z: [M]<sup>+</sup> Calcd for C<sub>17</sub>H<sub>17</sub>N 236.1440, found 236.1440.

In a separate reaction, 2-vinylpyridine (677 μL, 6 mmol, 1 equiv), BF<sub>3</sub>·OEt<sub>2</sub> (395 μL, 3 mmol, 0.5 equiv), and *trans*-1-phenyl-1,3-butadiene (1.65 g, 10 mmol, 2 equiv), were reacted in a 25mL r.b. flask fitted with a condenser with amounts of reagents adjusted to meet the larger scale. General procedure was followed except for the reaction vessel, which was open to air. The product was isolated as a yellow oil (785.0 mg, 3.34 mmol, 53%).

**(1S,6S)-6-(pyridin-2-yl)cyclohex-2-en-1-yl acetate (2.13a) and**

**(1R,5R)-5-(pyridin-2-yl)cyclohex-2-en-1-yl acetate (2.13b)**



(1S,6S)-6-(pyridin-2-yl)cyclohex-2-en-1-yl acetate and (1R,5R)-5-(pyridin-2-yl)cyclohex-2-en-1-yl acetate were prepared according to the general Diels-Alder procedure using 2-vinylpyridine (215 μL, 2 mmol, 1 equiv), BF<sub>3</sub>·OEt<sub>2</sub> (132 μL, 1 mmol, 0.5 equiv), and *trans*-1-acetoxy-1,3-butadiene (474 μL, 4 mmol, 2 equiv) in acetonitrile (4 mL). The resulting mixture was stirred at 70 °C for 24 hr. After workup, the reaction mixture was purified on an alumina flash column (5% to 15% EtOAc/hexanes) to give product **2.13a** and **2.13b** as a yellow oil (307.9 mg, 1.42 mmol,

71% yield). Regioselectivity determined as 20:1 based on NMR integration of **2.13a**:**2.13b**. Diastereoselectivity determined as >99:1 based on the absence of diastereomeric peaks on NMR.

**TLC** (Vanillin, 25% EtOAc/Hexanes)  $R_f = 0.63$ .

**$^1\text{H}$  NMR (2.13a)** (600 MHz,  $\text{CDCl}_3$ ): 8.51 (dd,  $J = 5.6, 1.7$  Hz, 1H), 7.59 (td,  $J = 7.7, 1.7$  Hz, 1H), 7.19 (d,  $J = 7.7$  Hz, 1H), 7.13 – 7.08 (m, 1H), 6.03 – 6.06 (m, 1H), 5.96 – 5.89 (m, 1H), 5.53 (d,  $J = 4.5$  Hz, 1H), 3.18 (dt,  $J = 12.8, 3.2$  Hz, 1H), 2.36 – 2.27 (m, 1H), 2.24 – 2.11 (m, 2H), 1.98 – 1.93 (m, 1H), 1.74 (s, 3H).

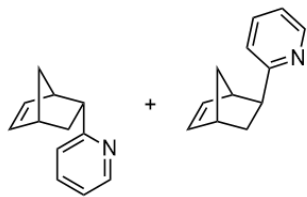
**$^{13}\text{C}$  NMR (2.13a)** (151 MHz,  $\text{CDCl}_3$ ):  $\delta$  170.1, 161.4, 149.0, 135.9, 133.3, 124.8, 122.1, 121.5, 68.5, 45.9, 25.8, 21.3, 20.8.

**HRMS** (EI/QTOF)  $m/z$ :  $[\text{M}]^+$  Calcd for  $\text{C}_{13}\text{H}_{15}\text{NO}_2$  218.1182, found 218.1178.

In a separate reaction, 2-vinylpyridine (4.80 mL, 40 mmol, 1 equiv),  $\text{BF}_3 \cdot \text{OEt}_2$  (2.75 mL, 20 mmol, 0.5 equiv), and *trans*-1-acetoxy-1,3-butadiene (10.0 g, 90 mmol, 2 equiv) using the general Diels-Alder procedure above, with amounts of reagents adjusted to meet the larger scale. The product was isolated as a yellow oil (4.95 g, 20 mmol, 51%).

**2-((1S,2R,4R)-bicyclo[2.2.1]heptan-2-yl)pyridine (2.14a) and**

**2-((1S,2S,4R)-bicyclo[2.2.1]heptan-2-yl)pyridine (2.14b)**



2-((1S,2R,4R)-bicyclo[2.2.1]heptan-2-yl)pyridine and 2-((1S,2S,4R)-bicyclo[2.2.1]heptan-2-yl)pyridine were prepared according to the general Diels-Alder procedure using 2-vinylpyridine (215  $\mu$ L, 2 mmol, 1 equiv),  $\text{BF}_3 \cdot \text{OEt}_2$  (132  $\mu$ L, 1 mmol, 0.5 equiv), and freshly distilled cyclopentadiene (264  $\mu$ L, 4 mmol, 2 equiv) in acetonitrile (4 mL). The resulting mixture was stirred at 70  $^\circ\text{C}$  for 24 hr. After workup, the reaction mixture was purified on an alumina flash column (5% to 15% EtOAc/hexanes) to give products **2.14a** and **2.14b** as a colorless oil (341.9 mg, 1.99 mmol, 99% yield). Diastereoselectivity determined as >20:1 based on NMR integration of **2.14a**:**2.14b**.

**TLC** (Vanillin, 25% EtOAc/Hexanes)  $R_f = 0.49$ .

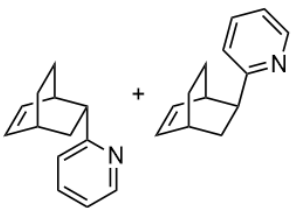
**$^1\text{H}$  NMR (2.14a)** (600 MHz,  $\text{CDCl}_3$ ):  $\delta$  8.46 (dd,  $J = 4.8, 1.9$  Hz, 1H), 7.49 (td,  $J = 7.7, 1.9$  Hz, 1H), 7.06 – 6.99 (m, 2H), 6.20 (dd,  $J = 5.7, 3.0$  Hz, 1H), 5.73 (dd,  $J = 5.7, 3.0$  Hz, 1H), 3.56 (ddd,  $J = 8.9, 4.1, 3.0$  Hz, 1H), 3.25 (s, 1H), 2.93 (s, 1H), 2.19 (dd,  $J = 8.9, 4.1$  Hz, 1H), 1.51 – 1.44 (m, 3H).

**$^{13}\text{C}$  NMR (2.14a)** (151 MHz,  $\text{CDCl}_3$ ):  $\delta$  146.1, 135.1, 129.7, 121.0, 47.7, 45.8, 45.0, 40.7, 40.6.

**HRMS** (EI/QTOF)  $m/z$ :  $[\text{M}]^+$  Calcd for  $\text{C}_{12}\text{H}_{13}\text{N}$  172.1127, found 172.1125.

**2-((1R,2R,4R)-bicyclo[2.2.2]oct-5-en-2-yl)pyridine (2.15a) and**

**2-((1R,2S,4R)-bicyclo[2.2.2]oct-5-en-2-yl)pyridine (2.15b)**



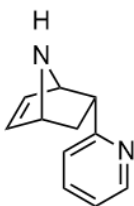
2-((1R,2R,4R)-bicyclo[2.2.2]oct-5-en-2-yl)pyridine and 2-((1R,2S,4R)-bicyclo[2.2.2]oct-5-en-2-yl)pyridine were prepared according to the general Diels-Alder procedure using 2-vinylpyridine (215  $\mu$ L, 2 mmol, 1 equiv),  $\text{BF}_3 \cdot \text{OEt}_2$  (132  $\mu$ L, 1 mmol, 0.5 equiv), and 1,3-cyclohexadiene (380  $\mu$ L, 4 mmol, 2 equiv) in acetonitrile (4 mL). The resulting mixture was stirred at 70  $^\circ\text{C}$  for 24 hr. After workup, the reaction mixture was purified on a silica flash column (5% to 15% EtOAc/hexanes) to give products **2.15a** and **2.15b** as a colorless oil (186.9 mg, 1.02 mmol, 51% yield). Diastereoselectivity determined as >20:1 based on NMR integration of **2.15a**:**2.15b**.

**TLC** (Vanillin, 25% EtOAc/Hexanes)  $R_f = 0.53$ .

**$^1\text{H}$  NMR (2.15a)** (600 MHz,  $\text{CDCl}_3$ ):  $\delta$  8.46 (dd,  $J = 4.9, 1.9$  Hz, 1H), 7.52 (td,  $J = 7.7, 1.9$  Hz, 1H), 7.11 (d,  $J = 7.7$  Hz, 1H), 7.03 (dd,  $J = 7.7, 4.9$  Hz, 1H), 6.37 – 6.41 (m, 1H), 6.17 – 6.09 (m, 1H), 3.19 (dd,  $J = 10.0, 5.9$  Hz, 1H), 2.80 – 2.74 (m, 1H), 2.69 – 2.62 (m, 1H), 2.07 (dd,  $J = 12.8, 10.0$  Hz, 1H), 1.78 – 1.72 (m, 1H), 1.69 – 1.62 (m, 1H), 1.62 – 1.54 (m, 1H), 1.36 – 1.26 (m, 2H).  
 **$^{13}\text{C}$  NMR (2.15a)** (151 MHz,  $\text{CDCl}_3$ ):  $\delta$  166.5, 148.6, 136.0, 135.1, 131.9, 121.5, 120.8, 45.7, 35.7, 34.2, 30.2, 27.1, 24.3.

**HRMS** (EI/QTOF)  $m/z$ :  $[\text{M}]^+$  Calcd for  $\text{C}_{13}\text{H}_{15}\text{N}$  186.1283, found 186.1280.

**(1R,4R,5R)-5-(pyridin-2-yl)-7-azabicyclo[2.2.1]hept-2-ene (2.16)**



(1R,4R,5R)-5-(pyridin-2-yl)-7-azabicyclo[2.2.1]hept-2-ene was prepared according to the general Diels-Alder procedure using 2-vinylpyridine (215  $\mu$ L/mg, 2 mmol, 1 equiv),  $\text{BF}_3 \cdot \text{OEt}_2$  (132  $\mu$ L, 1

mmol, 0.5 equiv), and pyrrole (277  $\mu$ L, 4 mmol, 2 equiv) in acetonitrile (4 mL). The resulting mixture was stirred at 70  $^{\circ}$ C for 24 hr. After workup, the reaction mixture was purified on an alumina flash column (5% to 15% EtOAc/hexanes) to give product **2.16** as a brown solid (191.1 mg, 1.11 mmol, 55% yield). Diastereoselectivity determined as >99:1 based on the absence of diastereomeric peaks on NMR.

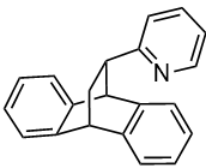
**TLC** (Vanillin, 25% EtOAc/Hexanes)  $R_f$  = 0.16.

**$^1\text{H}$  NMR** (600 MHz,  $\text{CDCl}_3$ ):  $\delta$  8.92 (br s, 1H), 8.60 – 8.54 (m, 1H), 7.60 (td,  $J$  = 7.5, 1.9 Hz, 1H), 7.14 (dd,  $J$  = 7.5, 1.9 Hz, 2H), 6.68 – 6.62 (m, 1H), 6.10 (d,  $J$  = 3.0 Hz, 1H), 5.93 (d,  $J$  = 3.0 Hz, 1H), 3.13 (dd,  $J$  = 7.6, 5.6 Hz, 2H), 3.07 (dd,  $J$  = 7.6, 5.6 Hz, 2H).

**$^{13}\text{C}$  NMR** (151 MHz,  $\text{CDCl}_3$ ):  $\delta$  161.3, 149.0, 136.7, 132.0, 123.4, 121.3, 116.3, 107.9, 105.2, 38.0, 27.0.

**HRMS** (EI/QTOF)  $m/z$ :  $[\text{M}]^+$  Calcd for  $\text{C}_{11}\text{H}_{12}\text{N}_2$  173.1079, found 173.1075.

### 2-((9S,10S,12R)-9,10-dihydro-9,10-ethanoanthracen-12-yl)pyridine (**2.17**)



2-((9S,10S,12R)-9,10-dihydro-9,10-ethanoanthracen-12-yl)pyridine was prepared according to the general Diels-Alder procedure using 2-vinylpyridine (215  $\mu$ L, 2 mmol, 1 equiv),  $\text{BF}_3 \cdot \text{OEt}_2$  (132  $\mu$ L, 1 mmol, 0.5 equiv), and anthracene (713 mg, 4 mmol, 2 equiv) in acetonitrile (4 mL). The resulting mixture was stirred at 70  $^{\circ}$ C for 72 hr. After workup, the reaction mixture was purified on a silica flash column (5% to 15% EtOAc/hexanes) to give product **2.17** as a yellow solid (250.0 mg, 0.88 mmol, 44% yield).

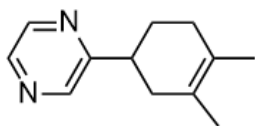
**TLC** (Vanillin, 25% EtOAc/Hexanes)  $R_f = 0.65$ .

**$^1\text{H NMR}$**  (600 MHz,  $\text{CDCl}_3$ ):  $\delta$  8.47 (d,  $J = 4.1$  Hz, 1H), 7.41 – 7.35 (m, 3H), 7.34 – 7.30 (m, 1H), 7.15 – 7.11 (m, 3H), 7.06 (dd,  $J = 7.4, 4.1$  Hz, 1H), 6.98 (td,  $J = 7.4, 1.2$  Hz, 1H), 6.88 (d,  $J = 6.7$  Hz, 1H), 6.19 (d,  $J = 8.1$  Hz, 1H), 4.47 – 4.43 (m, 2H), 3.59 (dd,  $J = 10.4, 2.6$  Hz, 1H), 2.33 (ddd,  $J = 12.9, 10.4, 2.6$  Hz, 1H), 2.00 (dd,  $J = 12.9, 2.6$  Hz, 1H).

**$^{13}\text{C NMR}$**  (151 MHz,  $\text{CDCl}_3$ ):  $\delta$  163.2, 147.8, 144.1, 143.5, 143.5, 140.0, 136.6, 126.1, 125.9, 125.9, 125.8, 125.4, 123.7, 123.4, 123.0, 121.7, 121.5, 50.5, 46.5, 44.4, 34.3.

**HRMS** (EI/QTOF)  $m/z$ :  $[\text{M}]^+$  Calcd for  $\text{C}_{21}\text{H}_{17}\text{N}$  284.1440, found 288.1434.

### 2-(3,4-dimethylcyclohex-3-en-1-yl)pyrazine (**2.18**)



2-(3,4-dimethylcyclohex-3-en-1-yl)pyrazine was prepared according to the general Diels-Alder procedure using 2-vinylpyrazine (204  $\mu\text{L}$ , 2 mmol, 1 equiv),  $\text{BF}_3 \cdot \text{OEt}_2$  (132  $\mu\text{L}$ , 1 mmol, 0.5 equiv), and 2,3-dimethylbutadiene (456  $\mu\text{L}$ , 4 mmol, 2 equiv) in acetonitrile (4 mL). The resulting mixture was stirred at 70  $^\circ\text{C}$  for 24 hr. After workup, the reaction mixture was purified on a silica flash column (5% to 15% EtOAc/hexanes) to give product **2.18** as an orange oil. (180.5 mg, 0.96 mmol, 48% yield).

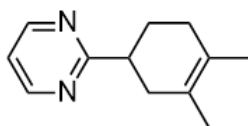
**TLC** (Vanillin, 25% EtOAc/Hexanes)  $R_f = 0.62$ .

**$^1\text{H NMR}$**  (600 MHz,  $\text{CDCl}_3$ ):  $\delta$  8.51 – 8.44 (m, 2H), 8.37 (d,  $J = 2.5$  Hz, 1H), 3.02 – 2.93 (m, 1H), 2.34 – 2.25 (m, 1H), 2.21 – 2.12 (m, 2H), 2.04 – 1.91 (m, 2H), 1.86 – 1.77 (m, 1H), 1.63 (s, 3H), 1.62 (s, 3H).

$^{13}\text{C}$  NMR (151 MHz,  $\text{CDCl}_3$ ):  $\delta$  161.2, 144.0, 143.6, 142.2, 125.5, 124.6, 40.5, 37.3, 31.7, 28.8, 19.0, 18.9.

HRMS (EI/QTOF)  $m/z$ :  $[\text{M}]^+$  Calcd for  $\text{C}_{12}\text{H}_{26}\text{N}_2$  189.1392, found 189.1389.

### 2-(3,4-dimethylcyclohex-3-en-1-yl)pyrimidine (2.19)



2-(3,4-dimethylcyclohex-3-en-1-yl)pyrimidine was prepared according to the general Diels-Alder procedure using 2-vinylpyrimidine (212  $\mu\text{L}$ , 2 mmol, 1 equiv),  $\text{BF}_3 \cdot \text{OEt}_2$  (132  $\mu\text{L}$ , 1 mmol, 0.5 equiv), and 2,3-dimethylbutadiene (456  $\mu\text{L}$ , 4 mmol, 2 equiv) in acetonitrile (4 mL). The resulting mixture was stirred at 70  $^\circ\text{C}$  for 24 hr. After workup, the reaction mixture was purified on a silica flash column (5% to 15% EtOAc/hexanes) to give product **18** as a yellow oil (248.5 mg, 1.32 mmol, 66% yield).

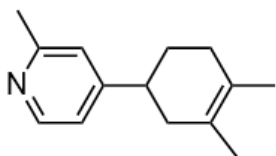
TLC (Vanillin, 25% EtOAc/Hexanes)  $R_f$  = 0.59.

$^1\text{H}$  NMR (600 MHz,  $\text{CDCl}_3$ ):  $\delta$  8.62 (d,  $J$  = 4.9 Hz, 2H), 7.06 (t,  $J$  = 4.9 Hz, 1H), 3.06 (ddd,  $J$  = 12.3, 11.1, 5.3 Hz, 1H), 2.42 – 2.31 (m, 1H), 2.22 – 2.12 (m, 2H), 2.02 (dd,  $J$  = 12.3, 5.3 Hz, 1H), 1.95 – 1.99 (m, 1H), 1.76 – 1.73 (m, 1H), 1.59 (s, 6H).

$^{13}\text{C}$  NMR (151 MHz,  $\text{CDCl}_3$ ):  $\delta$  174.2, 156.9, 125.3, 124.7, 118.4, 44.1, 36.6, 32.0, 28.7, 19.0, 18.8.

HRMS (EI/QTOF)  $m/z$ :  $[\text{M}]^+$  Calcd for  $\text{C}_{12}\text{H}_{26}\text{N}_2$  189.1392, found 189.1387.

#### 4-(3,4-dimethylcyclohex-3-en-1-yl)-2-methylpyridine (2.20)



4-(3,4-dimethylcyclohex-3-en-1-yl)-2-methylpyridine was prepared according to the general Diels-Alder procedure using 2-methyl-4-vinylpyridine (238  $\mu\text{L}$ , 2 mmol, 1 equiv),  $\text{BF}_3 \cdot \text{OEt}_2$  (132  $\mu\text{L}$ , 1 mmol, 0.5 equiv), and 2,3-dimethylbutadiene (456  $\mu\text{L}$ , 4 mmol, 2 equiv) in acetonitrile (4 mL). The resulting mixture was stirred at 70  $^\circ\text{C}$  for 24 hr. After workup, the reaction mixture was purified on a silica flash column (5% to 15% EtOAc/hexanes) to give product **2.20** as a colorless oil (269.1 mg, 1.33 mmol, 67% yield).

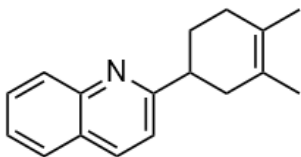
**TLC** (Vanillin, 25% EtOAc/Hexanes)  $R_f = 0.30$ .

**$^1\text{H NMR}$**  (600 MHz,  $\text{CDCl}_3$ ):  $\delta$  8.36 (d,  $J = 5.2$  Hz, 1H), 6.99 (d,  $J = 1.7$  Hz, 1H), 6.94 (dd,  $J = 5.2, 1.7$  Hz, 1H), 2.76 – 2.67 (m, 1H), 2.52 (s, 3H), 2.17 – 2.03 (m, 3H), 2.02 – 1.95 (m, 1H), 1.85 – 1.88 (m, 1H), 1.70 – 1.64 (m, 1H), 1.63 (s, 6H).

**$^{13}\text{C NMR}$**  (151 MHz,  $\text{CDCl}_3$ ):  $\delta$  157.9, 156.8, 148.6, 125.7, 124.7, 122.0, 119.6, 40.2, 38.8, 31.8, 31.8, 29.5, 24.2, 19.0, 18.8.

**HRMS** (EI/QTOF)  $m/z$ :  $[\text{M}]^+$  Calcd for  $\text{C}_{14}\text{H}_{19}\text{N}$  202.1596, found 202.1591.

#### 2-(3,4-dimethylcyclohex-3-en-1-yl)quinoline (2.21)



2-(3,4-dimethylcyclohex-3-en-1-yl)quinoline was prepared according to the general Diels-Alder procedure using 2-vinylquinoline (301  $\mu\text{L}/\text{mg}$ , 2 mmol, 1 equiv),  $\text{BF}_3 \cdot \text{OEt}_2$  (132  $\mu\text{L}$ , 1 mmol, 0.5 equiv), and 2,3-dimethylbutadiene (456  $\mu\text{L}$ , 4 mmol, 2 equiv) in acetonitrile (4 mL). The resulting mixture was stirred at 70  $^\circ\text{C}$  for 24 hr. After workup, the reaction mixture was purified on a silica flash column (5% to 15% EtOAc/hexanes) to give product **2.21** as an orange oil (422.2 mg, 1.78 mmol, 89% yield).

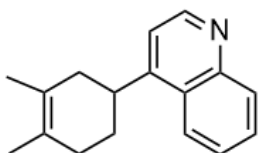
**TLC** (Vanillin, 25% EtOAc/Hexanes)  $R_f = 0.80$ .

**$^1\text{H NMR}$**  (600 MHz,  $\text{CDCl}_3$ ):  $\delta$  8.12 (dt,  $J = 8.5, 0.9$  Hz, 1H), 8.07 (dd,  $J = 8.5, 0.9$  Hz, 1H), 7.72 (dd,  $J = 8.1, 1.4$  Hz, 1H), 7.64 (ddd,  $J = 8.5, 6.8, 1.4$  Hz, 1H), 7.43 (ddd,  $J = 8.1, 6.8, 1.4$  Hz, 1H), 7.29 (d,  $J = 8.5$  Hz, 1H), 3.21 (ddd,  $J = 12.1, 10.9, 5.4$  Hz, 1H), 2.38 – 2.31 (m, 1H), 2.29 – 2.16 (m, 2H), 2.08 – 1.94 (m, 2H), 1.91 – 1.81 (m, 1H), 1.63 (s, 6H).

**$^{13}\text{C NMR}$**  (151 MHz,  $\text{CDCl}_3$ ):  $\delta$  166.1, 146.7, 137.4, 130.5, 129.8, 128.1, 127.5, 127.0, 126.0, 125.5, 124.7, 119.7, 43.4, 37.7, 31.9, 29.2, 18.9.

**HRMS** (EI/QTOF)  $m/z$ :  $[\text{M}]^+$  Calcd for  $\text{C}_{17}\text{H}_{19}\text{N}$  238.1596, found 238.1592.

#### 4-(3,4-dimethylcyclohex-3-en-1-yl)quinoline (**2.22**)



4-(3,4-dimethylcyclohex-3-en-1-yl)quinoline was prepared according to the general Diels-Alder procedure using 4-vinylquinoline (282  $\mu\text{L}$ , 2 mmol, 1 equiv),  $\text{BF}_3 \cdot \text{OEt}_2$  (132  $\mu\text{L}$ , 1 mmol, 0.5 equiv), and 2,3-dimethylbutadiene (456  $\mu\text{L}$ , 4 mmol, 2 equiv) in acetonitrile (4 mL). The resulting mixture was stirred at 70  $^\circ\text{C}$  for 24 hr. After workup, the reaction mixture was purified on a silica

flash column (5% to 15% EtOAc/hexanes) to give product **2.22** as a yellow oil (360.4 mg, 1.52 mmol, 76% yield).

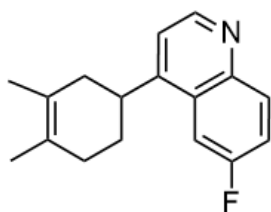
**TLC** (Vanillin, 25% EtOAc/Hexanes)  $R_f = 0.58$ .

**$^1\text{H NMR}$**  (600 MHz,  $\text{CDCl}_3$ ):  $\delta$  8.78 (d,  $J = 4.7$  Hz, 1H), 8.12 (d,  $J = 8.4$  Hz, 1H), 8.04 (d,  $J = 6.7$  Hz, 1H), 7.62 (dd,  $J = 8.4, 6.7$  Hz, 1H), 7.48 (dd,  $J = 8.4, 6.7$  Hz, 1H), 7.22 (s, 1H), 3.55 (ddd,  $J = 11.0, 8.0, 5.3$  Hz, 1H), 2.13 – 2.20 (m, 2H), 2.14 – 2.05 (m, 1H), 1.93 – 1.96 (m, 1H), 1.91 (d,  $J = 12.5$  Hz, 1H), 1.80 (ddd,  $J = 12.5, 11.0, 5.3$  Hz, 1H), 1.63 (s, 3H), 1.60 (s, 3H).

**$^{13}\text{C NMR}$**  (151 MHz,  $\text{CDCl}_3$ ):  $\delta$  153.9, 149.6, 147.4, 129.6, 129.2, 127.1, 126.5, 125.7, 124.8, 123.1, 117.6, 38.9, 35.3, 31.9, 29.2, 19.0, 18.9.

**HRMS** (EI/QTOF)  $m/z$ :  $[\text{M}]^+$  Calcd for  $\text{C}_{17}\text{H}_{19}\text{N}$  238.1596, found 238.1592.

#### 4-(3,4-dimethylcyclohex-3-en-1-yl)-6-fluoroquinoline (2.23)



4-(3,4-dimethylcyclohex-3-en-1-yl)-6-fluoroquinoline was prepared according to the general Diels-Alder procedure using 6-fluoro-4-vinylquinoline (346 mg, 2 mmol, 1 equiv),  $\text{BF}_3 \cdot \text{OEt}_2$  (132  $\mu\text{L}$ , 1 mmol, 0.5 equiv), and 2,3-dimethylbutadiene (456  $\mu\text{L}$ , 4 mmol, 2 equiv) in acetonitrile (4 mL). The resulting mixture was stirred at 70  $^\circ\text{C}$  for 24 hr. After workup, the reaction mixture was purified on a silica flash column (5% to 15% EtOAc/hexanes) to give product **2.23** as a yellow solid (390.3 mg, 1.62 mmol, 81% yield).

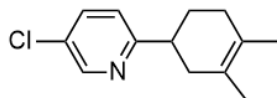
**TLC** (Vanillin, 25% EtOAc/Hexanes)  $R_f = 0.57$ .

**<sup>1</sup>H NMR** (600 MHz, CDCl<sub>3</sub>): δ 8.72 (d, J = 4.7 Hz, 1H), 8.08 (dd, J = 9.2, 5.6 Hz, 1H), 7.60 (dd, J = 10.4, 2.8 Hz, 1H), 7.36 (ddd, J = 9.2, 7.9, 2.8 Hz, 1H), 7.19 (d, J = 4.7 Hz, 1H), 3.36 (ddd, J = 10.7, 5.1, 2.8 Hz, 1H), 2.23 – 2.10 (m, 2H), 2.09 – 2.01 (m, 1H), 1.96 – 1.92 (m, 1H), 1.91 – 1.84 (m, 1H), 1.75 (ddd, J = 12.6, 11.0, 5.4 Hz, 1H), 1.59 (s, 3H), 1.57 (s, 3H).

**<sup>13</sup>C NMR** (151 MHz, CDCl<sub>3</sub>): δ 161.4, 159.7, 153.1, 153.1, 149.0, 148.9, 144.6, 132.2, 132.1, 127.9, 127.9, 125.7, 124.7, 119.3, 119.2, 118.1, 106.9, 106.7, 38.6, 38.6, 35.5, 31.7, 29.1, 18.9, 18.8.

**HRMS** (EI/QTOF) m/z: [M]<sup>+</sup> Calcd for C<sub>16</sub>H<sub>16</sub>NF 242.1346, found 242.1346.

### 5-chloro-2-(3,4-dimethylcyclohex-3-en-1-yl)pyridine (2.25)



5-chloro-2-(3,4-dimethylcyclohex-3-en-1-yl)pyridine was prepared according to the general Diels-Alder procedure using 5-chloro-2-vinylpyridine (252 μL, 2 mmol, 1 equiv), BF<sub>3</sub>·OEt<sub>2</sub> (132 μL, 1 mmol, 0.5 equiv), and 2,3-dimethylbutadiene (456 μL, 4 mmol, 2 equiv) in acetonitrile (4 mL). The resulting mixture was stirred at 70 °C for 24 hr. After workup, the reaction mixture was purified on a silica flash column (5% to 15% EtOAc/hexanes) to give product **2.25** as a colorless oil (380.0 mg, 1.72 mmol, 86% yield).

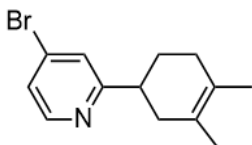
**TLC** (Vanillin, 25% EtOAc/Hexanes) R<sub>f</sub> = 0.44.

**<sup>1</sup>H NMR** (800 MHz, CDCl<sub>3</sub>): δ 8.51 (d, J = 5.9 Hz, 1H), 7.60 (d, J = 7.2 Hz, 1H), 7.15 (dd, J = 7.2, 5.9 Hz, 1H), 2.97 (s, 1H), 2.19 – 2.25 (m, 3H), 2.01 (s, 2H), 1.78 (dd, J = 11.9, 5.9 Hz, 1H), 1.68 (s, 6H).

$^{13}\text{C}$  NMR (201 MHz,  $\text{CDCl}_3$ ):  $\delta$  164.2, 147.9, 136.1, 129.3, 125.5, 124.8, 122.0, 42.4, 37.9, 31.3, 29.3, 19.1, 18.9.

HRMS (EI/QTOF)  $m/z$ :  $[\text{M}]^+$  Calcd for  $\text{C}_{13}\text{H}_{16}\text{NCl}$  222.1050, found 222.1051.

#### 4-bromo-2-(3,4-dimethylcyclohex-3-en-1-yl)pyridine (2.26)



4-bromo-2-(3,4-dimethylcyclohex-3-en-1-yl)pyridine was prepared according to the general Diels-Alder procedure using 4-bromo-2-vinylpyridine (368 mg, 2 mmol, 1 equiv),  $\text{BF}_3 \cdot \text{OEt}_2$  (132  $\mu\text{L}$ , 1 mmol, 0.5 equiv), and 2,3-dimethylbutadiene (456  $\mu\text{L}$ , 4 mmol, 2 equiv) in acetonitrile (4 mL). The resulting mixture was stirred at 70  $^\circ\text{C}$  for 24 hr. After workup, the reaction mixture was purified on a silica flash column (5% to 15% EtOAc/hexanes) to give product **2.26** as a colorless oil (418.9 mg, 1.58 mmol, 79% yield).

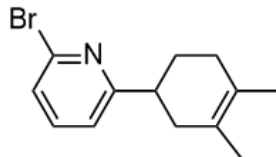
TLC (Vanillin, 25% EtOAc/Hexanes)  $R_f$  = 0.45.

$^1\text{H}$  NMR (800 MHz,  $\text{CDCl}_3$ ):  $\delta$  8.36 (s, 1H), 7.36 (s, 1H), 7.28 (d,  $J$  = 2.6 Hz, 1H), 2.97 – 2.90 (m, 1H), 2.28 – 2.23 (m, 1H), 2.22 – 2.15 (m, 2H), 2.06 – 2.00 (m, 1H), 2.01 – 1.94 (m, 1H), 1.74 – 1.79 (m, 1H), 1.66 (s, 6H).

$^{13}\text{C}$  NMR (201 MHz,  $\text{CDCl}_3$ ):  $\delta$  167.6, 149.9, 133.1, 125.4, 124.7, 124.6, 124.5, 42.9, 38.0, 32.0, 29.1, 19.1, 18.9.

HRMS (EI/QTOF)  $m/z$ :  $[\text{M}]^+$  Calcd for  $\text{C}_{13}\text{H}_{16}\text{NBr}$  266.0545, found 266.0547.

## 2-bromo-6-(3,4-dimethylcyclohex-3-en-1-yl)pyridine (2.24)



2-bromo-6-(3,4-dimethylcyclohex-3-en-1-yl)pyridine was prepared according to the general Diels-Alder procedure using 2-bromo-6-vinylpyridine (368 mg, 2 mmol, 1 equiv),  $\text{BF}_3 \cdot \text{OEt}_2$  (132  $\mu\text{L}$ , 1 mmol, 0.5 equiv), and 2,3-dimethylbutadiene (456  $\mu\text{L}$ , 4 mmol, 2 equiv) in acetonitrile (4 mL). The resulting mixture was stirred at 70 °C for 48 hr. After workup, the reaction mixture was purified on a silica flash column (2% to 5% EtOAc/hexanes) to give product **2.24** as a colorless oil (244.7 mg, 0.92 mmol, 46% yield).

**TLC** (Vanillin, 25% EtOAc/Hexanes)  $R_f = 0.88$ .

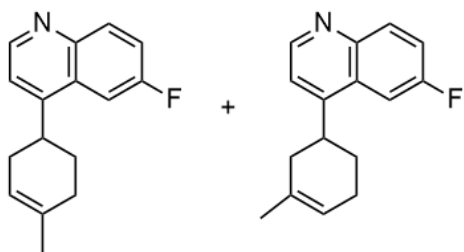
**$^1\text{H NMR}$**  (600 MHz,  $\text{CDCl}_3$ ):  $\delta$  7.44 (t,  $J = 7.7$  Hz, 1H), 7.28 (dd,  $J = 7.7, 0.9$  Hz, 1H), 7.10 (dd,  $J = 7.7, 0.9$  Hz, 1H), 2.92 (ddd,  $J = 12.2, 9.5, 6.2$  Hz, 1H), 2.25 – 2.17 (m, 2H), 2.12 – 2.14 (m, 1H), 2.01 – 1.91 (m, 2H), 1.78 – 1.69 (m, 1H), 1.63 (s, 6H).

**$^{13}\text{C NMR}$**  (151 MHz,  $\text{CDCl}_3$ ):  $\delta$  167.8, 141.5, 138.6, 125.4, 125.3, 124.6, 119.7, 42.6, 37.7, 31.8, 29.1, 19.0, 18.9.

**HRMS** (EI/QTOF)  $m/z$ :  $[\text{M}]^+$  Calcd for  $\text{C}_{13}\text{H}_{16}\text{NBr}$  266.0545, found 266.0548.

## 6-fluoro-4-(4-methylcyclohex-3-en-1-yl)quinoline (2.38a) and

## 6-fluoro-4-(3-methylcyclohex-3-en-1-yl)quinoline (2.38b)



6-fluoro-4-(4-methylcyclohex-3-en-1-yl) quinoline and 6-fluoro-4-(3-methylcyclohex-3-en-1-yl) quinoline were prepared according to the general Diels-Alder procedure using 6-fluoro-4-vinylquinoline (346 mg, 2 mmol, 1 equiv),  $\text{BF}_3 \cdot \text{OEt}_2$  (132  $\mu\text{L}$ , 1 mmol, 0.5 equiv), and isoprene (398  $\mu\text{L}$ , 4 mmol, 2 equiv) in acetonitrile (4 mL). The resulting mixture was stirred at 70 °C for 24 hr. After workup, the reaction mixture was purified on a silica flash column (5% to 15% EtOAc/hexanes) to give products **2.38a** and **2.38b** as a yellow oil (354.8 mg, 1.39 mmol, 70% yield). Regioselectivity determined as 3:1 based on NMR integration of **2.38a**:**2.38b**.

**TLC** (Vanillin, 25% EtOAc/Hexanes)  $R_f = 0.53$ .

**$^1\text{H}$  NMR (2.38a and 2.38b)**  $^1\text{H}$  NMR (600 MHz,  $\text{CDCl}_3$ )  $\delta$  8.77 (dd,  $J = 5.8, 4.5$  Hz, 1H), 8.12 – 8.05 (m, 1H), 7.66 (dd,  $J = 10.5, 3.0$  Hz, 1H), 7.42 (ddd,  $J = 9.2, 7.9, 3.0$  Hz, 1H), 7.25 (d,  $J = 7.9$  Hz, 1H), 5.54 – 5.46 (m, 1H), 3.52 – 3.36 (m, 1H), 2.36 – 2.40 (m, 1H), 2.24 – 2.08 (m, 2H), 2.01 – 2.04 (m, 1H), 1.99 (s, 1H), 1.86 – 1.92 (m, 1H), 1.71 (s, 3H).

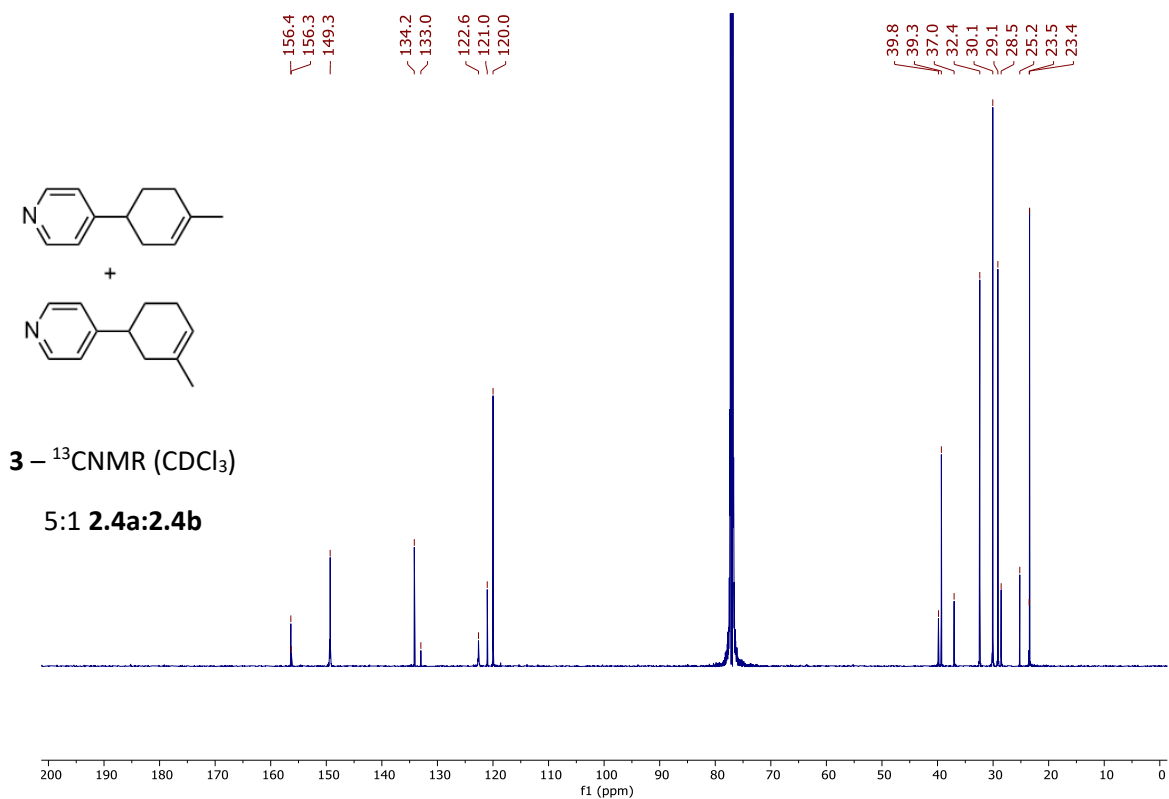
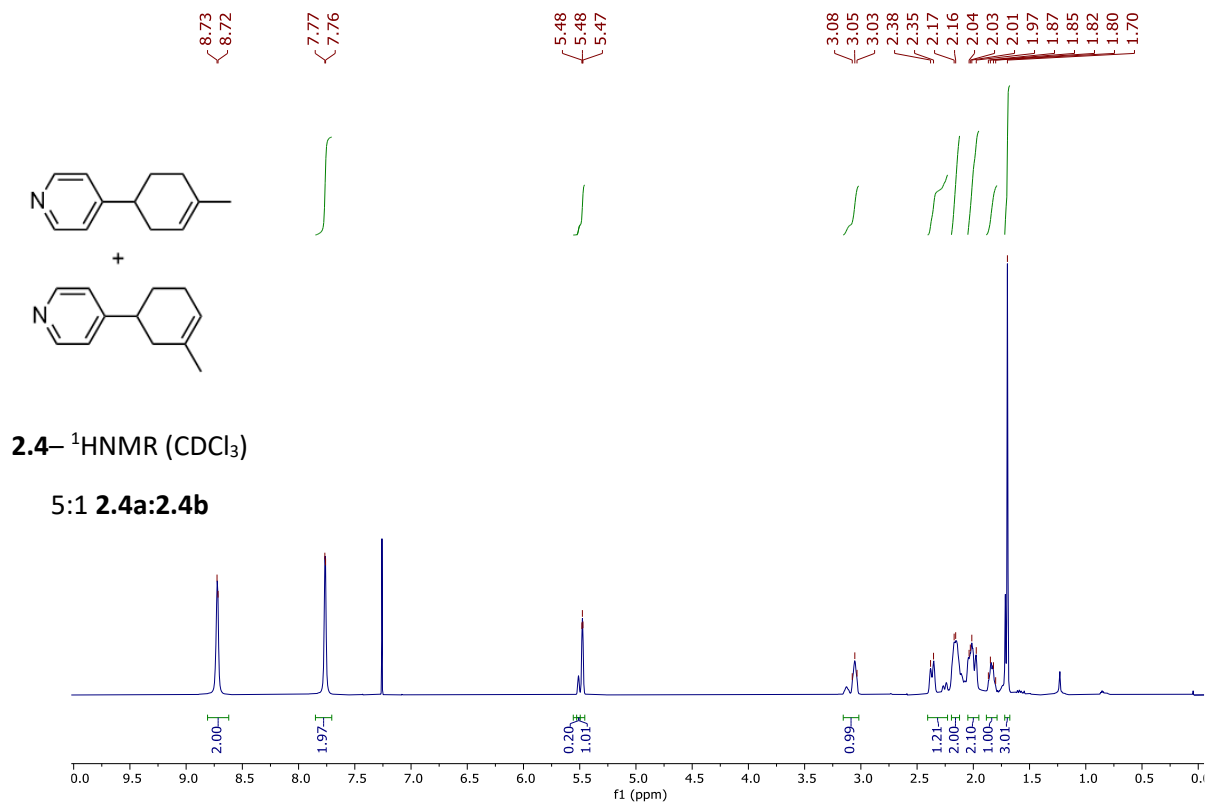
**$^{13}\text{C}$  NMR (2.38a and 2.38b)** (151 MHz,  $\text{CDCl}_3$ ):  $\delta$  161.3, 159.7, 152.2, 152.2, 149.6, 149.6, 149.6, 145.4, 134.2, 133.2, 132.8, 132.8, 132.7, 132.7, 127.9, 127.8, 121.1, 120.3, 120.2, 119.1, 119.0, 119.0, 118.9, 118.2, 118.1, 106.8, 106.8, 106.7, 106.6, 37.0, 35.0, 34.6, 32.4, 30.3, 28.9, 28.4, 25.4, 23.5, 23.4.

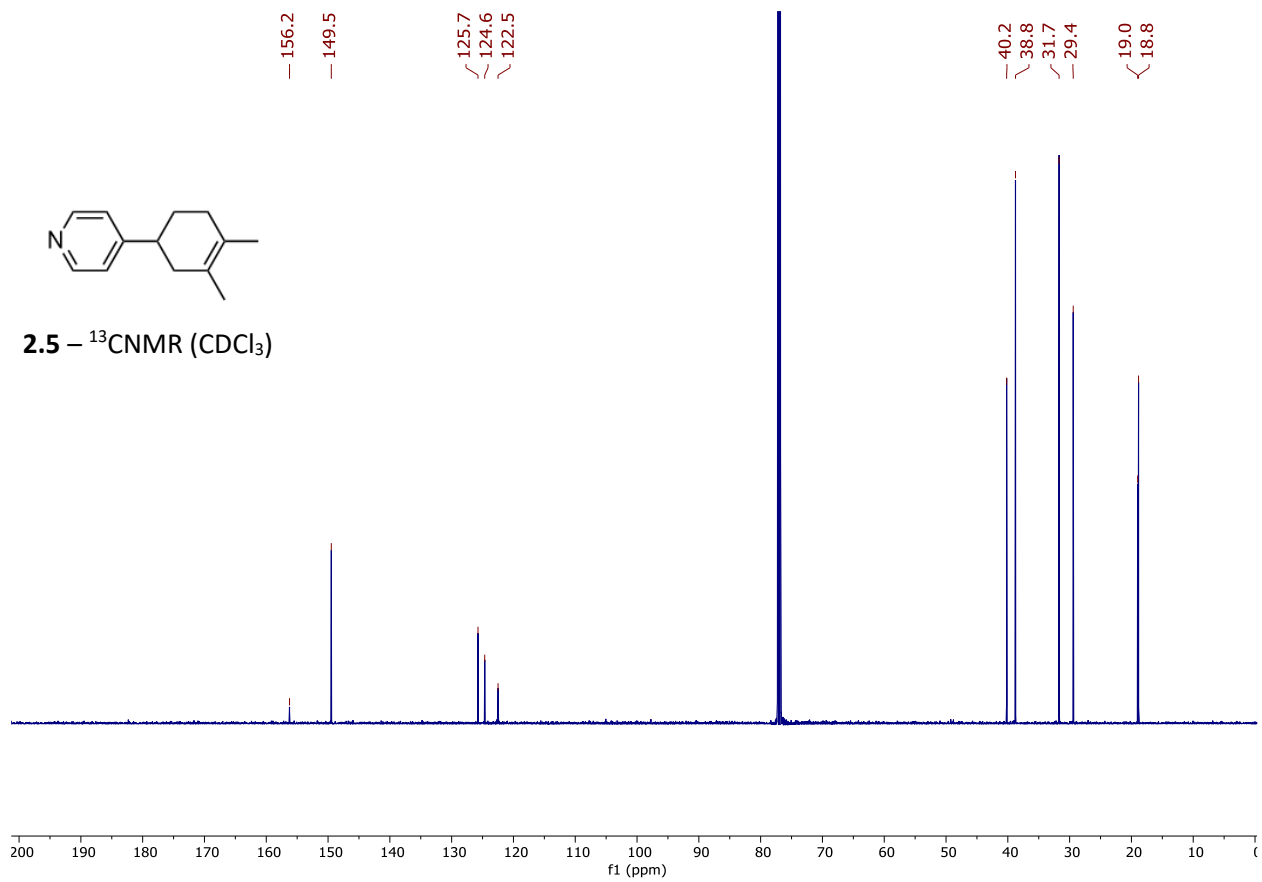
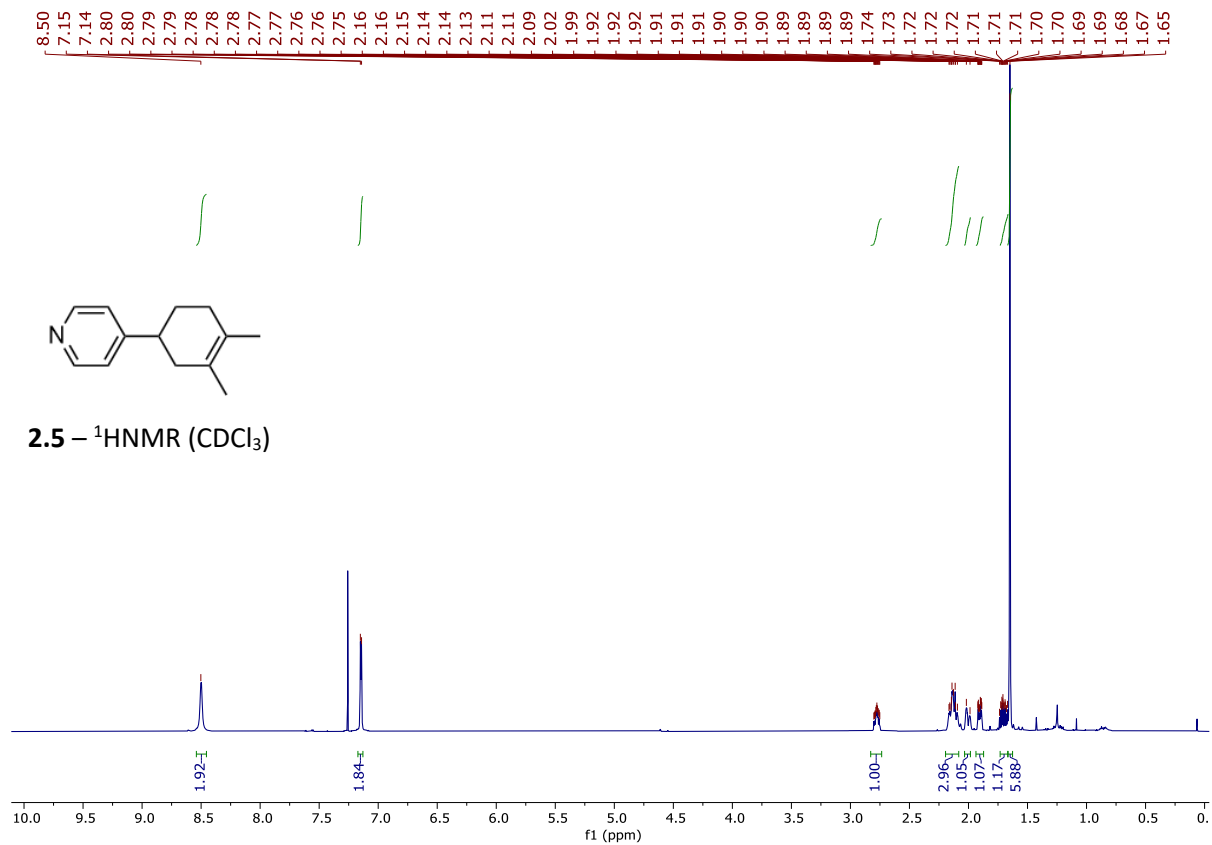
**HRMS** (EI/QTOF)  $m/z$ :  $[\text{M}]^+$  Calcd for  $\text{C}_{17}\text{H}_{16}\text{NF}$  256.1502, found 256.1499.

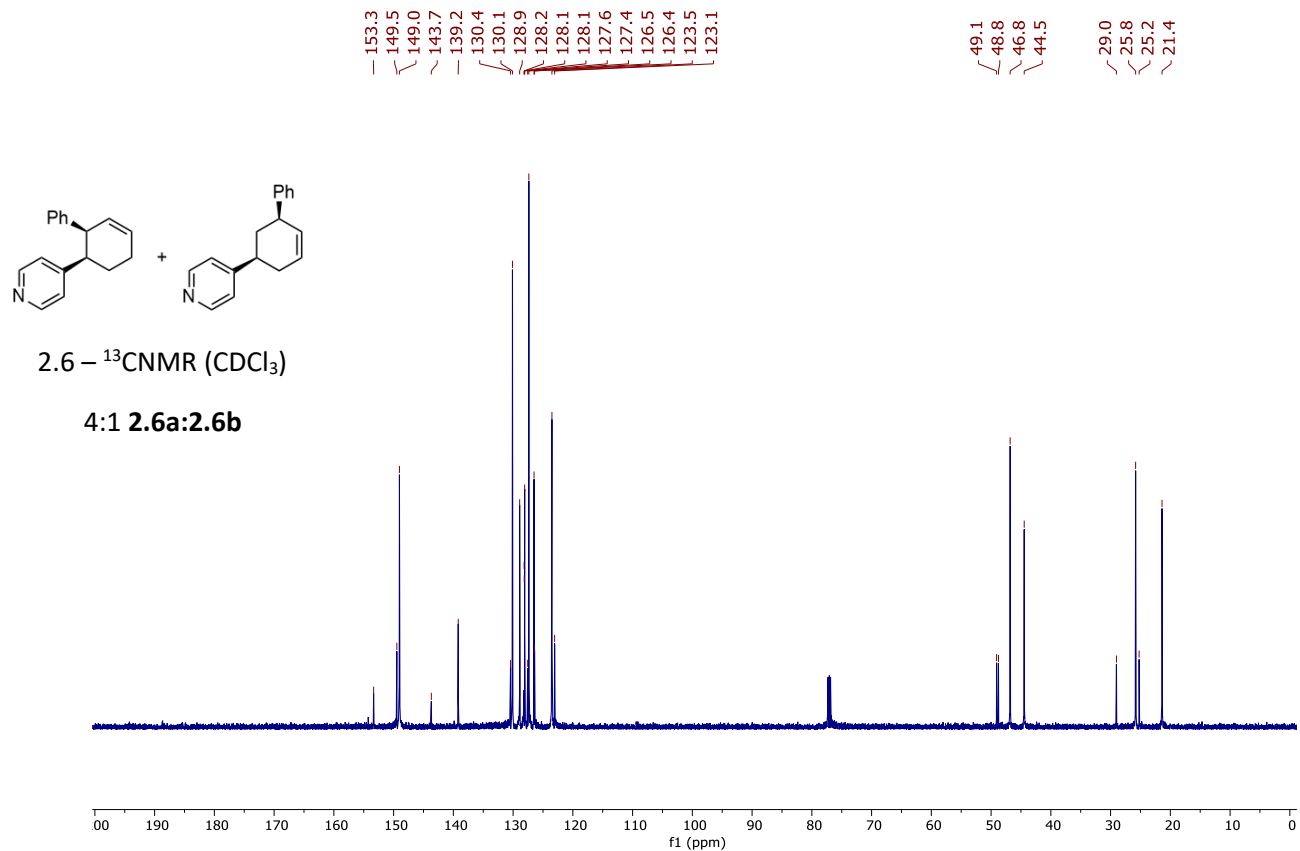
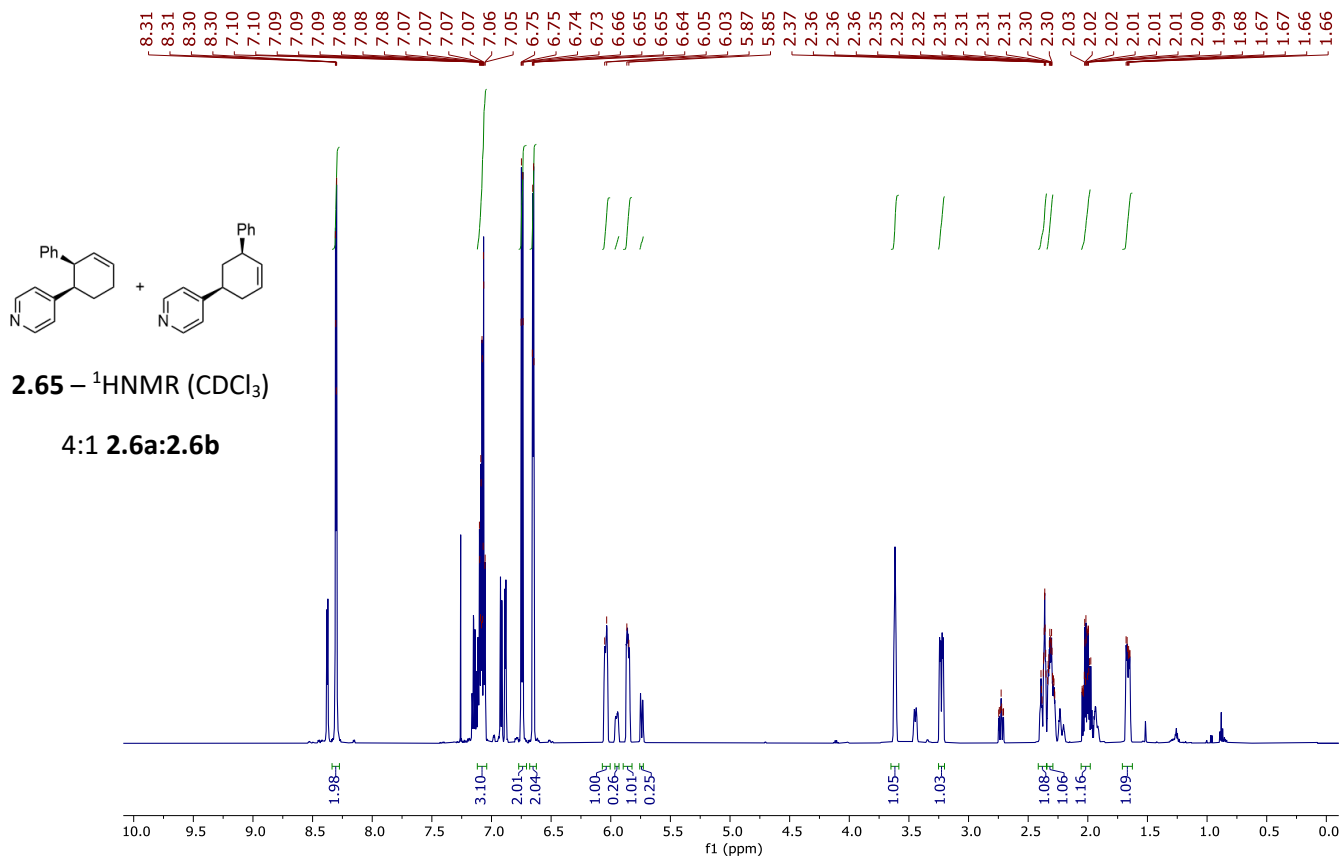
## A.6 References

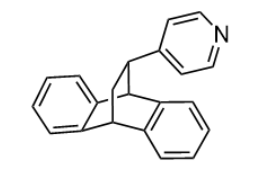
- (1) Zhang, M.; Xie, J.; Zhu, C. A General Deoxygenation Approach for Synthesis of Ketones from Aromatic Carboxylic Acids and Alkenes. *Nat. Commun.* 2018 91 **2018**, 9 (1), 1–10.
- (2) Wang, S.; Li, X.; Liu, H.; Xu, L.; Zhuang, J.; Li, J.; Li, H.; Wang, W. Organocatalytic Enantioselective Direct Additions of Aldehydes to 4-Vinylpyridines and Electron-Deficient Vinylarenes and Their Synthetic Applications. *J. Am. Chem. Soc.* **2015**, 137 (6), 2303–2310.
- (3) Martins, M. A. P.; Freitag, R.; Zanatta, N. <sup>13</sup>C NMR Chemical Shifts of Heterocycles: Empirical Substituent Effects in 5-Halomethylisoxazoles. <http://dx.doi.org/10.1080/00387019408006976> **2006**, 27 (9), 1227–1240.
- (4) Chen, J.; Fu, Y.; Yu, Y.; Wang, J.-R.; Guo, Y.-W.; Li, H.; Wang, W. Enantioselective [4 + 2] Cycloaddition Reaction of Vinylquinolines with Dienals Enabled by Synergistic Organocatalysis. *Org. Lett.* **2020**, 22 (15), 6061–6066.
- (5) Crisp, G.; Papadopoulos, S. Palladium-Mediated Transformations of Heteroaromatic Triflates. *Aust. J. Chem.* **1989**, 42 (2), 279–285.
- (6) Li, Y.; Guo, F.; Zha, Z.; Wang, Z. Iron-Catalyzed Synthesis of 2-Vinylquinolines via Sp<sup>3</sup> C-H Functionalization and Subsequent C-N Cleavage. *Chem. - An Asian J.* **2013**, 8 (3), 534–537.

# A.7 NMR Spectra

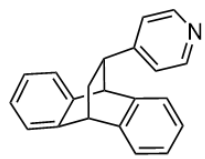
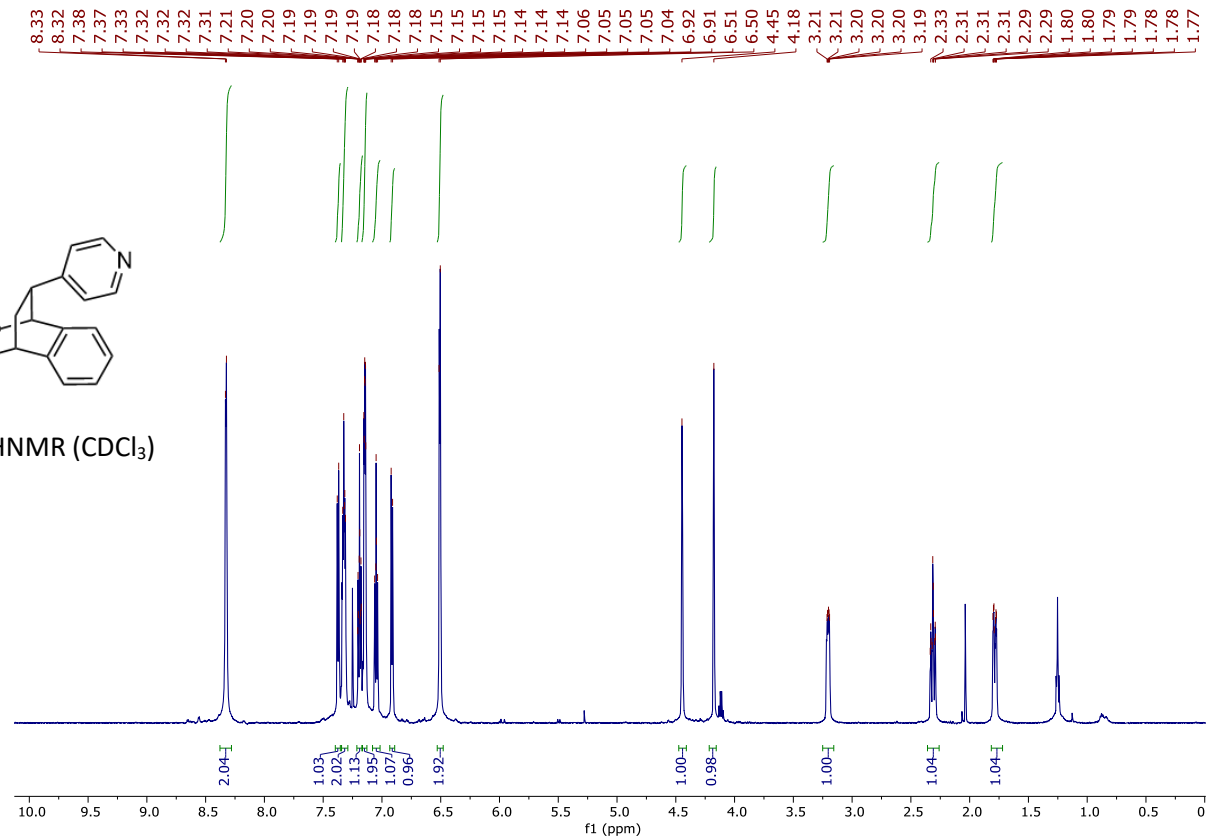




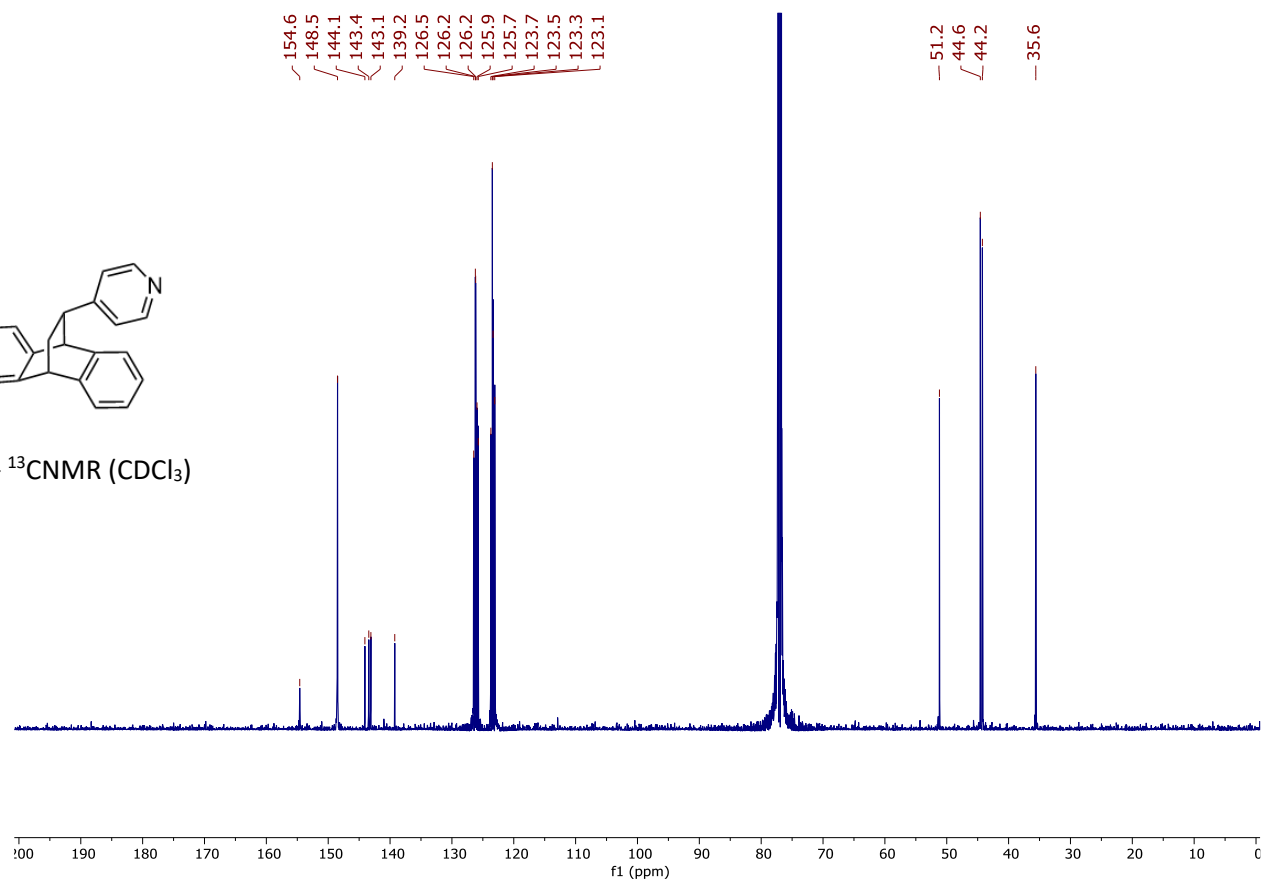


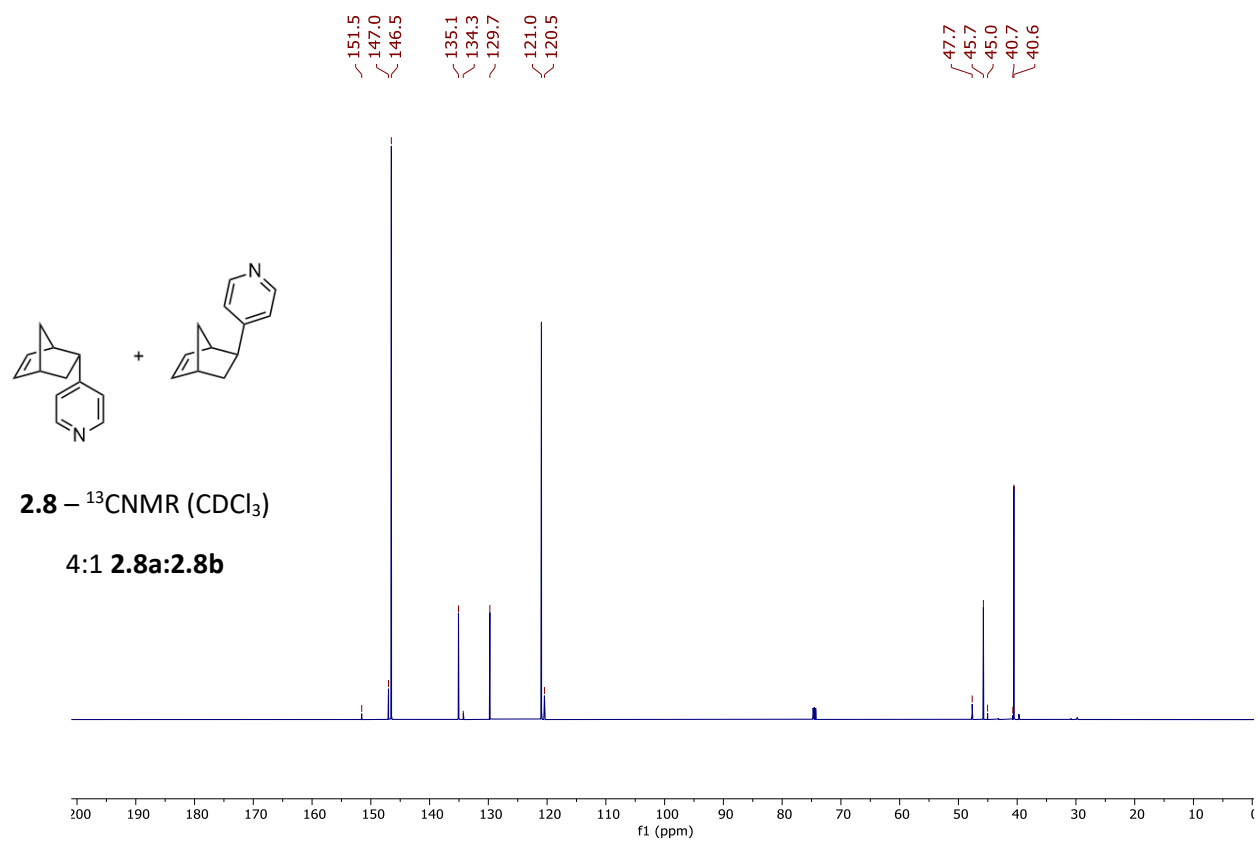
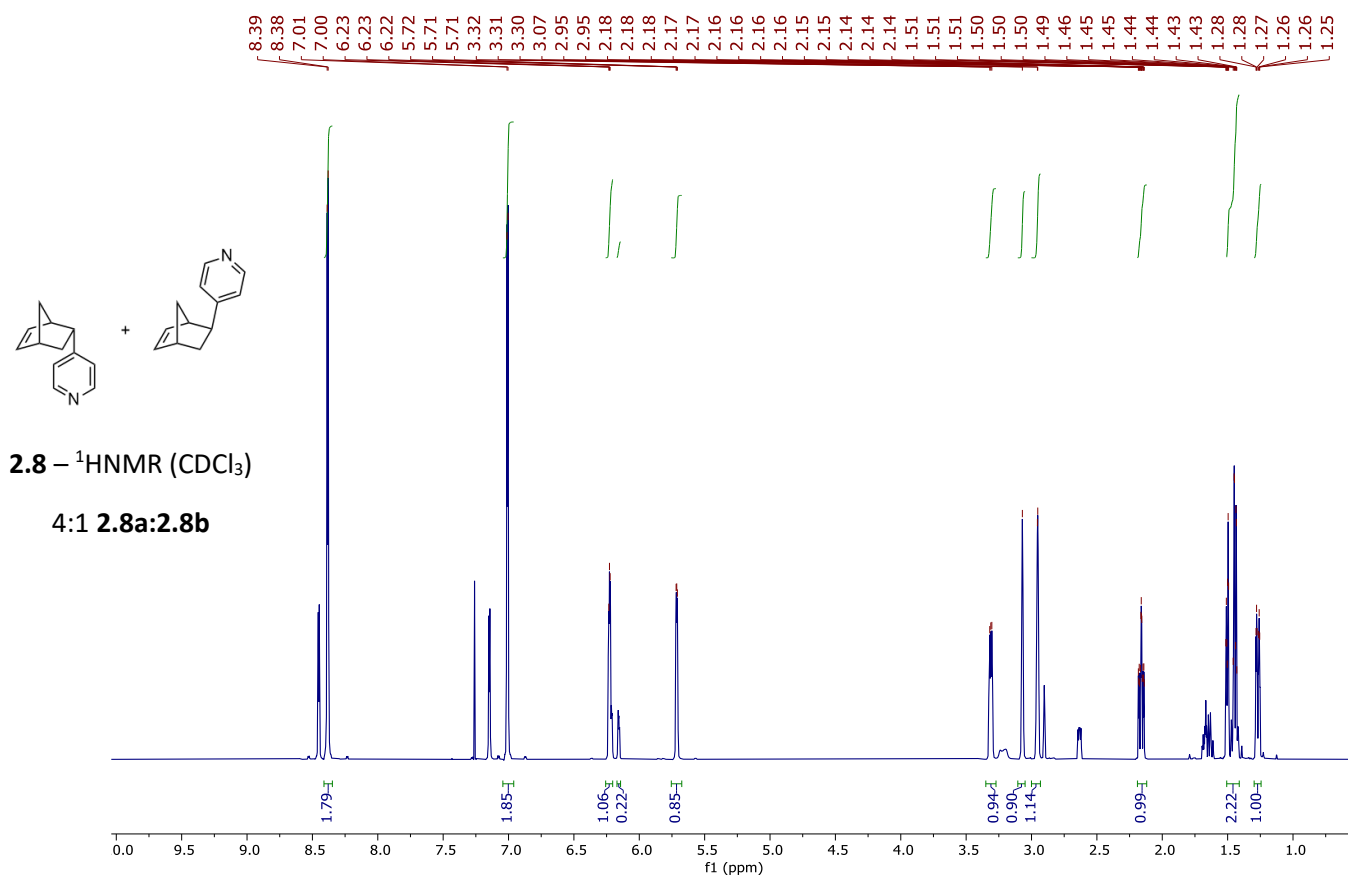


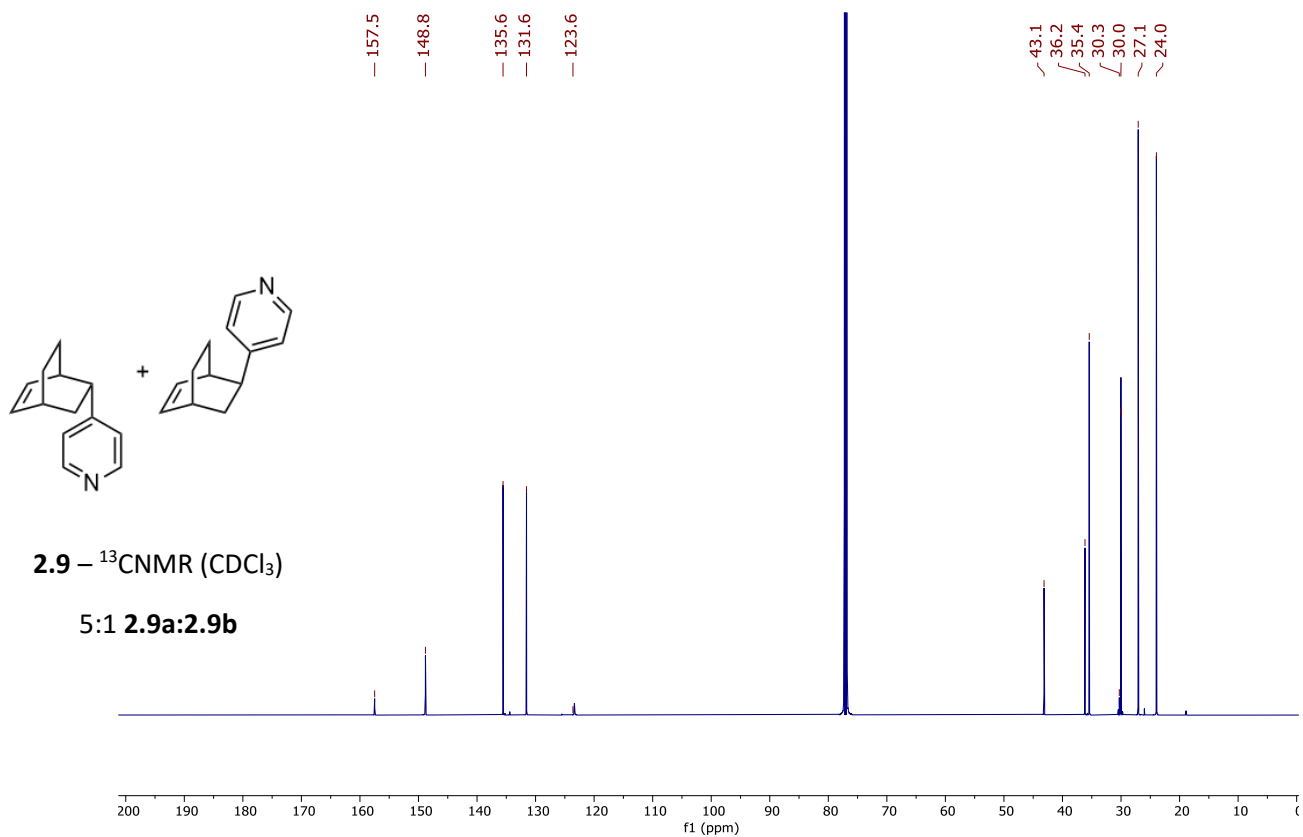
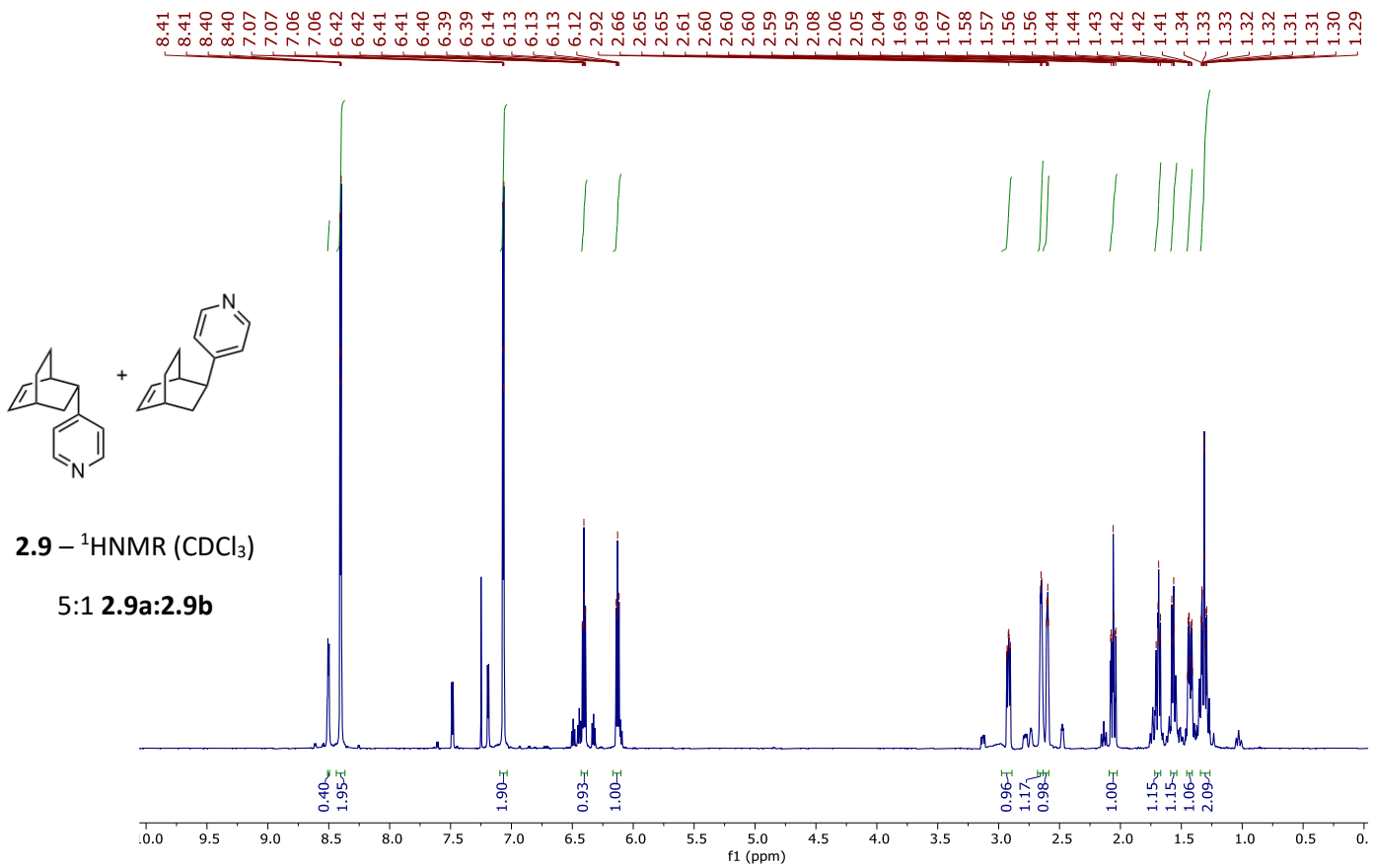
2.7 – <sup>1</sup>HNMR (CDCl<sub>3</sub>)

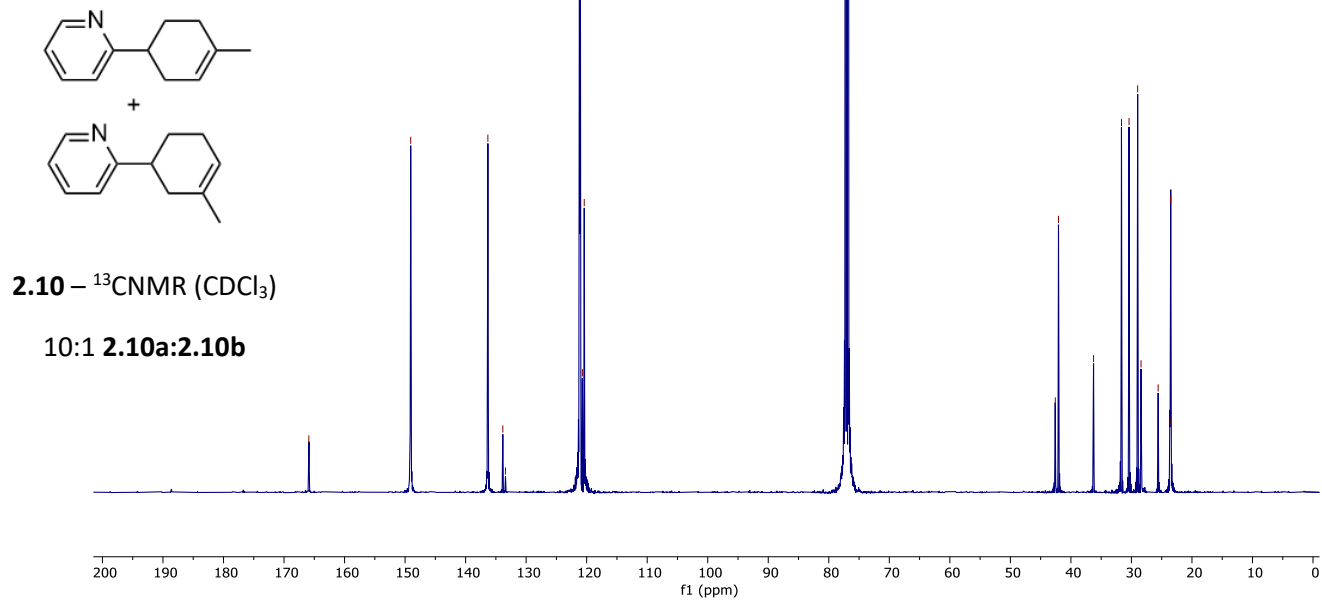
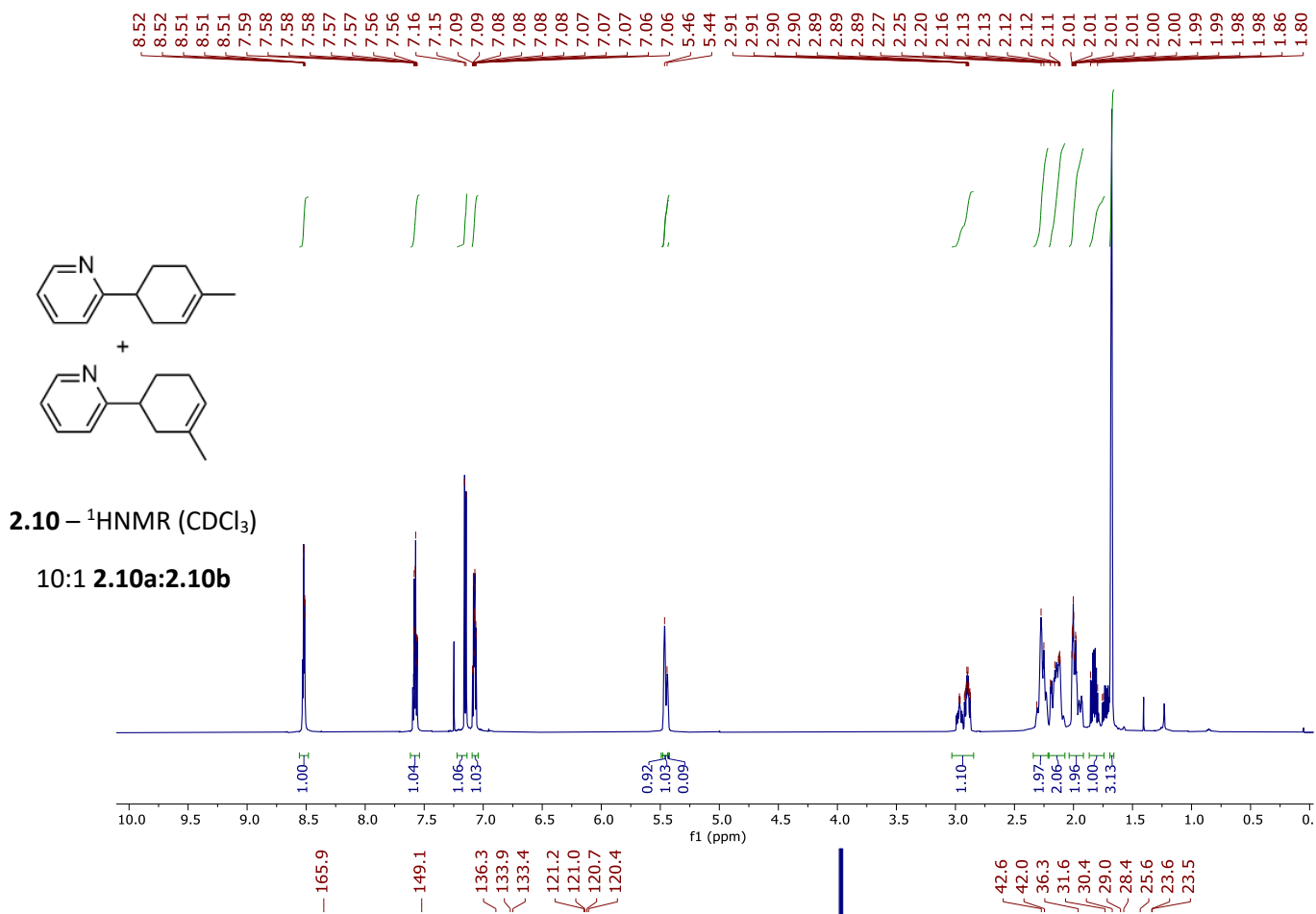


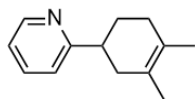
2.7 – <sup>13</sup>CNMR (CDCl<sub>3</sub>)



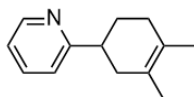
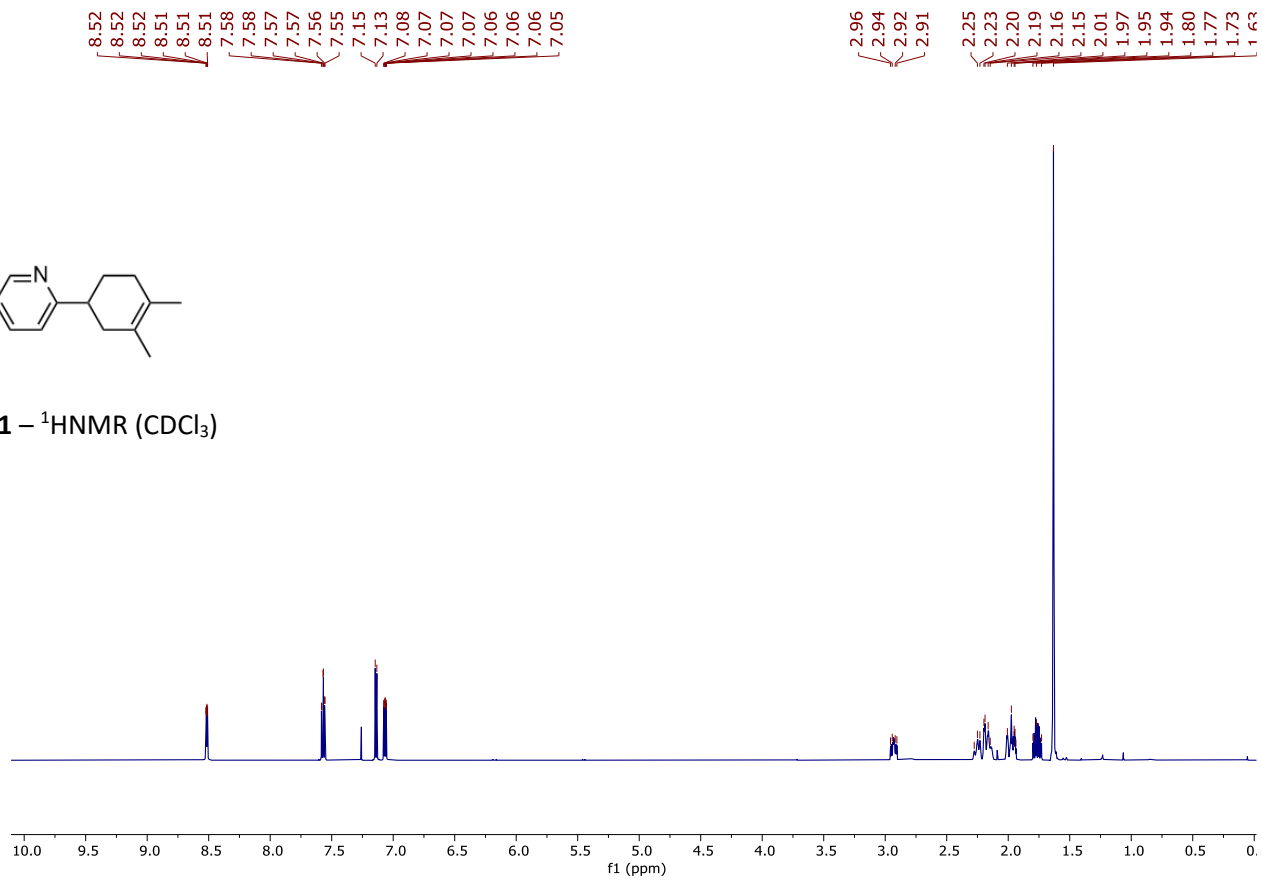




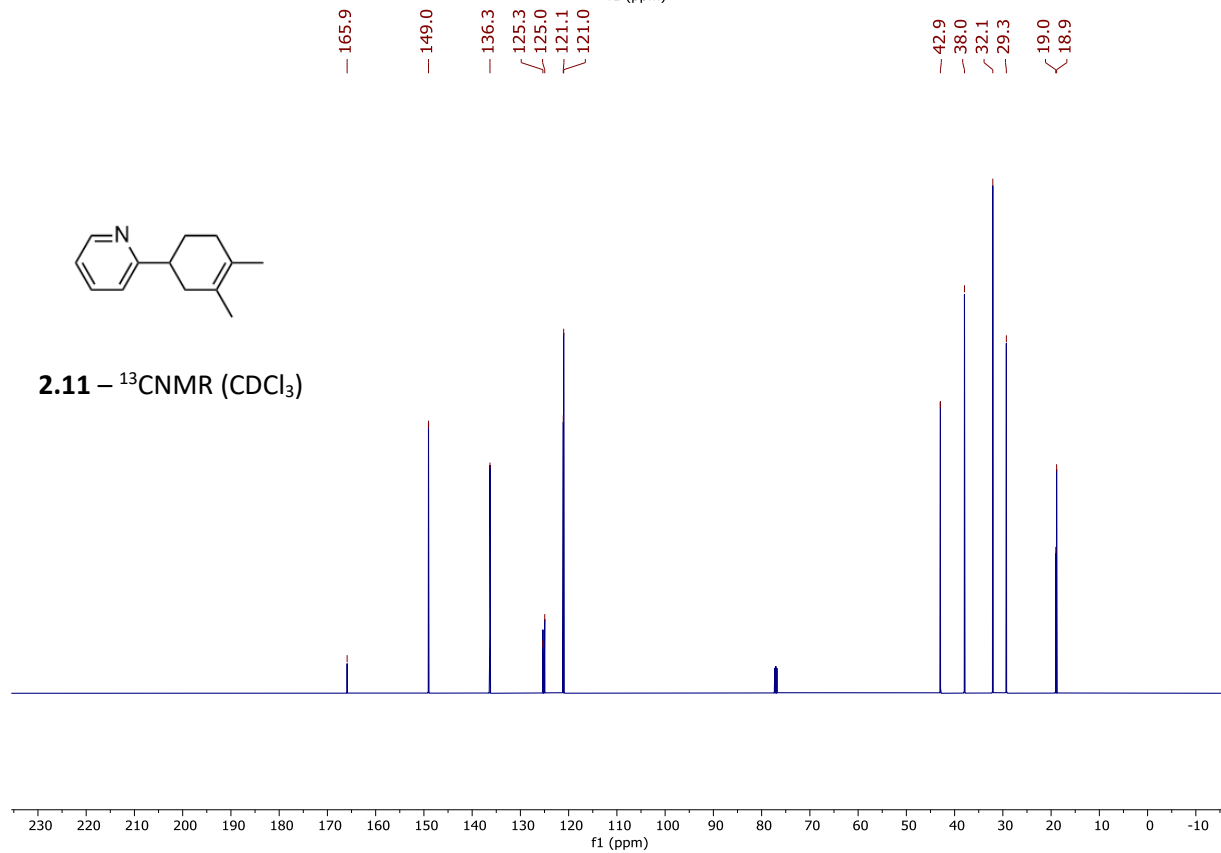


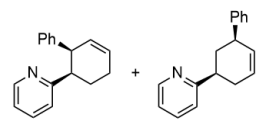


2.11 –  $^1\text{H}$ NMR ( $\text{CDCl}_3$ )



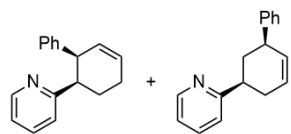
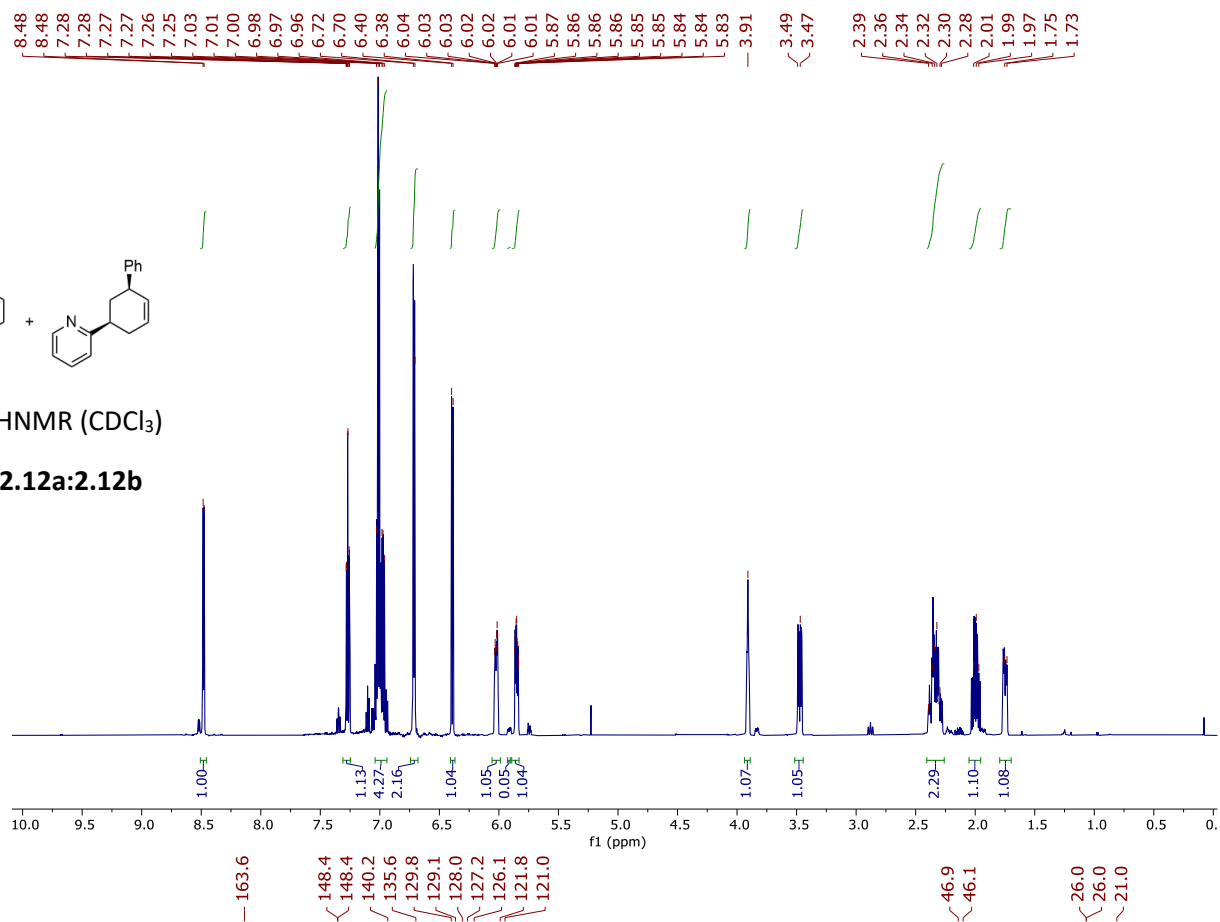
2.11 –  $^{13}\text{C}$ NMR ( $\text{CDCl}_3$ )





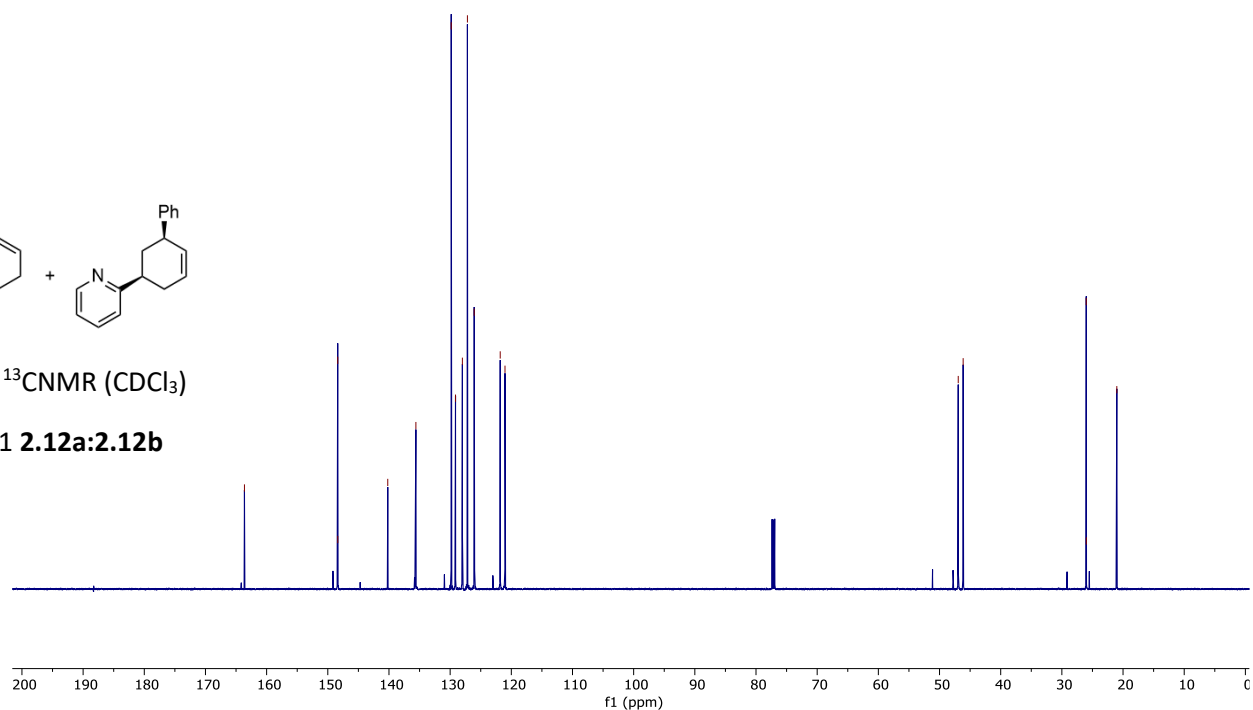
2.12 –  $^1\text{H}$ NMR ( $\text{CDCl}_3$ )

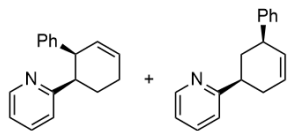
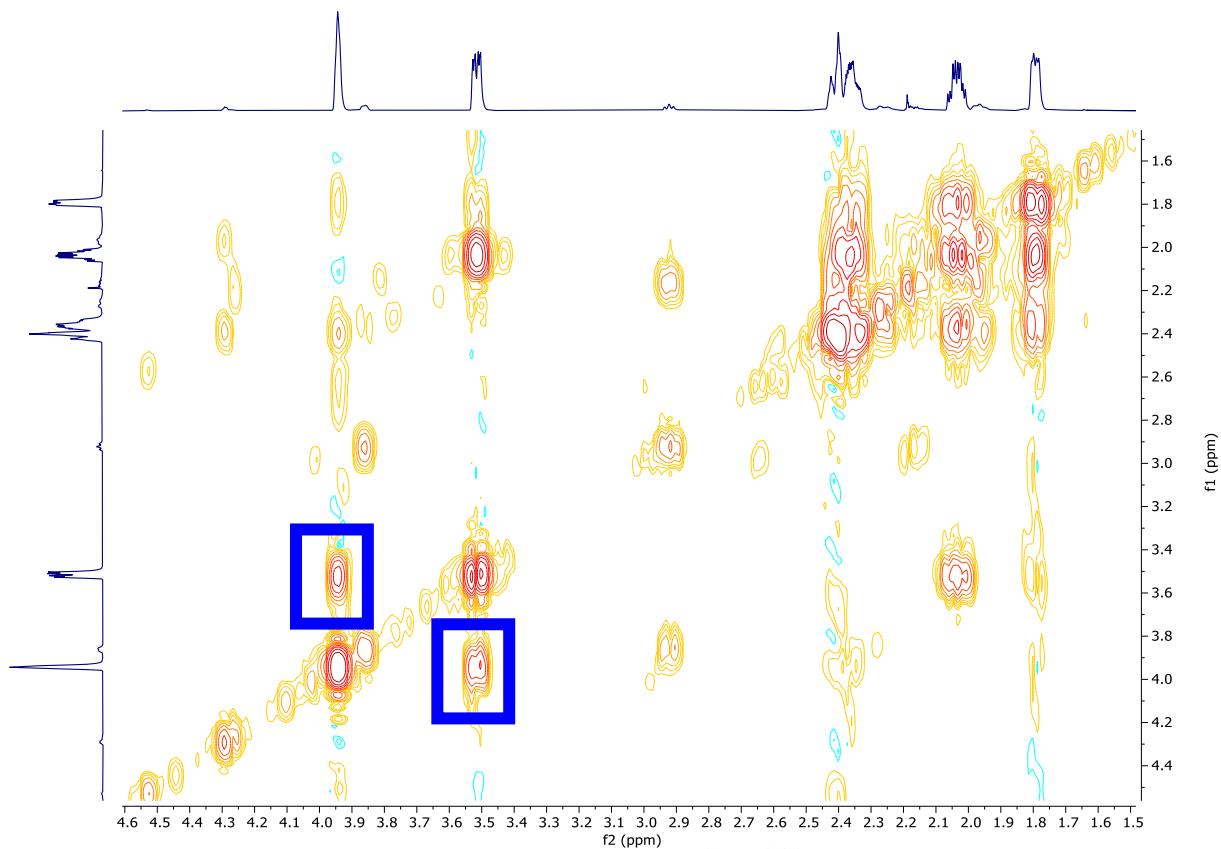
>20:1 2.12a:2.12b



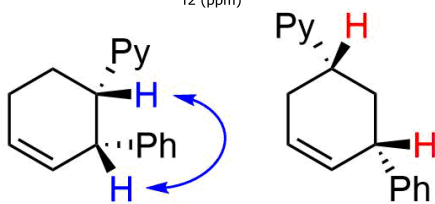
2.12 –  $^{13}\text{C}$ NMR ( $\text{CDCl}_3$ )

>20:1 2.12a:2.12b

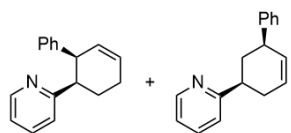
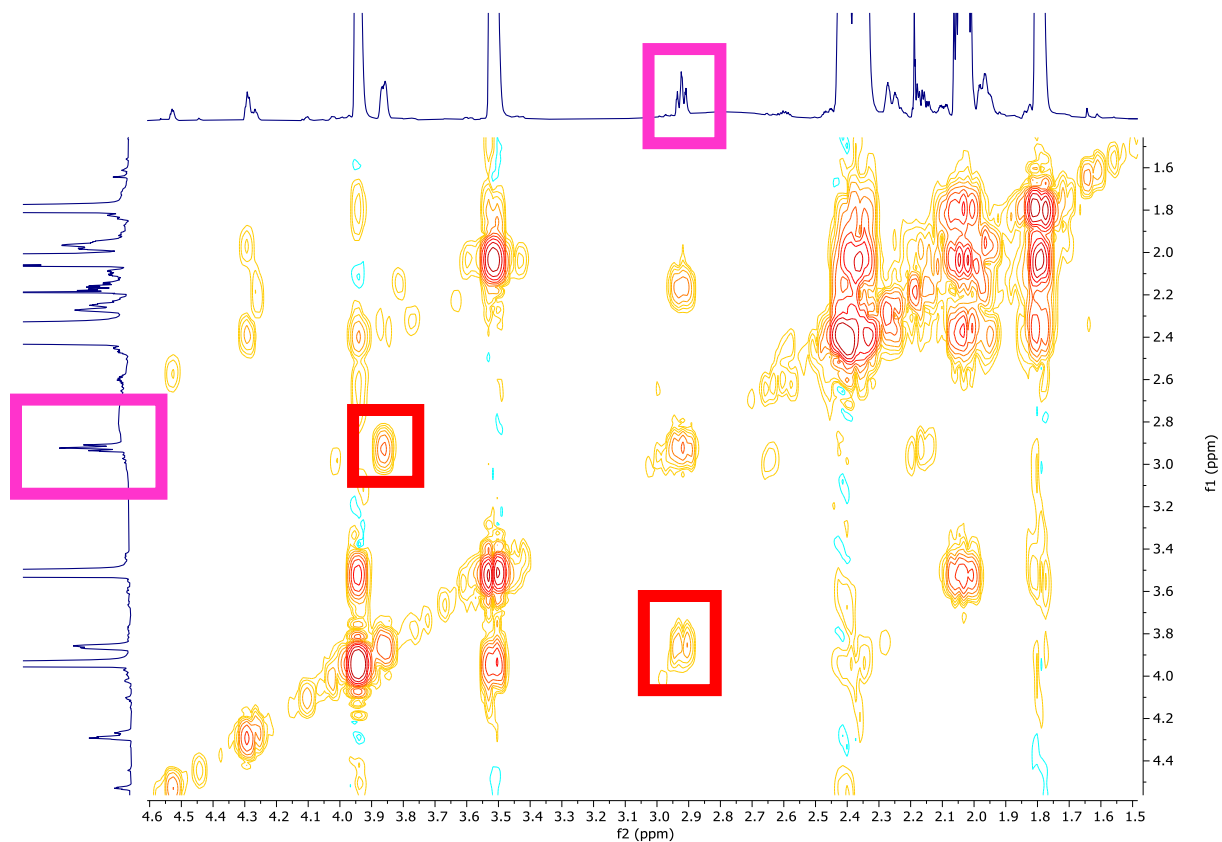




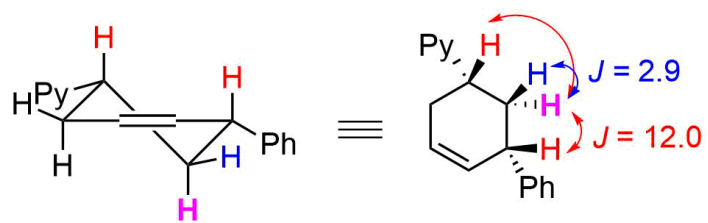
2.12 –  $^{13}\text{H}$ -COSY NMR in aliphatic region ( $\text{CDCl}_3$ )



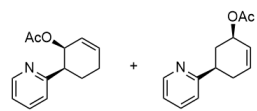
$^3J$  coupling between methine protons on major isomer



2.12 –  $^{13}\text{H}$ -COSY NMR in aliphatic region ( $\text{CDCl}_3$ )

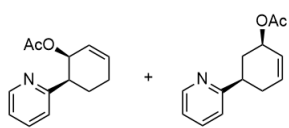
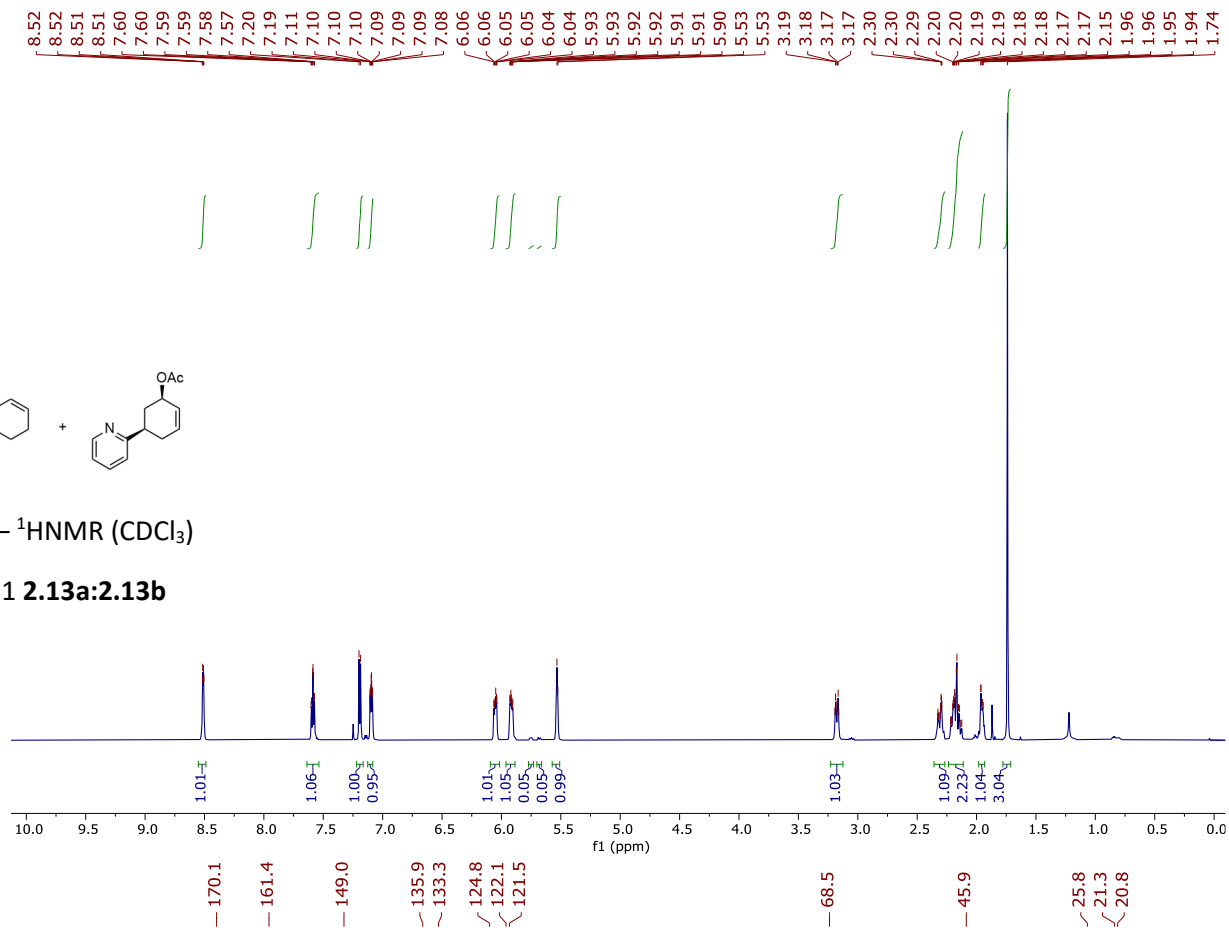


minor isomer td,  $J = 12.0, 2.9$   
coupling to visible minor methine peak



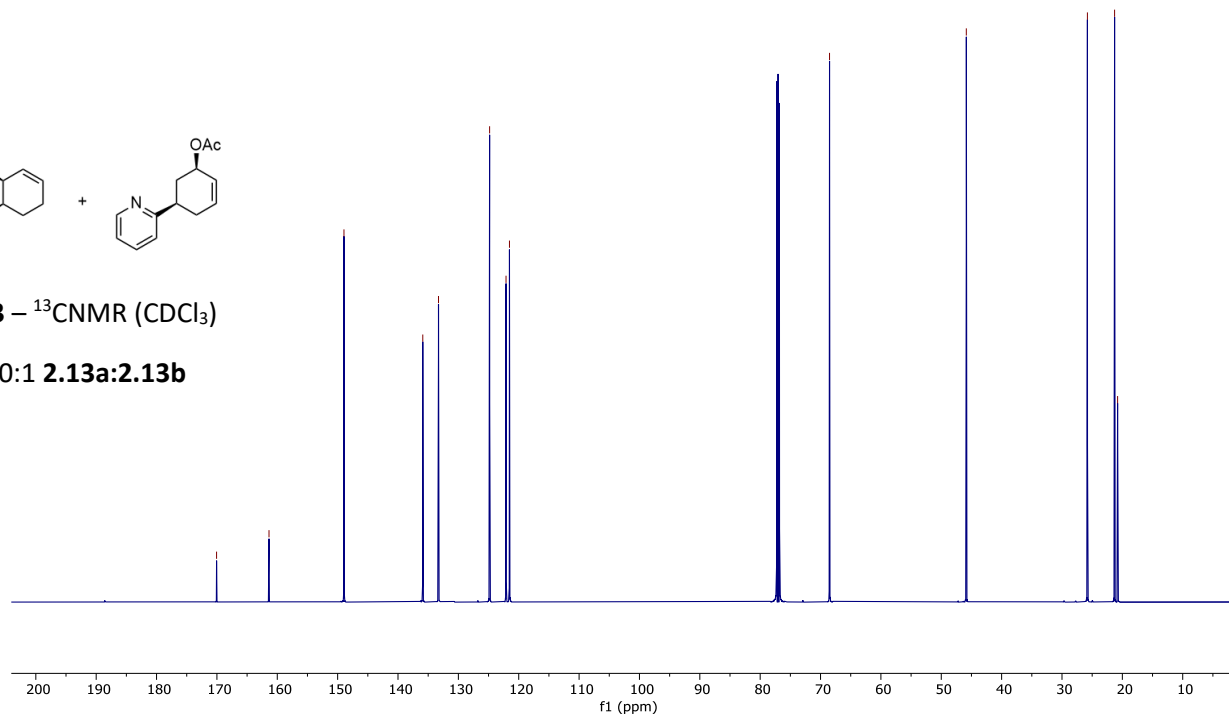
**2.13** –  $^1\text{H}$ NMR ( $\text{CDCl}_3$ )

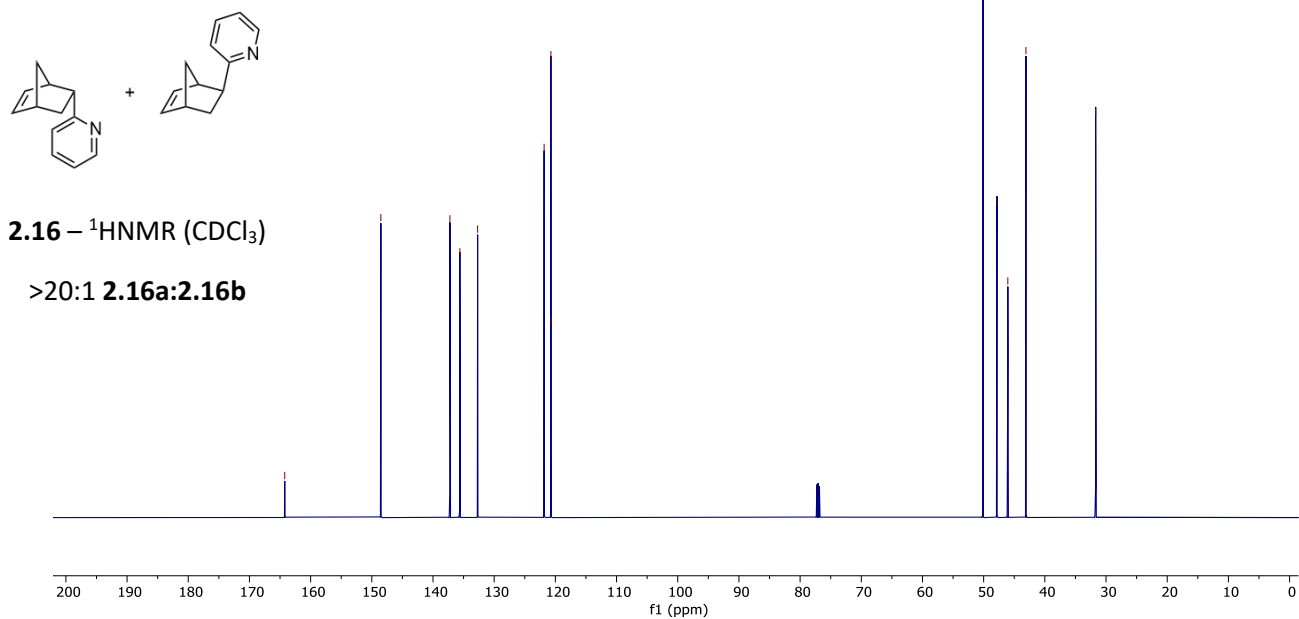
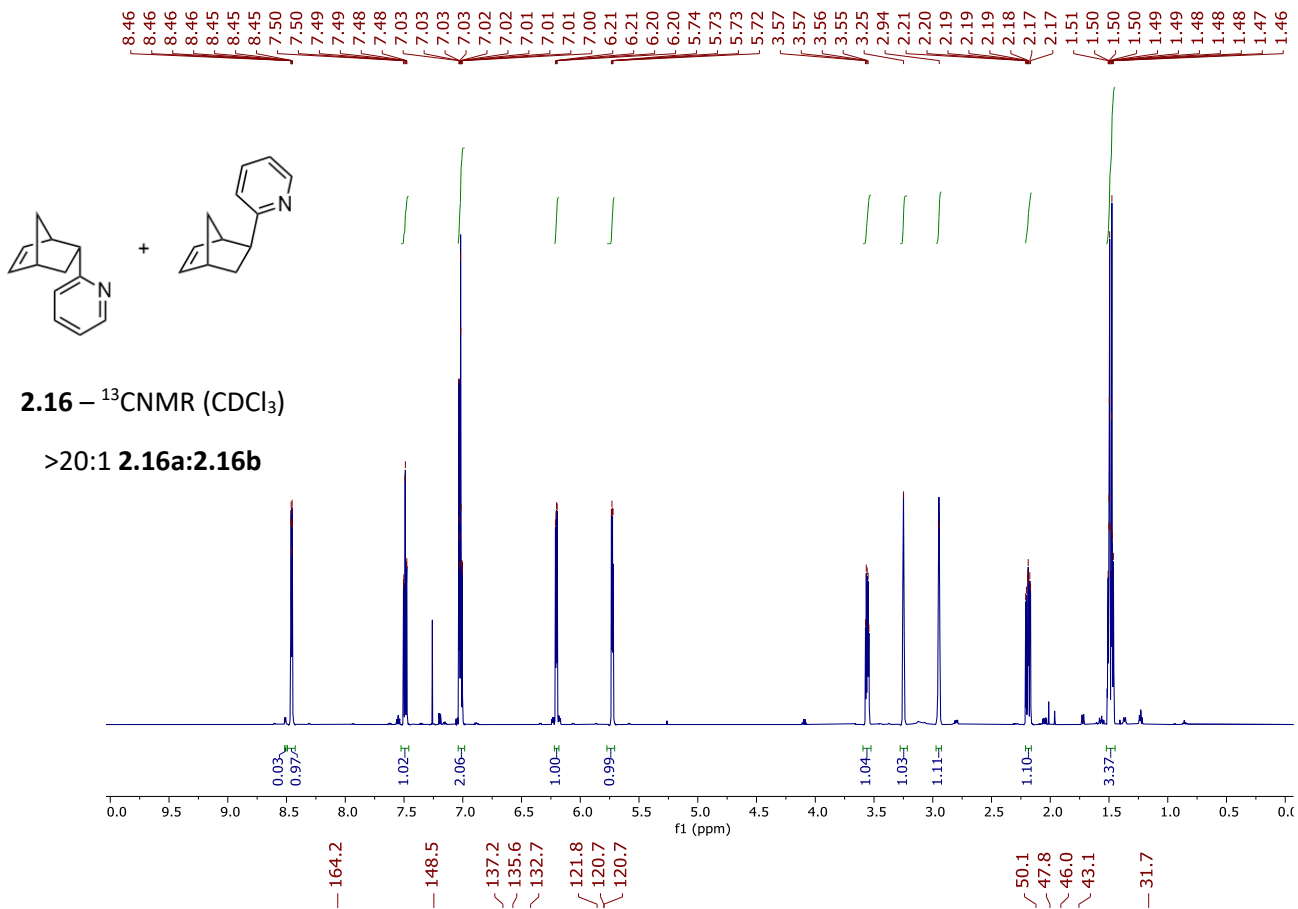
20:1 **2.13a**:**2.13b**

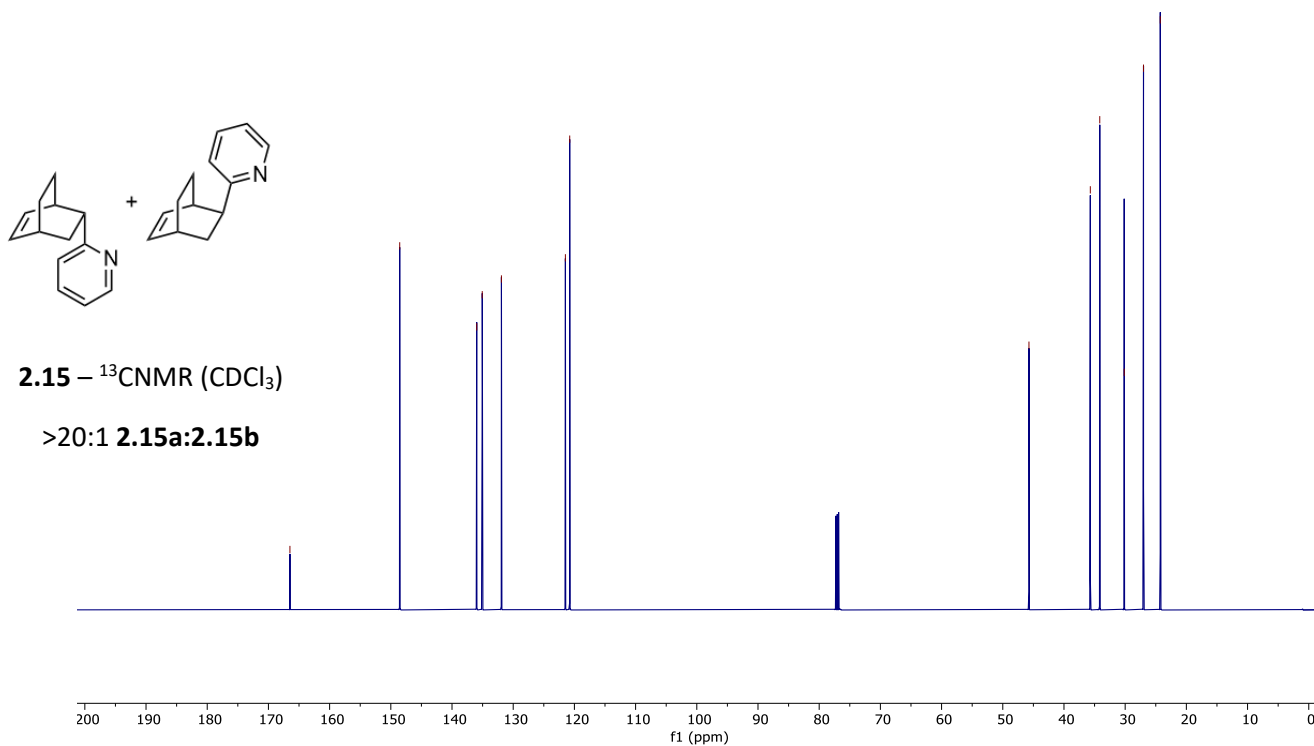
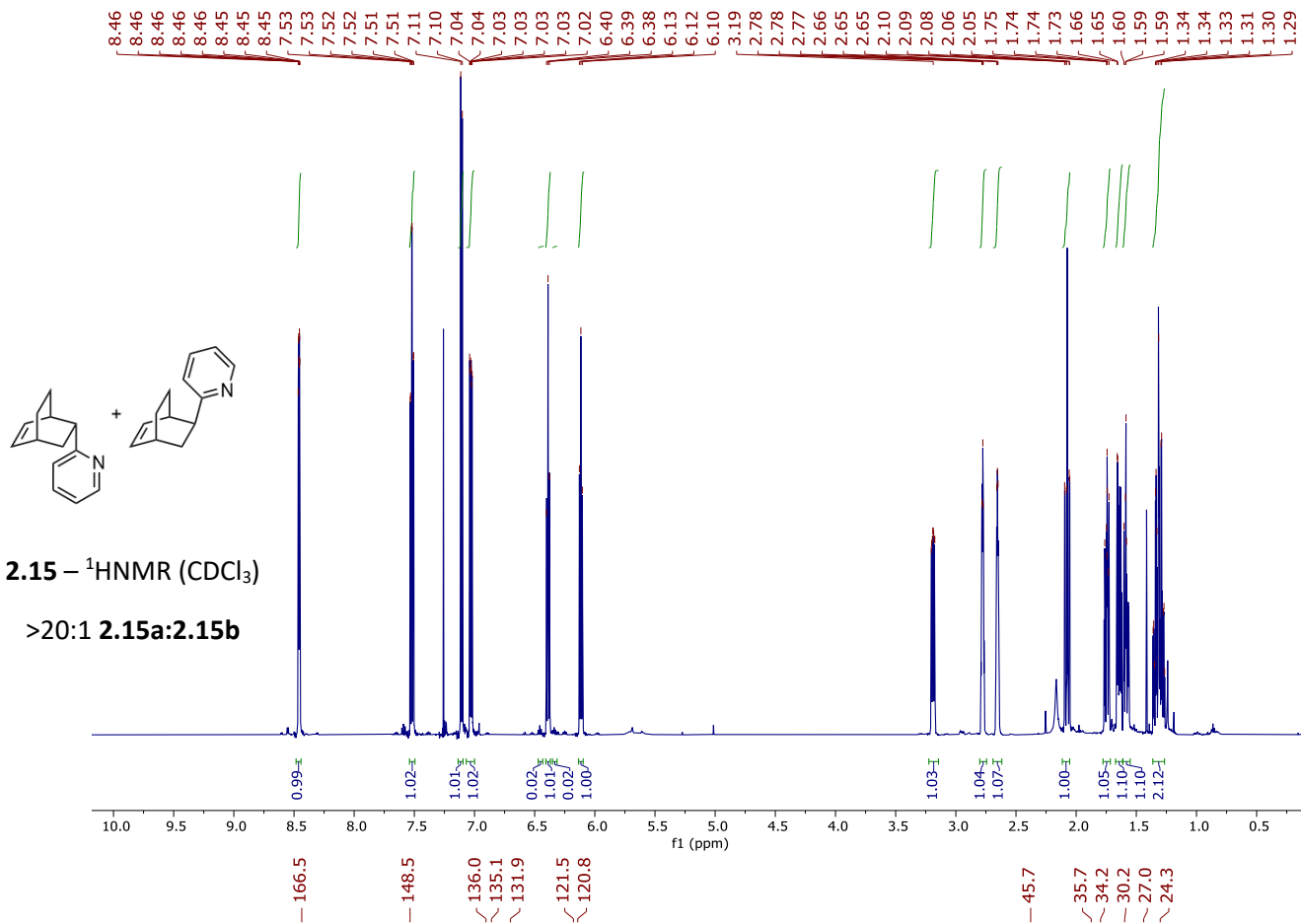


**2.13** –  $^{13}\text{C}$ NMR ( $\text{CDCl}_3$ )

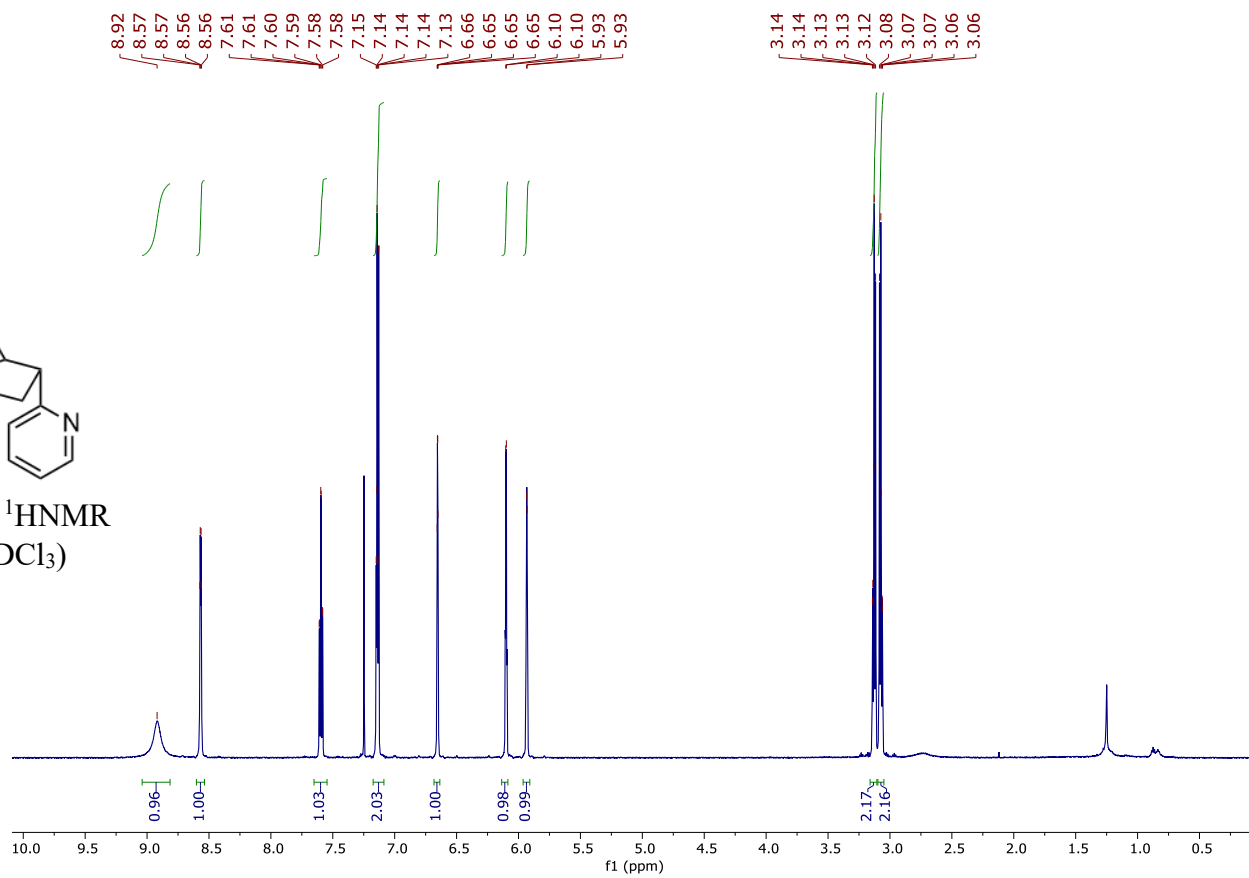
20:1 **2.13a**:**2.13b**



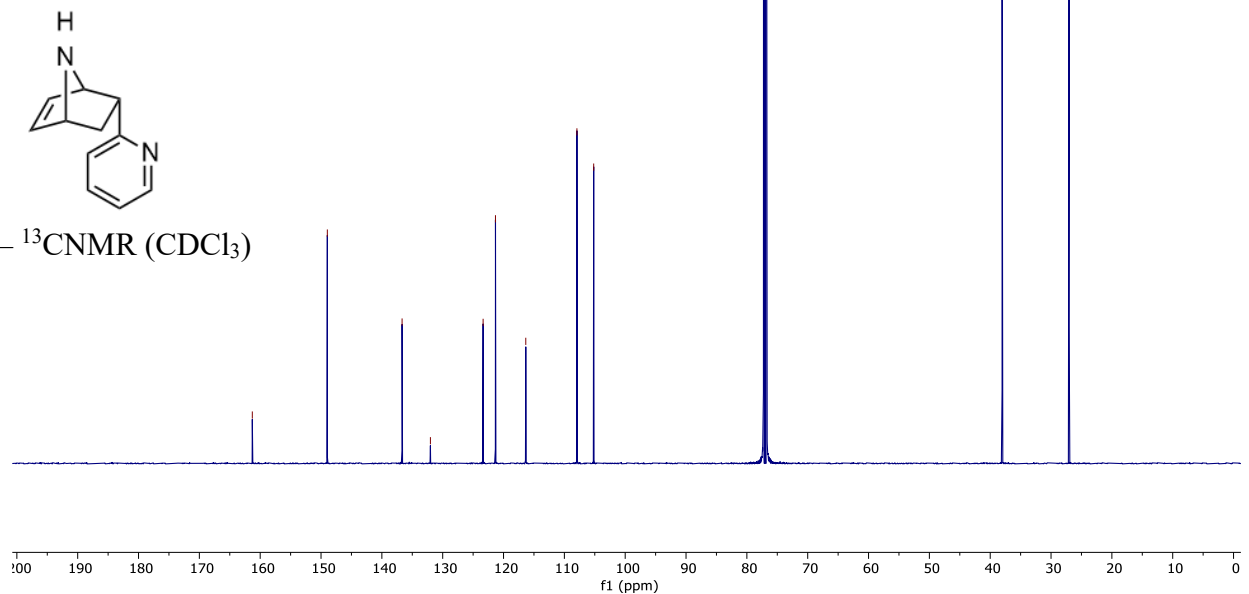


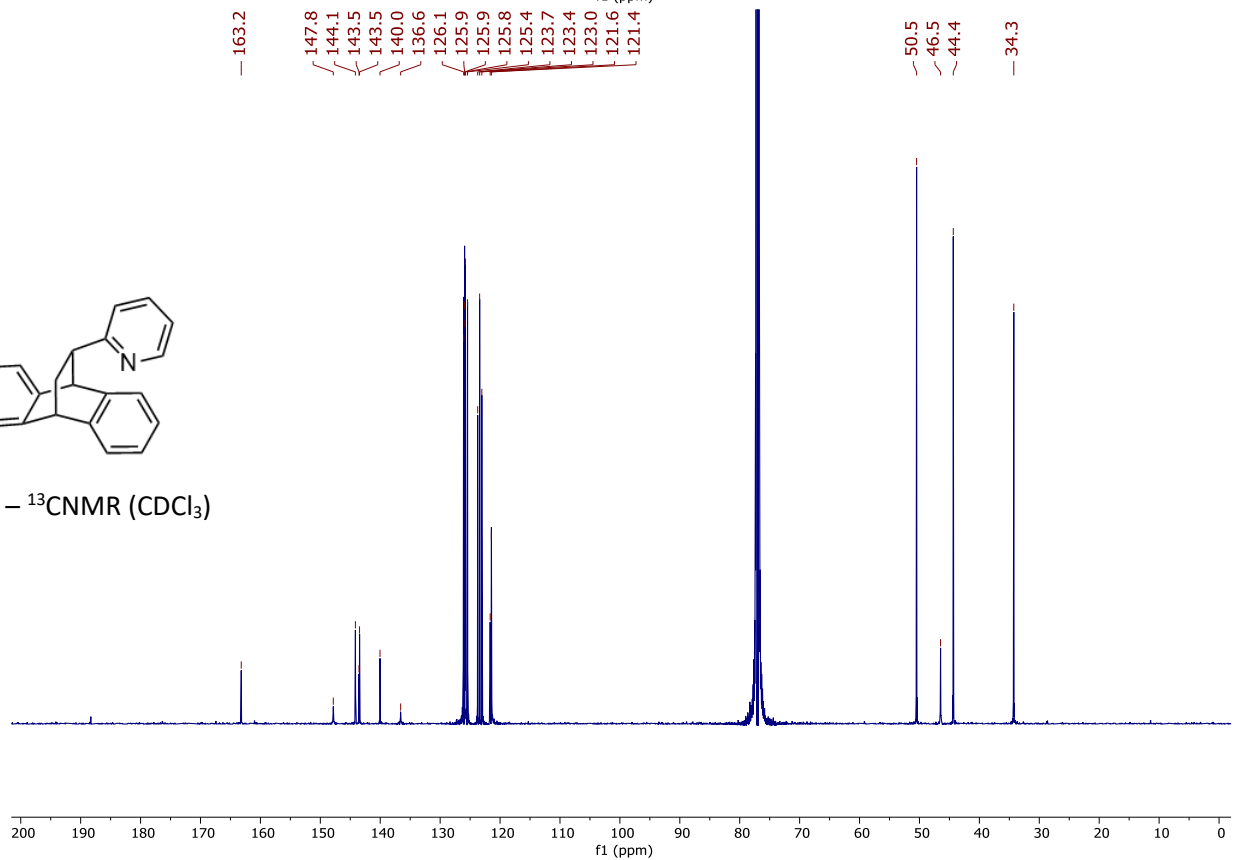
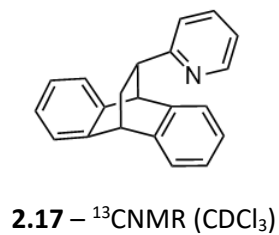
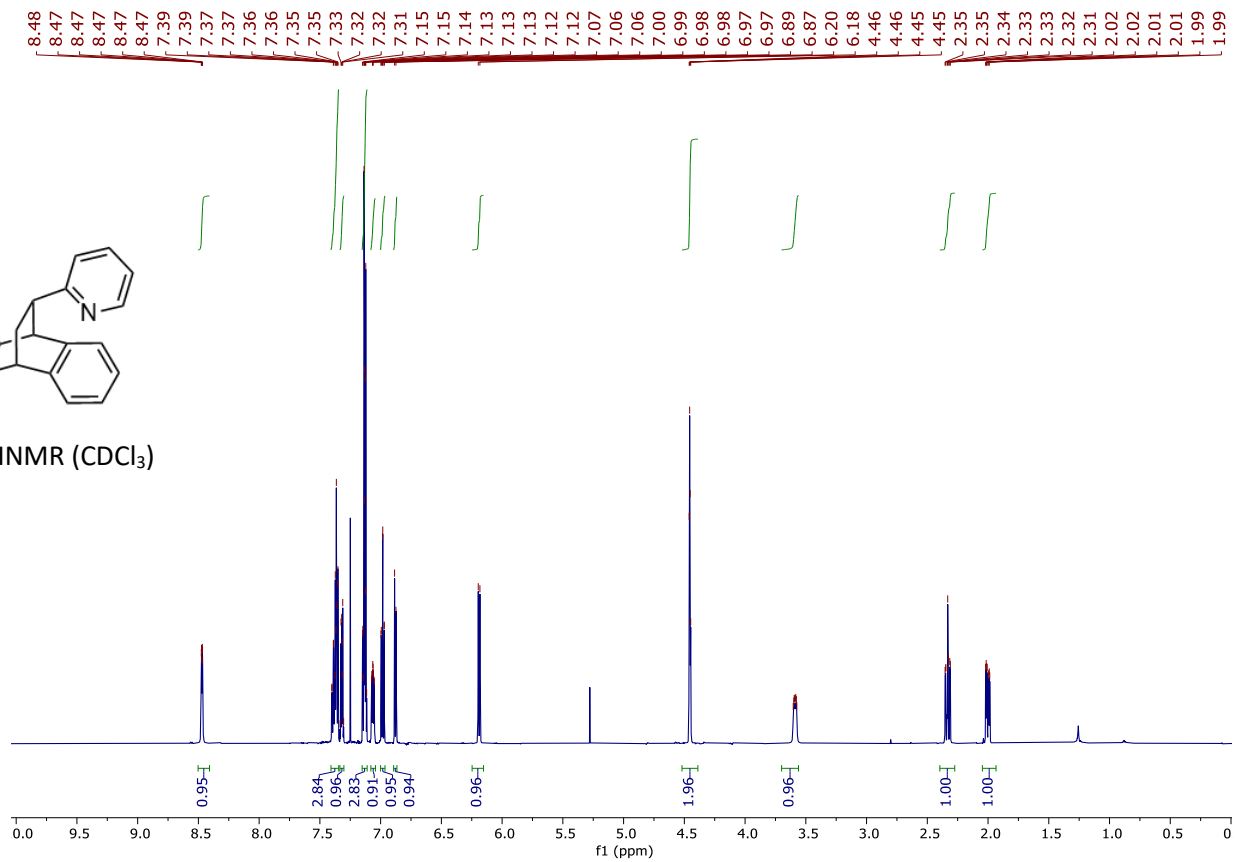
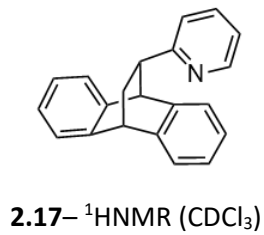


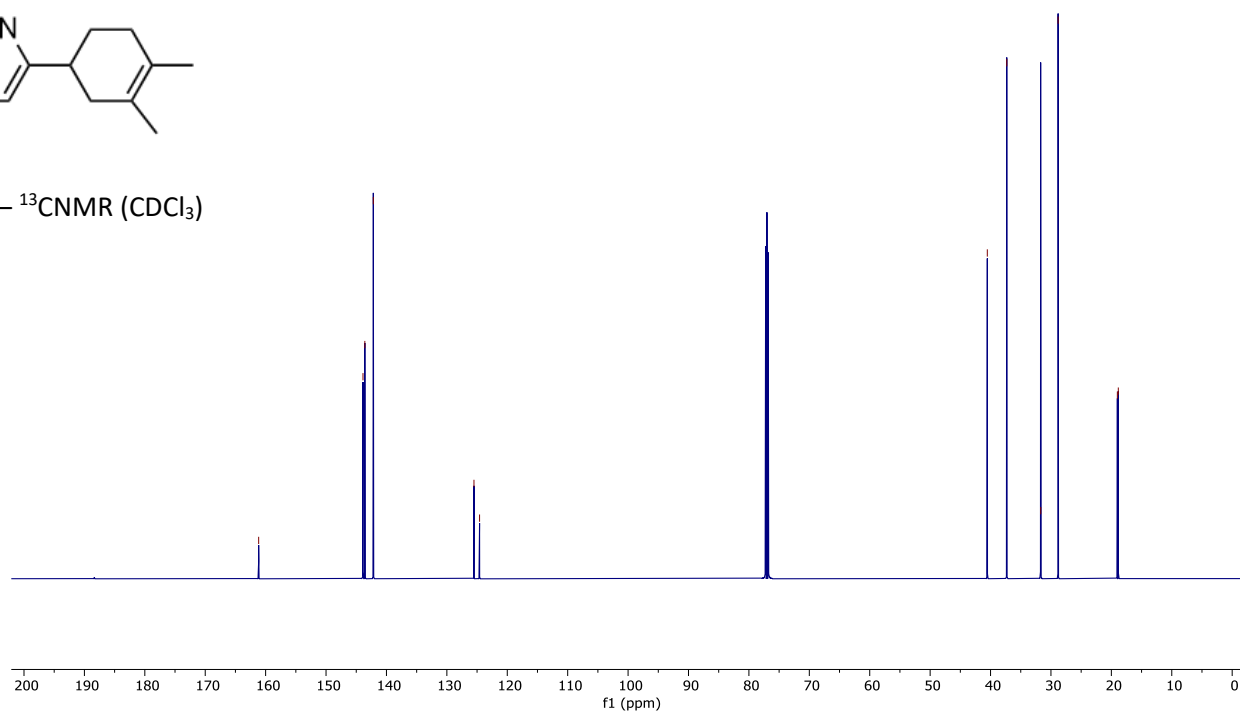
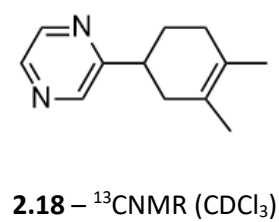
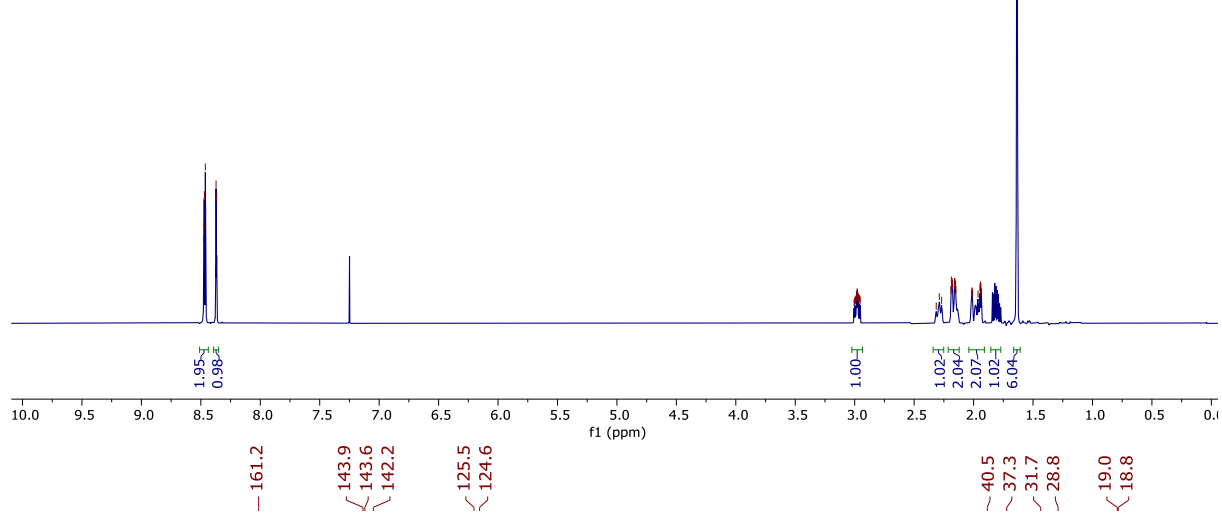
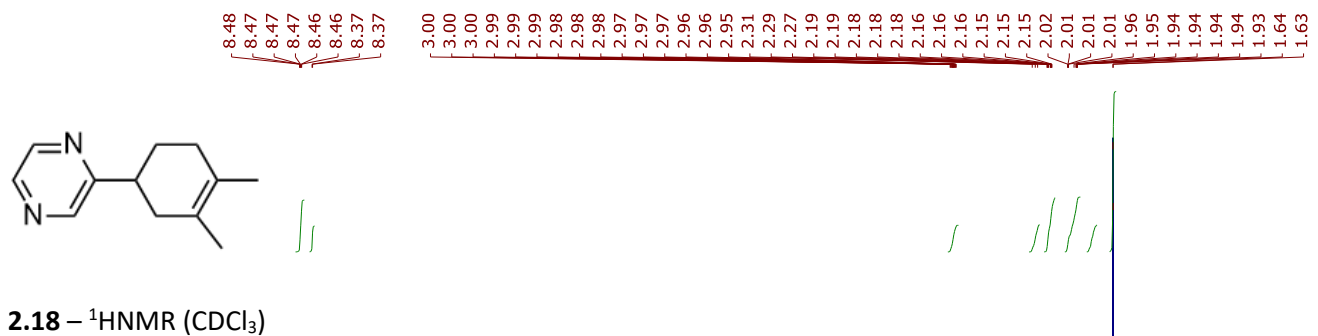
2.14 – <sup>1</sup>H NMR  
(CDCl<sub>3</sub>)

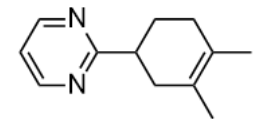


2.14 – <sup>13</sup>C NMR (CDCl<sub>3</sub>)

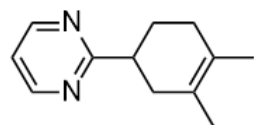
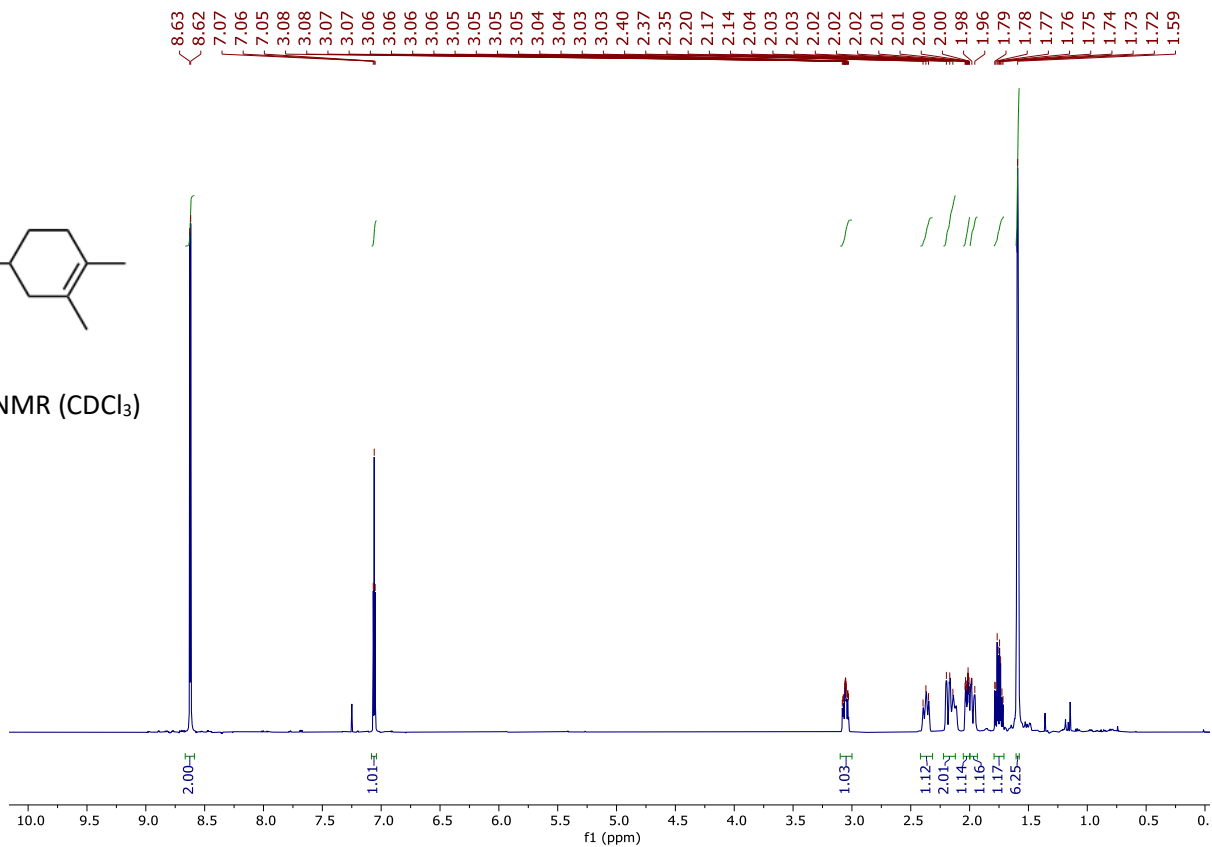




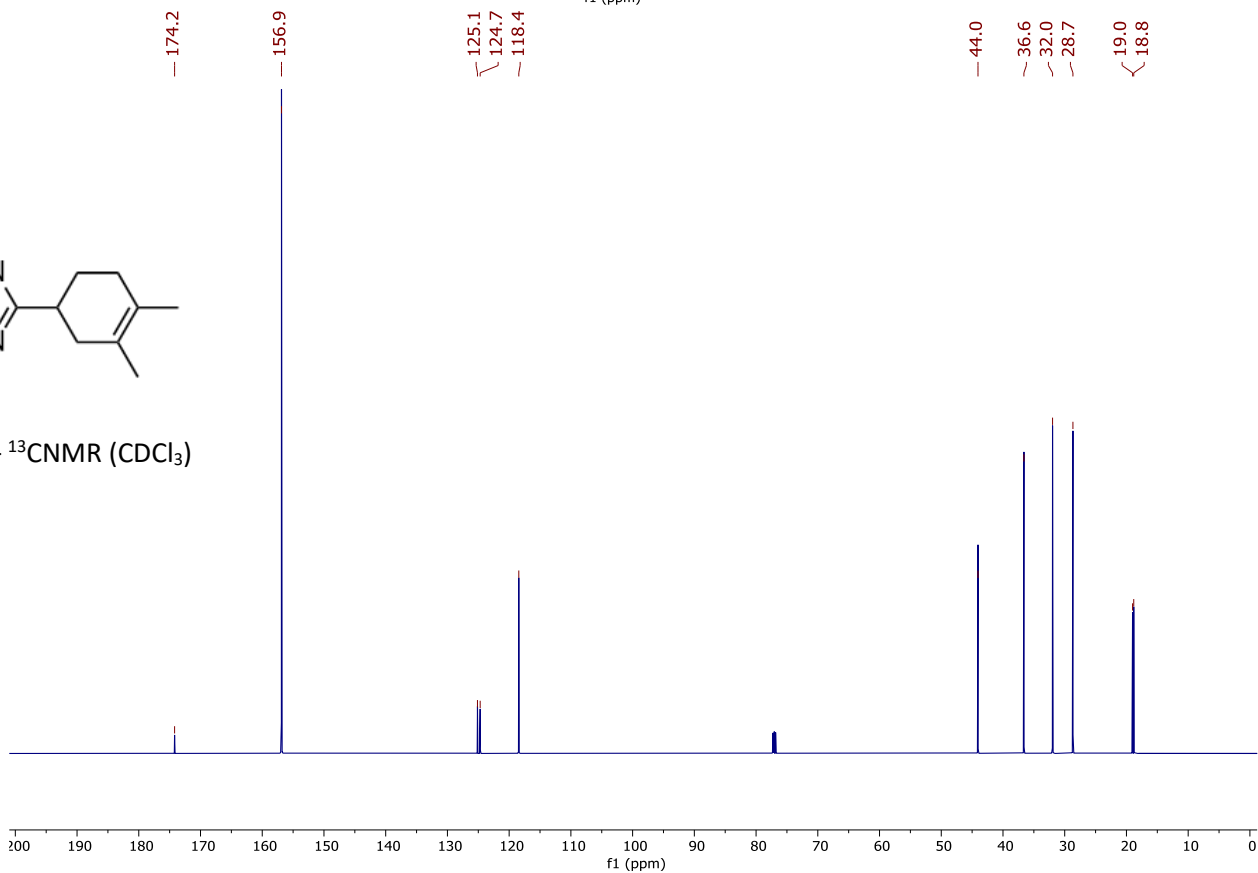


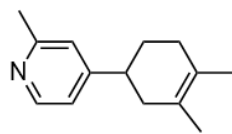


2.19 –  $^1\text{H}$ NMR ( $\text{CDCl}_3$ )

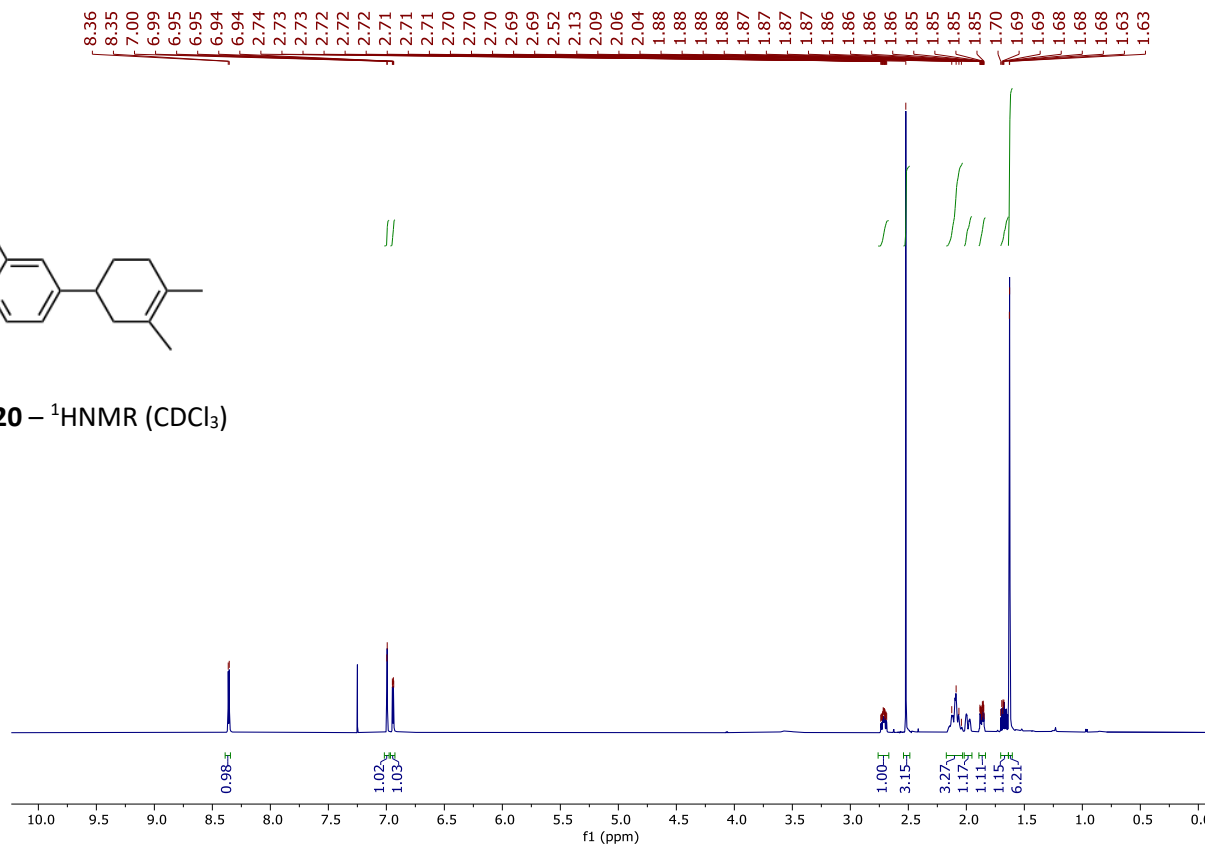


2.19 –  $^{13}\text{C}$ NMR ( $\text{CDCl}_3$ )



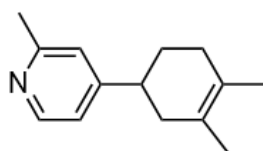


2.20 – <sup>1</sup>HNMR (CDCl<sub>3</sub>)

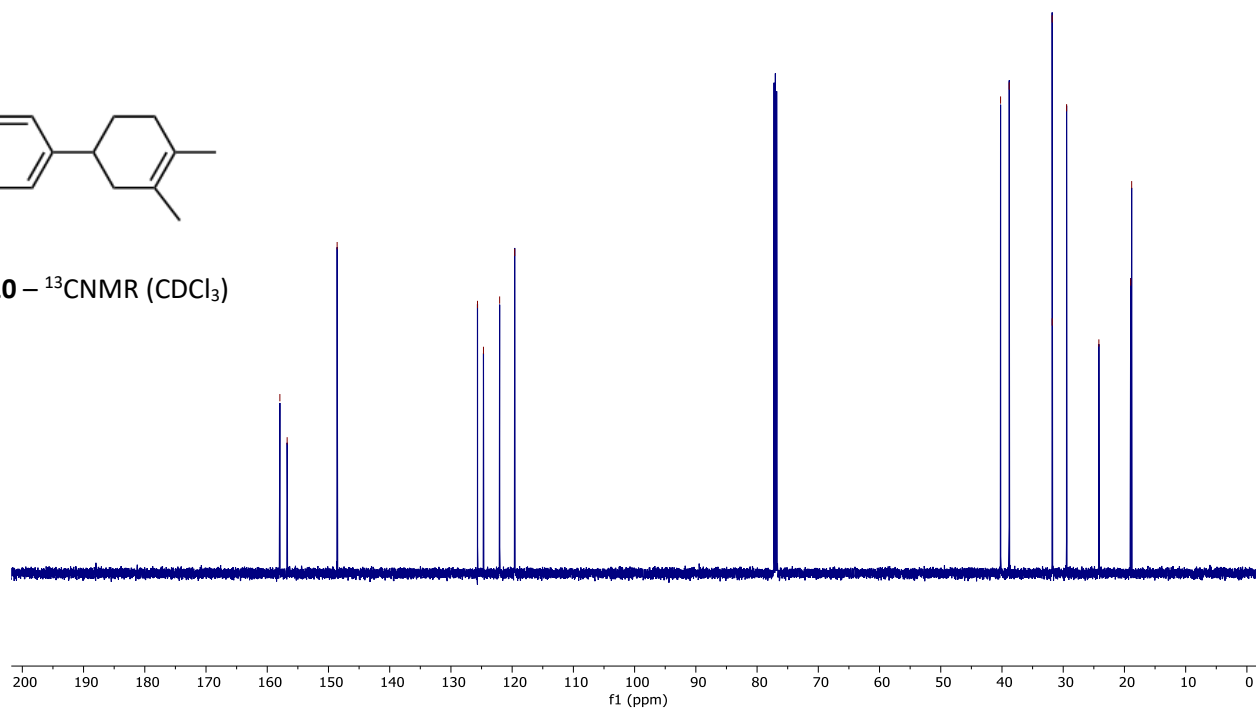


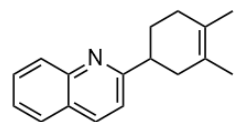
157.9  
156.7  
148.6  
125.7  
124.7  
122.0  
119.6

40.2  
38.8  
31.8  
31.8  
29.4  
24.2  
19.0  
18.8

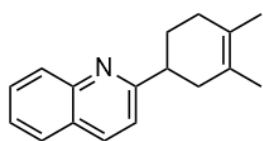
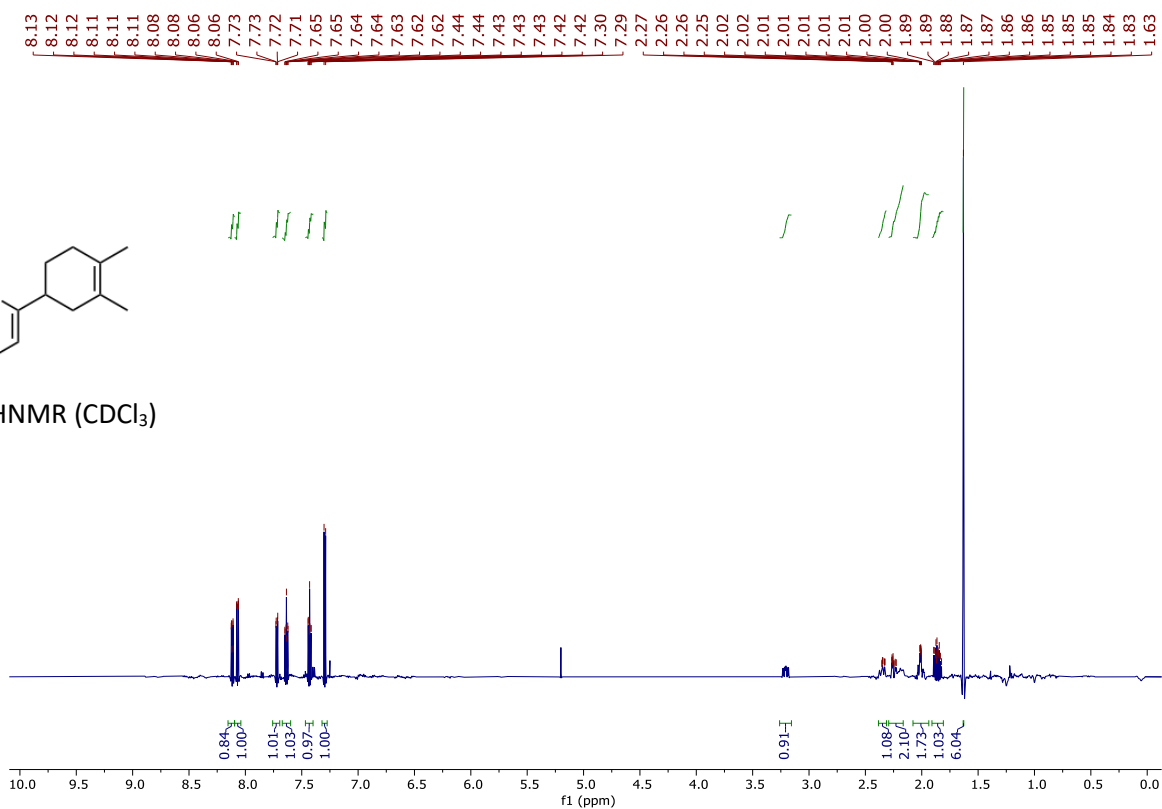


2.20 – <sup>13</sup>CNMR (CDCl<sub>3</sub>)

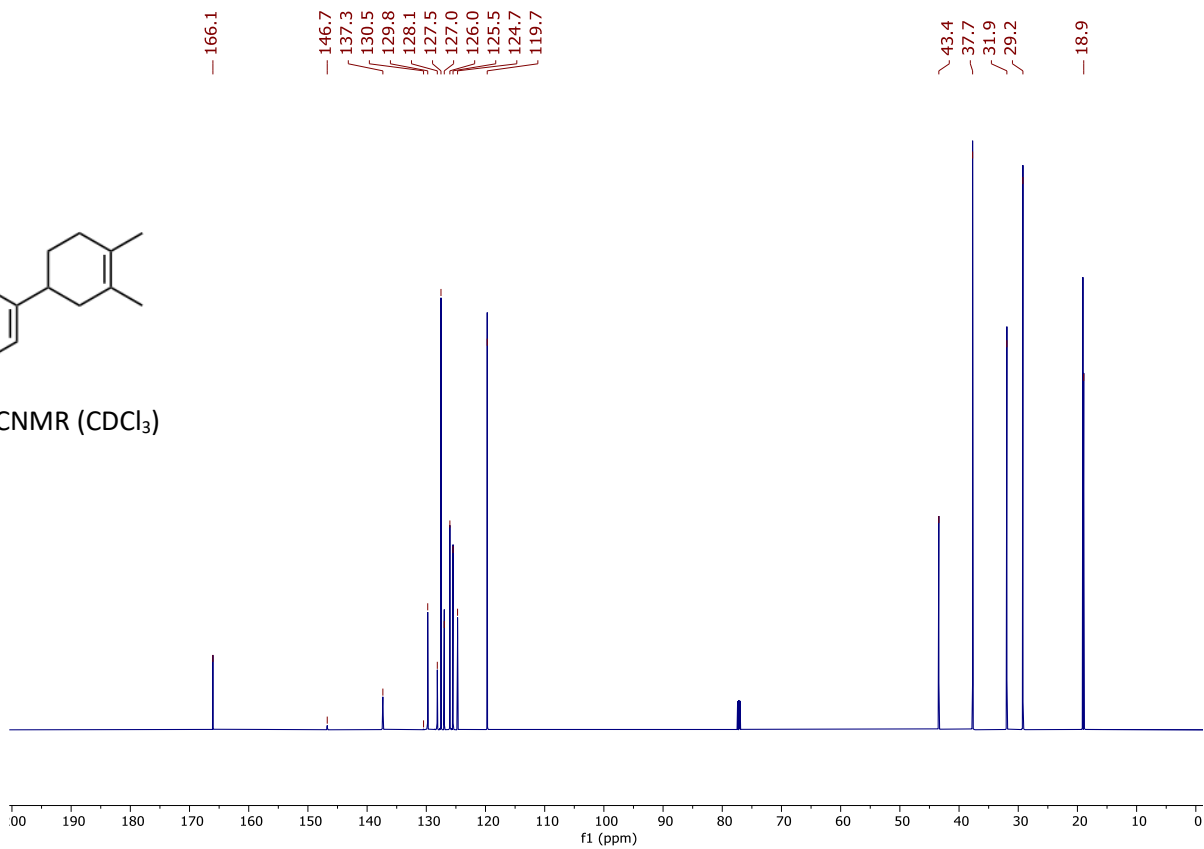


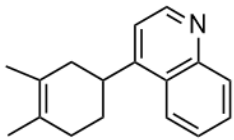


2.21 –  $^1\text{H}$ NMR ( $\text{CDCl}_3$ )

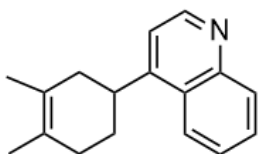
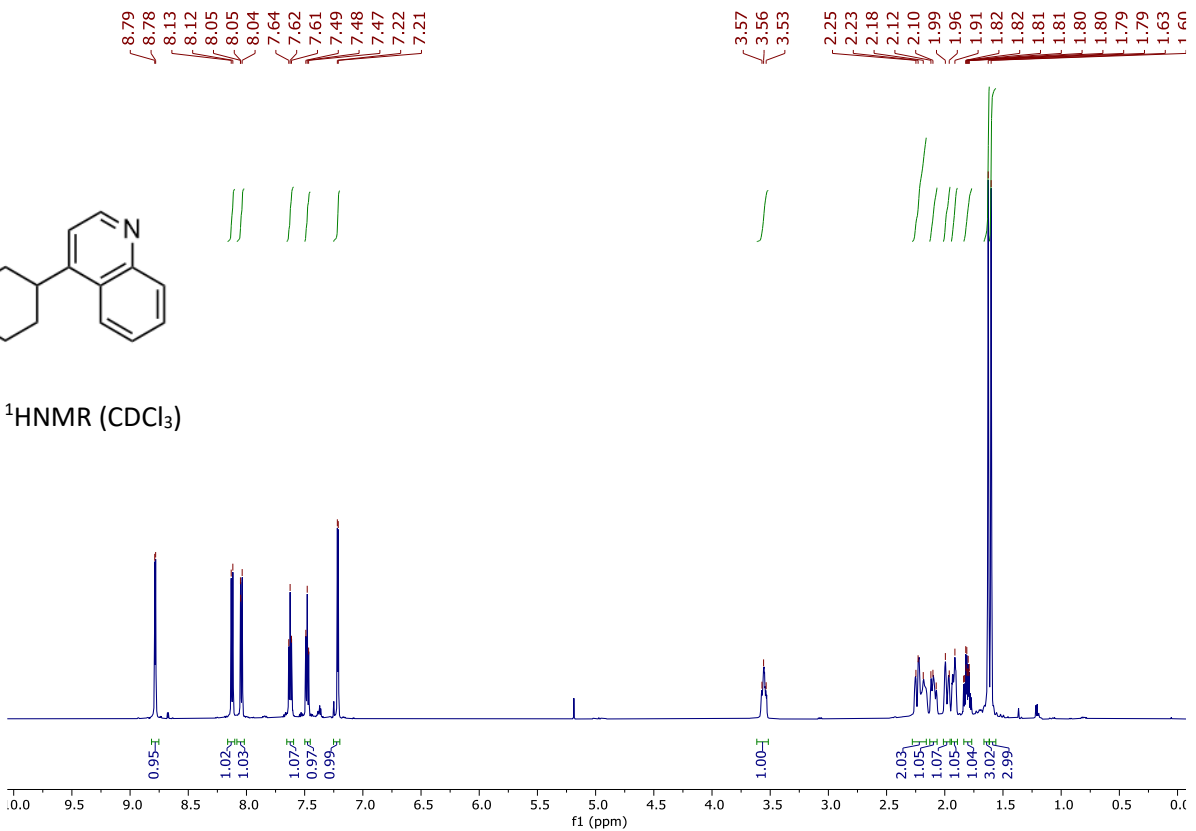


2.21 –  $^{13}\text{C}$ NMR ( $\text{CDCl}_3$ )

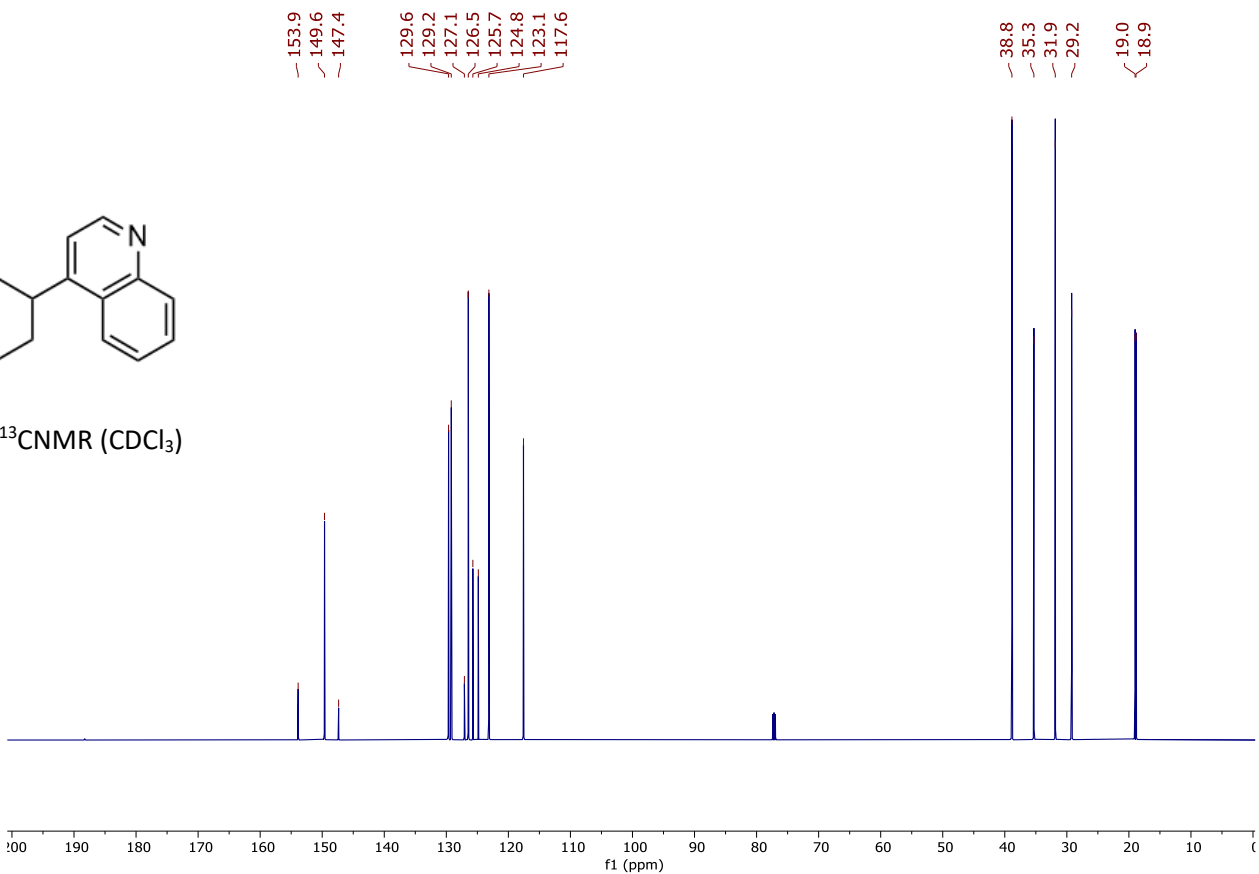




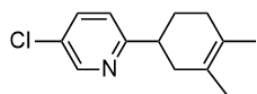
2.22 –  $^1\text{H}$ NMR ( $\text{CDCl}_3$ )



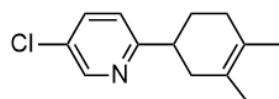
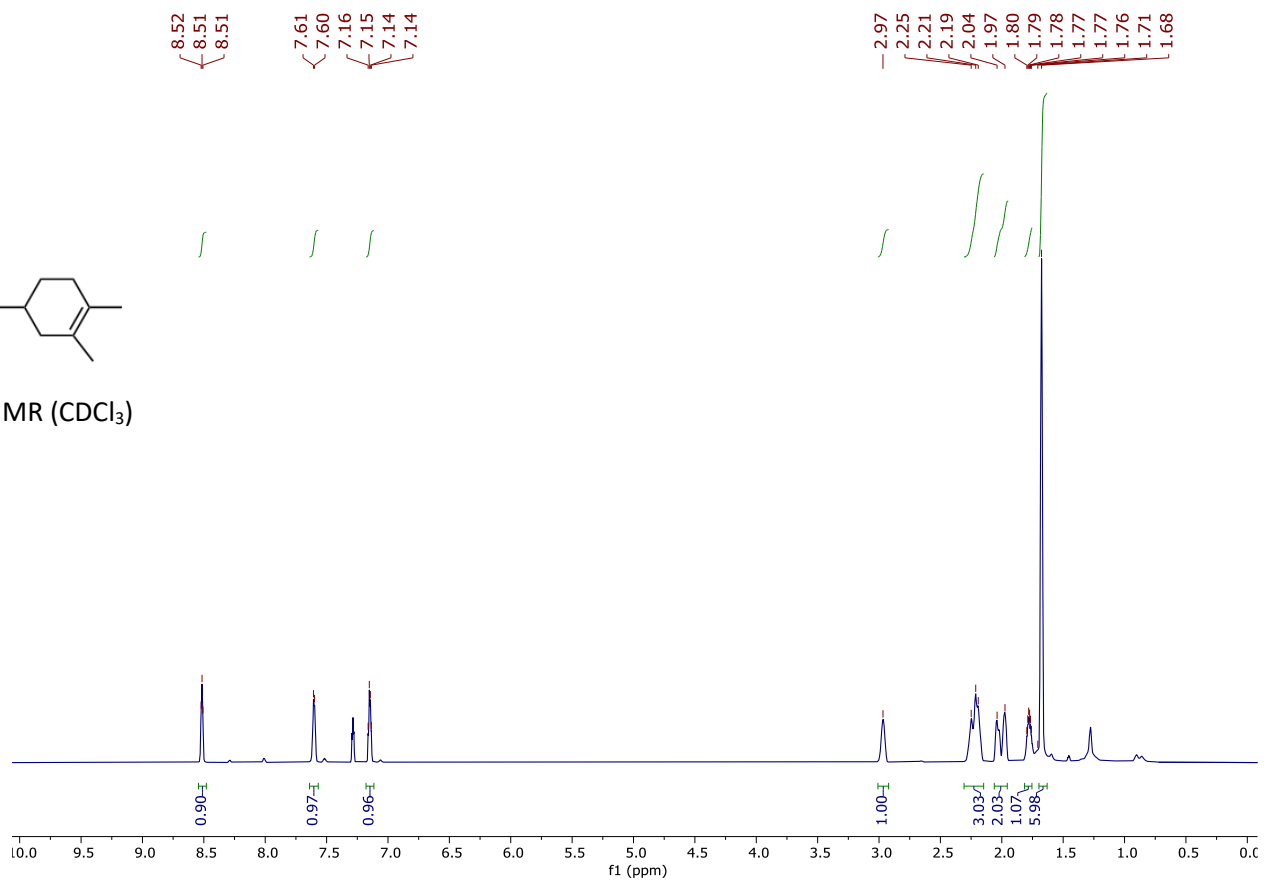
2.22 –  $^{13}\text{C}$ NMR ( $\text{CDCl}_3$ )



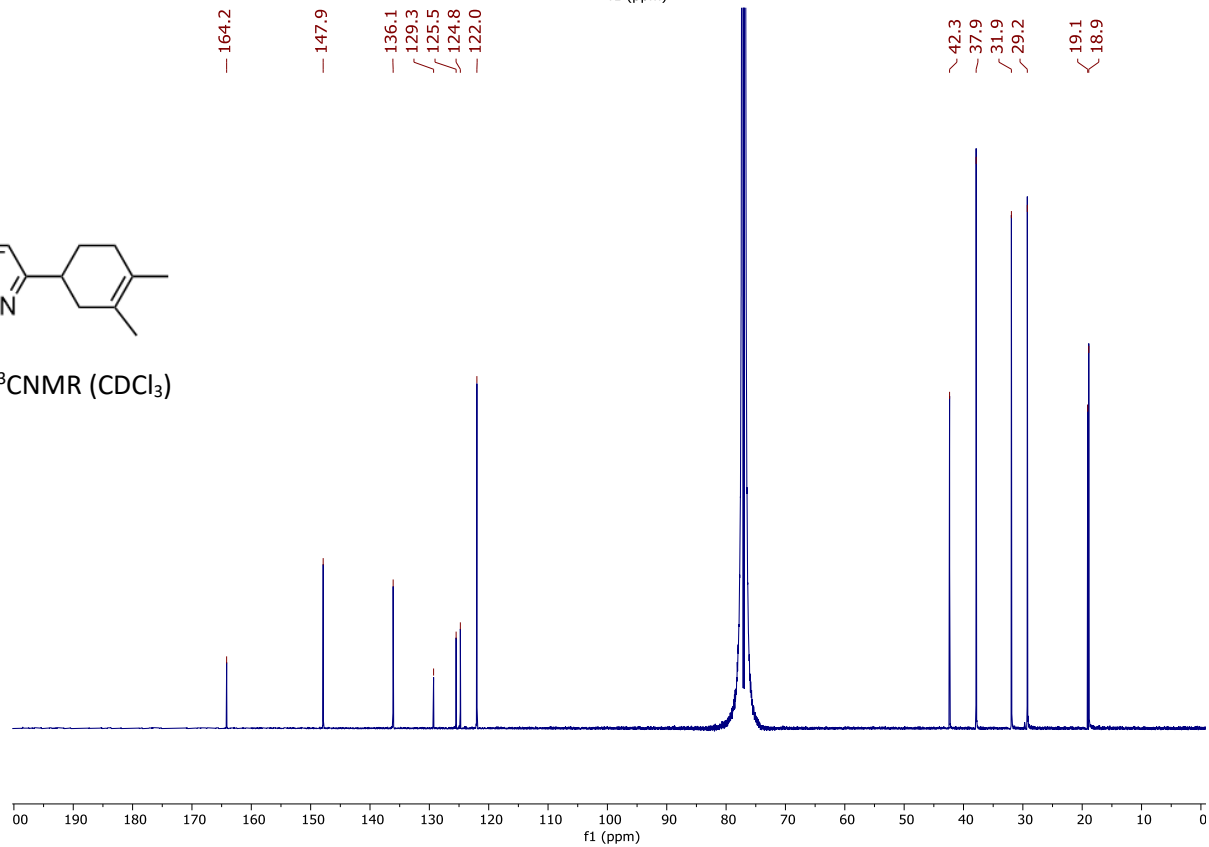


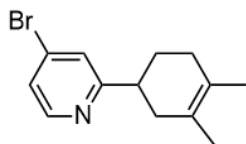


2.25 –  $^1\text{H}$ NMR ( $\text{CDCl}_3$ )

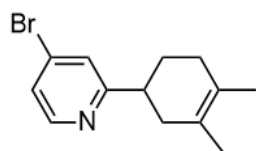
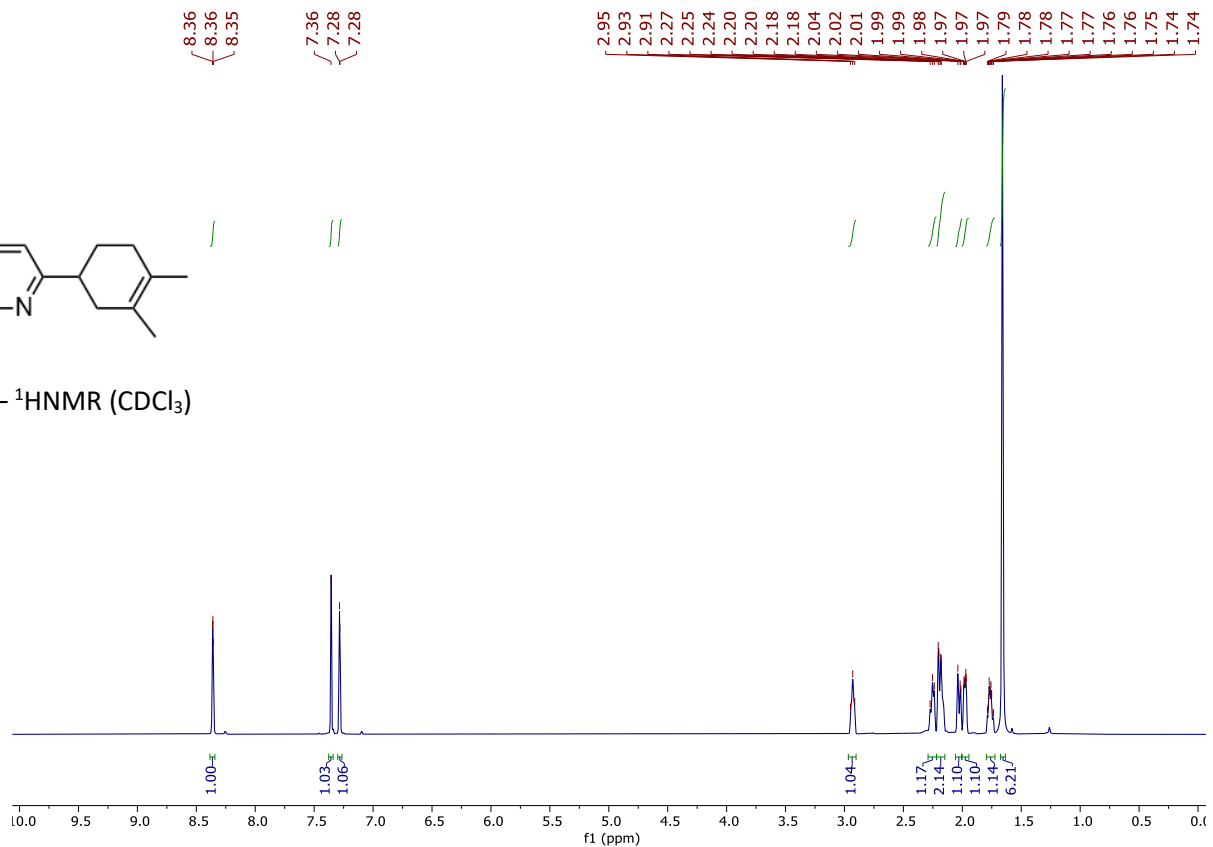


2.25 –  $^{13}\text{C}$ NMR ( $\text{CDCl}_3$ )

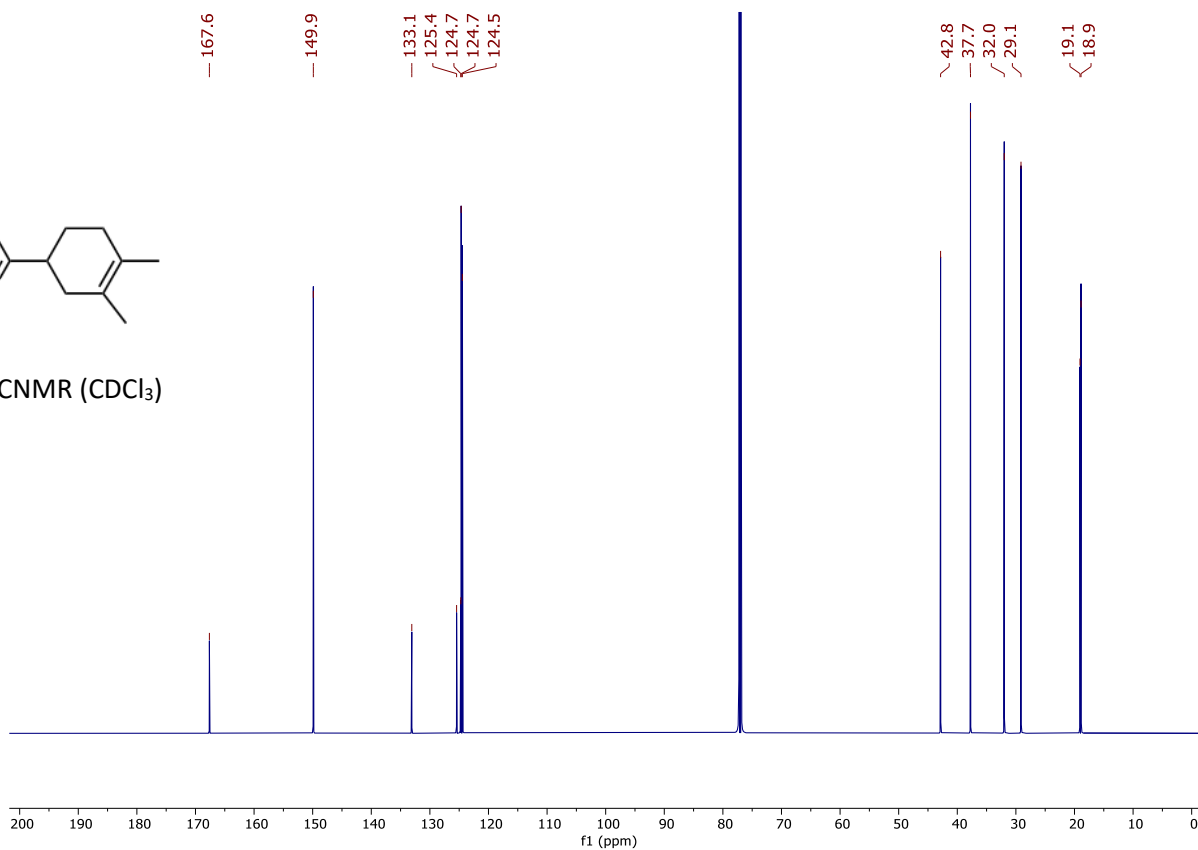


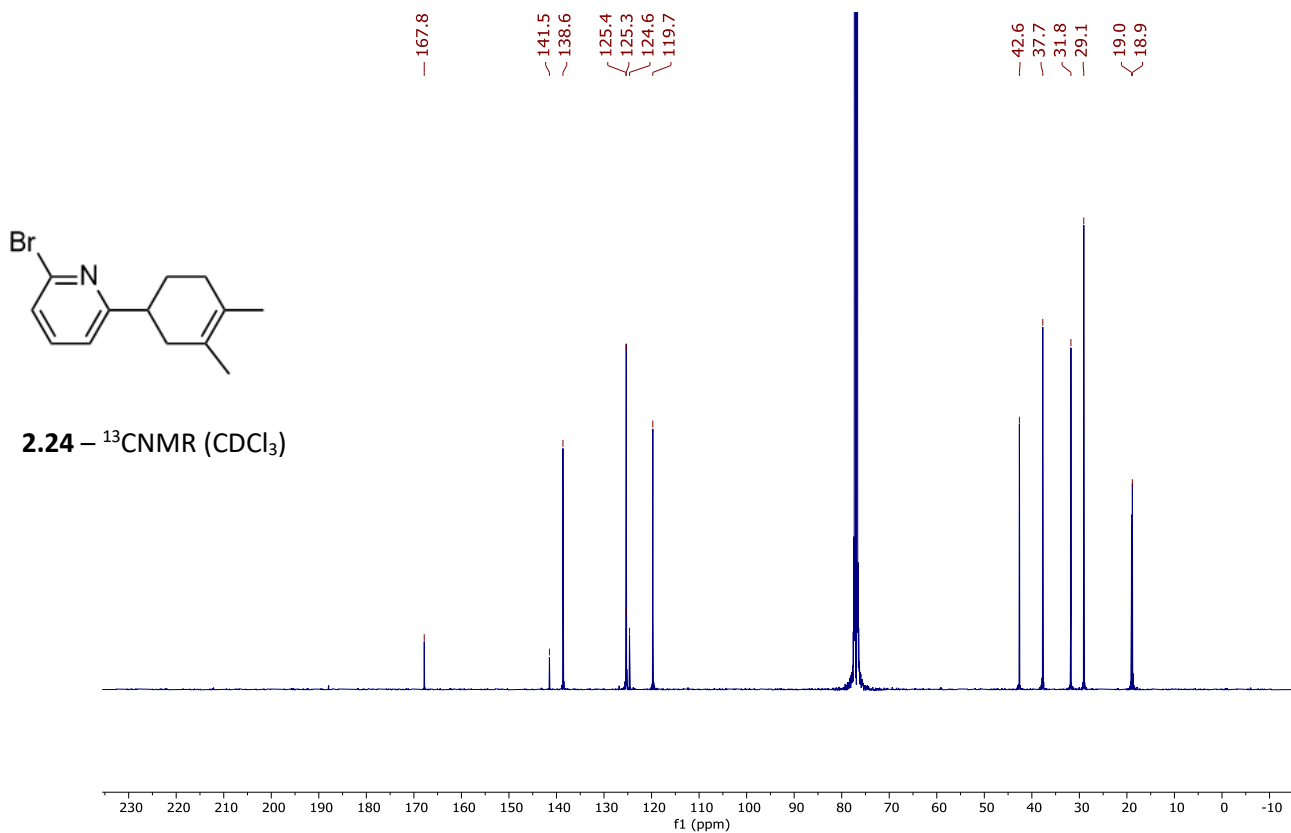
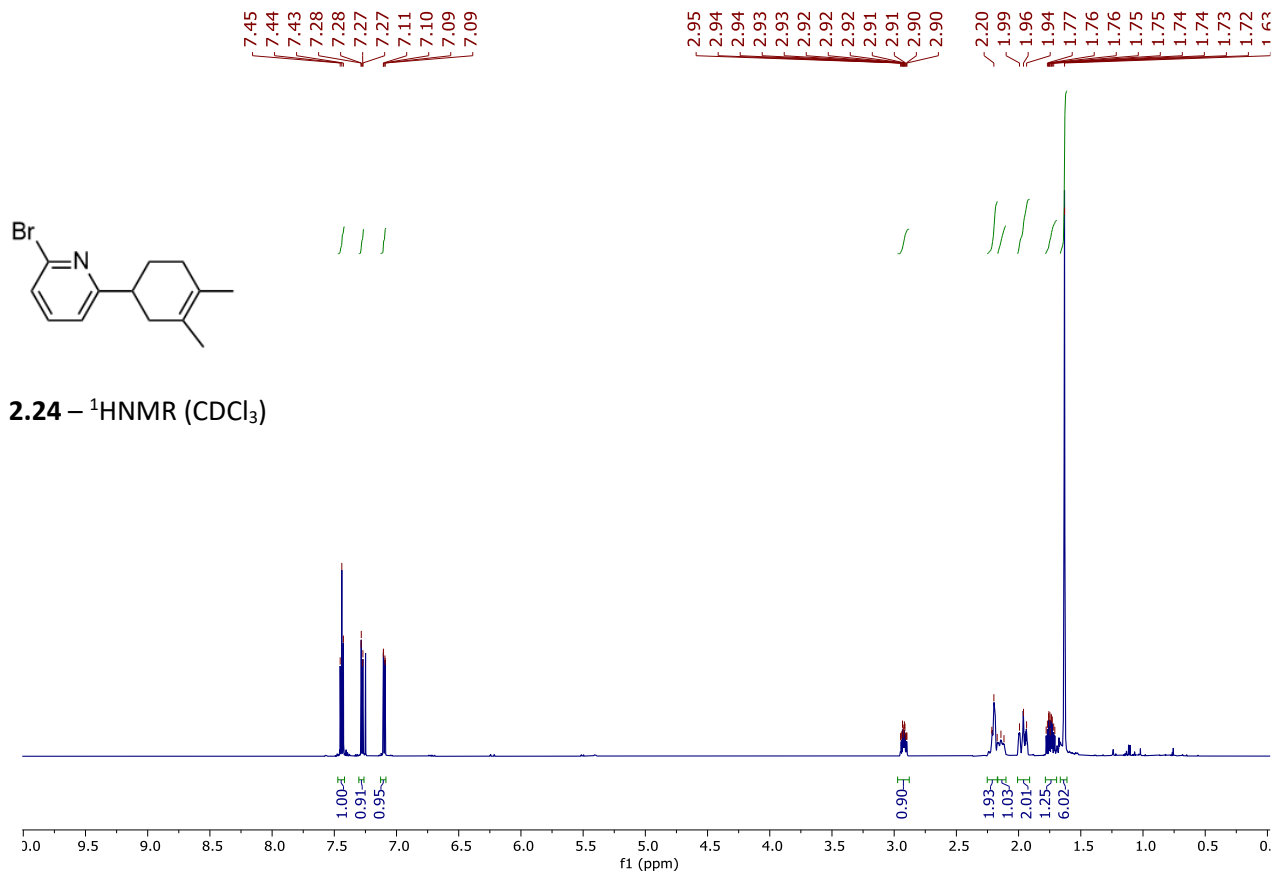


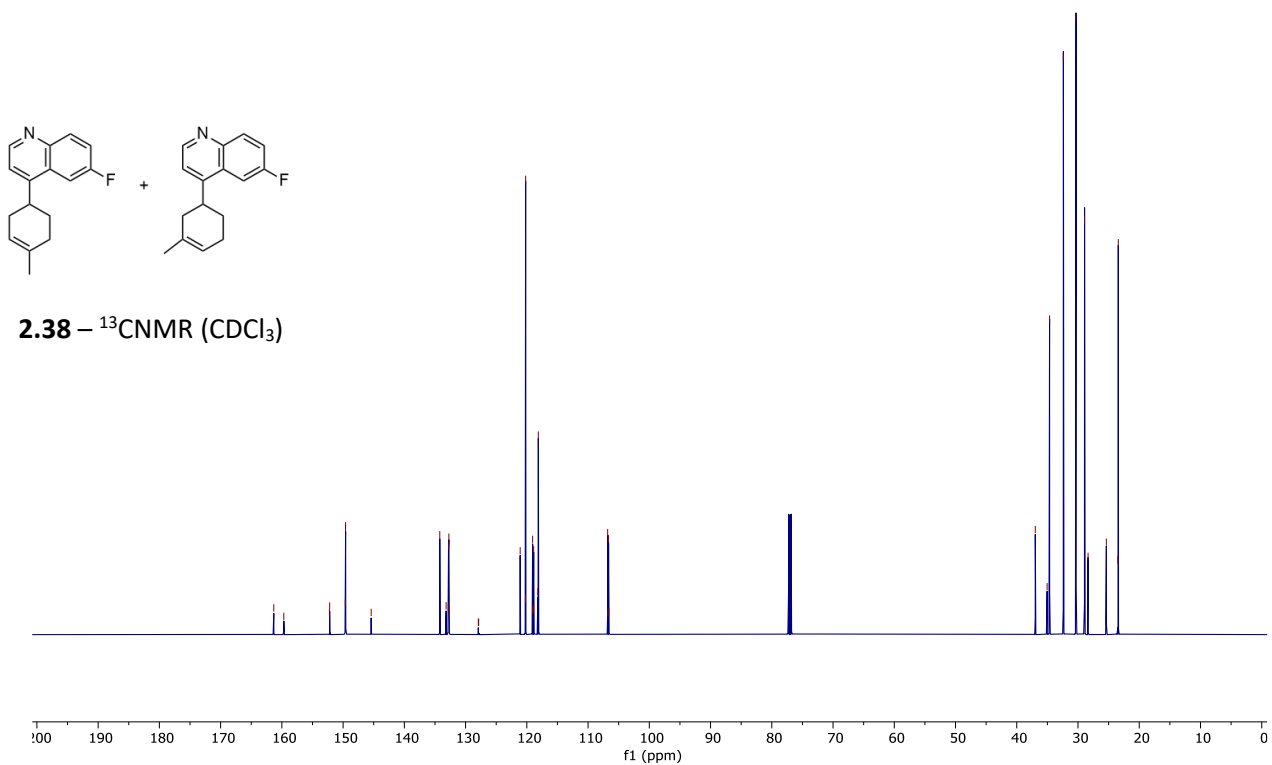
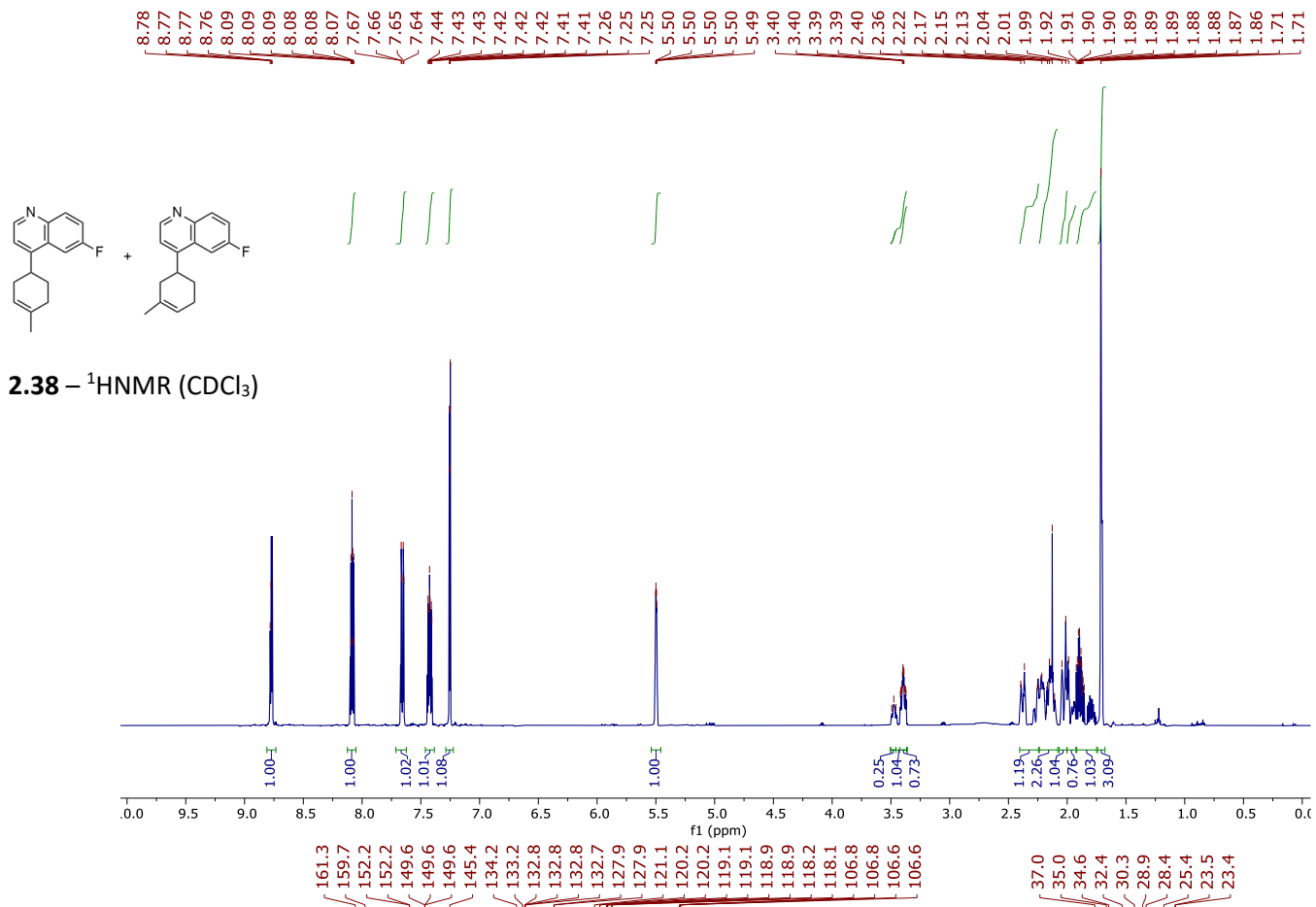
2.26 –  $^1\text{H}$ NMR ( $\text{CDCl}_3$ )



2.26 –  $^{13}\text{C}$ NMR ( $\text{CDCl}_3$ )







## B – Appendix 2:

### Chapter 3 Experimental Data

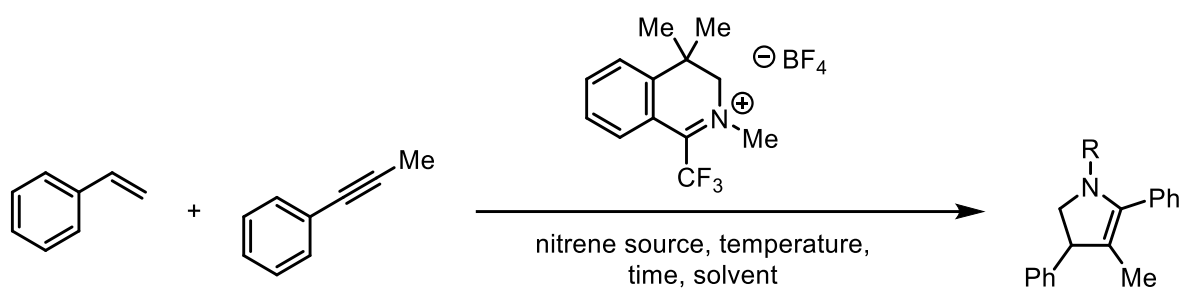
#### B.1 General methods

**Materials and Methods:** All reagents were obtained commercially in the highest available purity and used without further purification unless otherwise mentioned. Anhydrous solvents were obtained from a solvent purification system utilizing activated alumina columns under a positive pressure of argon. Reactions carried out at temperatures above room temperature (23 °C) were conducted in a pre-heated oil bath or on a pre-heated aluminum block. Cyclization reactions were performed inside a glovebox or using Schlenk techniques under N<sub>2</sub> atmosphere in 2-dram vials equipped with a magnetic stir bar unless otherwise noted. Flash column chromatography was performed using silica (400 mesh) or purchased pre-packaged for auto-column elution from Teledyne Isco. Elution of compounds was monitored by UV and anisaldehyde stain on TLC.

**Instrumentation:** <sup>1</sup>H and <sup>13</sup>C NMR spectra were measured on a Varian Inova 600 (600 MHz) or Bruker Avance III 800 (800 MHz) spectrometer and acquired at 300 K. Chemical shifts are reported in parts per million (ppm δ) referenced to the residual <sup>1</sup>H or <sup>13</sup>C resonance of the solvent. The following abbreviations are used singularly or in combination to indicate the multiplicity of signals: s - singlet, d - doublet, t - triplet, q - quartet, m – multiplet, br – broad, and ap – apparent. High-resolution mass spectrometry was obtained using an Agilent Q-TOF APCI spectrometer.

## B.2 Screening and Reaction Optimization

Reaction conditions were screened with the cyclization of styrene and 1-phenyl-1-propyne using the following general procedure: To a 1 dr vial equipped with a PTFE stir bar and charged with styrene (11  $\mu$ L, 0.1 mmol, 1 equiv) in dichloromethane (500  $\mu$ L) was added 1-phenyl-1-propyne (36  $\mu$ L, 0.3 mmol, 3 equiv), TMI-NBs (75 mg, 0.15 mmol, 1.5 equiv), and iminium catalyst (6.3 mg, 20  $\mu$ mol, 0.2 equiv) unless otherwise noted. The vial was placed in an aluminum heating block pre-heated to the specified temperature or on a stir plate at room temperature and allowed to stir for the specified time. Upon reaction completion, the mixture was cooled to room temperature, filtered through a silica plug with 20 mL dichloromethane, and NMR yield was obtained with 3-methyl nitrobenzoate as an internal standard.



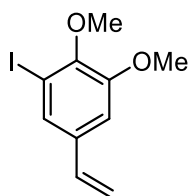
	eq. alkyne	nitrene source	eq. nitrene source	solvent	catalyst loading (mol %)	reaction temperature (°C)	reaction time (h)	NMR yield (%)
1	1	PhINTs	1	DCM	20	23	18	5
2	2	PhINTs	1	DCM	20	23	18	9
3	3	PhINTs	1	DCM	20	23	18	14

4	3	PhINTs	1.5	DCM	20	23	18	21
5	3	PhINTs	2	DCM	20	23	18	19
6	3	TMI-NBs	1.5	DCM	20	23	18	54
7	3	PhINBs	1.5	DCM	20	23	18	3
8	3	TMI-NTs	1.5	DCM	20	23	18	11
9	3	TMI-Tces	1.5	DCM	20	23	18	16
10	3	PhINTces	1.5	DCM	20	23	18	15
11	3	PhINTs	1.5	MeCN	20	23	18	20
12	3	PhINTs	1.5	DCE	20	23	18	5
13	3	PhINTs	1.5	THF	20	23	18	0
14	3	PhINTs	1.5	DMF	20	23	18	3
15	3	PhINTs	1.5	9:1 DCM:hexanes	20	23	18	9
16	3	PhINTs	1.5	DCM	10	23	18	0
17	3	PhINTs	1.5	DCM	15	23	18	16
18	3	PhINTs	1.5	DCM	30	23	18	22
19	3	TMI-NBs	1.5	DCM	0	23	18	0
20	3	TMI-NBs	1.5	DCM	20	4	18	trace
21	3	TMI-NBs	1.5	DCM	20	30	18	13
22	3	TMI-NBs	1.5	DCM	20	40	18	trace
23	3	PhINTs	1.5	DCM	20	23	24	30
24	3	TMI-NBs	1.5	DCM	20	23	24	62

## B.3 Reagent and Substrate Synthesis

Substrates **B.1** – **B.5** were prepared according to literature procedure.

### 1-iodo-2,3-dimethoxy-5-vinylbenzene (**B.1**)

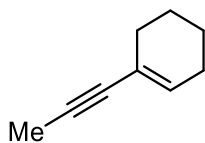


$^1\text{H NMR}$  (600 MHz,  $\text{CDCl}_3$ )  $\delta$  7.45 (d, 1H,  $J = 2.0$  Hz), 7.17 (d, 1H,  $J = 2.0$  Hz), 6.67 (dd, 1H,  $J = 10.8, 17.5$  Hz), 5.79 (d, 1H,  $J = 17.5$  Hz), 5.21 (d, 1H,  $J = 10.8$  Hz), 3.92 (s, 3H), 3.79 (s, 3H) ppm.

$^{13}\text{C NMR}$  (151 MHz,  $\text{CDCl}_3$ )  $\delta$  154.1, 149.4, 136.0, 135.3, 128.4, 114.2, 111.8, 92.6, 60.3, 56.1 ppm.

NMR spectra are consistent with literature reports.<sup>1</sup>

### 1-(prop-1-yn-1-yl)cyclohex-1-ene (**B.2**)

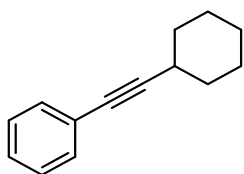


**<sup>1</sup>H NMR** (600 MHz, CDCl<sub>3</sub>): δ 6.02 – 5.98 (m, 1H), 2.13 – 2.01 (m, 4H), 1.94 (s, 3H), 1.68 – 1.52 (m, 4H).

**<sup>13</sup>C NMR** (151 MHz, CDCl<sub>3</sub>): δ 133.0, 121.1, 83.0, 81.9, 29.8, 25.7, 22.7, 21.5, 4.3.

NMR spectra are consistent with literature reports.<sup>2</sup>

**(cyclohexylethynyl)benzene (B.3)**

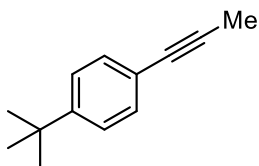


**<sup>1</sup>H NMR** (600 MHz, CDCl<sub>3</sub>): δ 7.39 – 7.41 (m, 1H), 7.25 – 7.29 (m, 4H), 2.59 – 2.61 (m, 1H), 1.88 – 2.90 (m, 2H), 1.74 – 1.77 (m, 2H), 1.52 – 1.55 (m, 3H), 1.34 – 1.36 (m, 3H).

**<sup>13</sup>C NMR** (151 MHz, CDCl<sub>3</sub>): δ 131.8, 128.4, 127.6, 124.3, 94.7, 80.7, 32.9, 29.9, 26.2, 25.1.

NMR spectra are consistent with literature reports.<sup>3</sup>

**1-(tert-butyl)-4-(prop-1-yn-1-yl)benzene (B.4)**

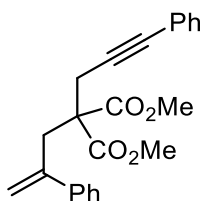


**<sup>1</sup>H NMR** (600 MHz, CDCl<sub>3</sub>): δ 7.35–7.28 (m, 4H), 2.04 (s, 3H), 1.30 (s, 9H).

**<sup>13</sup>C NMR** (151 MHz, CDCl<sub>3</sub>): δ 152.8, 131.8, 125.7, 122.4, 92.5, 79.2, 34.7, 31.1, 3.8.

NMR spectra are consistent with literature reports.<sup>4</sup>

### dimethyl 2-(2-phenylallyl)-2-(3-phenylprop-2-yn-1-yl)malonate (B.5)



<sup>1</sup>H NMR (600 MHz, CDCl<sub>3</sub>): δ 7.85 (d, *J* = 8.3 Hz, 1H), 7.49 – 7.15 (m, 10H), 5.32 (s, 1H), 4.94 (s, 1H), 3.45 (s, 6H), 2.96 (s, 2H), 2.38 (s, 2H).

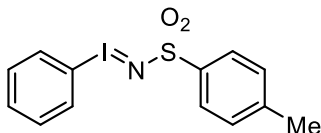
<sup>13</sup>C NMR (151 MHz, CDCl<sub>3</sub>): δ 170.9, 146.6, 141.0, 131.8, 128.4, 127.8, 127.5, 122.2, 112.8, 87.0, 80.8, 56.5, 52.2, 38.6, 22.6.

NMR spectra are consistent with literature reports.<sup>5</sup>

## B.4 Nitrene Precursor Synthesis

Nitrene precursors **B.6** - **B.9** were prepared according to literature procedure.

### (B.6) 4-methyl-N-(phenyl-λ<sup>3</sup>-iodaneylidene)benzenesulfonamide (PhINTs)

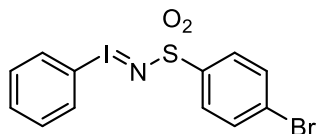


**<sup>1</sup>H NMR** (600 MHz, DMSO-*d*<sub>6</sub>): δ 7.71 (d, *J* = 7.8 Hz, 2H), 7.48-7.44 (m, 3H), 7.30-7.28 (m, 2H), 7.07 (d, *J* = 7.8 Hz, 2H), 2.23 (s, 3H).

**<sup>13</sup>C NMR** (151 MHz, DMSO-*d*<sub>6</sub>): δ 148.2, 131.7, 131.0, 128.3, 127.8, 127.1, 123.5, 110.2, 31.3 ppm.

NMR spectra are consistent with literature reports.<sup>6</sup>

**(B.7) 4-bromo-N-(phenyl-λ<sup>3</sup>-iodaneylidene)benzenesulfonamide (PhINBs)**

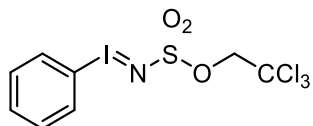


**<sup>1</sup>H NMR** (600 MHz, DMSO-*d*<sub>6</sub>): δ 7.74 – 7.72 (m, 2H), 7.53 – 7.41 (m, 5H), 7.27 – 7.23 (m, 2H).

**<sup>13</sup>C NMR** (151 MHz, DMSO-*d*<sub>6</sub>): δ 145.6, 132.9, 130.9, 130.1, 128.7, 127.1, 122.9, 119.0 ppm.

NMR spectra are consistent with literature reports.<sup>7</sup>

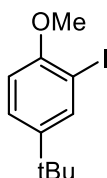
**(B.8) 2,2,2-trichloroethyl (phenyl-λ<sup>3</sup>-iodaneylidene)sulfamate (PhINTces)**



**<sup>1</sup>H NMR** (600 MHz, DMSO-*d*<sub>6</sub>): δ 8.10 (dd, *J* = 7.7, 1.2 Hz, 2H), 7.64 – 7.60 (m, 1H), 7.51 (t, *J* = 7.7 Hz, 2H), 4.22 (s, 2H) ppm.

NMR spectra are consistent with literature reports.<sup>8</sup>

**(B.9) 4-(tert-butyl)-2-iodo-1-methoxybenzene**



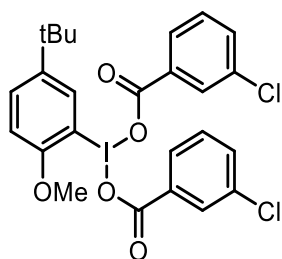
4-(*tert*-butyl)-2-iodo-1-methoxybenzene

<sup>1</sup>H NMR (600 MHz, CDCl<sub>3</sub>): δ 7.76 (d, J = 2.4 Hz, 1H), 7.30 (dd, J = 8.5, 2.4 Hz, 1H), 6.77 (d, J = 8.5 Hz, 1H), 3.89 (s, 3H), 1.22 (s, 9H) ppm.

<sup>13</sup>C NMR (151 MHz, CDCl<sub>3</sub>): δ 155.8, 145.8, 135.7, 125.4, 109.5, 84.2, 54.7, 34.1, 30.8.

NMR spectra are consistent with literature reports.<sup>9</sup>

**(B.10) (5-(tert-butyl)-2-methoxyphenyl)-λ<sup>3</sup>-iodanediyl bis(3-chlorobenzoate)**



**(5-(tert-butyl)-2-methoxyphenyl)-λ<sup>3</sup>-iodanediyl bis(3-chlorobenzoate)** was prepared by adding meta-Chloroperoxybenzoic acid (2 equiv) portionwise to a solution of **B.9** (1 equiv) in anhydrous dichloromethane (0.10 M) cooled to 0°C under magnetic stirring. After addition, the solution was warmed to rt and stirred for 3 hours. Upon completion, the mixture was cooled to

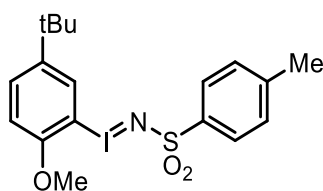
0°C and quenched with 2x solvent volume of cold DI water. The resulting biphasic mixture was extracted 3x with DCM, washed with brine, dried over MgSO<sub>4</sub>, and concentrated at room temperature *in vacuo* (product is thermally unstable) to yield an off-white oil. The oil was precipitated into an off-white solid upon addition of hexanes, then washed with a solution of 10% EtOH in hexanes to yield pure product **B.10** as off-white crystals (87% yield).

<sup>1</sup>H NMR (600 MHz, CDCl<sub>3</sub>) δ 8.25 (s, 1H), 7.84 (s, 2H), 7.78 (d, J = 7.8 Hz, 2H), 7.65 (d, J = 8.6 Hz, 1H), 7.43 (d, J = 7.8 Hz, 2H), 7.28 (t, J = 7.8 Hz, 2H), 7.14 (d, J = 8.6 Hz, 1H), 3.95 (s, 3H), 1.37 (s, 9H) ppm.

<sup>13</sup>C NMR (151 MHz, CDCl<sub>3</sub>) δ 170.1, 154.3, 146.2, 134.7, 134.1, 132.3, 132.3, 131.7, 130.1, 129.5, 128.2, 113.8, 111.7, 57.2, 57.0, 34.6, 31.3 ppm.

**Elemental Analysis:** Calcd for C<sub>25</sub>H<sub>23</sub>O<sub>5</sub>Cl<sub>2</sub>I: C 49.94, H 3.86, N 0.00; found C 49.77 H 3.78 N 0.05.

**(3.17) N-((5-(tert-butyl)-2-methoxyphenyl)-λ<sup>3</sup>-iodaneylidene)-4-methylbenzenesulfonamide (TMI-NTs)**



**N-((5-(tert-butyl)-2-methoxyphenyl)-λ<sup>3</sup>-iodaneylidene)-4-methylbenzenesulfonamide** was prepared according to modified literature procedure.<sup>55</sup> P-toluenesulfonamide (1 equiv) and KOH (2.5 equiv) were dissolved in MeOH (0.30 M) and cooled to 0°C under magnetic stirring. Product **B.10** (1 equiv) was then added portionwise and stirred for 30 minutes. The resulting mixture was warmed to rt and stirred 3 hours under N<sub>2</sub>. Upon completion, the mixture was

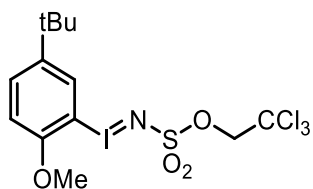
cooled to 0°C and quenched with 2x solvent volume of ice chips. The resulting precipitate was collected over vacuum filtration and washed with cold hexanes to yield pure product **3.17** as a white powder (54% yield).

**<sup>1</sup>H NMR** (600 MHz, CDCl<sub>3</sub>) δ 7.81 (d, J = 7.9 Hz, 2H), 7.64 (d, J = 2.2 Hz, 1H), 7.40 (dd, J = 8.5, 2.2 Hz, 1H), 7.14 (d, J = 7.9 Hz, 2H), 6.81 (d, J = 8.5 Hz, 1H), 3.86 (s, 3H), 2.33 (s, 3H), 1.26 (s, 9H) ppm.

**<sup>13</sup>C NMR** (151 MHz, CDCl<sub>3</sub>) δ 152.9, 147.9, 141.7, 140.2, 129.5, 129.2, 127.0, 126.5, 111.1, 102.6, 56.8, 35.0, 31.3, 21.4 ppm.

**Elemental Analysis:** Calcd for C<sub>18</sub>H<sub>22</sub>NO<sub>3</sub>SI: C 47.07, H 4.83, N 3.05; found C 46.74, H 4.81, N 2.89.

**(3.18) 2,2,2-trichloroethyl ((5-(tert-butyl)-2-methoxyphenyl)-λ<sup>3</sup>-iodaneylidene)sulfamate (TMI-NTces)**



**2,2,2-trichloroethyl ((5-(tert-butyl)-2-methoxyphenyl)-λ<sup>3</sup>-iodaneylidene) sulfamate** was prepared according to modified literature procedure.<sup>55</sup> 2,2,2-trichloroethyl sulfamate (H<sub>2</sub>NTces) (1 equiv) and KOH (2.5 equiv) were dissolved in MeOH (0.25 M) and cooled to 0°C under magnetic stirring. Product **B.10** (1 equiv) was then added portionwise and stirred for 30 minutes. The resulting mixture was warmed to rt and stirred 3 hours under N<sub>2</sub>. Upon completion, the mixture was cooled to 0°C and quenched with 2x solvent volume of ice chips. The resulting

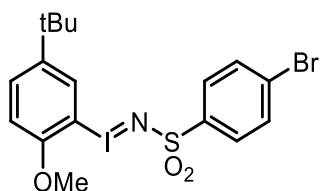
precipitate was collected over vacuum filtration and washed with cold hexanes and diethyl ether to yield pure product **3.18** as off-white crystals (62% yield).

$^1\text{H NMR}$  (600 MHz,  $\text{CDCl}_3$ )  $\delta$  7.88 (s, 1H), 7.52 (d,  $J = 8.5$  Hz, 1H), 6.93 (d,  $J = 8.5$  Hz, 1H), 4.57 (s, 2H), 3.94 (s, 3H), 1.34 (s, 9H) ppm.

$^{13}\text{C NMR}$  (151 MHz,  $\text{CDCl}_3$ )  $\delta$  153.1, 148.4, 130.5, 127.3, 111.5, 103.2, 94.7, 78.1, 57.1, 35.1, 31.3 ppm.

**Elemental Analysis:** Calcd for  $\text{C}_{13}\text{H}_{17}\text{NO}_4\text{SCl}_3\text{I}$ : C 30.23, H 3.32, N 2.71; found C 30.52, H 3.22, N 2.61.

**(3.19) N-((5-(tert-butyl)-2-methoxyphenyl)- $\lambda^3$ -iodaneylidene)-4-bromobenzenesulfonamide (TMI-NBs)**



**N-((5-(tert-butyl)-2-methoxyphenyl)- $\lambda^3$ -iodaneylidene)-4-bromobenzenesulfonamide** was prepared according to modified literature procedure.<sup>55</sup> 4-bromobenzenesulfonamide (1 equiv) and KOH (2.5 equiv) were dissolved in MeOH (0.30 M) and cooled to  $0^\circ\text{C}$  under magnetic stirring. Product **B.10** (1 equiv) was then added portionwise and stirred for 30 minutes. The resulting mixture was warmed to rt and stirred 3 hours under  $\text{N}_2$ . Upon completion, the mixture was cooled to  $0^\circ\text{C}$  and quenched with 2x solvent volume of ice chips. The resulting precipitate was collected over vacuum filtration and washed with cold hexanes to yield pure product **3.19** as an off-white powder (64% yield).

**<sup>1</sup>H NMR** (600 MHz, CDCl<sub>3</sub>) δ 7.76 (d, *J* = 8.5 Hz, 1H), 7.61 (d, *J* = 2.2 Hz, 1H), 7.47 – 7.40 (m, 2H), 6.82 (d, *J* = 8.5 Hz, 1H), 3.87 (s, 3H), 1.26 (s, 9H) ppm.

**<sup>13</sup>C NMR** (151 MHz, CDCl<sub>3</sub>) δ 153.0, 147.9, 142.2, 131.7, 129.9, 128.6, 127.0, 125.9, 111.2, 102.5, 56.8, 34.9, 31.2 ppm.

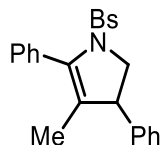
**Elemental Analysis:** Calcd for C<sub>17</sub>H<sub>19</sub>NO<sub>3</sub>SBrI: C 38.95, H 3.65, N 2.67; found C 38.90, H 3.60, N 2.77

## B.5 General [2+2+1] reaction procedure

To a 2 dr vial equipped with a PTFE stir bar and charged with alkene (1.0 mmol, 1 equiv) in dichloromethane (5 mL) was added alkyne (3.0 mmol, 3 equiv), TMI-NBs (786 mg, 1.5 mmol, 1.5 equiv), and iminium catalyst (65.6 mg, 200 μmol, 0.2 equiv). The vial was placed on a stir plate at room temperature under an inert environment and allowed to stir for 24 hours. Upon reaction completion, the mixture was quenched with water, washed with brine, dried over MgSO<sub>4</sub>, and concentrated *in vacuo*. The crude mixture was then purified by flash chromatography on silica deactivated with 5% triethylamine in 6.25% ethyl acetate in hexanes, or neutral alumina.

## B.6 Characterization of [2+2+1] Products

(3.11) 1-((4-bromophenyl)sulfonyl)-4-methyl-3,5-diphenyl-2,3-dihydro-1H-pyrrole



1-((4-bromophenyl)sulfonyl)-4-methyl-3,5-diphenyl-2,3-dihydro-1H-pyrrole was prepared according to the general procedure using styrene (115  $\mu$ L, 1.00 mmol, 1 equiv) and 1-phenyl-1-propyne (366  $\mu$ L, 3.00 mmol, 3 equiv). After workup, the reaction mixture was purified on a neutral alumina flash column (0% to 10% EtOAc/hexanes) to give product **3.11** as a white solid (282 mg, 620  $\mu$ mol, 62% yield).

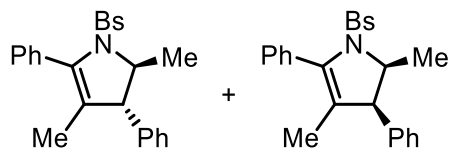
**TLC** (20% EtOAc/Hexanes)  $R_f$  = 0.46, stains orange on anisaldehyde.

**$^1\text{H}$  NMR** (600 MHz,  $\text{CDCl}_3$ )  $\delta$  7.55 (dd,  $J$  = 9.0 Hz, 3.6 Hz, 2H), 7.38 – 7.42 (m, 7H), 7.19 – 7.21 (m, 3H), 6.76 (t,  $J$  = 2.4 Hz, 2H), 4.36 (td,  $J$  = 10.8 Hz, 2.4 Hz, 1H), 3.73 – 3.76 (m, 1H), 3.66 – 3.69 (m, 1H), 1.43 (s, 3H) ppm.

**$^{13}\text{C}$  NMR** (151 MHz,  $\text{CDCl}_3$ )  $\delta$  141.8, 132.1, 132.1, 129.8, 129.6, 129.0, 128.4, 128.0, 127.8, 127.4, 127.0, 57.5, 51.5, 12.7 ppm.

**HRMS** (APCI/QTOF)  $m/z$ :  $[\text{M}+\text{H}]^+$  Calcd for  $\text{C}_{23}\text{H}_{20}\text{NO}_2\text{SBr}$  454.0471, found 454.0463.

**(3.20a + 3.20b) 1-((4-bromophenyl)sulfonyl)-2,4-dimethyl-3,5-diphenyl-2,3-dihydro-1H-pyrrole**



1-((4-bromophenyl)sulfonyl)-2,4-dimethyl-3,5-diphenyl-2,3-dihydro-1H-pyrrole was prepared according to the general procedure using *trans*- $\beta$ -methylstyrene (118  $\mu$ L, 1.00 mmol, 1 equiv) and 1-phenyl-1-propyne (366  $\mu$ L, 3.00 mmol, 3 equiv). After workup, the reaction mixture was purified on a deactivated silica flash column (0% to 15% EtOAc/hexanes) to give products **3.20a** and **3.20b** as a yellow solid (357 mg, 763  $\mu$ mol, 76% yield). Diastereoselectivity determined as 3:1 favoring the *trans* product based on NMR integration of **3.20a:3.20b**.

**TLC** (20% EtOAc/Hexanes)  $R_f = 0.65$ , stains yellow on anisaldehyde.

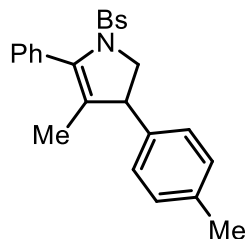
**$^1\text{H NMR}$**  (3.20a, major) (600 MHz,  $\text{CDCl}_3$ )  $\delta$  7.47 (d,  $J = 9.0$  Hz, 2H), 7.38 – 7.43 (m, 6H), 7.30 (d,  $J = 9.0$  Hz, 2H), 7.10 (t,  $J = 6.6$  Hz, 2H), 6.45 (d,  $J = 5.4$  Hz, 2H), 3.82 – 3.84 (m, 1H), 3.21 (d,  $J = 3.0$  Hz, 1H), 1.61 (d,  $J = 6.6$  Hz, 3H), 1.51 (s, 3H) ppm.

**$^1\text{H NMR}$**  (3.20b, minor) (600 MHz,  $\text{CDCl}_3$ )  $\delta$  7.63 (d,  $J = 9.0$  Hz, 2H), 7.54 (d,  $J = 9.0$  Hz, 2H), 7.26 – 7.36 (m, 5H), 7.16 (t,  $J = 6.6$  Hz, 3H), 6.94 (d,  $J = 7.2$  Hz, 2H), 4.49 (dq,  $J = 9.6$  Hz, 7.8 Hz, 1H), 3.82 – 3.84 (m, 1H), 1.50 (s, 3H), 1.03 (d,  $J = 7.8$  Hz, 3H) ppm.

**$^{13}\text{C NMR}$**  (mixture) (151 MHz,  $\text{CDCl}_3$ )  $\delta$  141.8, 139.0, 136.8, 136.6, 135.9, 132.8, 132.4, 132.1, 132.0, 129.8, 129.8, 129.5, 129.4, 129.3, 128.9, 128.7, 128.7, 128.4, 128.2, 128.1, 127.8, 127.8, 127.7, 127.2, 126.8, 126.7, 123.3, 122.4, 65.5, 61.0, 60.5, 55.8, 24.3, 19.1, 13.3, 12.4 ppm.

**HRMS** (APCI/QTOF)  $m/z$ :  $[\text{M}+\text{H}]^+$  Calcd for  $\text{C}_{24}\text{H}_{22}\text{NO}_2\text{SBr}$  468.0628, found 468.0619.

**(3.21) 1-((4-bromophenyl)sulfonyl)-4-methyl-5-phenyl-3-(p-tolyl)-2,3-dihydro-1H-pyrrole**



1 - ((4-bromophenyl)sulfonyl) – 4 – methyl – 5 – phenyl – 3 - (p-tolyl) - 2,3 – dihydro - 1H-pyrrole was prepared according to the general procedure using 4-methylstyrene (132  $\mu\text{L}$ , 1.00 mmol, 1 equiv) and 1-phenyl-1-propyne (366  $\mu\text{L}$ , 3.00 mmol, 3 equiv). After workup, the reaction mixture was purified on a neutral alumina flash column (0% to 10% EtOAc/hexanes) to give product 3.21 as a pink oil (329 mg, 704  $\mu\text{mol}$ , 70% yield).

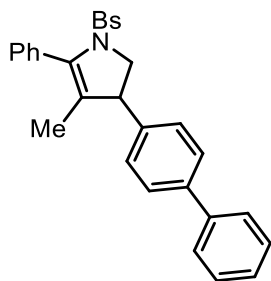
**TLC** (20% EtOAc/Hexanes)  $R_f = 0.66$ , stains orange on anisaldehyde.

**<sup>1</sup>H NMR** (600 MHz, CDCl<sub>3</sub>) δ 7.48 (d, J = 9.0 Hz, 2H), 7.30 – 7.37 (m, 7H), 6.94 (d, J = 9.0 Hz, 2H), 6.58 (d, J = 9.0 Hz, 2H), 4.28 (dd, J = 12.0 Hz, 11.6 Hz, 1H), 3.65 (dd, J = 12.0 Hz, 6.6 Hz, 1H), 3.57 (dd, J = 11.6 Hz, 6.6 Hz, 1H), 2.25 (s, 3H), 1.38 (d, J = 1.8 Hz, 3H) ppm.

**<sup>13</sup>C NMR** (151 MHz, CDCl<sub>3</sub>) δ 138.8, 137.4, 136.6, 132.1, 132.0, 129.8, 129.6, 129.4, 129.3, 128.4, 127.9, 127.7, 127.3, 126.3, 57.6, 51.1, 21.0, 12.8 ppm.

**HRMS** (APCI/QTOF) m/z: [M+H]<sup>+</sup> Calcd for C<sub>24</sub>H<sub>22</sub>NO<sub>2</sub>SBr 468.0628, found 468.0621.

**(3.22) 3-([1,1'-biphenyl]-4-yl)-1-((4-bromophenyl)sulfonyl)-4-methyl-5-phenyl-2,3-dihydro-1H-pyrrole**



3-([1,1'-biphenyl]-4-yl)-1-((4-bromophenyl)sulfonyl)-4-methyl-5-phenyl-2,3-dihydro-1H-pyrrole was prepared according to the general procedure using 4-phenylstyrene (118 μL, 1.00 mmol, 1 equiv) and 1-phenyl-1-propyne (366 μL, 3.00 mmol, 3 equiv). After workup, the reaction mixture was purified on a deactivated silica flash column (0% to 15% EtOAc/hexanes) to give product **3.22** as a white solid (272 mg, 513 μmol, 51% yield).

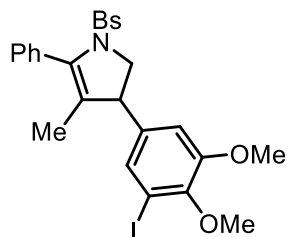
**TLC** (20% EtOAc/Hexanes) R<sub>f</sub> = 0.40, stains brown on anisaldehyde.

**<sup>1</sup>H NMR** (600 MHz, CDCl<sub>3</sub>) δ 7.57 – 7.58 (m, 4H), 7.41 – 7.45 (m, 10H), 7.35 (t, J = 7.8 Hz, 2H), 6.83 (d, J = 7.8 Hz, 2H), 4.39 (dd, J = 12.0 Hz, 9.6 Hz, 1H), 3.79 (dd, J = 12.0 Hz, 6.6 Hz, 1H), 3.73 (dd, J = 9.6 Hz, 6.6 Hz, 1H), 1.48 (d, J = 1.8 Hz, 3H) ppm.

$^{13}\text{C}$  NMR (151 MHz,  $\text{CDCl}_3$ )  $\delta$  140.8, 140.5, 140.0, 137.7, 135.9, 132.3, 132.1, 132.0, 130.0, 129.8, 129.6, 128.8, 128.5, 127.8, 127.4, 127.4, 127.0, 126.0, 57.5, 51.1, 12.8 ppm.

**HRMS** (APCI/QTOF)  $m/z$ :  $[\text{M}+\text{H}]^+$  Calcd for  $\text{C}_{29}\text{H}_{24}\text{NO}_2\text{SBr}$  530.0784, found 530.0777.

**(3.24) 1-((4-bromophenyl)sulfonyl)-3-(3-iodo-4,5-dimethoxyphenyl)-4-methyl-5-phenyl-2,3-dihydro-1H-pyrrole**



1-((4-bromophenyl)sulfonyl)-3-(3-iodo-4,5-dimethoxyphenyl)-4-methyl-5-phenyl-2,3-dihydro-1H-pyrrole was prepared according to the general procedure using 3-iodo-4,5-dimethoxystyrene (186  $\mu\text{L}$ , 1.00 mmol, 1 equiv) and 1-phenyl-1-propyne (366  $\mu\text{L}$ , 3.00 mmol, 3 equiv). After workup, the reaction mixture was purified on a deactivated silica flash column (0% to 50% EtOAc/hexanes) to give product **3.24** as a colorless oil (443 mg, 695  $\mu\text{mol}$ , 70% yield).

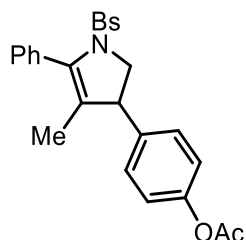
**TLC** (20% EtOAc/Hexanes)  $R_f$  = 0.37, stains brown on anisaldehyde.

$^1\text{H}$  NMR (600 MHz,  $\text{CDCl}_3$ )  $\delta$  7.57 (d,  $J$  = 9.0 Hz, 2H), 7.35 – 7.39 (m, 8H), 6.85 (s, 1H), 6.55 (s, 1H), 4.30 (t,  $J$  = 11.8 Hz, 1H), 3.77 – 3.79 (m, 7H), 3.61 (t,  $J$  = 10.2 Hz, 1H), 1.42 (s, 3H) ppm.

$^{13}\text{C}$  NMR (151 MHz,  $\text{CDCl}_3$ )  $\delta$  152.9, 148.1, 139.7, 137.9, 136.2, 132.1, 132.1, 131.6, 129.9, 129.6, 129.5, 128.3, 127.8, 125.4, 56.1, 56.0, 50.9, 29.7, 12.6 ppm.

**HRMS** (APCI/QTOF)  $m/z$ :  $[\text{M}+\text{H}]^+$  Calcd for  $\text{C}_{25}\text{H}_{23}\text{NO}_4\text{SBrI}$  639.9649, found 639.9638.

**(3.25) 4-(1-((4-bromophenyl)sulfonyl)-4-methyl-5-phenyl-2,3-dihydro-1H-pyrrol-3-yl)phenyl acetate**



4-(1-((4-bromophenyl)sulfonyl)-4-methyl-5-phenyl-2,3-dihydro-1H-pyrrol-3-yl)phenyl acetate was prepared according to the general procedure using 4-acetoxystyrene (153  $\mu\text{L}$ , 1.00 mmol, 1 equiv) and 1-phenyl-1-propyne (366  $\mu\text{L}$ , 3.00 mmol, 3 equiv). After workup, the reaction mixture was purified on a deactivated silica flash column (0% to 30% EtOAc/hexanes) to give product **3.25** as a yellow oil (295 mg, 577  $\mu\text{mol}$ , 58% yield).

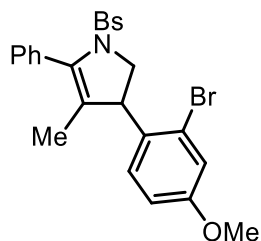
**TLC** (20% EtOAc/Hexanes)  $R_f = 0.39$ , stains orange on anisaldehyde.

**$^1\text{H NMR}$**  (600 MHz,  $\text{CDCl}_3$ )  $\delta$  7.56 (d,  $J = 9.0$  Hz, 2H), 7.38 – 7.42 (m, 7H), 6.92 (d,  $J = 9.0$  Hz, 2H), 6.77 (d,  $J = 9.0$  Hz, 2H), 4.36 (dd,  $J = 12.6$  Hz, 10.8 Hz, 1H), 3.75 (dd,  $J = 12.6$  Hz, 6.0 Hz, 1H), 3.70 (dd,  $J = 10.8$  Hz, 6.0 Hz, 1H), 2.30 (s, 3H), 1.46 (s, 3H) ppm.

**$^{13}\text{C NMR}$**  (151 MHz,  $\text{CDCl}_3$ )  $\delta$  169.4, 149.6, 139.4, 139.4, 139.4, 137.9, 135.9, 132.2, 131.9, 129.9, 129.6, 128.6, 128.3, 127.8, 125.7, 121.9, 57.5, 21.2, 12.8 ppm.

**HRMS** (APCI/QTOF)  $m/z$ :  $[\text{M}+\text{H}]^+$  Calcd for  $\text{C}_{25}\text{H}_{22}\text{NO}_4\text{SBr}$  512.0526, found 512.0526.

**(3.26) 3-(2-bromo-4-methoxyphenyl)-1-((4-bromophenyl)sulfonyl)-4-methyl-5-phenyl-2,3-dihydro-1H-pyrrole**



3-(2-bromo-4-methoxyphenyl)-1-((4-bromophenyl)sulfonyl)-4-methyl-5-phenyl-2,3-dihydro-1H-pyrrole was prepared according to the general procedure using 2-bromo-4-methoxystyrene (156  $\mu\text{L}$ , 1.00 mmol, 1 equiv) and 1-phenyl-1-propyne (366  $\mu\text{L}$ , 3.00 mmol, 3 equiv). After workup, the reaction mixture was purified on a neutral alumina flash column (0% to 20% EtOAc/hexanes) to give product **3.26** as a white solid (269 mg, 479  $\mu\text{mol}$ , 48% yield).

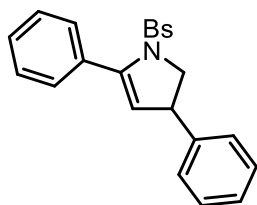
**TLC** (20% EtOAc/Hexanes)  $R_f = 0.69$ , stains yellow on anisaldehyde.

**$^1\text{H NMR}$**  (600 MHz,  $\text{CDCl}_3$ )  $\delta$  7.41 – 7.47 (m, 7H), 7.39 (d,  $J = 9.0$  Hz, 3H), 7.07 (d,  $J = 1.8$  Hz, 1H), 6.56 (dd,  $J = 9.6$  Hz, 1.8 Hz, 1H), 6.24 (d,  $J = 9.6$  Hz, 1H), 4.39 (dd,  $J = 13.6$  Hz, 7.2 Hz, 1H), 4.00 (dd,  $J = 7.2$  Hz, 5.4 Hz, 1H), 3.79 (s, 3H), 3.69 (dd,  $J = 13.6$  Hz, 5.4 Hz, 1H), 1.53 (s, 3H) ppm.

**$^{13}\text{C NMR}$**  (151 MHz,  $\text{CDCl}_3$ )  $\delta$  158.7, 132.1, 132.0, 131.7, 129.7, 129.5, 129.4, 128.6, 128.3, 127.9, 127.8, 125.2, 118.5, 113.2, 64.8, 56.8, 55.6, 13.1 ppm.

**HRMS** (APCI/QTOF)  $m/z$ :  $[\text{M}+\text{H}]^+$  Calcd for  $\text{C}_{24}\text{H}_{21}\text{NO}_3\text{SBr}_2$  561.9682, found 561.9672.

### (3.27) 1-((4-bromophenyl)sulfonyl)-3,5-diphenyl-2,3-dihydro-1H-pyrrole



1-((4-bromophenyl)sulfonyl)-3,5-diphenyl-2,3-dihydro-1H-pyrrole was prepared according to the general procedure using styrene (115  $\mu\text{L}$ , 1.00 mmol, 1 equiv) and phenylacetylene (329  $\mu\text{L}$ , 3.00 mmol, 3 equiv). After workup, the reaction mixture was purified on a deactivated silica flash column (0% to 15% EtOAc/hexanes) to give product **3.27** as a white solid (198 mg, 450  $\mu\text{mol}$ , 45% yield).

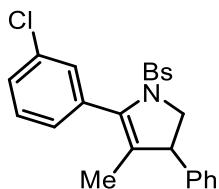
**TLC** (20% EtOAc/Hexanes)  $R_f = 0.49$ , stains purple on anisaldehyde.

**$^1\text{H NMR}$**  (600 MHz,  $\text{CDCl}_3$ )  $\delta$  7.59 – 7.60 (m, 2H), 7.51 (d,  $J = 7.8$  Hz, 2H), 7.38 – 7.40 (m, 5H), 7.18 – 7.19 (m, 3H), 6.81 – 6.83 (m, 2H), 5.47 (d,  $J = 2.4$  Hz, 1H), 4.47 (dd,  $J = 12.6$  Hz, 10.2 Hz, 1H), 3.87 (dd,  $J = 12.6$  Hz, 10.2 Hz, 1H), 3.77 (td,  $J = 10.2$  Hz, 2.4 Hz) ppm.

**$^{13}\text{C NMR}$**  (151 MHz,  $\text{CDCl}_3$ ) 145.7, 142.3, 135.4, 132.3, 132.1, 129.2, 128.7, 128.3, 128.2, 128.2, 128.0, 127.0, 126.9, 119.8, 59.8, 45.9 ppm.

**HRMS** (APCI/QTOF)  $m/z$ :  $[\text{M}+\text{H}]^+$  Calcd for  $\text{C}_{22}\text{H}_{18}\text{NO}_2\text{SBr}$  440.0315, found 440.0314.

**(3.28) 1-((4-bromophenyl)sulfonyl)-5-(3-chlorophenyl)-4-methyl-3-phenyl-2,3-dihydro-1H-pyrrole**



1-((4-bromophenyl)sulfonyl)-5-(3-chlorophenyl)-4-methyl-3-phenyl-2,3-dihydro-1H-pyrrole was prepared according to the general procedure using styrene (115  $\mu\text{L}$ , 1.00 mmol, 1 equiv) and 3-chloro-1-phenyl-1-propyne (403  $\mu\text{L}$ , 3.00 mmol, 3 equiv). After workup, the reaction mixture was purified on a deactivated silica flash column (0% to 15% EtOAc/hexanes) to give product **3.28** as a white solid (237 mg, 487  $\mu\text{mol}$ , 49% yield).

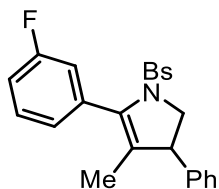
**TLC** (20% EtOAc/Hexanes)  $R_f = 0.54$ , stains red on anisaldehyde.

**$^1\text{H NMR}$**  (600 MHz,  $\text{CDCl}_3$ )  $\delta$  7.57 (d,  $J = 9.0$  Hz, 2H), 7.40 (d,  $J = 9.0$  Hz, 2H), 7.34 – 7.35 (m, 4H), 7.20 – 7.21 (m, 3H), 6.75 – 6.76 (m, 2H), 4.36 (dd,  $J = 12.0$  Hz, 9.6 Hz, 1H), 3.75 (dd,  $J = 12.0$  Hz, 7.8 Hz, 1H), 3.68 – 3.70 (m, 1H), 1.44 (d,  $J = 1.2$  Hz, 3H) ppm.

$^{13}\text{C}$  NMR (151 MHz,  $\text{CDCl}_3$ )  $\delta$  141.4, 136.3, 135.8, 133.9, 132.2, 129.5, 129.1, 128.8, 128.5, 128.2, 128.0, 127.4, 127.1, 57.4, 51.6, 12.7 ppm.

HRMS (APCI/QTOF)  $m/z$ :  $[\text{M}+\text{H}]^+$  Calcd for  $\text{C}_{23}\text{H}_{19}\text{NO}_2\text{SClBr}$  488.0081, found 488.0075.

**(3.30) 1-((4-bromophenyl)sulfonyl)-5-(3-fluorophenyl)-4-methyl-3-phenyl-2,3-dihydro-1H-pyrrole**



1-((4-bromophenyl)sulfonyl)-5-(3-fluorophenyl)-4-methyl-3-phenyl-2,3-dihydro-1H-pyrrole was prepared according to the general procedure using styrene (115  $\mu\text{L}$ , 1.00 mmol, 1 equiv) and 3'-fluoro-1-phenyl-1-propyne (383  $\mu\text{L}$ , 3.00 mmol, 3 equiv). After workup, the reaction mixture was purified on a deactivated silica flash column (0% to 20% EtOAc/hexanes) to give product **3.30** as a colorless oil (183 mg, 388  $\mu\text{mol}$ , 39% yield).

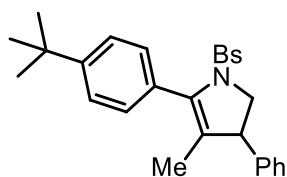
TLC (20% EtOAc/Hexanes)  $R_f$  = 0.38, stains red on anisaldehyde.

$^1\text{H}$  NMR (600 MHz,  $\text{CDCl}_3$ )  $\delta$  7.58 (d,  $J$  = 12.4 Hz, 2H), 7.42 (d,  $J$  = 12.4 Hz, 2H), 7.37 (q,  $J$  = 6.6 Hz, 1H), 7.19 – 7.23 (m, 4H), 7.12 – 7.14 (m, 1H), 7.07 (td,  $J$  = 9.6 Hz, 3.0 Hz, 1H), 6.73 – 6.74 (m, 2H), 4.35 (dd,  $J$  = 13.8 Hz, 7.8 Hz, 1H), 3.74 (dd,  $J$  = 12.0 Hz, 7.8 Hz, 1H), 3.65 – 3.68 (m, 1H), 1.44 (d,  $J$  = 1.2 Hz, 3H) ppm.

$^{13}\text{C}$  NMR (151 MHz,  $\text{CDCl}_3$ )  $\delta$  161.4, 141.4, 134.3, 132.2, 129.5, 129.3, 129.3, 128.8, 128.2, 127.4, 127.3, 127.1, 125.5, 125.5, 57.5, 51.6, 12.7 ppm.

HRMS (APCI/QTOF)  $m/z$ :  $[\text{M}+\text{H}]^+$  Calcd for  $\text{C}_{23}\text{H}_{19}\text{NO}_2\text{SBr}$  472.0377, found 472.0385.

**(3.31) 1-((4-bromophenyl)sulfonyl)-5-(4-(tert-butyl)phenyl)-4-methyl-3-phenyl-2,3-dihydro-1H-pyrrole**



1-((4-bromophenyl)sulfonyl)-5-(4-(tert-butyl)phenyl)-4-methyl-3-phenyl-2,3-dihydro-1H-pyrrole was prepared according to the general procedure using styrene (115  $\mu$ L, 1.00 mmol, 1 equiv) and 4'-tert-butyl-1-phenyl-1-propyne (517  $\mu$ L, 3.00 mmol, 3 equiv). After workup, the reaction mixture was purified on a deactivated silica flash column (0% to 15% EtOAc/hexanes) to give product **3.31** as a yellow solid (348 mg, 684  $\mu$ mol, 68% yield).

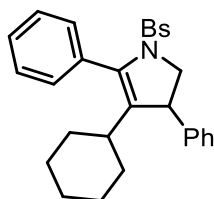
**TLC** (20% EtOAc/Hexanes)  $R_f$  = 0.64, stains purple on anisaldehyde.

**$^1\text{H NMR}$**  (600 MHz,  $\text{CDCl}_3$ )  $\delta$  7.51 – 7.54 (m, 4H), 7.41 – 7.43 (m, 4H), 7.18 – 7.20 (m, 3H), 6.83 – 6.85 (m, 2H), 4.47 (dd,  $J$  = 12.0 Hz, 7.8 Hz, 1H), 3.87 (dd,  $J$  = 7.8 Hz, 7.2 Hz, 1H), 3.74 – 3.77 (m, 1H), 1.59 (s, 3H), 1.37 (s, 9H) ppm.

**$^{13}\text{C NMR}$**  (151 MHz,  $\text{CDCl}_3$ )  $\delta$  145.6, 142.4, 135.5, 132.1, 129.5, 129.4, 128.7, 128.2, 127.8, 127.0, 126.9, 124.9, 119.4, 119.4, 59.8, 59.8, 45.9, 34.8, 31.3 ppm.

**HRMS** (APCI/QTOF)  $m/z$ :  $[\text{M}+\text{H}]^+$  Calcd for  $\text{C}_{27}\text{H}_{28}\text{NO}_2\text{SBr}$  calcd 510.1097, found 510.1083.

**(3.32) 1-((4-bromophenyl)sulfonyl)-4-cyclohexyl-3,5-diphenyl-2,3-dihydro-1H-pyrrole**



1-((4-bromophenyl)sulfonyl)-4-cyclohexyl-3,5-diphenyl-2,3-dihydro-1H-pyrrole was prepared according to the general procedure using styrene (115  $\mu$ L, 1.00 mmol, 1 equiv) and (cyclohexylethynyl)benzene (564  $\mu$ L, 3.00 mmol, 3 equiv). After workup, the reaction mixture was purified on a deactivated silica flash column (0% to 15% EtOAc/hexanes) to give product **3.32** as a colorless oil (251 mg, 481  $\mu$ mol, 48% yield).

**TLC** (20% EtOAc/Hexanes)  $R_f$  = 0.69, stains orange on anisaldehyde.

**$^1\text{H NMR}$**  (600 MHz,  $\text{CDCl}_3$ )  $\delta$  7.55 (d,  $J$  = 9.6 Hz, 2H), 7.34 – 7.38 (m, 7H), 7.12 – 7.17 (m, 3H), 6.71 (d,  $J$  = 5.4 Hz, 2H), 4.30 (t,  $J$  = 12.0 Hz, 1H), 3.88 (dd,  $J$  = 7.8 Hz, 5.4 Hz, 1H), 3.72 (dd,  $J$  = 12.0 Hz, 5.4 Hz, 1H), 2.03 (tt,  $J$  = 12.0 Hz, 3.6 Hz, 1H), 1.54 (s, 3H), 1.35 – 1.39 (m, 3H), 1.12 – 1.34 (m, 3H), 0.73 – 0.99 (m, 3H), 0.38 (qd,  $J$  = 13.2 Hz, 2.4 Hz, 1H) ppm.

**$^{13}\text{C NMR}$**  (151 MHz,  $\text{CDCl}_3$ ) 143.6, 137.2, 133.4, 132.1, 132.0, 130.1, 129.6, 128.5, 128.5, 127.7, 127.7, 127.5, 126.8, 125.6, 58.0, 47.1, 37.8, 33.5, 31.6, 26.4, 26.2, 25.6 ppm.

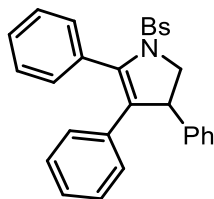
**HRMS** (APCI/QTOF)  $m/z$ :  $[\text{M}+\text{H}]^+$  Calcd for  $\text{C}_{28}\text{H}_{28}\text{NO}_2\text{SBr}$  522.1097, found 522.1094.

**$^1\text{H NMR}$**  (Xb) (600 MHz,  $\text{CDCl}_3$ )  $\delta$  7.54 (d,  $J$  = 8.4 Hz, 2H), 7.38 – 7.43 (m, 4 H), 7.06 – 7.08 (m, 6H), 6.65 (d,  $J$  = 8.4 Hz, 2H), 4.32 (t,  $J$  = 10.2 Hz, 1H), 3.72 (dd,  $J$  = 10.2 Hz, 3.6 Hz, 1H), 3.56 (dd,  $J$  = 10.2 Hz, 3.6 Hz, 1H), 1.34 – 1.38 (m, 1H), 0.23 – 0.40 (m, 3H), -0.12 – -0.13 (m, 1H) ppm.

**$^{13}\text{C NMR}$**  (mixture) (151 MHz,  $\text{CDCl}_3$ )  $\delta$  142.9, 142.5, 140.3, 138.8, 137.1, 136.1, 134.1, 132.4, 132.3, 132.2, 132.1, 130.3, 129.6, 129.5, 129.1, 129.1, 128.9, 128.8, 128.7, 128.6, 127.9, 127.8, 127.6, 127.3, 127.2, 127.0, 58.1, 58.1, 57.0, 48.6, 48.5, 47.3, 10.1, 9.9, 9.7, 9.7 ppm.

**HRMS** (APCI/QTOF)  $m/z$ :  $[\text{M}+\text{H}]^+$  Calcd for  $\text{C}_{25}\text{H}_{22}\text{NO}_2\text{SBr}$  480.0628, found 480.0619.

**(3.33) 1-((4-bromophenyl)sulfonyl)-3,4,5-triphenyl-2,3-dihydro-1H-pyrrole**



1-((4-bromophenyl)sulfonyl)-3,4,5-triphenyl-2,3-dihydro-1H-pyrrole was prepared according to the general procedure using styrene (115  $\mu$ L, 1.00 mmol, 1 equiv) and diphenylacetylene (534 mg, 3.00 mmol, 3 equiv). After workup, the reaction mixture was purified on a deactivated silica flash column (0% to 15% EtOAc/hexanes) to give product **3.33** as a white solid (268 mg, 520  $\mu$ mol, 52% yield).

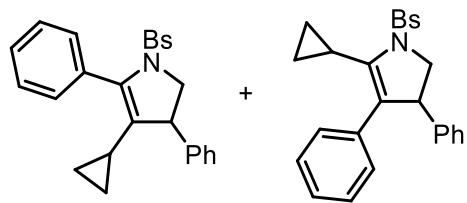
**TLC** (20% EtOAc/Hexanes)  $R_f$  = 0.60, stains red-orange on anisaldehyde.

**$^1\text{H NMR}$**  (600 MHz,  $\text{CDCl}_3$ )  $\delta$  7.51 (d,  $J$  = 9.0 Hz, 2H), 7.35 – 7.38 (m, 5H), 7.31 (t,  $J$  = 7.8 Hz, 2H), 7.14 – 7.16 (m, 3H), 6.92 – 6.95 (m, 5H), 6.65 – 6.66 (m, 2H), 4.51 (dd,  $J$  = 14.4 Hz, 7.8 Hz, 1H), 4.12 (dd,  $J$  = 7.8 Hz, 6.6 Hz, 1H), 4.00 (dd,  $J$  = 14.4 Hz, 6.6 Hz, 1H) ppm.

**$^{13}\text{C NMR}$**  (151 MHz,  $\text{CDCl}_3$ )  $\delta$  142.3, 139.4, 137.2, 134.3, 132.1, 131.7, 130.7, 129.3, 129.0, 128.8, 128.1, 128.0, 127.8, 127.7, 127.5, 126.9, 126.6, 58.6, 50.6 ppm.

**HRMS** (APCI/QTOF)  $m/z$ :  $[\text{M}+\text{H}]^+$  Calcd for  $\text{C}_{28}\text{H}_{22}\text{NO}_2\text{SBr}$  516.0638, found 516.0631.

**(3.34a and 3.34b) 1-((4-bromophenyl)sulfonyl)-4-cyclopropyl-3,5-diphenyl-2,3-dihydro-1H-pyrrole and 1-((4-bromophenyl)sulfonyl)-5-cyclopropyl-3,4-diphenyl-2,3-dihydro-1H-pyrrole**

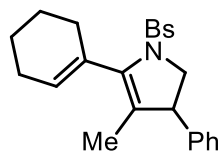


1-((4-bromophenyl)sulfonyl)-4-cyclopropyl-3,5-diphenyl-2,3-dihydro-1H-pyrrole and 1-((4-bromophenyl)sulfonyl)-5-cyclopropyl-3,4-diphenyl-2,3-dihydro-1H-pyrrole were prepared according to the general procedure using styrene (115  $\mu$ L, 1.00 mmol, 1 equiv) and (cyclopropylethynyl)benzene (366  $\mu$ L, 3.00 mmol, 3 equiv). After workup, the reaction mixture was purified on a deactivated silica flash column (0% to 25% EtOAc/hexanes) to give products **3.34a** and **Xb** as a yellow oil (231 mg, 481  $\mu$ mol, 48% yield). Regioselectivity determined as 2:1 based on NMR integration of **3.34a**:**3.34b**.

**TLC** (20% EtOAc/Hexanes)  $R_f$  = 0.35, stains brown on anisaldehyde.

**$^1\text{H NMR}$**  (Xa) (600 MHz,  $\text{CDCl}_3$ )  $\delta$  7.67 (d,  $J$  = 8.4 Hz, 2H), 7.59 (d,  $J$  = 8.4 Hz, 2H), 7.48 (d,  $J$  = 7.8 Hz, 1H), 7.31 (d,  $J$  = 7.8 Hz, 1H), 7.12 – 7.15 (m, 6H), 6.69 – 6.70 (m, 2H), 4.18 (t,  $J$  = 12.0, 1H), 4.16 – 4.17 (m, 1H), 3.68 (dd,  $J$  = 12.0 Hz, 3.6 Hz, 1H), 1.84 – 1.89 (m, 1H), 0.78 – 0.89 (m, 2H), 0.45 – 0.50 (m, 1H), 0.12 – 0.16 (m, 1H) ppm.

**(3.36) 1-((4-bromophenyl)sulfonyl)-5-(cyclohex-1-en-1-yl)-4-methyl-3-phenyl-2,3-dihydro-1H-pyrrole**



1-((4-bromophenyl)sulfonyl)-5-(cyclohex-1-en-1-yl)-4-methyl-3-phenyl-2,3-dihydro-1H-pyrrole was prepared according to the general procedure using styrene (115  $\mu$ L, 1.00 mmol, 1 equiv) and

1-cyclohexenyl-1-propyne (419  $\mu\text{L}$ , 3.00 mmol, 3 equiv). After workup, the reaction mixture was purified on a deactivated silica flash column (0% to 15% EtOAc/hexanes) to give product **3.36** as a yellow oil (92.3 mg, 202  $\mu\text{mol}$ , 20% yield).

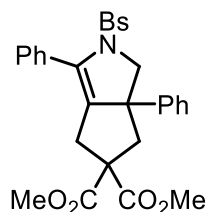
**TLC** (20% EtOAc/Hexanes)  $R_f = 0.66$ , stains yellow on anisaldehyde.

**$^1\text{H NMR}$**  (600 MHz,  $\text{CDCl}_3$ )  $\delta$  7.58 (d,  $J = 3.0$  Hz, 4H), 7.12 – 7.16 (m, 3H), 6.62 (dd,  $J = 9.0$  Hz, 3.0 Hz, 2H), 5.64 – 5.65 (m, 1H), 4.12 – 4.17 (m, 1H), 3.50 – 3.53 (m, 2H), 2.43 – 2.45 (m, 1H), 2.21 – 2.23 (m, 3H), 1.64 – 1.77 (m, 4H), 1.40 (d,  $J = 1.8$  Hz, 3H) ppm.

**$^{13}\text{C NMR}$**  (151 MHz,  $\text{CDCl}_3$ )  $\delta$  142.2, 140.1, 135.7, 132.0, 131.8, 129.7, 129.7, 129.5, 128.7, 128.6, 127.9, 127.8, 127.3, 126.8, 123.9, 57.0, 50.9, 27.9, 25.5, 22.5, 22.2, 12.8 ppm.

**HRMS** (APCI/QTOF)  $m/z$ :  $[\text{M}+\text{H}]^+$  Calcd for  $\text{C}_{23}\text{H}_{24}\text{NO}_2\text{SBr}$  458.0784, found 458.0784.

**(3.38) 1-dimethyl 2-((4-bromophenyl)sulfonyl)-3,6a-diphenyl-2,4,6,6a-tetrahydrocyclopenta [c]pyrrole-5,5(1H)-dicarboxylate**



**1-dimethyl 2-((4-bromophenyl)sulfonyl)-3,6a-diphenyl-2,4,6,6a-tetrahydrocyclopenta [c]pyrrole-5,5(1H)-dicarboxylate** was prepared according to the general procedure using

dimethyl 2-(2-phenylallyl)-2-(3-phenylprop-2-yn-1-yl)malonate (362 mg, 1.00 mmol, 1 equiv).

After workup, the reaction mixture was purified on a deactivated silica flash column (0% to 10% EtOAc/hexanes) to give product **3.38** as a white solid (172 mg, 289  $\mu\text{mol}$ , 29% yield).

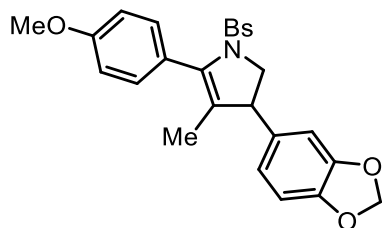
**TLC** (20% EtOAc/Hexanes)  $R_f = 0.62$ , stains chartreuse on anisaldehyde.

**<sup>1</sup>H NMR** (600 MHz, CDCl<sub>3</sub>) δ 7.75 (d, J = 9.0 Hz, 2H), 7.61 (d, J = 9.0 Hz, 2H), 7.27 – 7.30 (m, 7H), 7.20 – 7.23 (m, 3H), 4.15 (d, J = 18.0 Hz, 1H), 3.84 (s, 3H), 3.77 – 3.81 (m, 5H), 3.72 (d, J = 9.6 Hz, 1H), 3.26 (d, J = 16.8 Hz, 1H), 3.20 (d, J = 16.8 Hz, 1H) ppm.

**<sup>13</sup>C NMR** (151 MHz, CDCl<sub>3</sub>) δ 170.1, 169.3, 132.0, 131.6, 131.6, 129.6, 128.7, 128.2, 128.2, 128.0, 128.0, 128.0, 127.6, 127.2, 127.1, 126.9, 57.1, 55.4, 53.1, 52.5, 49.5, 45.9, 26.4 ppm.

**HRMS** (APCI/QTOF) m/z: [M+H]<sup>+</sup> Calcd for C<sub>25</sub>H<sub>24</sub>NO<sub>8</sub>SBr 596.0737, found 596.0733.

**(3.41) 3-(benzo[d][1,3]dioxol-4-yl)-1-((4-bromophenyl)sulfonyl)-5-(4-methoxyphenyl)-4-methyl-2,3-dihydro-1H-pyrrole**



3-(benzo[d][1,3]dioxol-4-yl)-1-((4-bromophenyl)sulfonyl)-5-(4-methoxyphenyl)-4-methyl-2,3-dihydro-1H-pyrrole was prepared according to general procedure using 5-vinylbenzo[d][1,3]dioxole (148 mg, 1.00 mmol, 1 equiv) and 1-methoxy-4-(prop-1-yn-1-yl)benzene (438 mg, 3.00 mmol, 3 equiv). After workup, the reaction mixture was purified on a deactivated silica flash column (0% to 20% EtOAc/hexanes) to give product **3.41** as a yellow solid (417 mg, 791 μmol, 79% yield).

**TLC** (20% EtOAc/Hexanes) R<sub>f</sub> = 0.51, stains orange on anisaldehyde.

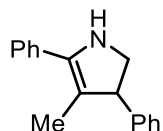
**<sup>1</sup>H NMR** (600 MHz, CDCl<sub>3</sub>) δ 7.55 (d, J = 9.0 Hz, 2H), 7.38 (d, J = 9.0 Hz, 2H), 7.32 (d, J = 9.0 Hz, 2H), 6.92 (d, J = 9.0 Hz, 2H), 6.63 (d, J = 8.4 Hz, 1H), 6.27 (dd, J = 8.4 Hz, 1.8 Hz, 1H), 6.15 (d, J = 1.8 Hz, 1H), 5.95 (d, J = 1.8 Hz, 1H), 5.92 (d, 1.8 Hz, 1H), 4.30 (dd, J = 13.2 Hz, 8.4

Hz, 1H), 3.85 (s, 3H), 3.68 (dd, J = 13.2 Hz, 4.8 Hz, 1H), 3.59 (dd, J = 8.4 Hz, 4.8 Hz, 1H), 1.42 (d, J = 1.2 Hz, 3H) ppm.

<sup>13</sup>C NMR (151 MHz, CDCl<sub>3</sub>) δ 135.9, 132.5, 132.0, 131.2, 130.7, 129.6, 128.0, 124.8, 124.1, 120.7, 113.2, 108.3, 107.3, 101.1, 57.5, 55.2, 51.0, 30.9, 12.7 ppm.

HRMS (APCI/QTOF) m/z: [M+H]<sup>+</sup> Calcd for C<sub>25</sub>H<sub>22</sub>NO<sub>5</sub>SBr 528.0475, found 528.0465.

### (B.11) 4-methyl-3,5-diphenyl-2,3-dihydro-1H-pyrrole



4-methyl-3,5-diphenyl-2,3-dihydro-1H-pyrrole was prepared according to literature procedure<sup>9</sup> combining product **3.11** (80.0 mg, 176 μmol, 1 equiv), 33% hydrochloric acid (92.3 μL, 880 mmol, 5 equiv), and zinc chloride (120 mg, 880 mmol 5 equiv) in 2.0 mL acetic acid. After workup, the reaction mixture was concentrated *in vacuo* and purified on a basic alumina flash column (0% to 10% EtOAc/hexanes) to give product **B.11** as a pink oil (35 mg, 176 μmol, 85% yield).

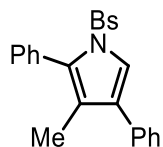
TLC (20% EtOAc/Hexanes) R<sub>f</sub> = 0.29, stains orange on anisaldehyde.

<sup>1</sup>H NMR (600 MHz, CDCl<sub>3</sub>) δ 7.80 – 7.81 (m, 2H), 7.40 – 7.43 (m, 3H), 7.28 (t, J = 7.8 Hz, 2H), 7.16 – 7.21 (m, 2H), 4.46 (ddd, J = 15.0 Hz, 7.2 Hz, 1.8 Hz, 1H), 4.13 (dd, J = 15.0 Hz, 5.4 Hz, 1H), 3.43 – 3.47 (m, 1H), 3.14 – 3.17 (m, 1H), 1.31 (d, J = 7.2 Hz, 3H) ppm.

<sup>13</sup>C NMR (151 MHz, CDCl<sub>3</sub>) δ 145.3, 133.8, 130.3, 128.8, 128.6, 128.0, 126.7, 126.5, 67.3, 52.2, 18.5 ppm.

HRMS (APCI/QTOF) m/z: [M+H]<sup>+</sup> Calcd for C<sub>17</sub>H<sub>17</sub>N 236.1434, found 246.1438.

**(B.12) 1-((4-bromophenyl)sulfonyl)-3-methyl-2,4-diphenyl-1H-pyrrole**



1-((4-bromophenyl)sulfonyl)-3-methyl-2,4-diphenyl-1H-pyrrole was prepared according to literature procedure<sup>10</sup> combining product **3.11** (25.0 mg, 55  $\mu$ mol, 1 equiv) and 2,3-Dichloro-5,6-dicyano-1,4-benzoquinone (DDQ) (31.0 mg, 140  $\mu$ mol, 2.5 equiv) in 1.0 mL toluene at 150°C for 36h. Upon completion, the crude reaction mixture was concentrated *in vacuo* and purified on a deactivated silica flash column (10% to 20% EtOAc/hexanes) to give product **B.12** as a pink solid (22.0 mg, 48.4  $\mu$ mol, 88% yield).

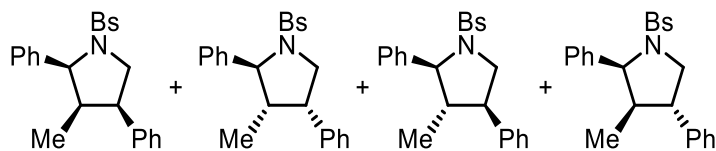
**TLC** (20% EtOAc/Hexanes)  $R_f$  = 0.87, stains white on anisaldehyde.

**<sup>1</sup>H NMR** (600 MHz, CDCl<sub>3</sub>)  $\delta$  7.48 (s, 1H), 7.45 (d,  $J$  = 14.4 Hz, 2H), 7.38 – 7.43 (m, 7H), 7.35 – 7.36 (m, 3H), 7.31 (tt,  $J$  = 6.6 Hz, 1.8 Hz, 1H), 7.20 (d,  $J$  = 14.4 Hz, 2H), 7.14 – 7.15 (m, 2H), 3.19 (s, 3H) ppm.

**<sup>13</sup>C NMR** (151 MHz, CDCl<sub>3</sub>)  $\delta$  137.5, 134.0, 132.1, 132.0, 130.4, 129.9, 129.2, 128.8, 128.6, 128.5, 128.1, 127.6, 127.1, 125.6, 122.9, 119.7, 11.2 ppm.

**HRMS** (APCI/QTOF)  $m/z$ :  $[M+H]^+$  Calcd for C<sub>23</sub>H<sub>18</sub>NO<sub>2</sub>SBr 452.0315, found 452.0309

**(B.12a – d) 1-((4-bromophenyl)sulfonyl)-3-methyl-2,4-diphenylpyrrolidine**



1-((4-bromophenyl)sulfonyl)-3-methyl-2,4-diphenylpyrrolidine was prepared according to literature procedure<sup>11</sup> combining product **3.11** (250 mg, 0.55 mmol, 1 equiv) with triethylsilane (439  $\mu$ L, 2.75 mmol, 5 equiv), trifluoroacetic acid (211 mL, 2.75 mmol, 5 equiv), and trifluoroacetic anhydride (382 mL, 2.75 mmol, 5 equiv) in 3.0 mL DCM with stirring at 0°C. The reaction mixture was then warmed to rt and stirred 36h. Upon completion, the crude reaction mixture was concentrated *in vacuo* and purified on deactivated silica flash column (0% to 5% EtOAc/hexanes) to give products **B.12a**, **B.12b**, and **B.12c** as a white solid (22.0 mg, 48.4  $\mu$ mol, 88% yield). Diastereoselectivity determined as 90:6:4:0 of **Xa:Xb:Xc:Xd** based on NMR integration.

**TLC** (20% EtOAc/Hexanes)  $R_f$  = 0.61, stains white on anisaldehyde.

**<sup>1</sup>H NMR (B.12a, major)** (600 MHz, CDCl<sub>3</sub>)  $\delta$  7.52 (d,  $J$  = 8.6 Hz, 2H), 7.42 (d,  $J$  = 8.6 Hz, 2H), 7.31 (t,  $J$  = 7.9 Hz, 2H), 7.27 – 7.23 (m, 6H), 7.17 (d,  $J$  = 7.9 Hz, 2H), 4.24 (d,  $J$  = 9.5 Hz, 1H), 4.17 (dd,  $J$  = 11.4, 7.8 Hz, 1H), 3.57 (t,  $J$  = 11.4 Hz, 1H), 2.70 (td,  $J$  = 11.4, 7.8 Hz, 1H), 2.26 (ddq,  $J$  = 11.4, 9.5, 6.5 Hz, 1H), 0.84 (d,  $J$  = 6.5 Hz, 3H).

**<sup>13</sup>C NMR (B.12a, major)** (151 MHz, CDCl<sub>3</sub>)  $\delta$  140.6, 138.4, 138.0, 132.0, 128.8, 128.8, 128.5, 127.7, 127.6, 127.5, 127.3, 127.2, 71.7, 56.0, 51.7, 51.6, 14.3 ppm.

**HRMS** (APCI/QTOF)  $m/z$ : [M+H]<sup>+</sup> Calcd for C<sub>23</sub>H<sub>18</sub>NO<sub>2</sub>SBr 455.0555, found 455.0564.

## B.7 Computational details

### Computational Method

Calculations were carried out with the Gaussian 16 program, Revision B.01. Geometry optimizations were performed with the B3LYP functional with the 6-311G(p,d) basis set. The conductor-like polarizable continuum (CPCM) solvation model was used with solvent parameters for chloroform.

### Full Gaussian Reference

Gaussian 16, Revision B.01, M. J. Frisch, G. W. Trucks, H. B. Schlegel, G. E. Scuseria, M. A. Robb, J. R. Cheeseman, G. Scalmani, V. Barone, G. A. Petersson, H. Nakatsuji, X. Li, M. Caricato, A. V. Marenich, J. Bloino, B. G. Janesko, R. Gomperts, B. Mennucci, H. P. Hratchian, J. V. Ortiz, A. F. Izmaylov, J. L. Sonnenberg, D. Williams-Young, F. Ding, F. Lipparini, F. Egidi, J. Goings, B. Peng, A. Petrone, T. Henderson, D. Ranasinghe, V. G. Zakrzewski, J. Gao, N. Rega, G. Zheng, W. Liang, M. Hada, M. Ehara, K. Toyota, R. Fukuda, J. Hasegawa, M. Ishida, T. Nakajima, Y. Honda, O. Kitao, H. Nakai, T. Vreven, K. Throssell, J. A. Montgomery, Jr., J. E. Peralta, F. Ogliaro, M. J. Bearpark, J. J. Heyd, E. N. Brothers, K. N. Kudin, V. N. Staroverov, T. A. Keith, R. Kobayashi, J. Normand, K. Raghavachari, A. P. Rendell, J. C. Burant, S. S. Iyengar, J. Tomasi, M. Cossi, J. M. Millam, M. Klene, C. Adamo, R. Cammi, J. W. Ochterski, R. L. Martin, K. Morokuma, O. Farkas, J. B. Foresman, and D. J. Fox, Gaussian, Inc., Wallingford CT, 2016.

Optimized Coordinates

**3.20a** (*trans* pyrroline)

C 0.77862700 -1.45348000 0.15589100	C -2.56189400 -1.40809900 1.26383300
C 2.01824800 -0.98270100 -0.04381100	C -3.08921100 -0.88252200 0.07992000
C 0.66848200 0.87900700 0.59933300	C -3.18506500 -2.46369800 1.93124100
H 0.55788300 1.39784000 1.54945300	C -4.27013000 -1.41049400 -0.43411800
C 2.14833400 0.48119200 0.30310800	H -2.57654700 -0.08233800 -0.44141900
H 2.49018300 1.04730000 -0.57027700	C -4.36981600 -2.99160300 1.41745000
N -0.10111500 -0.40926100 0.61291500	H -2.75007000 -2.87101400 2.83630500
S -1.07907800 -0.70115800 1.97666400	C -4.89851600 -2.45672500 0.24468900
O -0.48325400 -1.71613100 2.86224500	H -4.69249500 -1.01975500 -1.35212800
O -1.41424700 0.61978400 2.52803200	H -4.86527100 -3.81220800 1.92229200
C 3.11343300 0.77496900 1.44747900	Br -6.52057800 -3.17709900 -0.46033600
C 4.13384200 1.72314600 1.29279700	C 0.21988759 -2.85707772 -0.14297974
C 2.98078100 0.12335400 2.68164200	C -0.36069525 -3.12733966 -1.38247701
C 4.99755100 2.02211500 2.34835700	C 0.29432783 -3.85819942 0.82540145
H 4.25189300 2.22748800 0.33699500	C -0.86730567 -4.39827467 -1.65320164
C 3.83845300 0.42517200 3.74058400	H -0.41992280 -2.33764238 -2.14543972
H 2.20231800 -0.62442600 2.80900200	C -0.21150239 -5.12985280 0.55439710
C 4.84912800 1.37558900 3.57756400	H 0.75204548 -3.64541318 1.80230758
H 5.78449500 2.75853100 2.21254900	C -0.79238682 -5.39998937 -0.68460917
H 3.72085900 -0.08659000 4.69152100	H -1.32550678 -4.61119612 -2.62993738
H 5.51920500 1.60731300 4.40021900	H -0.15230048 -5.91911181 1.31796737

H -1.19184593 -6.40201655 -0.89831527	C 4.99755100 2.02211500 2.34835700
C 3.18499431 -1.80584517 -0.62064436	H 4.25189300 2.22748800 0.33699500
H 3.48171148 -2.54976755 0.08888959	C 3.83845300 0.42517200 3.74058400
H 2.87220691 -2.28163915 -1.52656055	H 2.20231800 -0.62442600 2.80900200
H 4.01172562 -1.15805340 -0.82504877	C 4.84912800 1.37558900 3.57756400
C 0.08754595 1.77175286 -0.51292512	H 5.78449500 2.75853100 2.21254900
H -0.85253720 2.17165341 -0.19476913	H 3.72085900 -0.08659000 4.69152100
H 0.76562693 2.57388936 -0.71708981	H 5.51920500 1.60731300 4.40021900
H -0.05408912 1.18999999 -1.39971884	C -2.56189400 -1.40809900 1.26383300
	C -3.08921100 -0.88252200 0.07992000
<b>3.20b</b> ( <i>cis</i> pyrroline)	C -3.18506500 -2.46369800 1.93124100
C 0.77862700 -1.45348000 0.15589100	C -4.27013000 -1.41049400 -0.43411800
C 2.01824800 -0.98270100 -0.04381100	H -2.57654700 -0.08233800 -0.44141900
C 0.66848200 0.87900700 0.59933300	C -4.36981600 -2.99160300 1.41745000
C 2.14833400 0.48119200 0.30310800	H -2.75007000 -2.87101400 2.83630500
H 2.49018300 1.04730000 -0.57027700	C -4.89851600 -2.45672500 0.24468900
N -0.10111500 -0.40926100 0.61291500	H -4.69249500 -1.01975500 -1.35212800
S -1.07907800 -0.70115800 1.97666400	H -4.86527100 -3.81220800 1.92229200
O -0.48325400 -1.71613100 2.86224500	Br -6.52057800 -3.17709900 -0.46033600
O -1.41424700 0.61978400 2.52803200	C 0.21988759 -2.85707772 -0.14297974
C 3.11343300 0.77496900 1.44747900	C -0.36069525 -3.12733966 -1.38247701
C 4.13384200 1.72314600 1.29279700	C 0.29432783 -3.85819942 0.82540145
C 2.98078100 0.12335400 2.68164200	C -0.86730567 -4.39827467 -1.65320164

H -0.41992280 -2.33764238 -2.14543972

C -0.21150239 -5.12985280 0.55439710

H 0.75204548 -3.64541318 1.80230758

C -0.79238682 -5.39998937 -0.68460917

H -1.32550678 -4.61119612 -2.62993738

H -0.15230048 -5.91911181 1.31796737

H -1.19184593 -6.40201655 -0.89831527

C 3.18499431 -1.80584517 -0.62064436

H 3.48171148 -2.54976755 0.08888959

H 2.87220691 -2.28163915 -1.52656055

H 4.01172562 -1.15805340 -0.82504877

C 0.51196232 1.61325936 1.94394263

H -0.46727569 2.04013487 2.00534469

H 0.64977923 0.91985947 2.74712574

H 1.24463280 2.38994589 2.01359883

H 0.26484461 1.49929146 -0.17346972

## B.8 Crystallographic Data

A colorless, block-like specimen of  $C_{23}H_{20}BrNO_2S$ , approximate dimensions 0.097 mm x 0.134 mm x 0.382 mm, was coated with Paratone oil and mounted on a MiTeGen MicroLoop. The X-ray intensity data were measured on a Bruker D8 Venture Kappa four-circle diffractometer system equipped with an Incoatec  $I\mu S$  3.0 micro-focus sealed X-ray tube (Mo  $K\alpha$ ,  $\lambda = 0.71073$  Å) and a HELIOS double bounce multilayer mirror monochromator.

The total exposure time was 0.91 hours. The frames were integrated with the Bruker SAINT software package<sup>1</sup> using a narrow-frame algorithm. The integration of the data using a monoclinic unit cell yielded a total of 43918 reflections to a maximum  $\theta$  angle of  $33.15^\circ$  (0.65 Å resolution), of which 7580 were independent (average redundancy 5.794, completeness = 99.7%,  $R_{int} = 6.67\%$ ,  $R_{sig} = 4.83\%$ ) and 5722 (75.49%) were greater than  $2\sigma(F^2)$ . The final cell constants of  $a = 20.7100(12)$  Å,  $b = 6.9933(4)$  Å,  $c = 14.4187(8)$  Å,  $\beta = 107.623(2)^\circ$ , volume =  $1990.3(2)$  Å<sup>3</sup>, are based upon the refinement of the XYZ-centroids of 9942 reflections above  $20\sigma(I)$  with  $5.657^\circ < 2\theta < 65.38^\circ$ . Data were corrected for absorption effects using the Multi-Scan method (SADABS).<sup>2</sup> The ratio of minimum to maximum apparent transmission was 0.746. The calculated minimum and maximum transmission coefficients (based on crystal size) are 0.4880 and 0.8160.

The structure was solved and refined using the Bruker SHELXTL Software Package<sup>3</sup> within

---

<sup>1</sup> Bruker (2012). *Saint; SADABS; APEX3*. Bruker AXS Inc., Madison, Wisconsin, USA.

<sup>2</sup> Krause, L., Herbst-Irmer, R., Sheldrick, G. M., Stalke, D. "Comparison of silver and molybdenum microfocus X-ray sources for single-crystal structure determination" *J. Appl. Cryst.* (2015) 48, 3-10. doi:10.1107/S1600576714022985

<sup>3</sup> Sheldrick, G. M. (2015). *Acta Cryst. A* **71**, 3-8.

APEX4<sup>1</sup> and OLEX2,<sup>4</sup> using the space group P 2<sub>1</sub>/c, with Z = 4 for the formula unit, C<sub>23</sub>H<sub>20</sub>BrNO<sub>2</sub>S. Non-hydrogen atoms were refined anisotropically. Hydrogen atoms were placed in geometrically calculated positions with  $U_{iso} = 1.2U_{equiv}$  of the parent atom ( $U_{iso} = 1.5U_{equiv}$  for methyl). The final anisotropic full-matrix least-squares refinement on F<sup>2</sup> with 254 variables converged at R1 = 3.80%, for the observed data and wR2 = 8.98% for all data. The goodness-of-fit was 1.029. The largest peak in the final difference electron density synthesis was 0.613 e<sup>-</sup>/Å<sup>3</sup> and the largest hole was -0.439 e<sup>-</sup>/Å<sup>3</sup> with an RMS deviation of 0.080 e<sup>-</sup>/Å<sup>3</sup>. On the basis of the final model, the calculated density was 1.516 g/cm<sup>3</sup> and F(000), 928 e<sup>-</sup>.

## Table 1. Sample and crystal data for Hilinski\_AED\_pyrroline\_X2.

<b>Identification code</b>	Hilinski_AED_pyrroline_X2
<b>Chemical formula</b>	C <sub>23</sub> H <sub>20</sub> BrNO <sub>2</sub> S
<b>Formula weight</b>	454.37 g/mol

---

<sup>4</sup> Dolomanov, O. V.; Bourhis, L. J.; Gildea, R. J.; Howard, J. A. K.; Puschmann, H. *J. Appl. Cryst.* (2009). **42**, 339-341.

<b>Temperature</b>	100(2) K
<b>Wavelength</b>	0.71073 Å
<b>Crystal size</b>	0.097 x 0.134 x 0.382 mm
<b>Crystal habit</b>	colorless block
<b>Crystal system</b>	monoclinic
<b>Space group</b>	P 2 <sub>1</sub> /c
<b>Unit cell dimensions</b>	a = 20.7100(12) Å     α = 90° b = 6.9933(4) Å     β = 107.623(2)° c = 14.4187(8) Å     γ = 90°
<b>Volume</b>	1990.3(2) Å <sup>3</sup>
<b>Z</b>	4
<b>Density (calculated)</b>	1.516 g/cm <sup>3</sup>
<b>Absorption coefficient</b>	2.189 mm <sup>-1</sup>
<b>F(000)</b>	928

**Table 2. Data collection and structure refinement for Hilinski\_AED\_pyrroline\_X2.**

**Diffractometer** Bruker D8 Venture Kappa four-circle diffractometer

<b>Radiation source</b>	Incoatec I $\mu$ S 3.0 micro-focus sealed X-ray tube (Mo K $\alpha$ , $\lambda = 0.71073 \text{ \AA}$ )
<b>Theta range for data collection</b>	2.83 to 33.15 $^\circ$
<b>Index ranges</b>	-31 $\leq h \leq 31$ , -10 $\leq k \leq 6$ , -22 $\leq l \leq 22$
<b>Reflections collected</b>	43918
<b>Independent reflections</b>	7580 [R(int) = 0.0667]
<b>Coverage of independent reflections</b>	99.7%
<b>Absorption correction</b>	Multi-Scan
<b>Max. and min. transmission</b>	0.8160 and 0.4880
<b>Structure solution technique</b>	direct methods
<b>Structure solution program</b>	SHELXT 2018/2 (Sheldrick, 2018)
<b>Refinement method</b>	Full-matrix least-squares on F $^2$
<b>Refinement program</b>	SHELXL-2019/1 (Sheldrick, 2019)
<b>Function minimized</b>	$\Sigma w(F_o^2 - F_c^2)^2$

<b>Data / restraints / parameters</b>	7580 / 0 / 254	
<b>Goodness-of-fit on F<sup>2</sup></b>	1.029	
<b>Δ/σ<sub>max</sub></b>	0.001	
<b>Final R indices</b>	5722 data; I>2σ(I)	R1 = 0.0380, wR2 = 0.0812
	all data	R1 = 0.0611, wR2 = 0.0898
<b>Weighting scheme</b>	w=1/[σ <sup>2</sup> (F <sub>o</sub> <sup>2</sup> )+(0.0320P) <sup>2</sup> +1.2087P] where P=(F <sub>o</sub> <sup>2</sup> +2F <sub>c</sub> <sup>2</sup> )/3	
<b>Largest diff. peak and hole</b>	0.613 and -0.439 eÅ <sup>-3</sup>	
<b>R.M.S. deviation from mean</b>	0.080 eÅ <sup>-3</sup>	

**Table 3. Atomic coordinates  
and equivalent isotropic  
atomic displacement**

## parameters ( $\text{\AA}^2$ ) for

### Hilinski\_AED\_pyrroline\_X2.

U(eq) is defined as one third of the trace of the orthogonalized  $U_{ij}$  tensor.

	x/a	y/b	z/c	U(eq)
Br1	0.03542(2)	0.15927(3)	0.43888(2)	0.02759(6)
S1	0.29909(2)	0.68690(5)	0.53146(3)	0.01562(8)
O1	0.27822(6)	0.88342(17)	0.51839(9)	0.0218(2)
O2	0.34318(6)	0.61243(17)	0.48060(9)	0.0195(2)
N1	0.33754(7)	0.66165(18)	0.64898(10)	0.0162(2)
C1	0.30386(10)	0.7479(2)	0.71707(13)	0.0222(3)
C2	0.29163(9)	0.5805(3)	0.77937(12)	0.0206(3)
C3	0.34063(8)	0.4321(2)	0.76494(12)	0.0172(3)
C4	0.36288(8)	0.4766(2)	0.68943(11)	0.0153(3)
C5	0.41220(8)	0.3718(2)	0.65356(11)	0.0150(3)
C6	0.46795(8)	0.4644(2)	0.63852(12)	0.0187(3)
C7	0.51545(8)	0.3613(2)	0.60845(13)	0.0211(3)
C8	0.50835(9)	0.1651(2)	0.59493(13)	0.0215(3)
C9	0.45291(9)	0.0720(2)	0.60953(13)	0.0227(3)

	<b>x/a</b>	<b>y/b</b>	<b>z/c</b>	<b>U(eq)</b>
C10	0.40467(9)	0.1747(2)	0.63794(12)	0.0188(3)
C11	0.36437(9)	0.2713(3)	0.83548(13)	0.0219(3)
C12	0.21848(9)	0.5137(3)	0.75442(13)	0.0255(4)
C13	0.19767(10)	0.3329(3)	0.71776(14)	0.0304(4)
C14	0.13023(11)	0.2768(5)	0.69829(15)	0.0452(6)
C15	0.08324(11)	0.4030(6)	0.71410(17)	0.0622(10)
C16	0.10339(12)	0.5832(6)	0.75007(18)	0.0558(8)
C17	0.17052(11)	0.6389(4)	0.77063(15)	0.0396(6)
C18	0.22562(8)	0.5445(2)	0.50126(11)	0.0156(3)
C19	0.23081(8)	0.3511(2)	0.48195(12)	0.0168(3)
C20	0.17350(8)	0.2366(2)	0.46066(12)	0.0195(3)
C21	0.11260(8)	0.3178(2)	0.46050(12)	0.0201(3)
C22	0.10633(9)	0.5111(3)	0.47884(13)	0.0211(3)
C23	0.16370(8)	0.6253(2)	0.49931(13)	0.0195(3)

**Table 4. Bond lengths (Å) for  
Hilinski\_AED\_pyrroline\_X2.**

Br1-C21	1.8919(16)	S1-O2	1.4311(12)
---------	------------	-------	------------

S1-O1	1.4359(12)	S1-N1	1.6491(14)
S1-C18	1.7592(16)	N1-C4	1.451(2)
N1-C1	1.493(2)	C1-C2	1.543(2)
C1-H1A	0.990000	C1-H1B	0.990000
C2-C3	1.509(2)	C2-C12	1.521(3)
C2-H2	1.000000	C3-C4	1.341(2)
C3-C11	1.496(2)	C4-C5	1.472(2)
C5-C6	1.397(2)	C5-C10	1.398(2)
C6-C7	1.391(2)	C6-H6	0.950000
C7-C8	1.387(2)	C7-H7	0.950000
C8-C9	1.390(3)	C8-H8	0.950000
C9-C10	1.389(2)	C9-H9	0.950000
C10-H10	0.950000	C11-H11A	0.980000
C11-H11B	0.980000	C11-H11C	0.980000
C12-C13	1.388(3)	C12-C17	1.396(3)
C13-C14	1.395(3)	C13-H13	0.950000
C14-C15	1.383(4)	C14-H14	0.950000
C15-C16	1.378(5)	C15-H15	0.950000
C16-C17	1.387(4)	C16-H16	0.950000
C17-H17	0.950000	C18-C19	1.392(2)
C18-C23	1.394(2)	C19-C20	1.387(2)

C19-H19	0.950000	C20-C21	1.382(2)
C20-H20	0.950000	C21-C22	1.391(2)
C22-C23	1.387(2)	C22-H22	0.950000
C23-H23	0.950000		

**Table 5. Bond angles (°) for  
Hilinski\_AED\_pyrroline\_X2.**

O2-S1-O1	119.64(7)	O2-S1-N1	107.64(7)
O1-S1-N1	105.66(7)	O2-S1-C18	107.79(7)
O1-S1-C18	107.80(7)	N1-S1-C18	107.82(7)
C4-N1-C1	106.26(12)	C4-N1-S1	120.79(10)
C1-N1-S1	117.14(11)	N1-C1-C2	105.56(13)
N1-C1-H1A	110.600000	C2-C1-H1A	110.600000
N1-C1-H1B	110.600000	C2-C1-H1B	110.600000
H1A-C1-H1B	108.800000	C3-C2-C12	114.81(15)
C3-C2-C1	101.86(13)	C12-C2-C1	115.01(15)
C3-C2-H2	108.300000	C12-C2-H2	108.300000
C1-C2-H2	108.300000	C4-C3-C11	127.12(15)
C4-C3-C2	111.30(14)	C11-C3-C2	121.28(14)

C3-C4-N1	111.21(14)	C3-C4-C5	127.98(15)
N1-C4-C5	120.50(13)	C6-C5-C10	119.29(14)
C6-C5-C4	121.20(14)	C10-C5-C4	119.46(14)
C7-C6-C5	120.26(15)	C7-C6-H6	119.900000
C5-C6-H6	119.900000	C8-C7-C6	120.12(16)
C8-C7-H7	119.900000	C6-C7-H7	119.900000
C7-C8-C9	119.95(15)	C7-C8-H8	120.000000
C9-C8-H8	120.000000	C10-C9-C8	120.21(15)
C10-C9-H9	119.900000	C8-C9-H9	119.900000
C9-C10-C5	120.16(15)	C9-C10-H10	119.900000
C5-C10-H10	119.900000	C3-C11-H11A	109.500000
C3-C11-H11B	109.500000	H11A-C11- H11B	109.500000
C3-C11-H11C	109.500000	H11A-C11- H11C	109.500000
H11B-C11- H11C	109.500000	C13-C12-C17	118.7(2)
C13-C12-C2	122.83(16)	C17-C12-C2	118.4(2)
C12-C13-C14	120.6(2)	C12-C13-H13	119.700000
C14-C13-H13	119.700000	C15-C14-C13	119.9(3)
C15-C14-H14	120.000000	C13-C14-H14	120.000000

C16-C15-C14	119.8(2)	C16-C15-H15	120.100000
C14-C15-H15	120.100000	C15-C16-C17	120.5(2)
C15-C16-H16	119.800000	C17-C16-H16	119.800000
C16-C17-C12	120.4(3)	C16-C17-H17	119.800000
C12-C17-H17	119.800000	C19-C18-C23	121.08(15)
C19-C18-S1	119.09(12)	C23-C18-S1	119.82(12)
C20-C19-C18	119.50(15)	C20-C19-H19	120.200000
C18-C19-H19	120.200000	C21-C20-C19	118.86(15)
C21-C20-H20	120.600000	C19-C20-H20	120.600000
C20-C21-C22	122.44(15)	C20-C21-Br1	118.97(13)
C22-C21-Br1	118.56(13)	C23-C22-C21	118.48(15)
C23-C22-H22	120.800000	C21-C22-H22	120.800000
C22-C23-C18	119.63(15)	C22-C23-H23	120.200000
C18-C23-H23	120.200000		

**Table 6. Torsion angles ( $^{\circ}$ ) for  
Hilinski\_AED\_pyrroline\_X2.**

O2-S1-N1-C4	-53.84(13)	O1-S1-N1-C4	177.25(12)
C18-S1-N1-C4	62.19(13)	O2-S1-N1-C1	173.95(12)

O1-S1-N1-C1	45.04(13)	C18-S1-N1-C1	-70.01(13)
C4-N1-C1-C2	-17.30(17)	S1-N1-C1-C2	121.19(13)
N1-C1-C2-C3	19.06(17)	N1-C1-C2-C12	- 105.77(16)
C12-C2-C3-C4	110.00(16)	C1-C2-C3-C4	-14.96(18)
C12-C2-C3- C11	-75.9(2)	C1-C2-C3-C11	159.15(15)
C11-C3-C4-N1	- 169.05(16)	C2-C3-C4-N1	4.64(19)
C11-C3-C4-C5	4.6(3)	C2-C3-C4-C5	178.24(15)
C1-N1-C4-C3	8.35(18)	S1-N1-C4-C3	- 128.29(13)
C1-N1-C4-C5	- 165.81(14)	S1-N1-C4-C5	57.56(18)
C3-C4-C5-C6	- 128.33(18)	N1-C4-C5-C6	44.8(2)
C3-C4-C5-C10	49.1(2)	N1-C4-C5-C10	- 137.84(15)
C10-C5-C6-C7	-0.1(2)	C4-C5-C6-C7	177.33(15)
C5-C6-C7-C8	-1.2(3)	C6-C7-C8-C9	1.3(3)
C7-C8-C9-C10	-0.2(3)	C8-C9-C10-C5	-1.1(3)

C6-C5-C10-C9	1.2(2)	C4-C5-C10-C9	- 176.26(15)
C3-C2-C12- C13	-2.3(2)	C1-C2-C12- C13	115.44(19)
C3-C2-C12- C17	176.65(16)	C1-C2-C12- C17	-65.6(2)
C17-C12-C13- C14	-0.6(3)	C2-C12-C13- C14	178.39(17)
C12-C13-C14- C15	1.0(3)	C13-C14-C15- C16	-0.7(3)
C14-C15-C16- C17	-0.1(4)	C15-C16-C17- C12	0.5(3)
C13-C12-C17- C16	-0.2(3)	C2-C12-C17- C16	- 179.20(18)
O2-S1-C18- C19	32.14(15)	O1-S1-C18- C19	162.56(13)
N1-S1-C18- C19	-83.80(14)	O2-S1-C18- C23	- 149.41(13)
O1-S1-C18- C23	-18.98(16)	N1-S1-C18- C23	94.65(14)
C23-C18-C19- C20	-0.2(2)	S1-C18-C19- C20	178.27(13)

C18-C19-C20- C21	-0.9(2)	C19-C20-C21- C22	1.4(3)
C19-C20-C21- Br1	- 176.40(12)	C20-C21-C22- C23	-0.9(3)
Br1-C21-C22- C23	176.94(13)	C21-C22-C23- C18	-0.2(3)
C19-C18-C23- C22	0.7(3)	S1-C18-C23- C22	- 177.72(13)

**Table 7. Anisotropic atomic displacement parameters ( $\text{\AA}^2$ ) for Hilinski\_AED\_pyrroline\_X2.**

The anisotropic atomic displacement factor exponent takes the form:  $-2\pi^2 [ h^2 a^{*2}$

$U_{11} + \dots + 2 h k a^* b^* U_{12} ]$

	$U_{11}$	$U_{22}$	$U_{33}$	$U_{23}$	$U_{13}$	$U_{12}$
Br1	0.01917(8)	0.03337(10)	0.03080(10)	-0.00069(8)	0.00843(7)	-0.00829(7)
S1	0.01579(17)	0.01453(16)	0.01697(17)	0.00187(14)	0.00560(14)	0.00047(13)
O1	0.0239(6)	0.0146(5)	0.0261(6)	0.0032(5)	0.0067(5)	0.0008(5)
O2	0.0178(5)	0.0235(5)	0.0192(6)	0.0019(5)	0.0084(4)	0.0000(5)
N1	0.0189(6)	0.0135(5)	0.0163(6)	-0.0012(5)	0.0053(5)	0.0013(5)

	<b>U<sub>11</sub></b>	<b>U<sub>22</sub></b>	<b>U<sub>33</sub></b>	<b>U<sub>23</sub></b>	<b>U<sub>13</sub></b>	<b>U<sub>12</sub></b>
C1	0.0287(9)	0.0193(7)	0.0203(8)	-0.0032(7)	0.0097(7)	0.0050(7)
C2	0.0226(8)	0.0244(8)	0.0155(7)	-0.0011(6)	0.0069(6)	0.0042(7)
C3	0.0165(7)	0.0182(7)	0.0161(7)	0.0001(6)	0.0038(6)	-0.0003(6)
C4	0.0145(6)	0.0145(6)	0.0161(7)	-0.0009(6)	0.0034(6)	-0.0018(5)
C5	0.0147(6)	0.0149(6)	0.0144(7)	0.0008(5)	0.0031(5)	0.0017(5)
C6	0.0158(7)	0.0175(7)	0.0223(8)	0.0000(6)	0.0051(6)	-0.0010(6)
C7	0.0157(7)	0.0244(8)	0.0238(8)	-0.0014(7)	0.0069(6)	0.0003(6)
C8	0.0211(7)	0.0232(8)	0.0191(7)	-0.0022(7)	0.0043(6)	0.0077(7)
C9	0.0294(9)	0.0168(7)	0.0222(8)	-0.0017(6)	0.0084(7)	0.0034(7)
C10	0.0218(7)	0.0155(6)	0.0199(7)	-0.0003(6)	0.0075(6)	-0.0024(6)
C11	0.0238(8)	0.0224(7)	0.0202(8)	0.0036(7)	0.0078(7)	0.0015(7)
C12	0.0203(8)	0.0428(10)	0.0157(7)	0.0067(8)	0.0088(6)	0.0058(8)
C13	0.0212(8)	0.0498(12)	0.0197(8)	0.0062(8)	0.0054(7)	-0.0062(8)
C14	0.0263(10)	0.0847(19)	0.0217(9)	0.0124(11)	0.0030(8)	-0.0190(11)
C15	0.0188(10)	0.142(3)	0.0250(11)	0.0222(16)	0.0057(8)	-0.0043(14)
C16	0.0278(11)	0.115(3)	0.0288(11)	0.0194(15)	0.0144(9)	0.0272(14)
C17	0.0305(10)	0.0690(16)	0.0218(9)	0.0106(10)	0.0118(8)	0.0214(11)
C18	0.0152(7)	0.0166(6)	0.0156(7)	0.0008(6)	0.0057(5)	0.0001(6)
C19	0.0160(6)	0.0175(7)	0.0174(7)	-0.0001(6)	0.0056(5)	0.0013(6)
C20	0.0197(7)	0.0184(7)	0.0201(8)	-0.0005(6)	0.0058(6)	-0.0005(6)

	<b>U<sub>11</sub></b>	<b>U<sub>22</sub></b>	<b>U<sub>33</sub></b>	<b>U<sub>23</sub></b>	<b>U<sub>13</sub></b>	<b>U<sub>12</sub></b>
C21	0.0159(7)	0.0254(8)	0.0192(7)	0.0016(7)	0.0054(6)	-0.0045(6)
C22	0.0166(7)	0.0246(8)	0.0234(8)	0.0022(7)	0.0080(6)	0.0037(6)
C23	0.0181(7)	0.0191(7)	0.0230(8)	0.0011(6)	0.0086(6)	0.0035(6)

**Table 8. Hydrogen atomic coordinates and isotropic atomic displacement parameters ( $\text{\AA}^2$ ) for Hilinski\_AED\_pyrroline\_X2.**

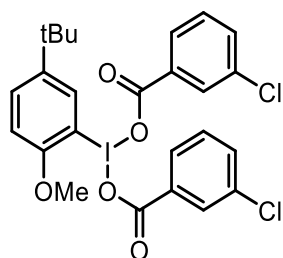
	<b>x/a</b>	<b>y/b</b>	<b>z/c</b>	<b>U(eq)</b>
H1A	0.2604	0.8085	0.6805	0.027000
H1B	0.3334	0.8458	0.7587	0.027000
H2	0.3069	0.6210	0.8491	0.025000
H6	0.4735	0.5984	0.6489	0.022000
H7	0.5528	0.4253	0.5971	0.025000
H8	0.5413	0.0944	0.5757	0.026000
H9	0.4480	-0.0623	0.6001	0.027000

	<b>x/a</b>	<b>y/b</b>	<b>z/c</b>	<b>U(eq)</b>
H10	0.3665	0.1109	0.6468	0.023000
H11A	0.3775	0.3215	0.9021	0.033000
H11B	0.4035	0.2090	0.8235	0.033000
H11C	0.3277	0.1781	0.8271	0.033000
H13	0.2297	0.2466	0.7058	0.037000
H14	0.1166	0.1520	0.6742	0.054000
H15	0.0372	0.3656	0.7002	0.075000
H16	0.0711	0.6698	0.7608	0.067000
H17	0.1839	0.7630	0.7959	0.047000
H19	0.2733	0.2979	0.4833	0.020000
H20	0.1760	0.1047	0.4464	0.023000
H22	0.0637	0.5637	0.4774	0.025000
H23	0.1608	0.7579	0.5119	0.023000

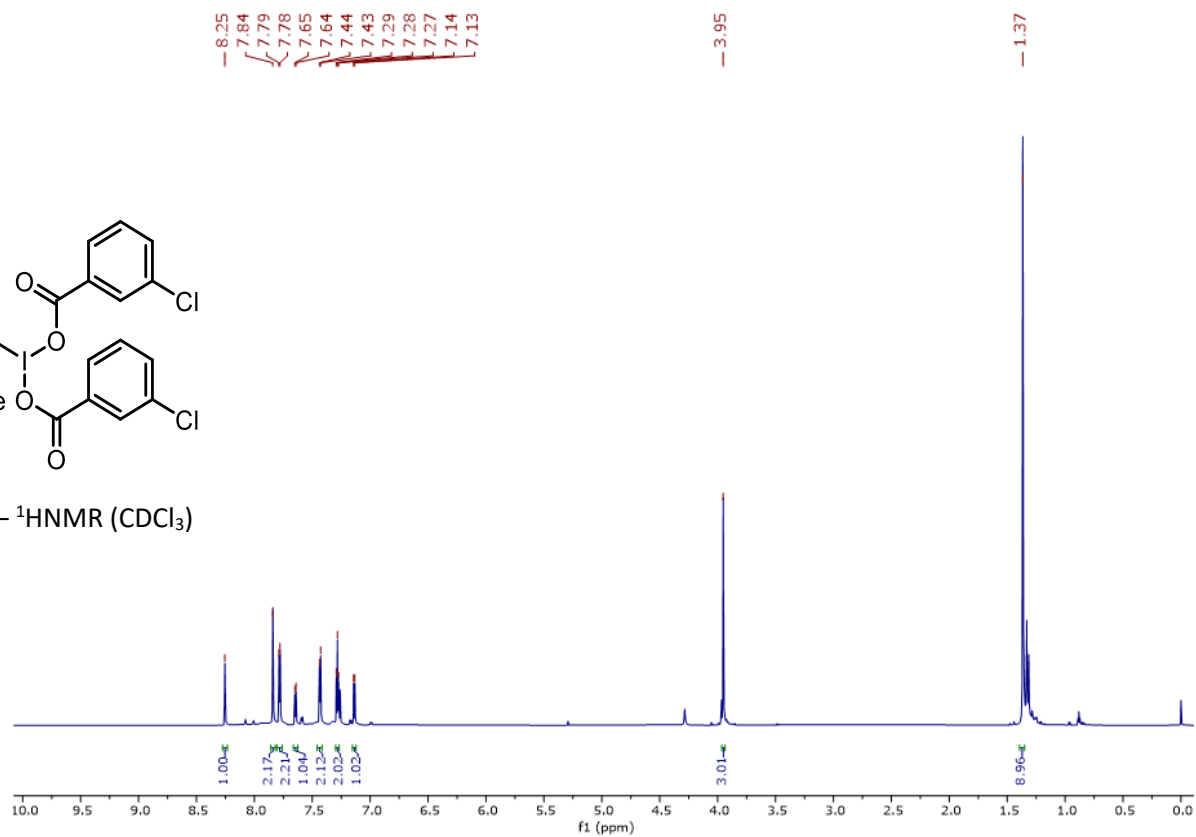
## B.9 References

- (1) Garfinkle, J.; Kimball, F. S.; Trzuppek, J. D.; Takizawa, S.; Shimamura, H.; Tomishima, M.; Boger, D. L. Total Synthesis of Chloropeptin II (Complestatin) and Chloropeptin I. *J. Am. Chem. Soc.* **2009**, *131* (44), 16036–16038.
- (2) Wech, F.; Gellrich, U. In Situ Formation of an Efficient Catalyst for the Semihydrogenation of Alkynes from Imidazolone and BH<sub>3</sub>. *ACS Catal.* **2022**, *12* (9), 5388–5396.
- (3) Wearing, E. R.; Blackmun, D. E.; Becker, M. R.; Schindler, C. S. 1- And 2-Azetines via Visible Light-Mediated [2 + 2]-Cycloadditions of Alkynes and Oximes. *J. Am. Chem. Soc.* **2021**, *143* (39), 16235–16242.
- (4) Son, Y.; Hwang, S.; Bak, S.; Kim, H. E.; Choi, J. H.; Chung, W. J.  $\alpha$ -Fluoroamine Synthesis via P(III)-Mediated Deoxygenative Geminal Fluorosulfonimidation of 1,2-Diketones. *Org. Biomol. Chem.* **2022**, *20* (16), 3263–3267.
- (5) Lu, B.; Li, C.; Zhang, L. Gold-Catalyzed Highly Regioselective Oxidation of C-C Triple Bonds without Acid Additives: Propargyl Moieties as Masked  $\alpha,\beta$ -Unsaturated Carbonyls. *J. Am. Chem. Soc.* **2010**, *132* (40), 14070–14072.
- (6) Jurberg, I. D.; Nome, R. A.; Crespi, S.; Atvars, T. D. Z.; König, B. Visible Light-Enhanced C–H Amination of Cyclic Ethers with Iminoiodinanes. *Adv. Synth. Catal.* **2022**, *364* (23), 4061–4068.
- (7) Combee, L. A.; Raya, B.; Wang, D.; Hilinski, M. K. Organocatalytic Nitrenoid Transfer: Metal-Free Selective Intermolecular C(Sp<sup>3</sup>)–H Amination Catalyzed by an Iminium Salt. *Chem. Sci.* **2018**, *9* (4), 935–939.
- (8) Iskra, J.; Murphree, S. S. Rapid Aerobic Iodination of Arenes Mediated by Hypervalent Iodine in Fluorinated Solvents. *Tetrahedron Lett.* **2017**, *58* (7), 645–648.
- (9) Yu, X.; Guo, Z.; Song, H.; Liu, Y.; Wang, Q. Hydration and Intramolecular Cyclization of Homopropargyl Sulfonamide Derivatives Catalyzed by Silver Hexafluoroantimonate(V): Synthesis of Structurally Diverse 2,3-Dihydro-1H-Pyrroles. *Adv. Synth. Catal.* **2018**, *360* (6), 1077–1081.
- (10) Schwalm, C. S.; Correia, C. R. D. Divergent Total Synthesis of the Natural Antimalarial Marinoquinolines A, B, C, E and Unnatural Analogues. *Tetrahedron Lett.* **2012**, *53* (36), 4836–4840.
- (11) Chung, M. C.; Chan, Y. H.; Chang, W. J.; Hou, D. R. Synthesis of 2,3-Dihydro-1H-Pyrroles by Intramolecular Cyclization of N-(3-Butynyl)-Sulfonamides. *Org. Biomol. Chem.* **2017**, *15* (17), 3783–3790.

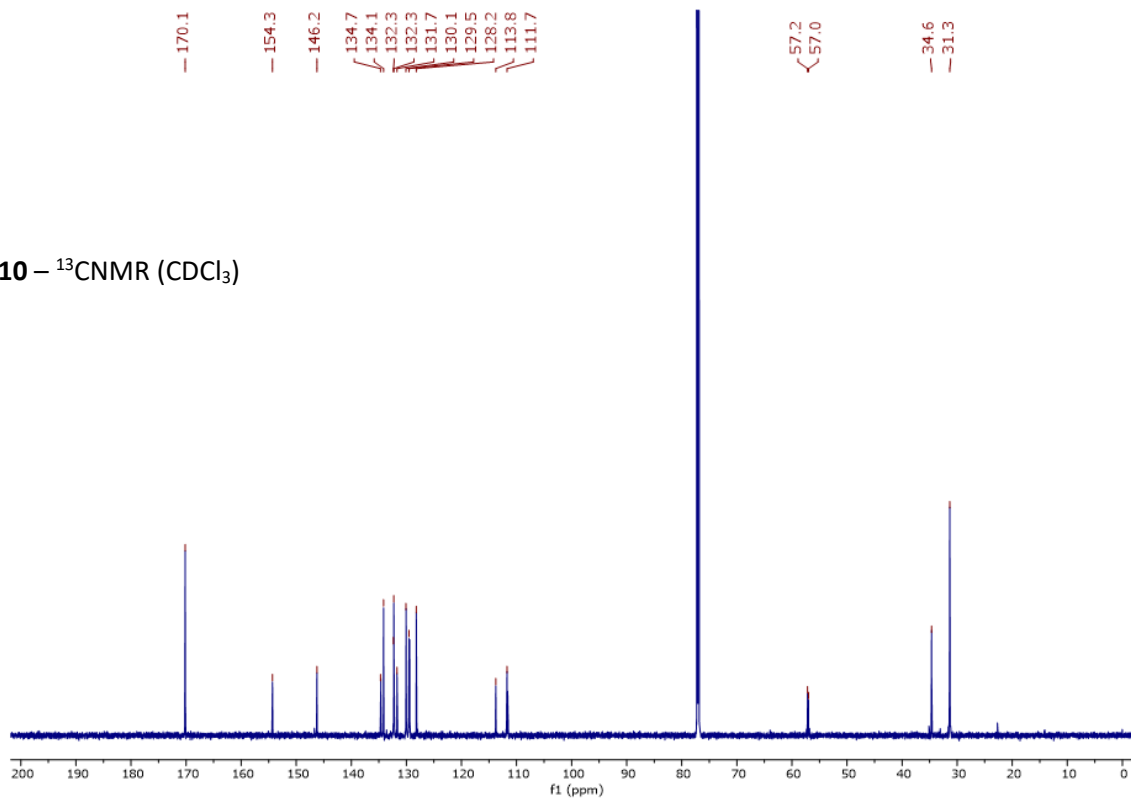
## B.10 NMR Spectra

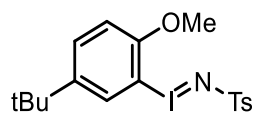


**B.10** –  $^1\text{H NMR}$  ( $\text{CDCl}_3$ )

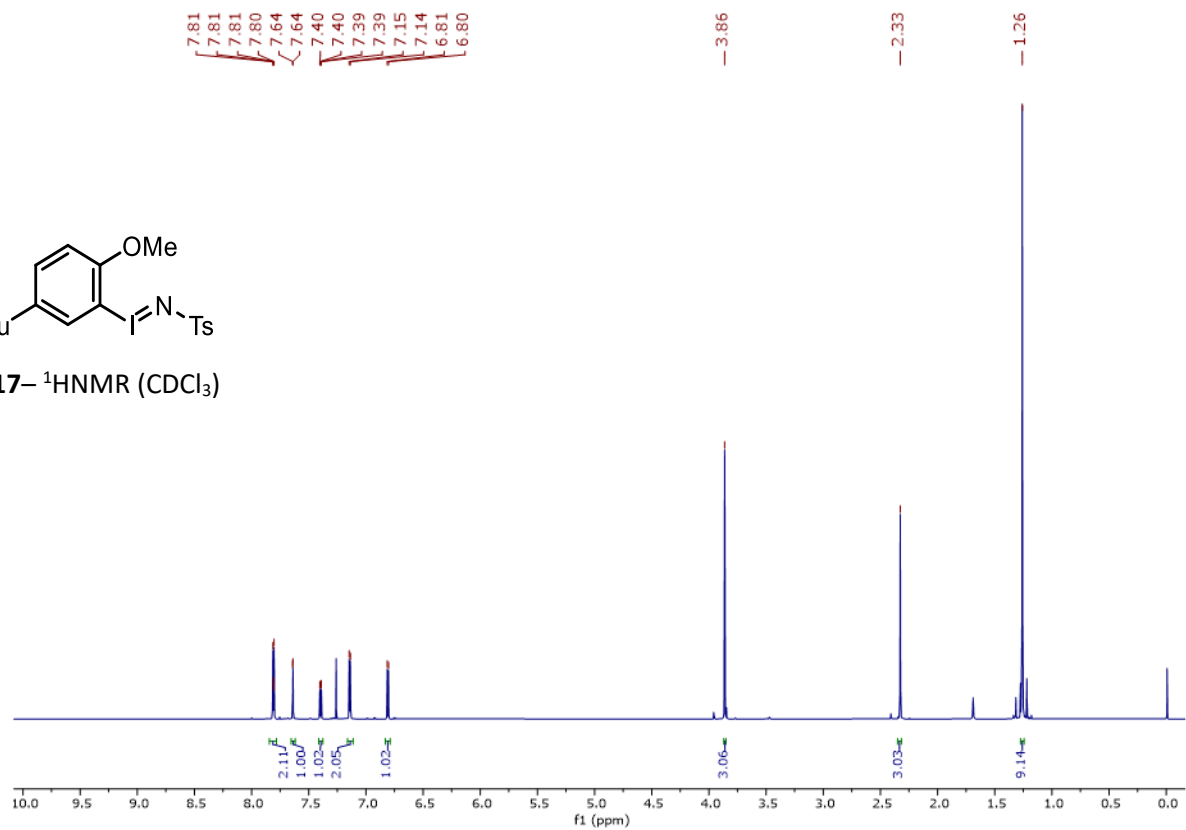


**B.10** –  $^{13}\text{C NMR}$  ( $\text{CDCl}_3$ )

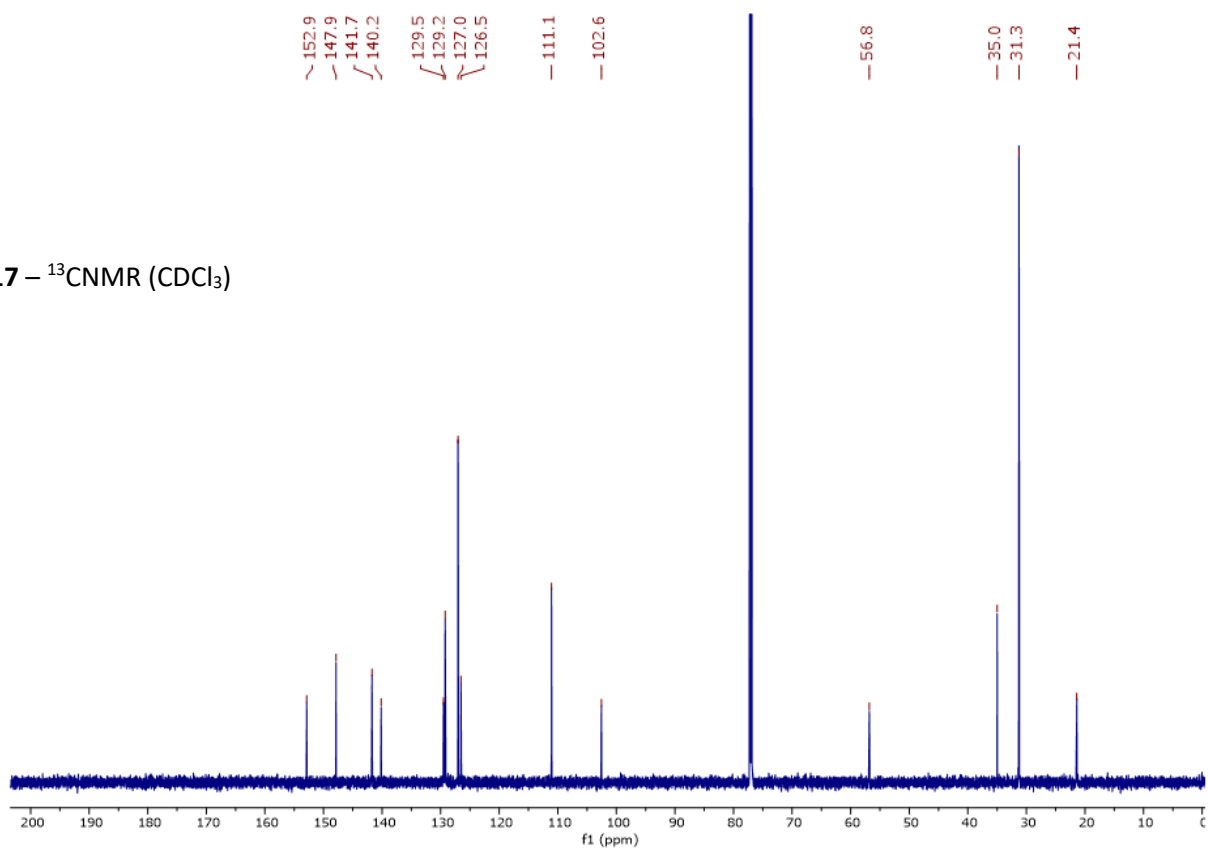


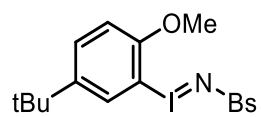


3.17-  $^1\text{H}$ NMR ( $\text{CDCl}_3$ )

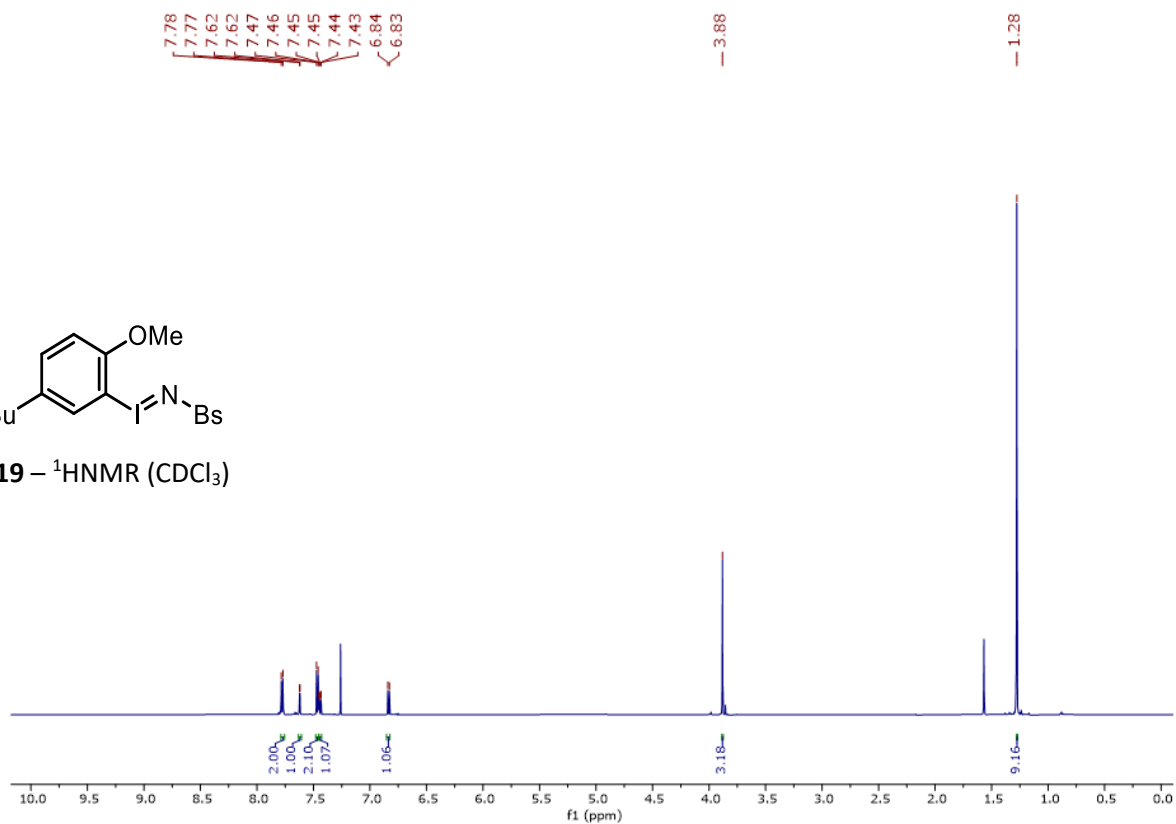


3.17 -  $^{13}\text{C}$ NMR ( $\text{CDCl}_3$ )

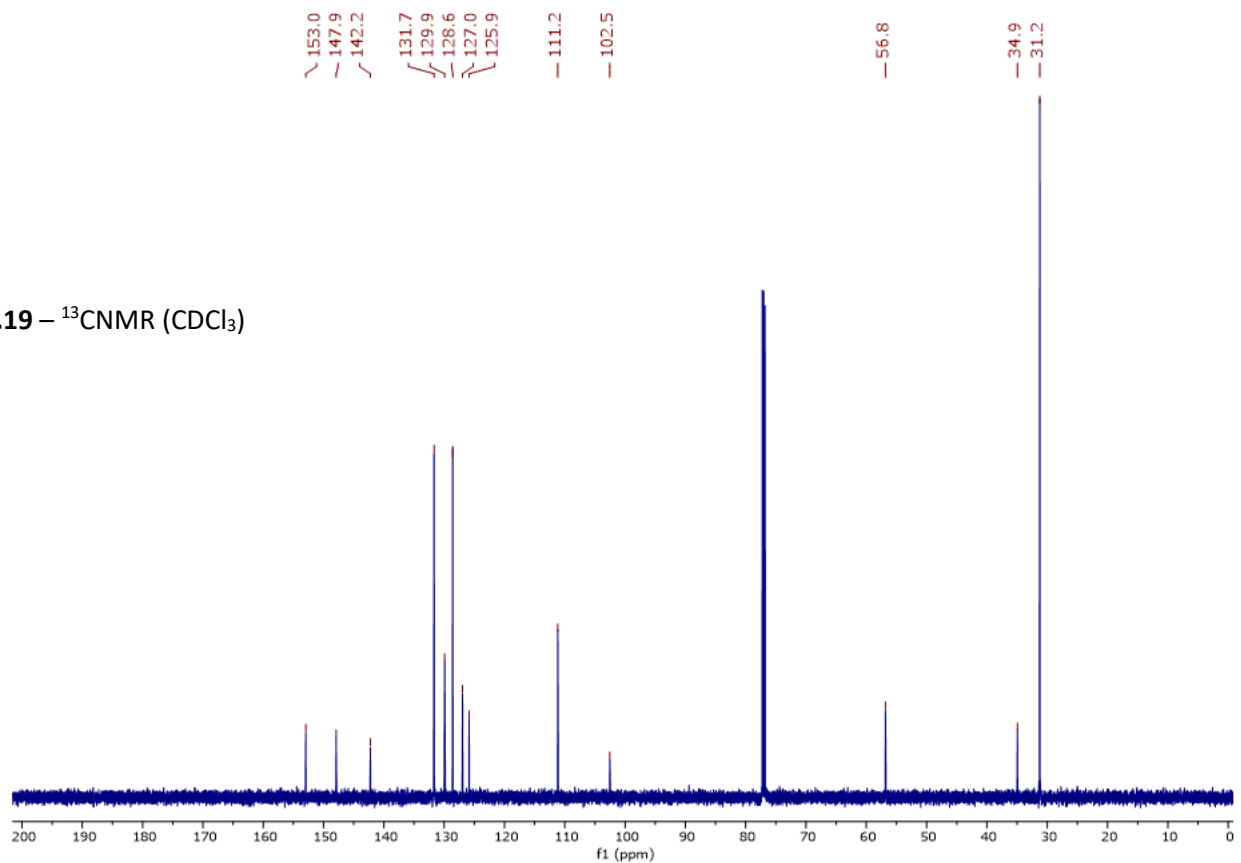


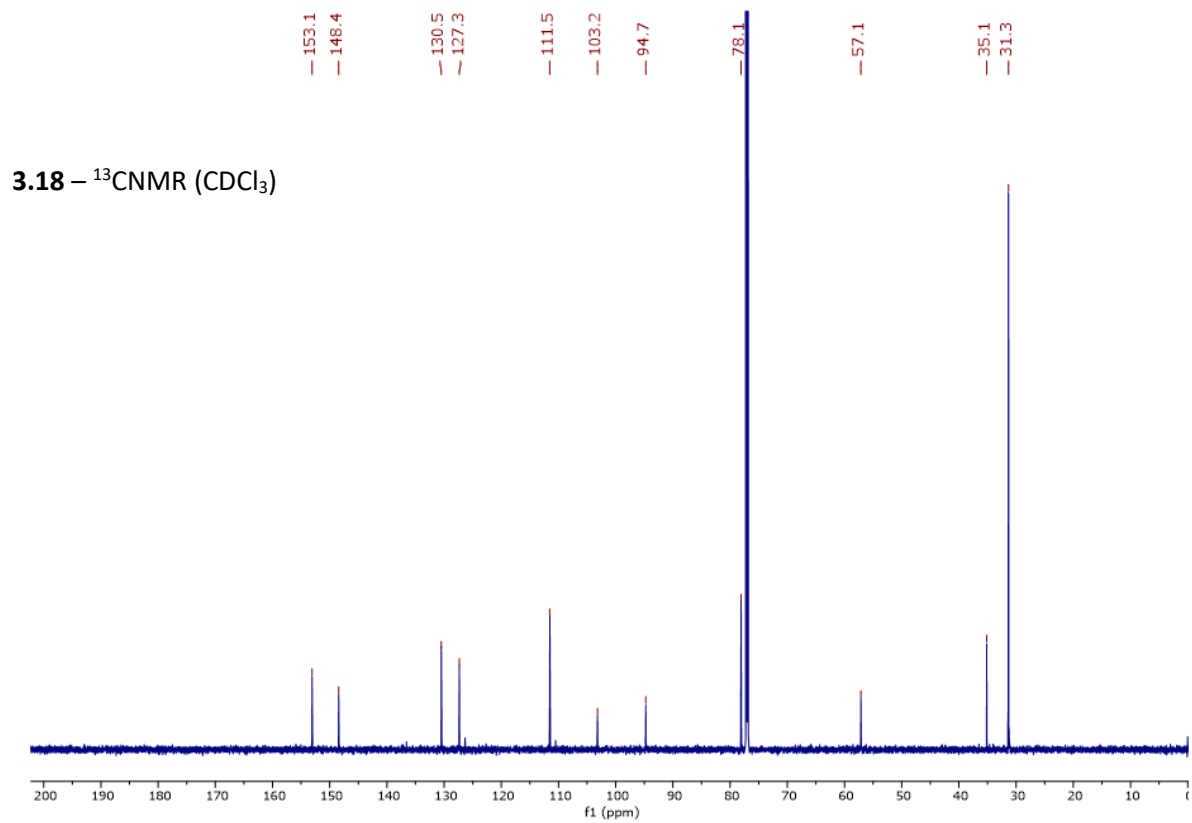
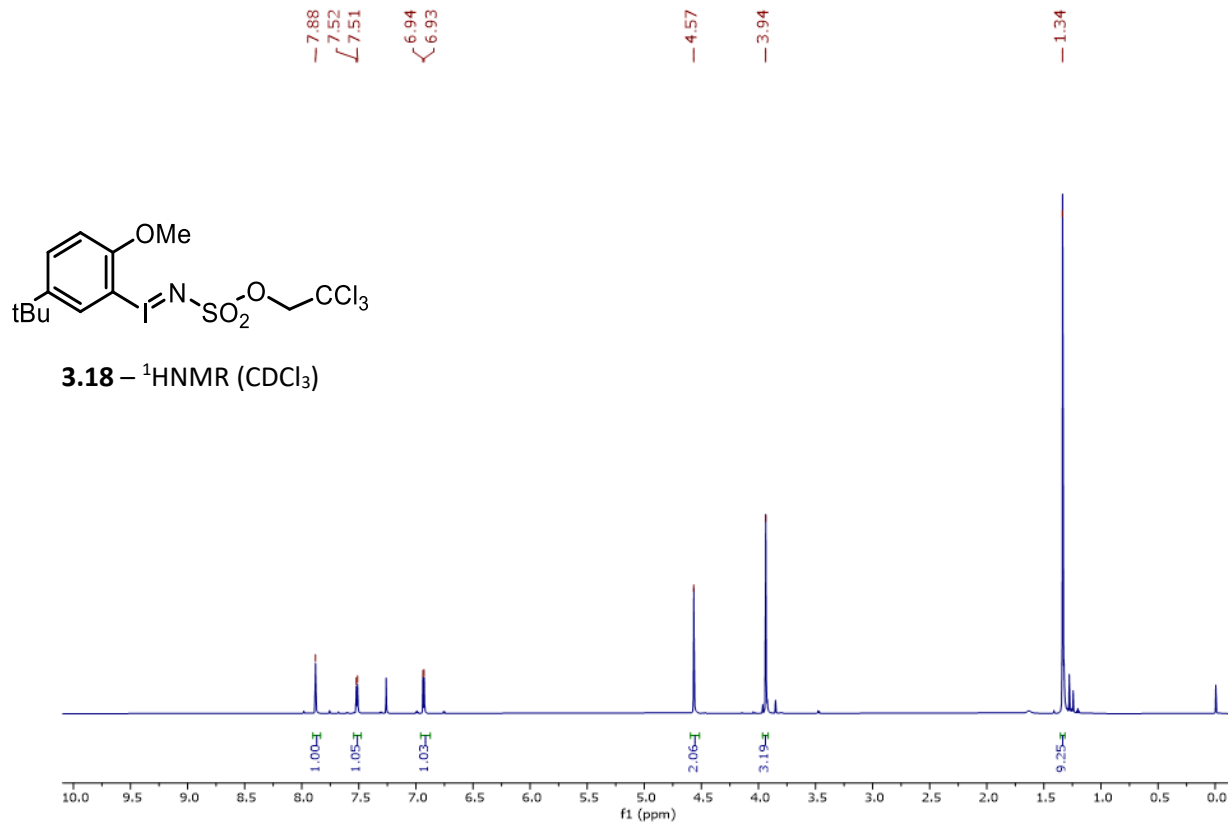


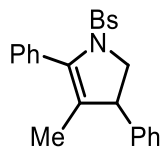
3.19 –  $^1\text{H}$ NMR ( $\text{CDCl}_3$ )



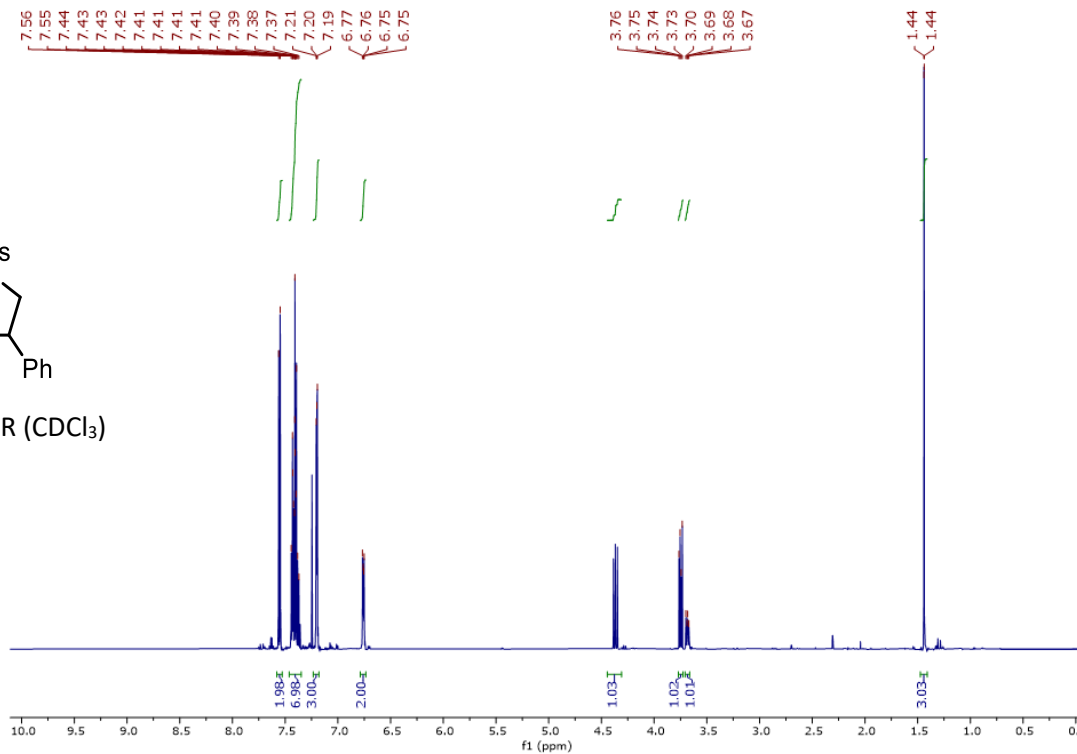
3.19 –  $^{13}\text{C}$ NMR ( $\text{CDCl}_3$ )





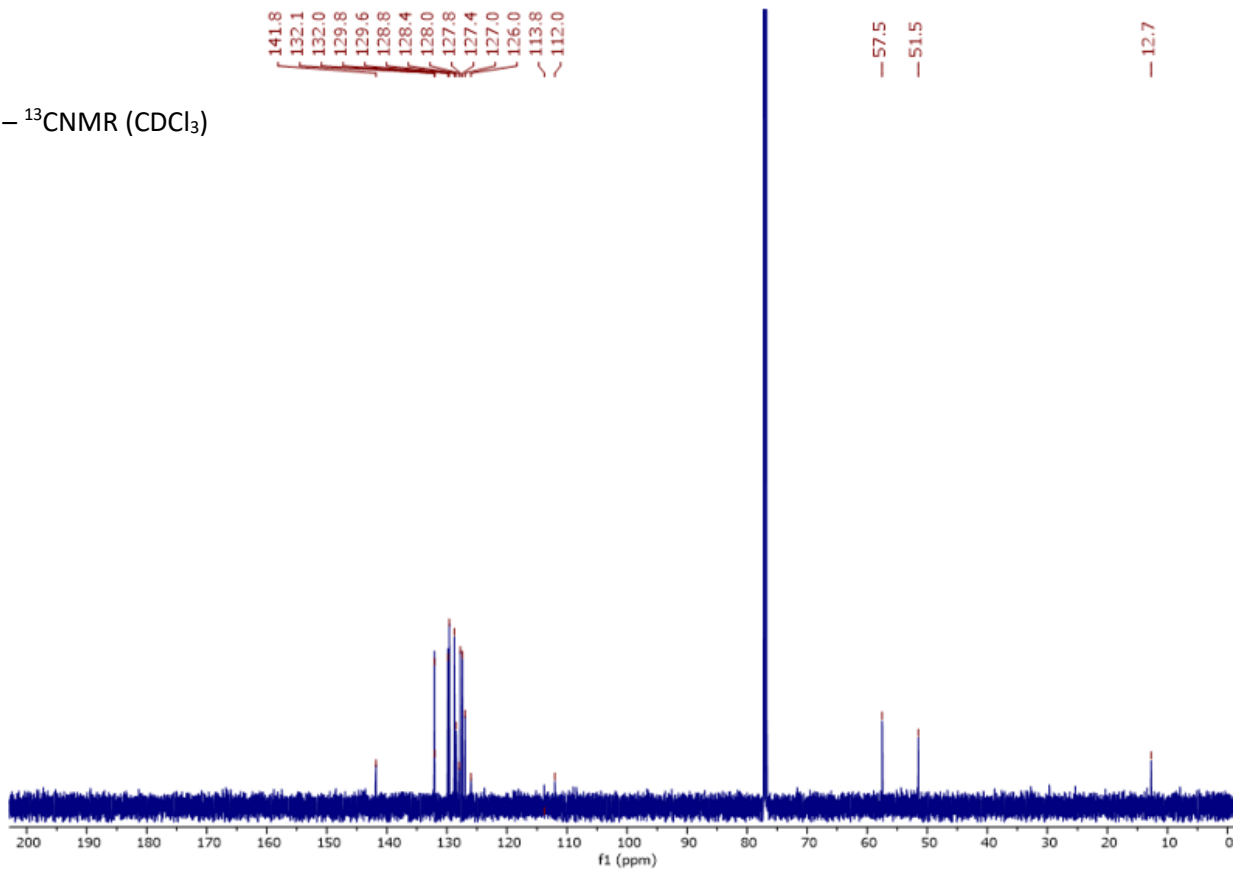


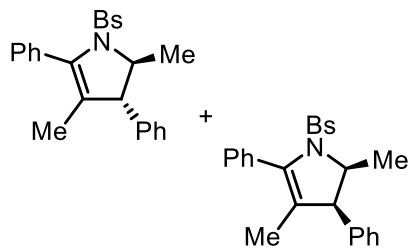
3.11 – <sup>1</sup>HNMR (CDCl<sub>3</sub>)



6.

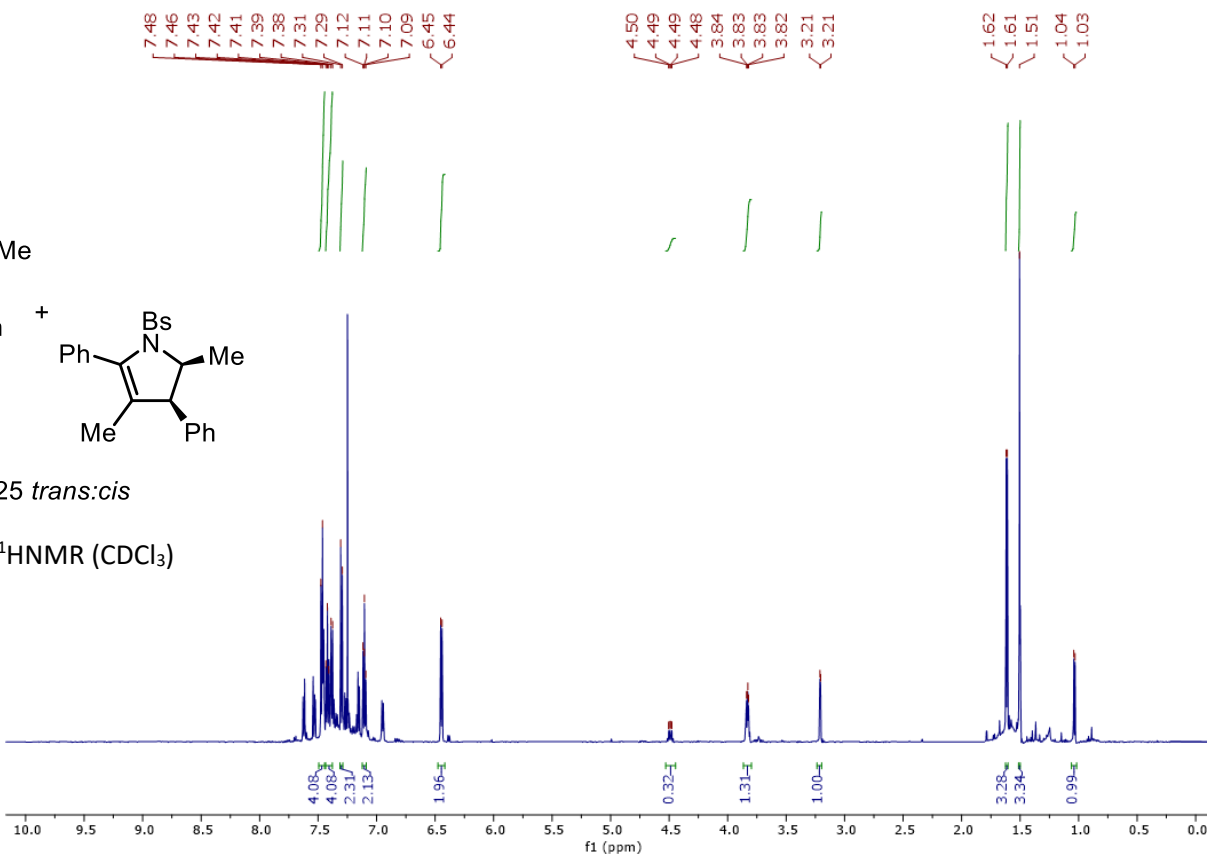
3.11 – <sup>13</sup>CNMR (CDCl<sub>3</sub>)



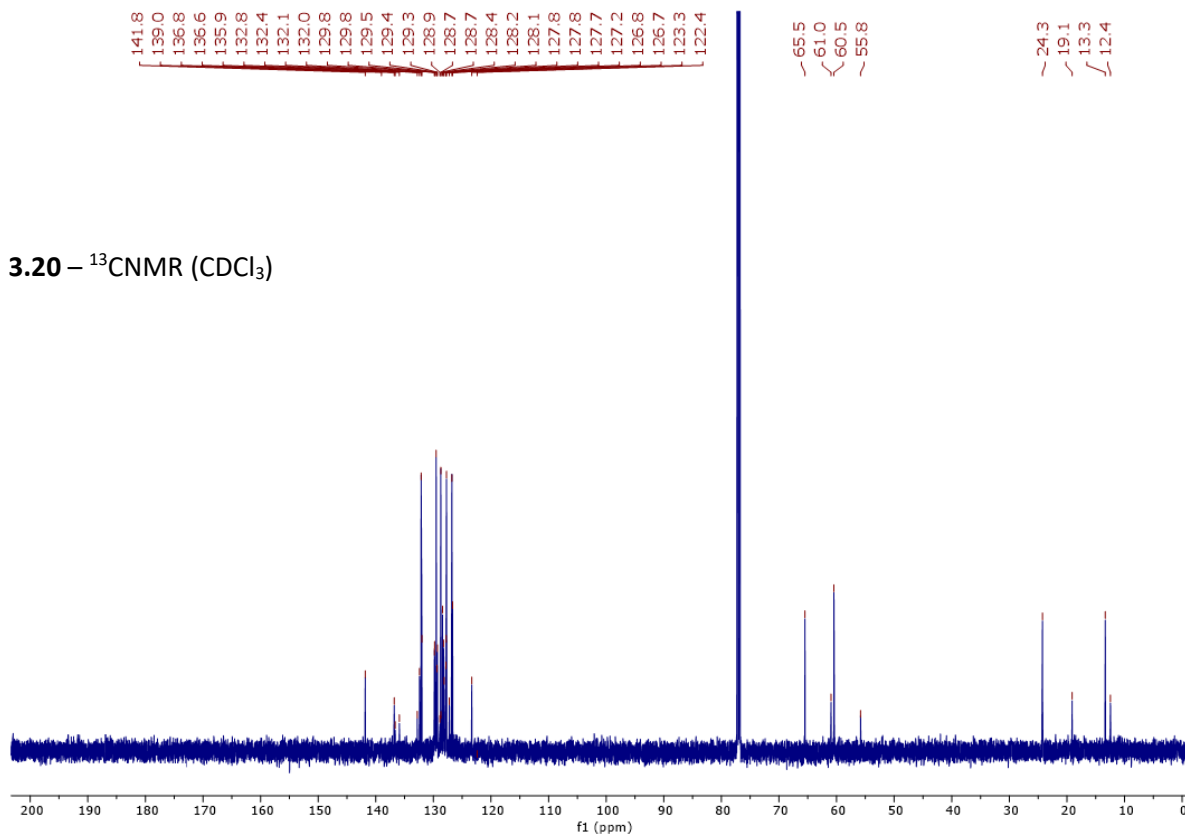


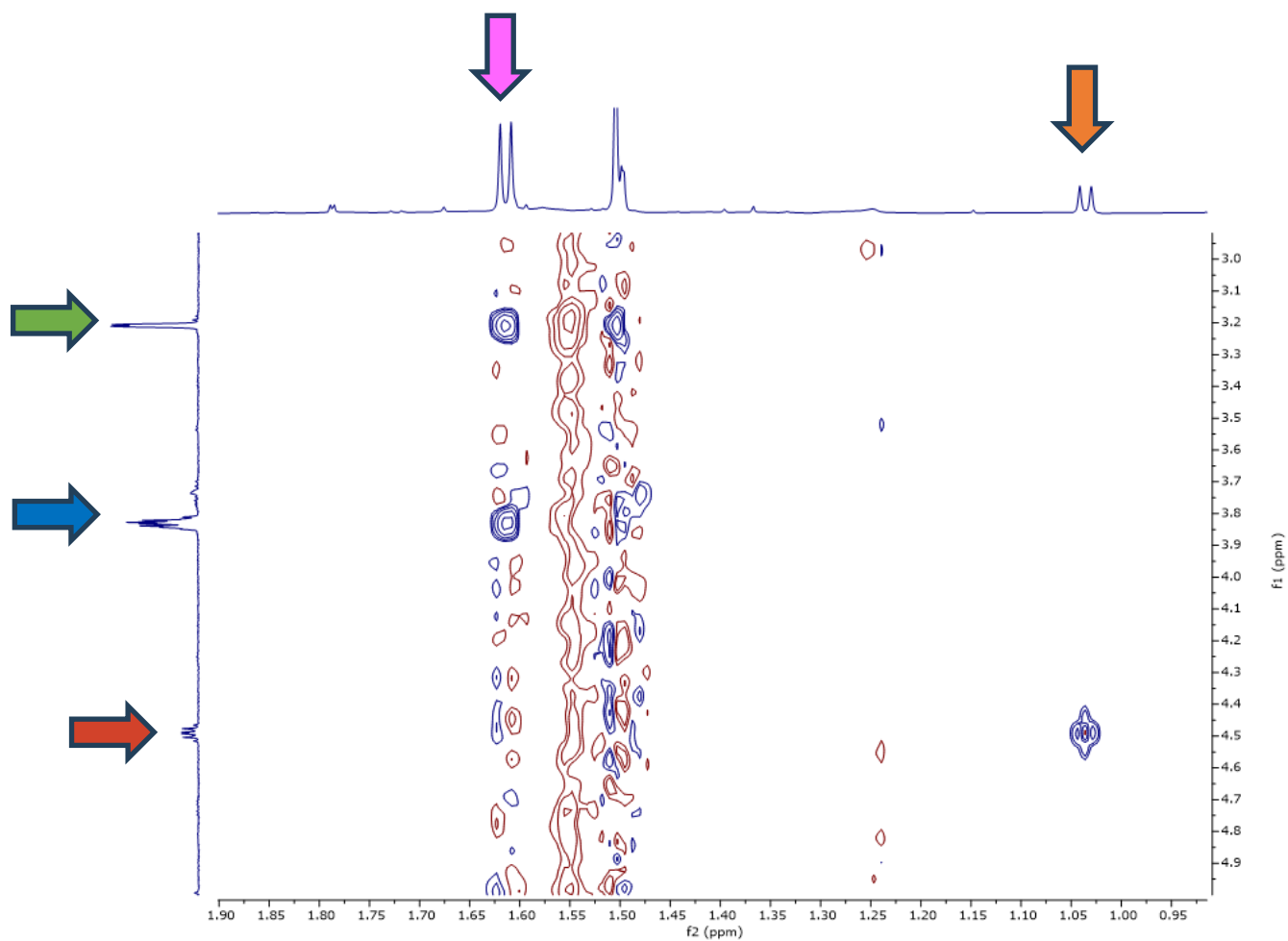
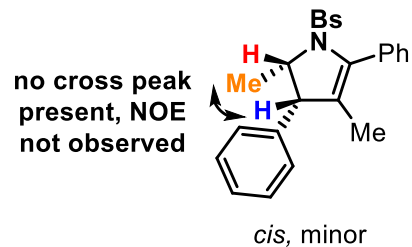
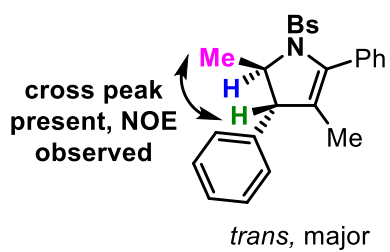
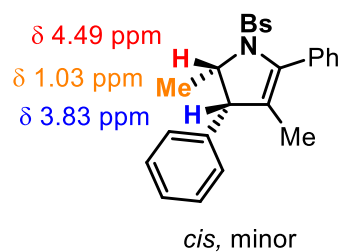
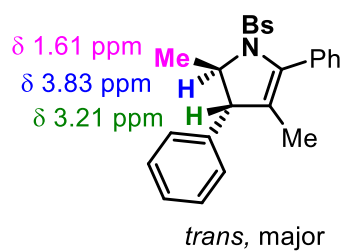
75:25 *trans*:*cis*

**3.20** –  $^1\text{H}$ NMR ( $\text{CDCl}_3$ )



**3.20** –  $^{13}\text{C}$ NMR ( $\text{CDCl}_3$ )





3.20 –  $^1\text{H}$ -NOESY NMR ( $\text{CDCl}_3$ )

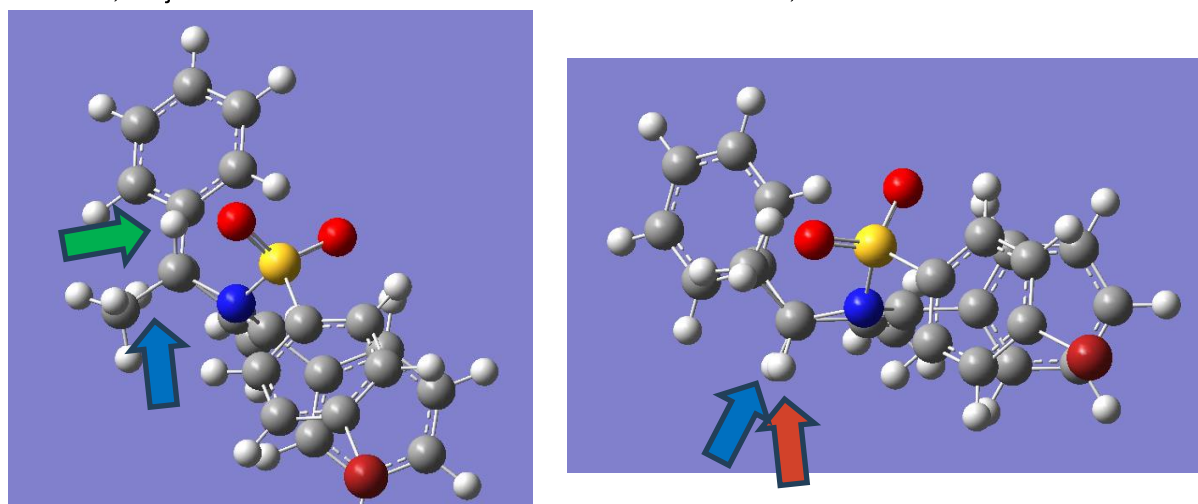
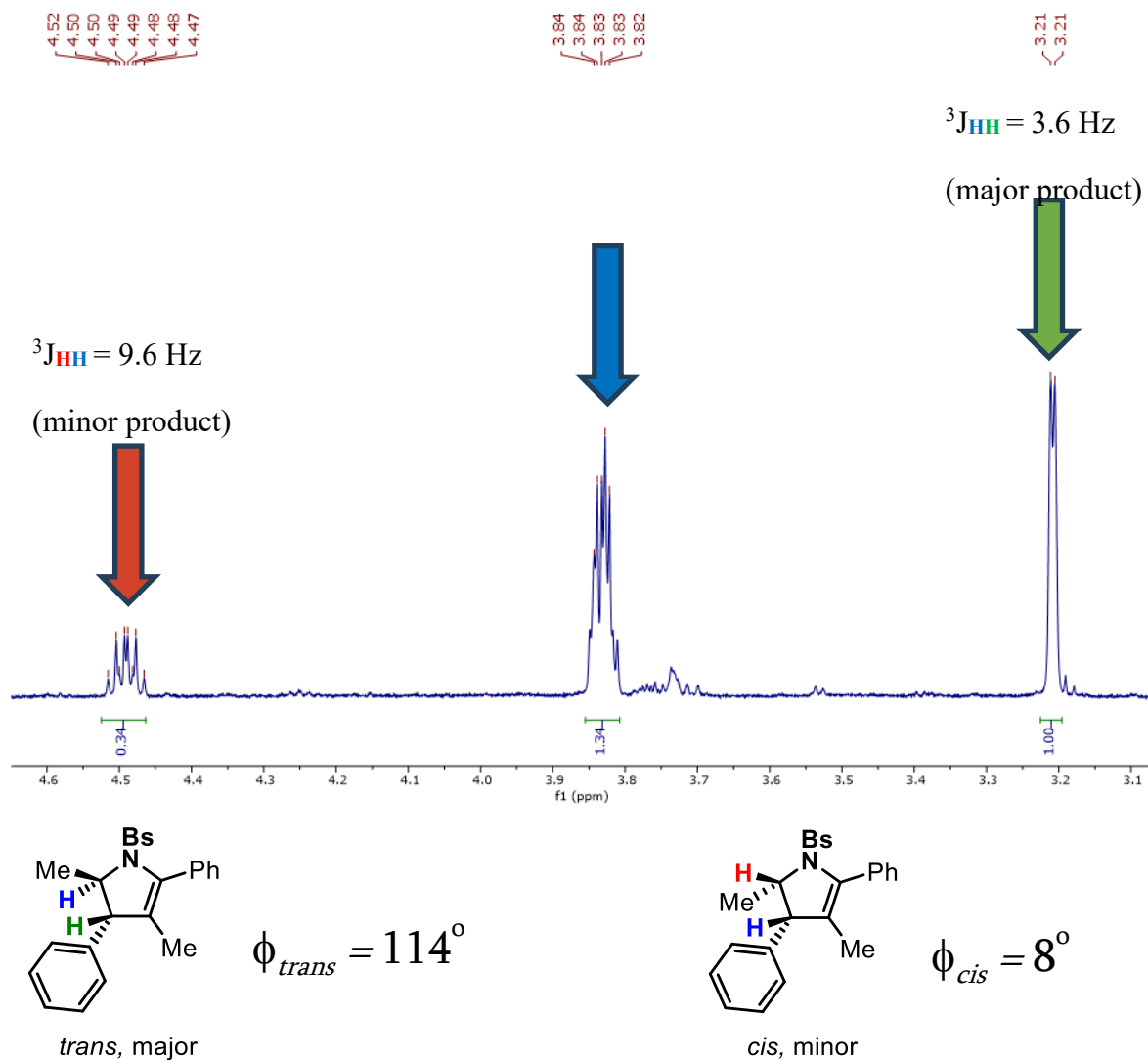
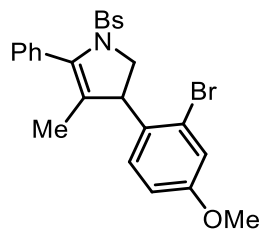
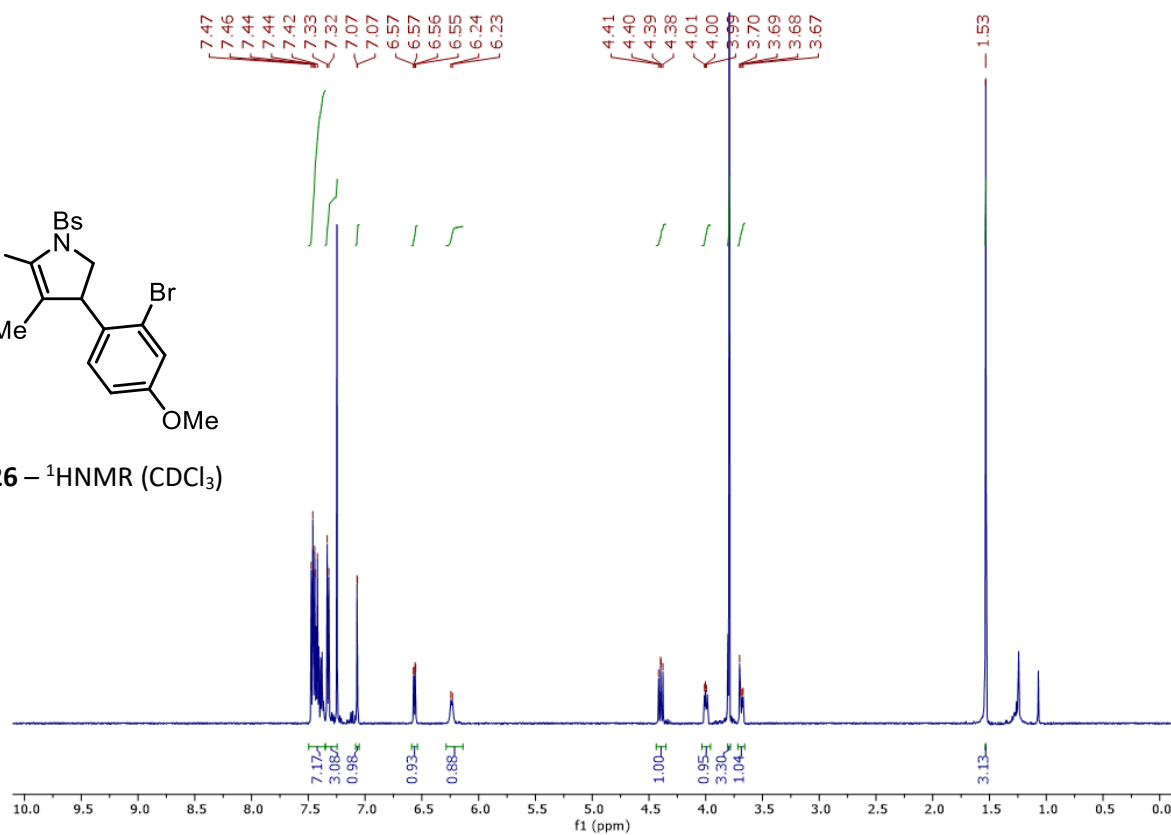


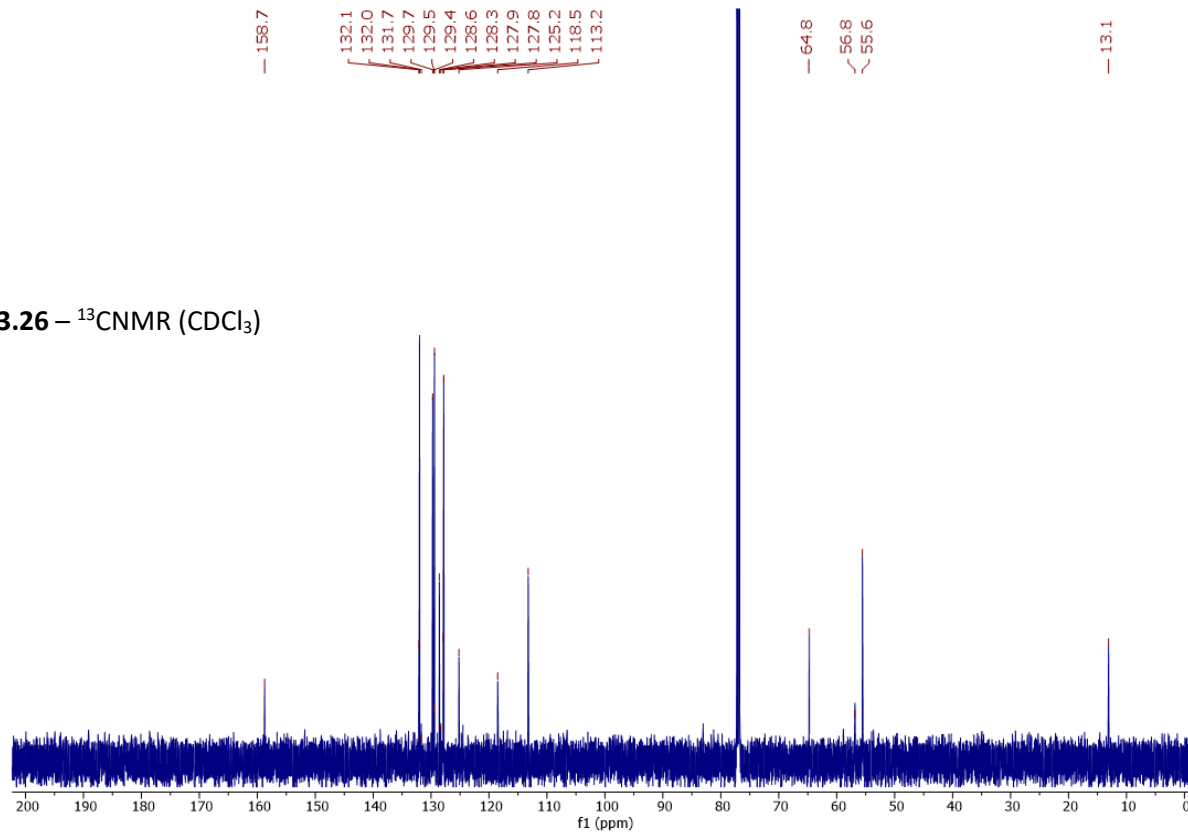
**Figure S1.** DFT geometry optimizations of *trans* and *cis* diastereomers of **3.20**. Dihedral angles of highlighted protons are consistent with their Karplus coupling values.

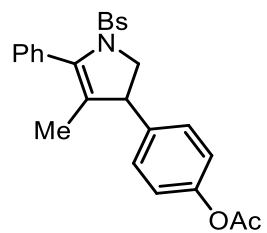


3.26 –  $^1\text{H}$ NMR ( $\text{CDCl}_3$ )

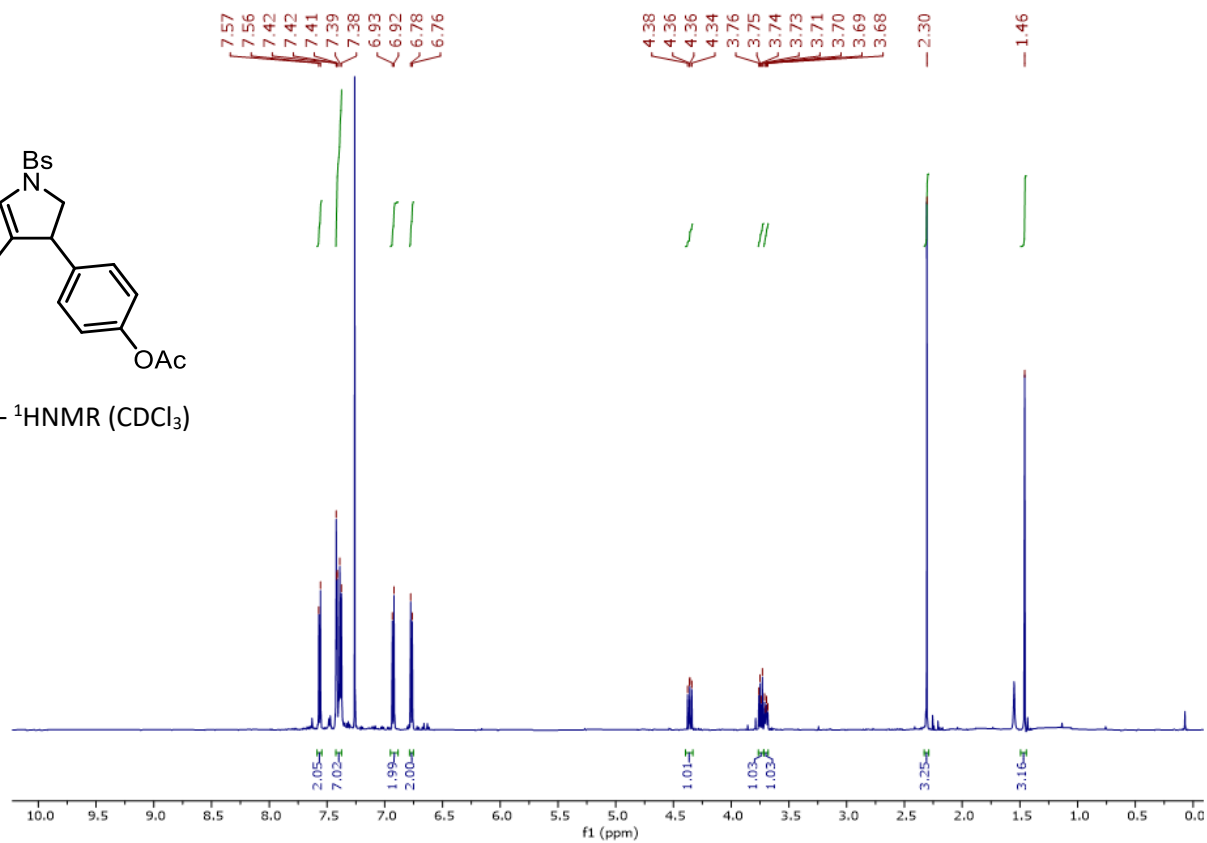


3.26 –  $^{13}\text{C}$ NMR ( $\text{CDCl}_3$ )

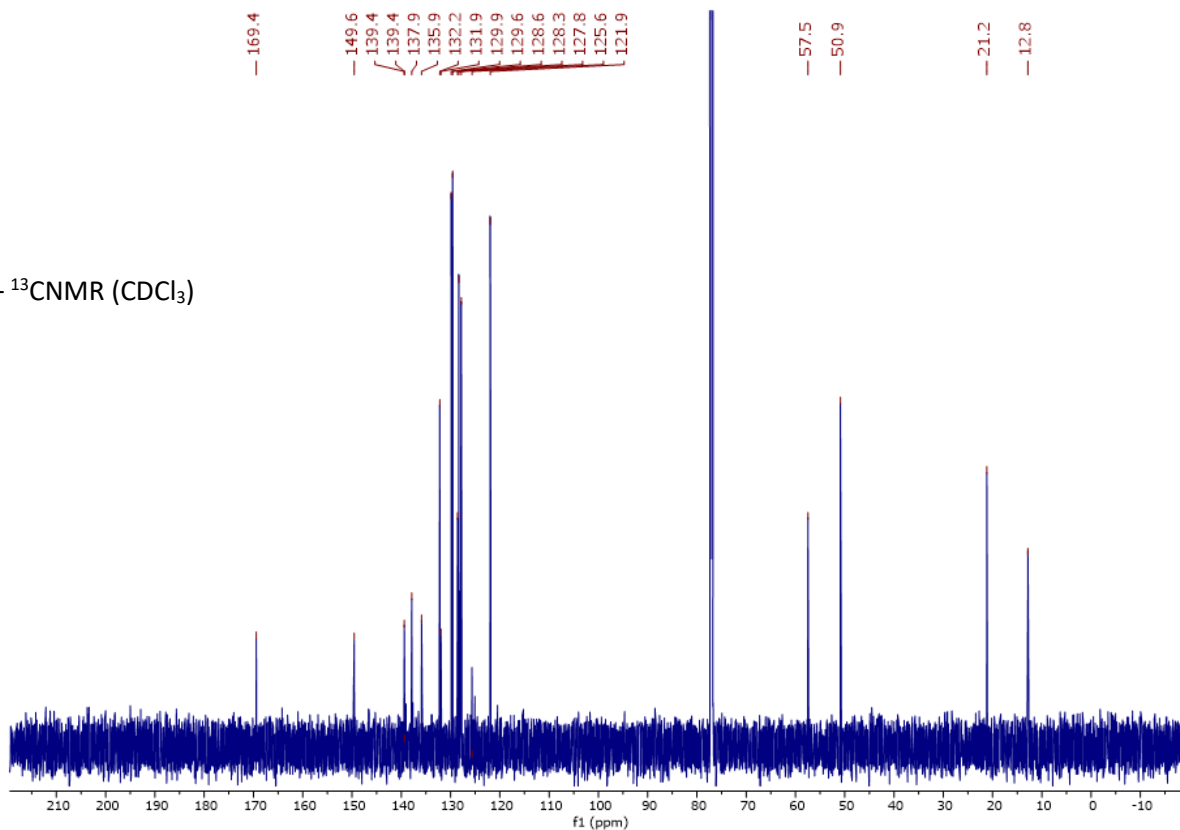


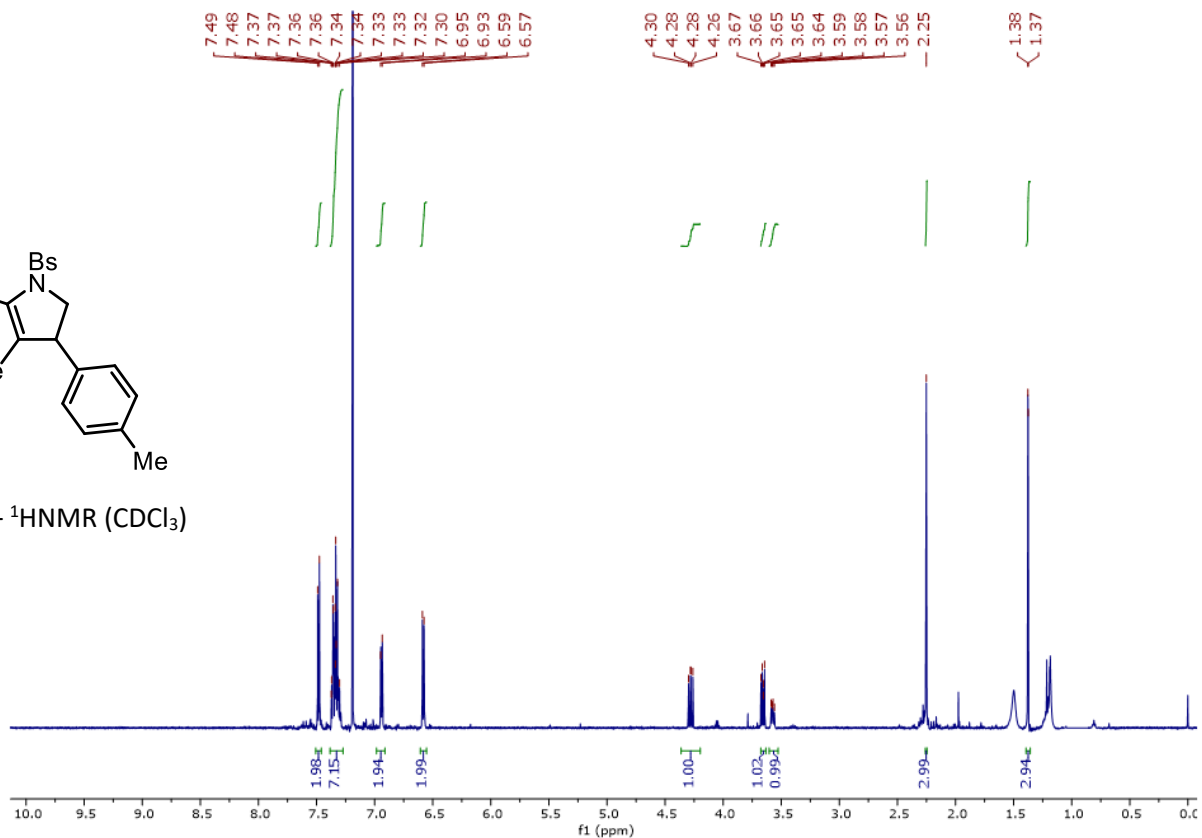
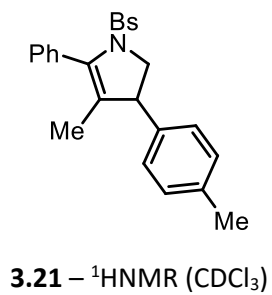


3.25 –  $^1\text{H}$ NMR ( $\text{CDCl}_3$ )

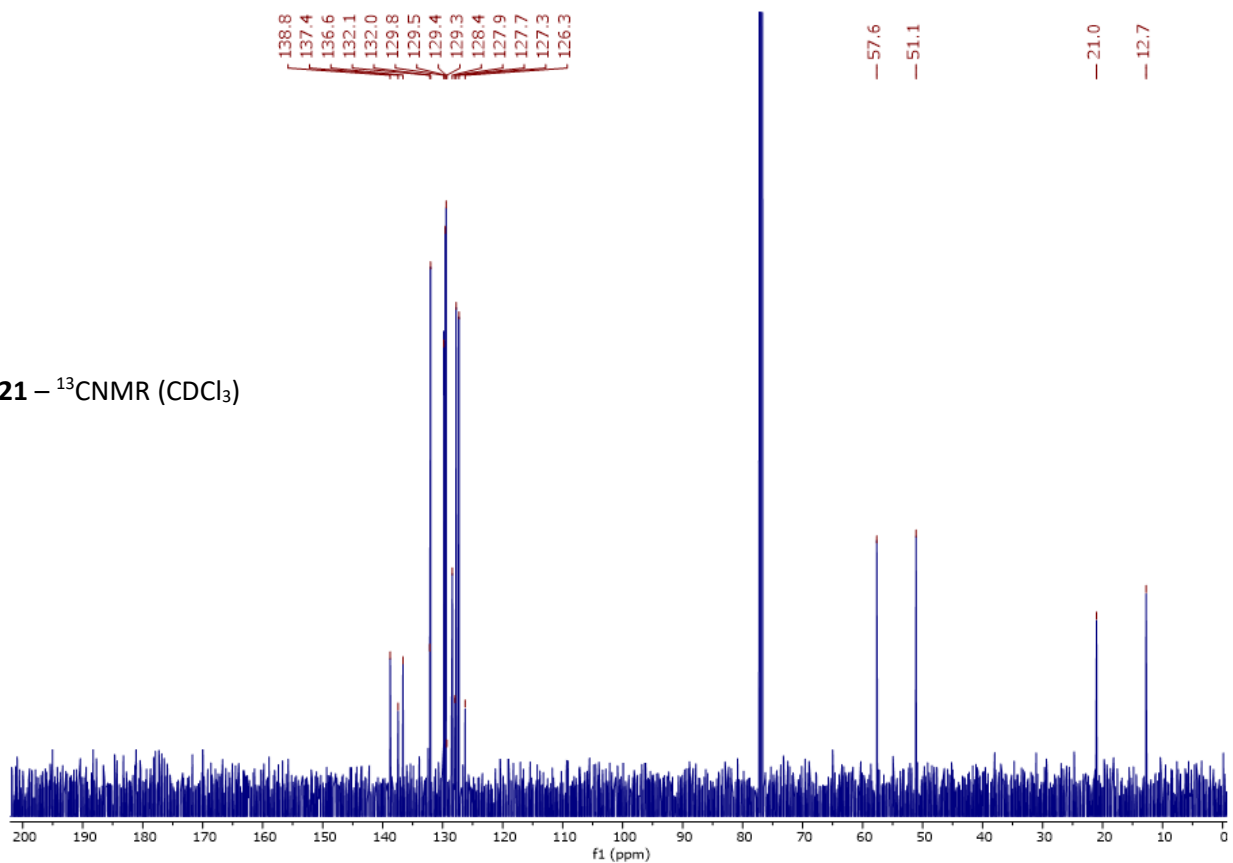


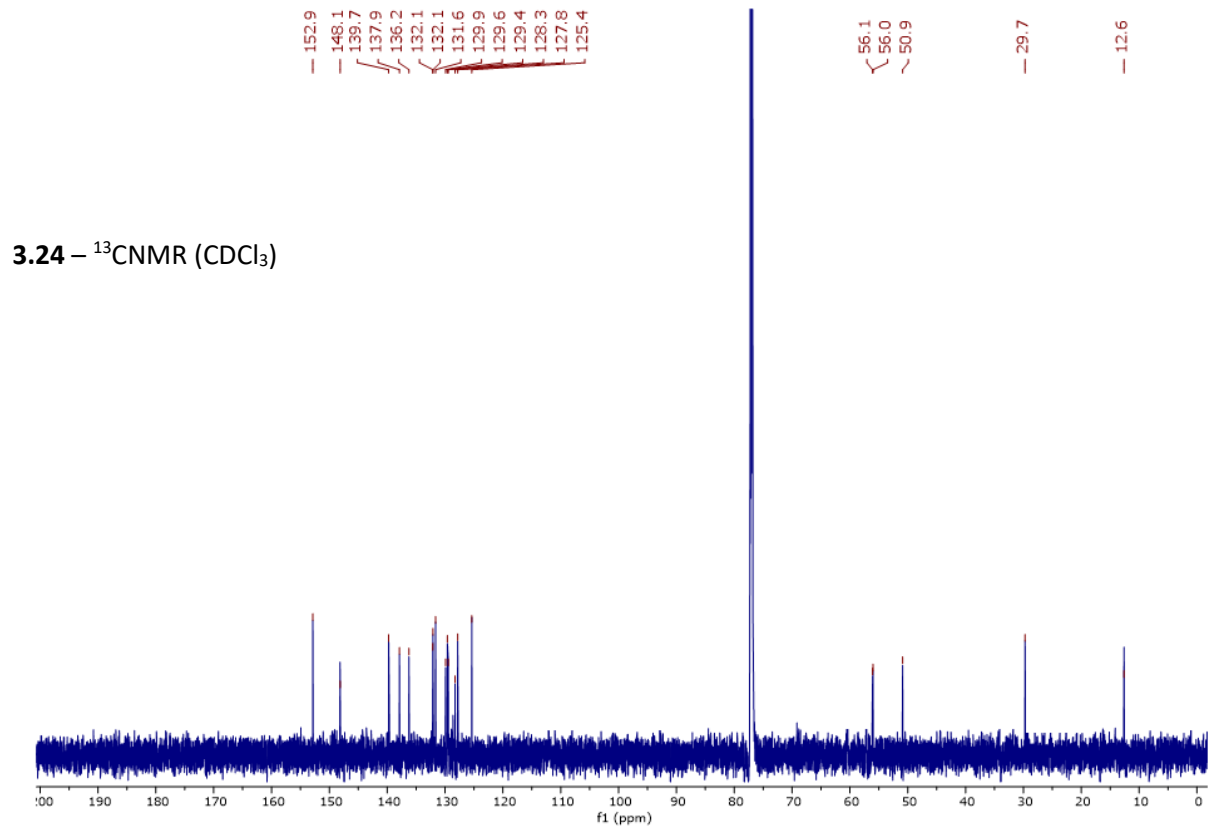
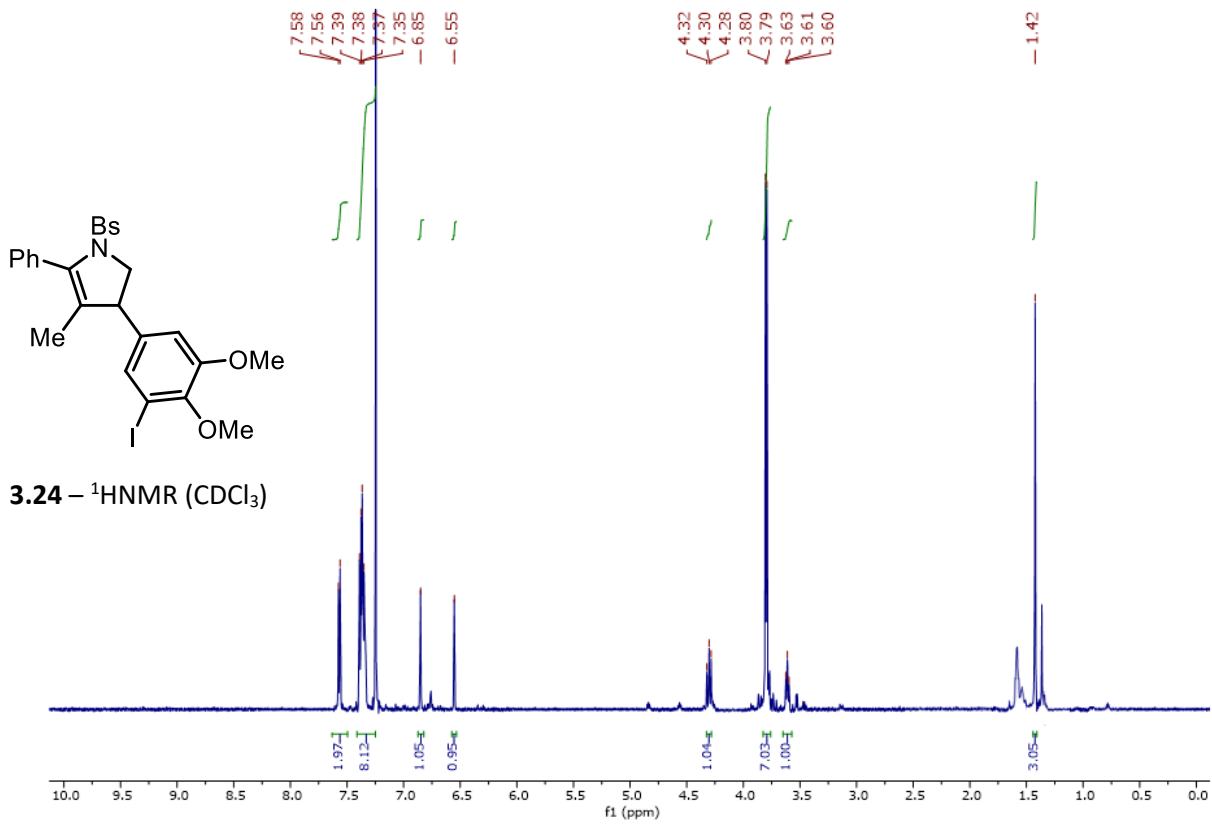
3.25 –  $^{13}\text{C}$ NMR ( $\text{CDCl}_3$ )

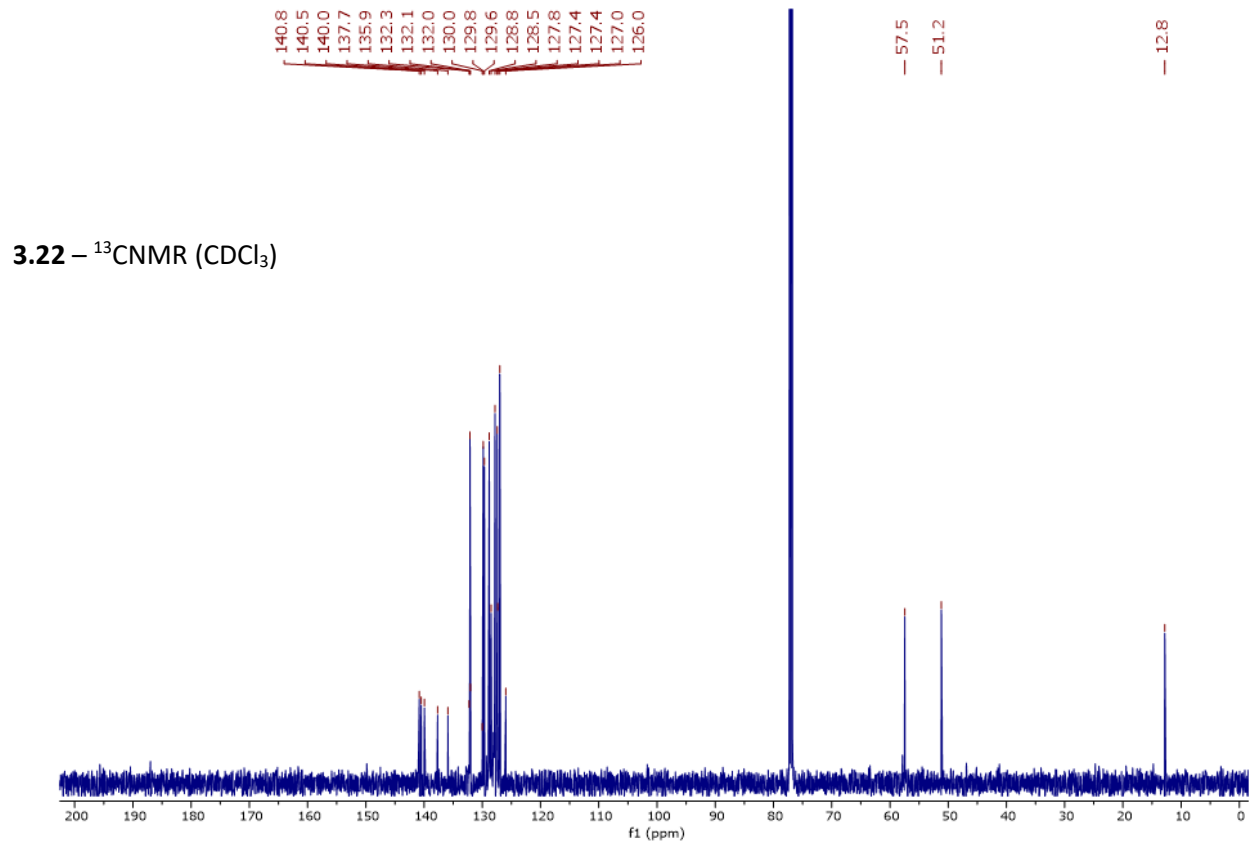
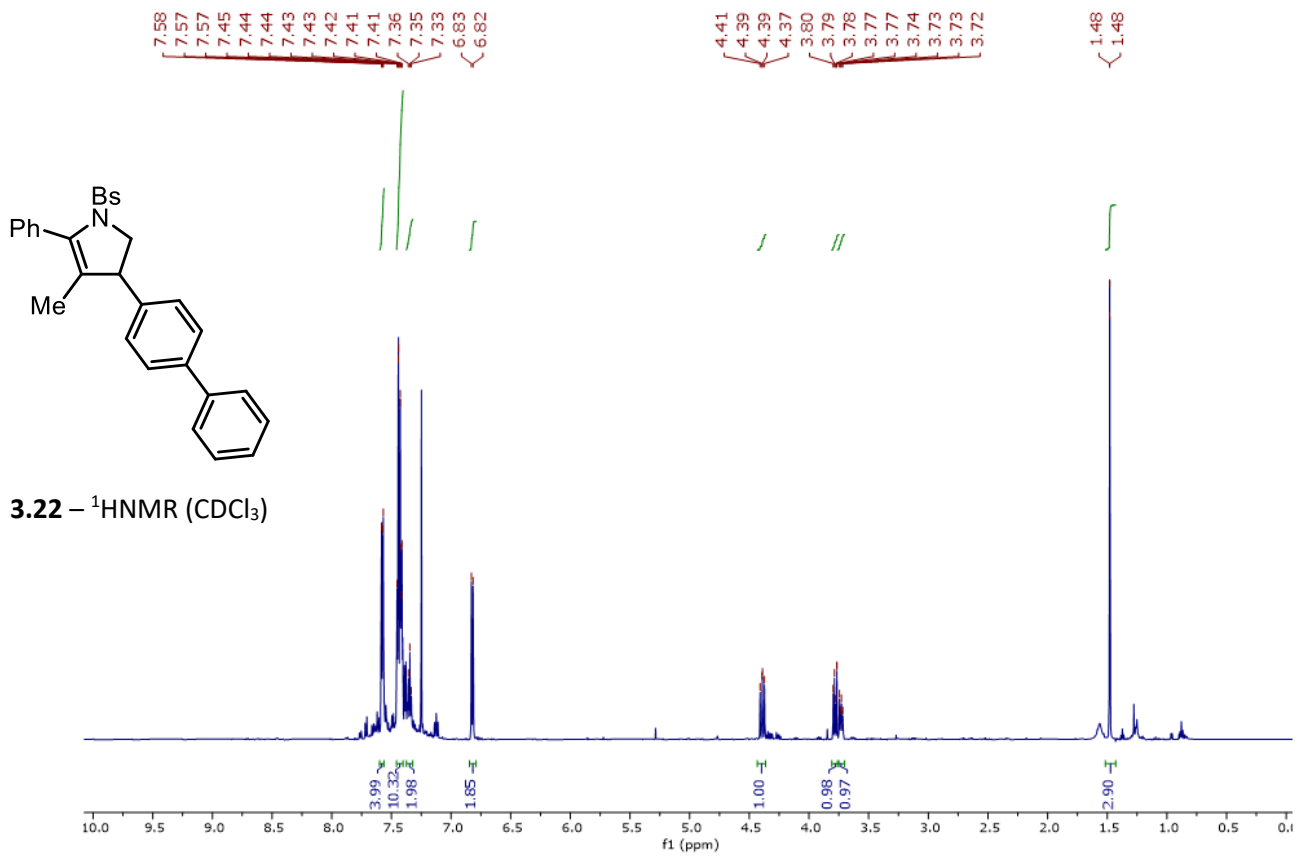


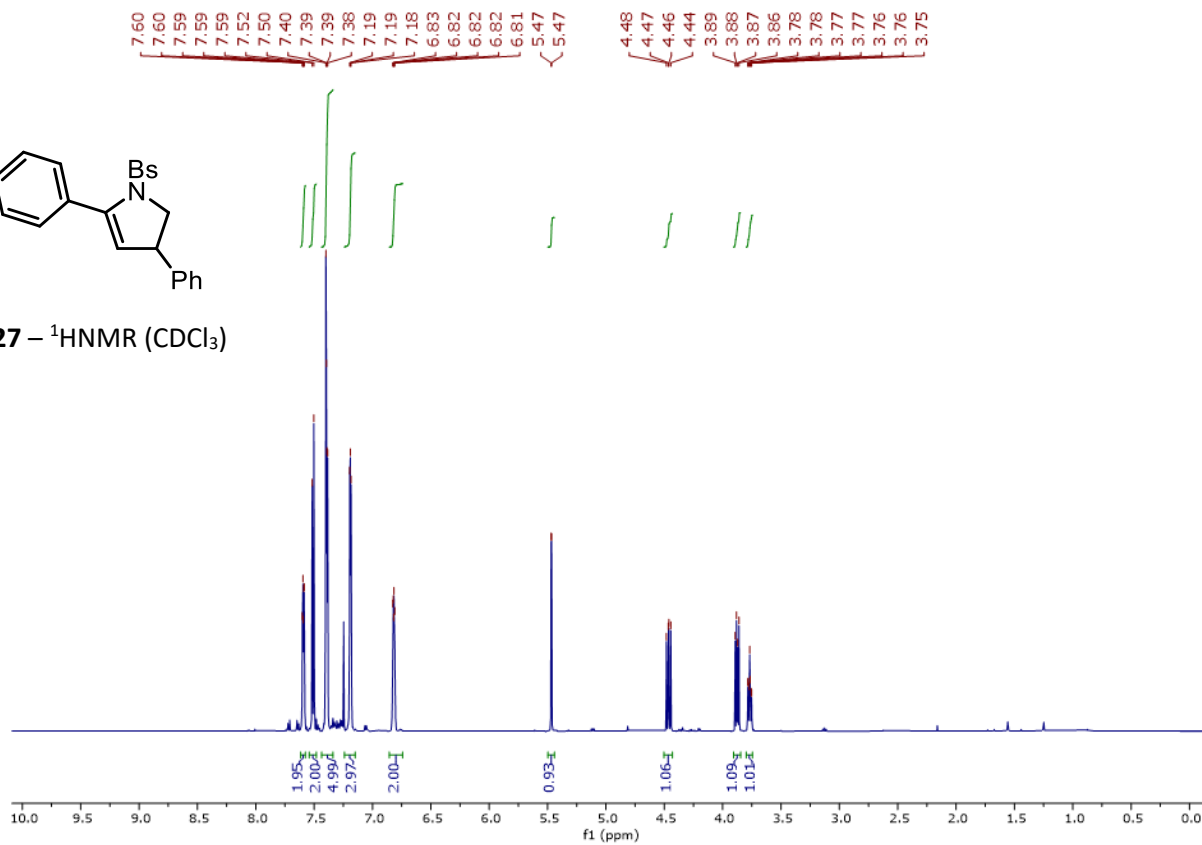
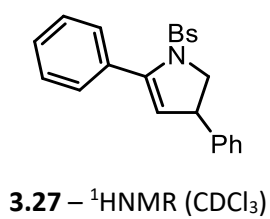


**3.21** –  $^{13}\text{C}$ NMR ( $\text{CDCl}_3$ )

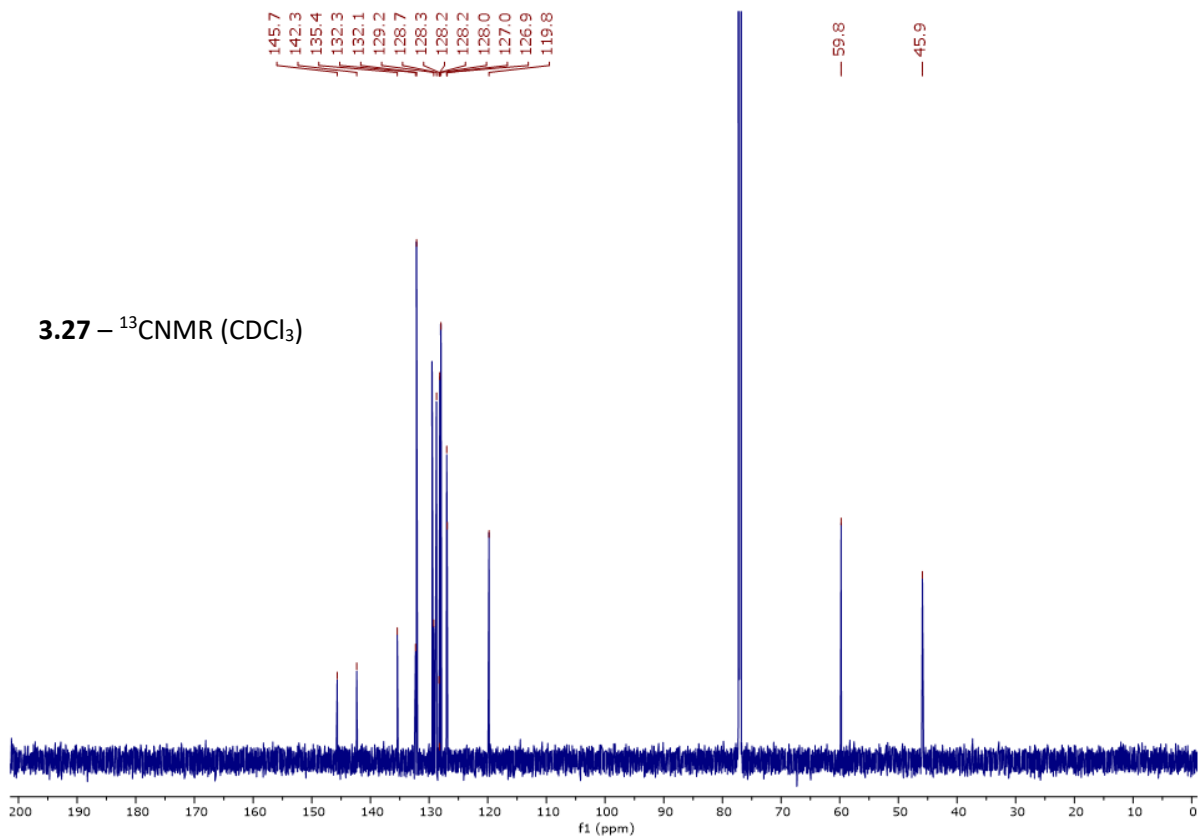


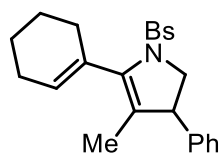




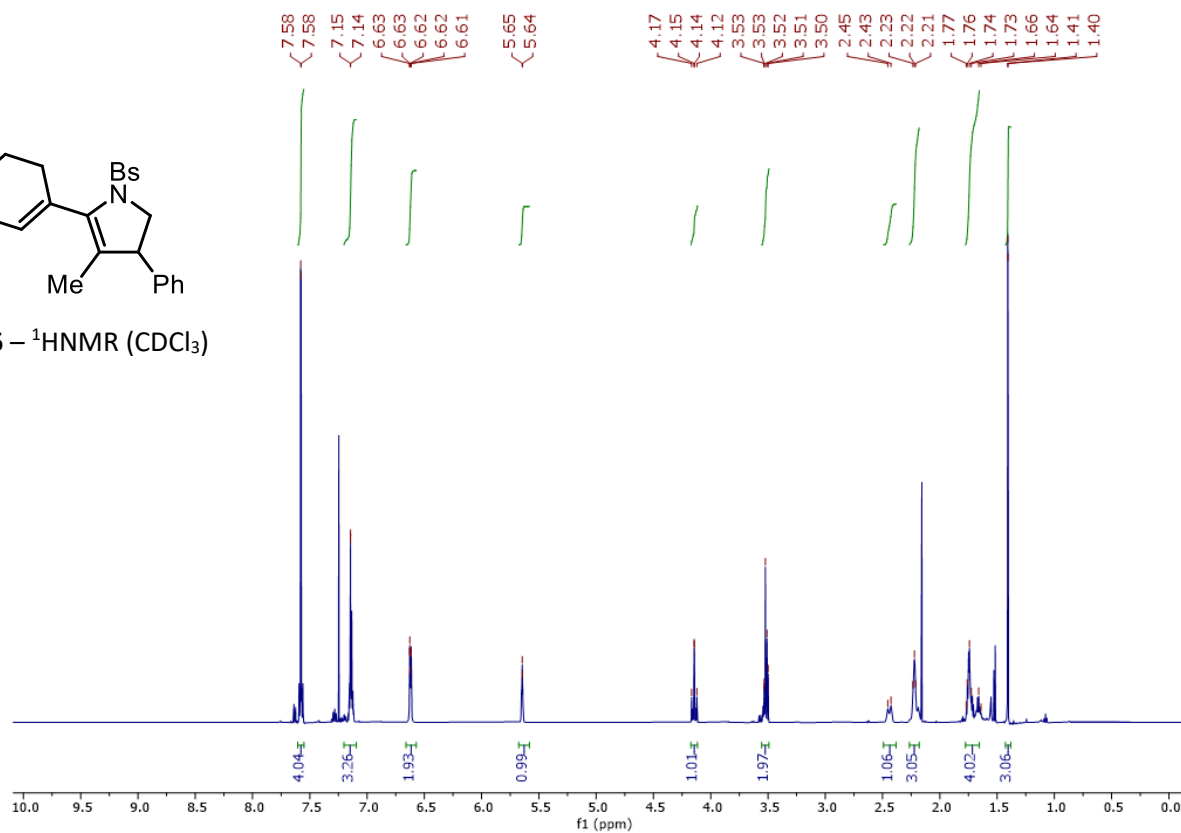


3.27 – <sup>13</sup>CNMR (CDCl<sub>3</sub>)

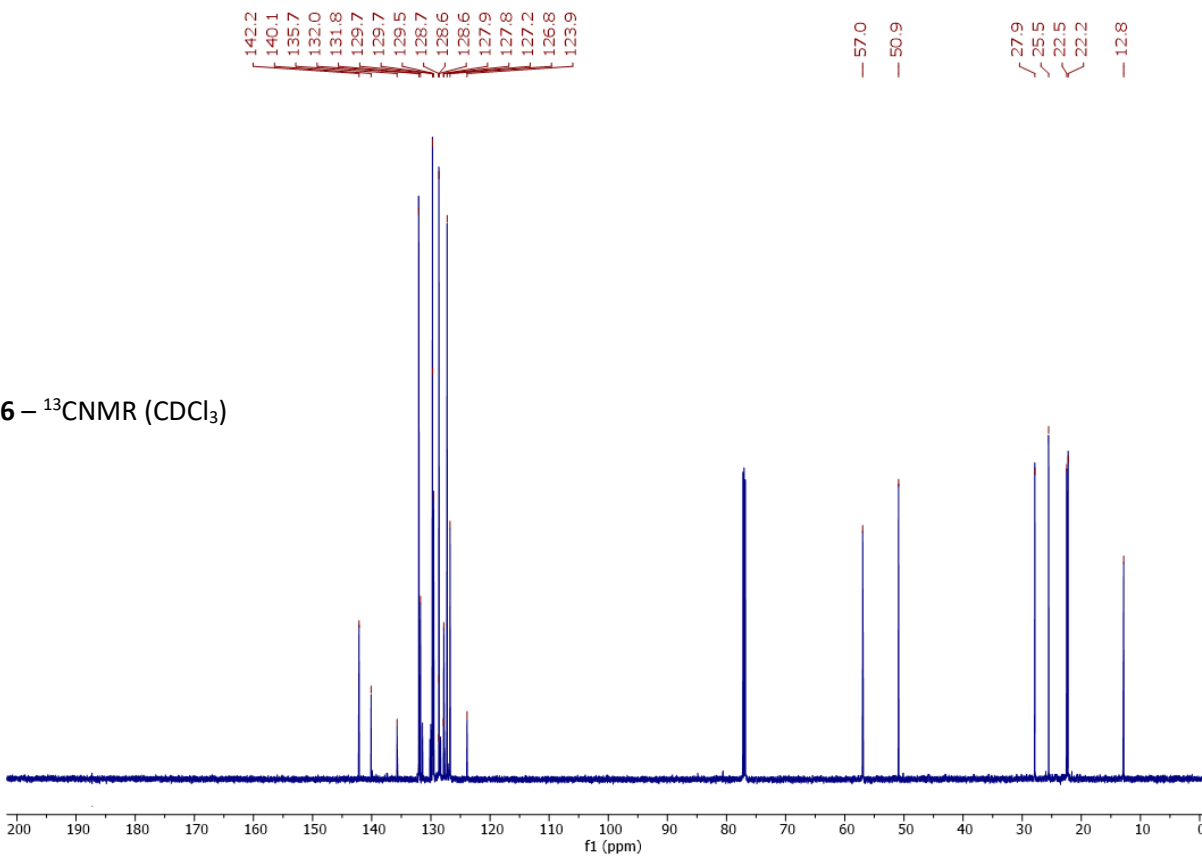


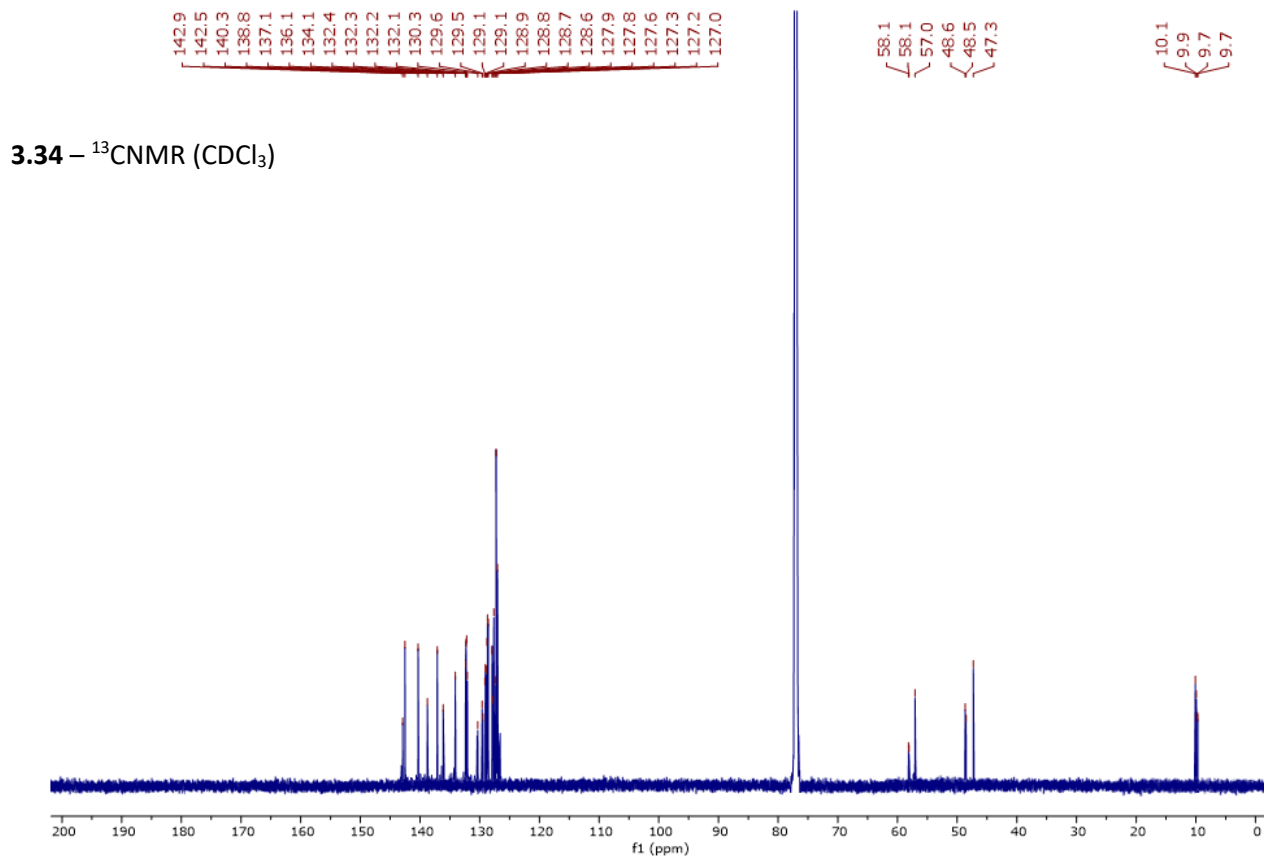
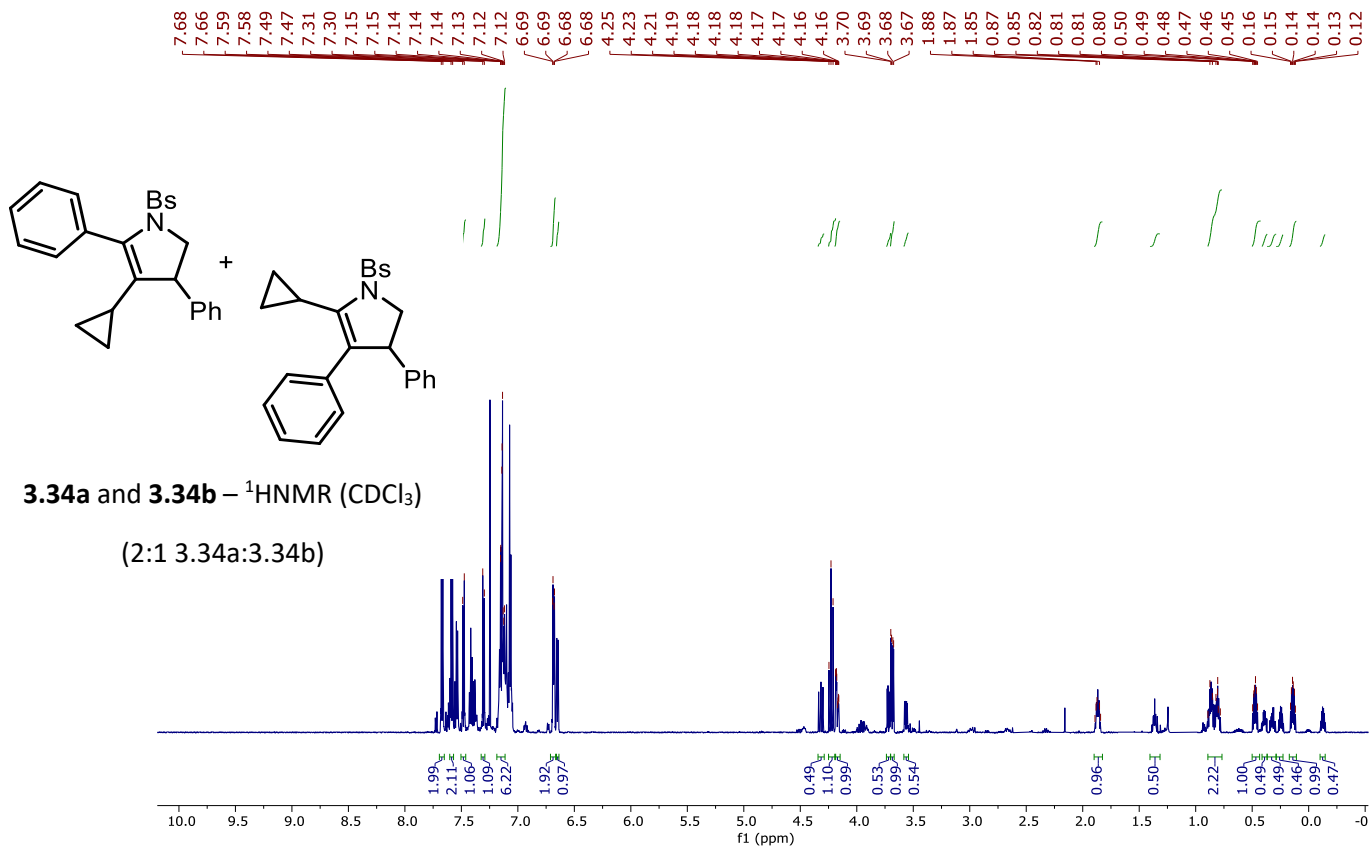


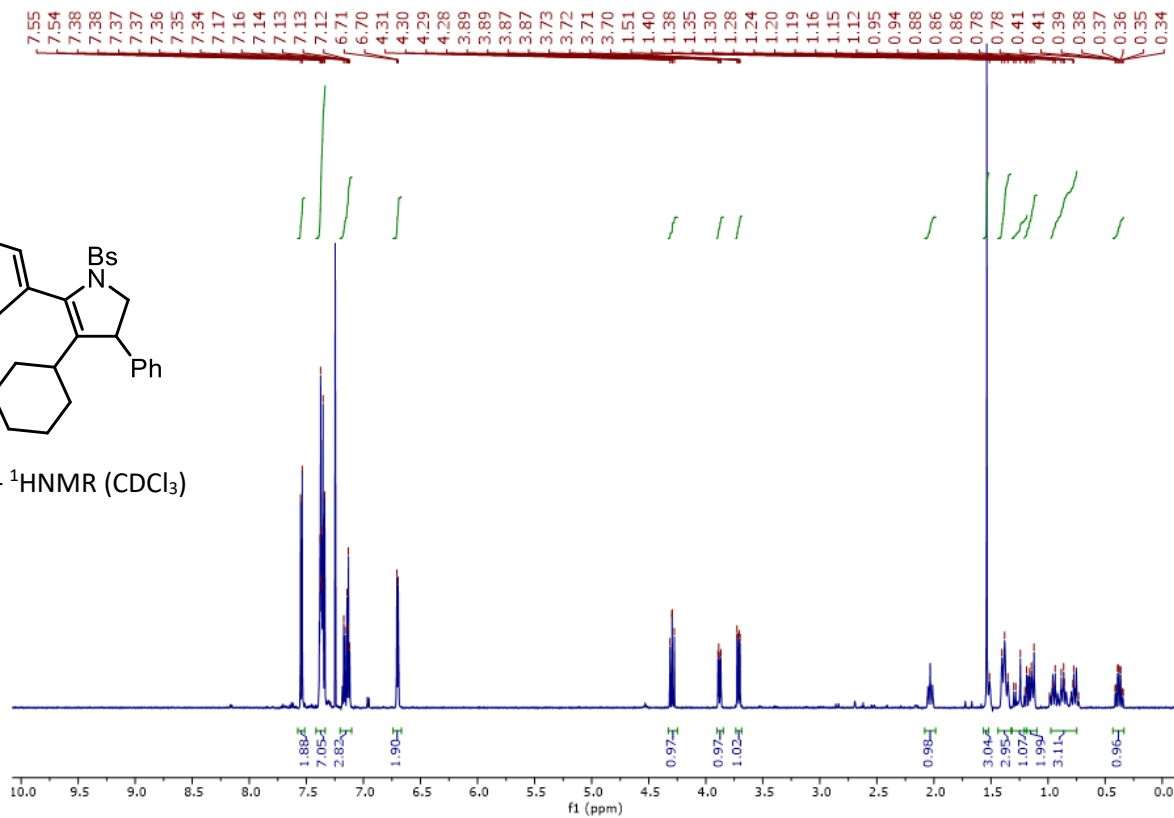
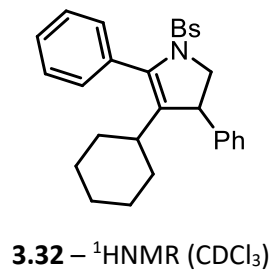
3.36 –  $^1\text{H}$ NMR ( $\text{CDCl}_3$ )



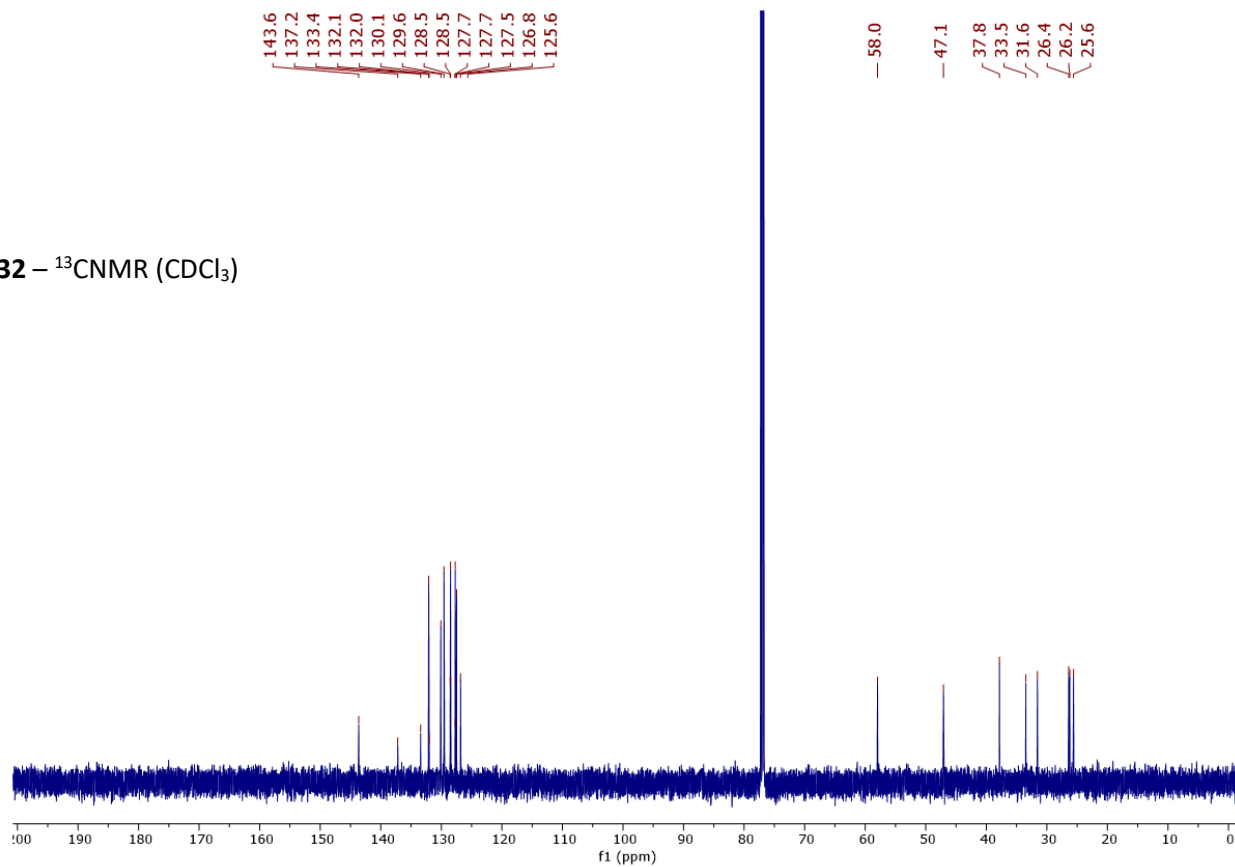
3.36 –  $^{13}\text{C}$ NMR ( $\text{CDCl}_3$ )

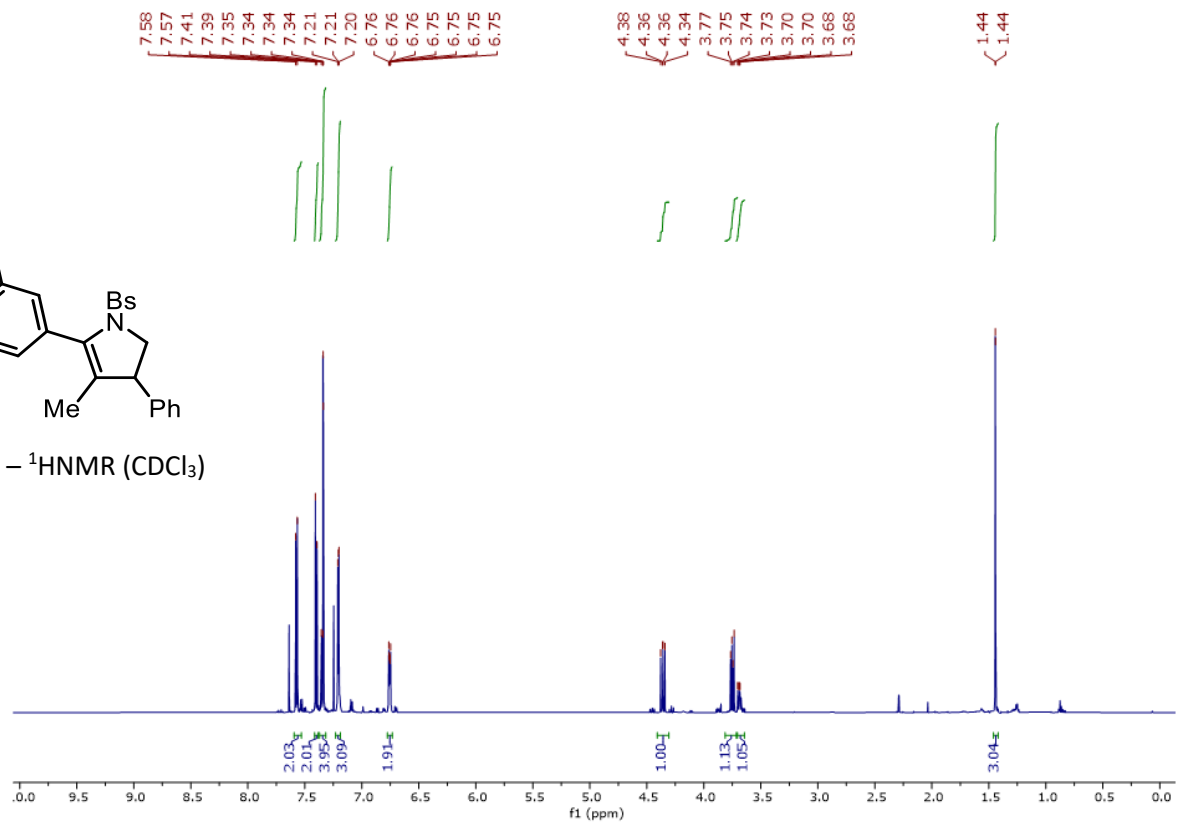
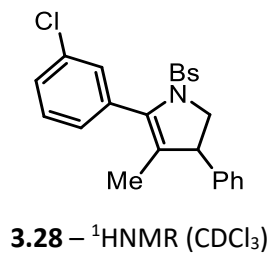




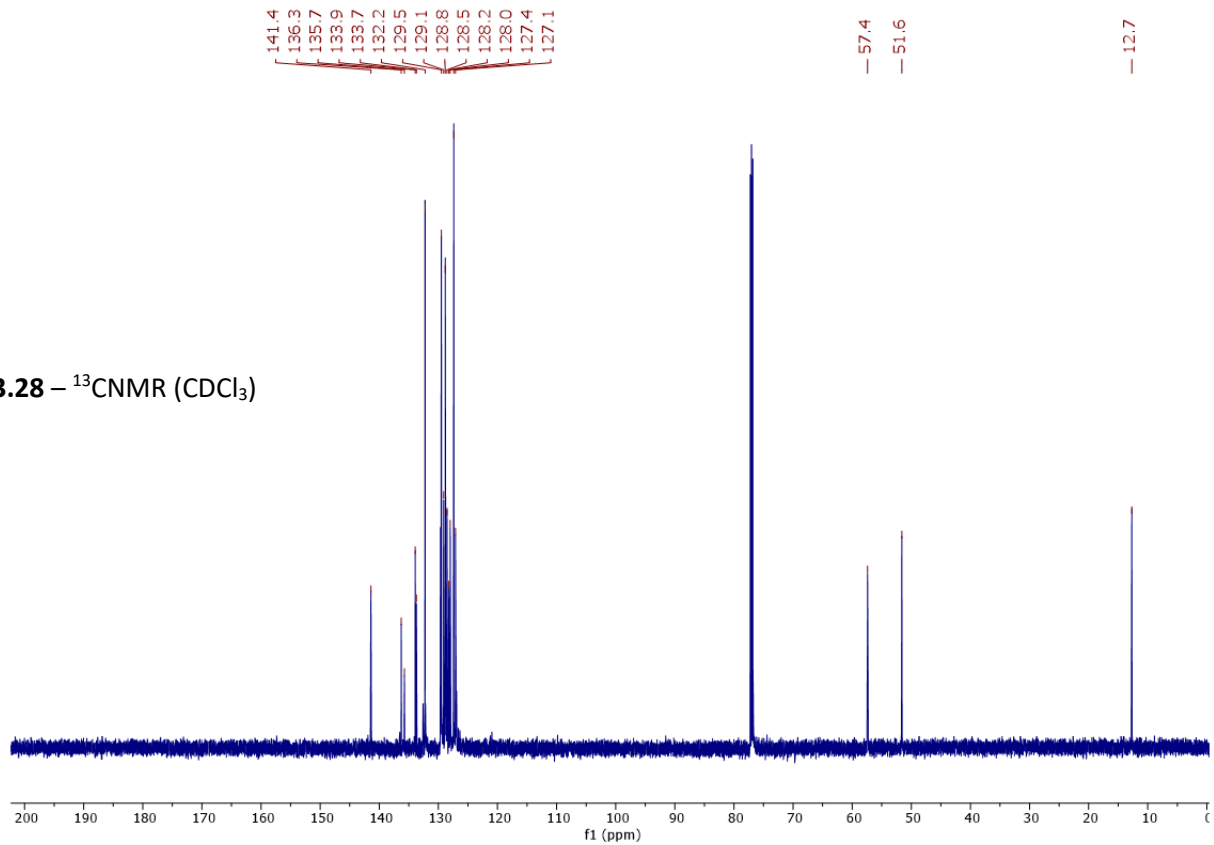


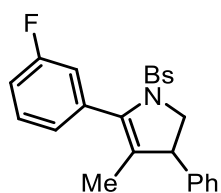
3.32 – <sup>13</sup>CNMR (CDCl<sub>3</sub>)



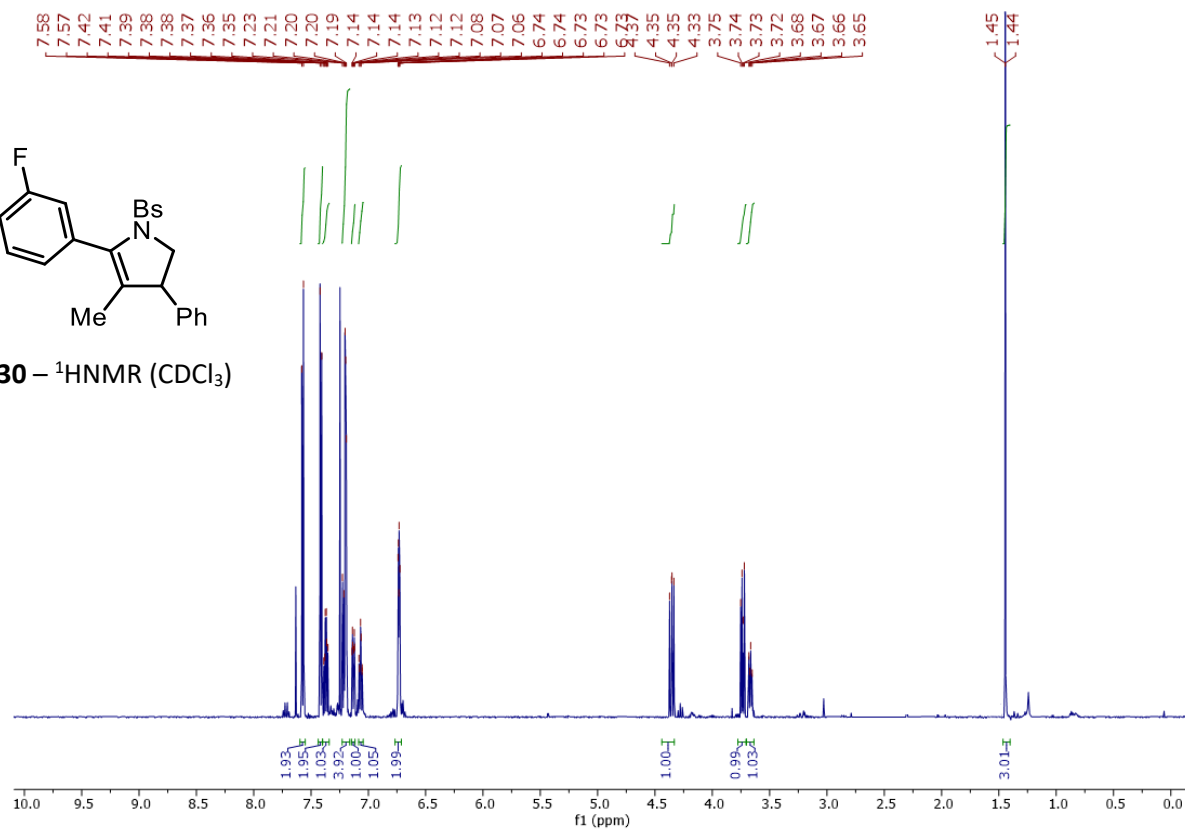


**3.28** –  $^{13}\text{C}$ NMR ( $\text{CDCl}_3$ )

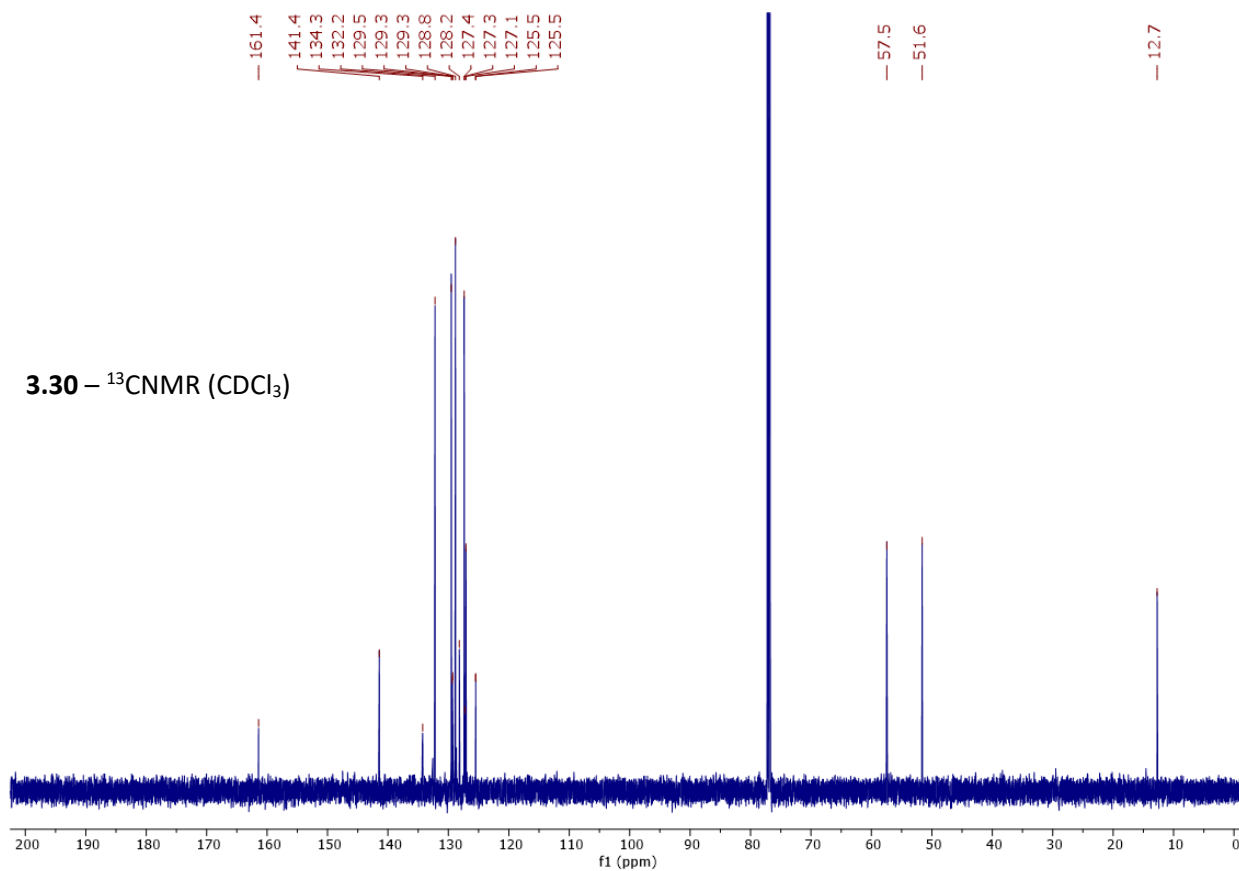


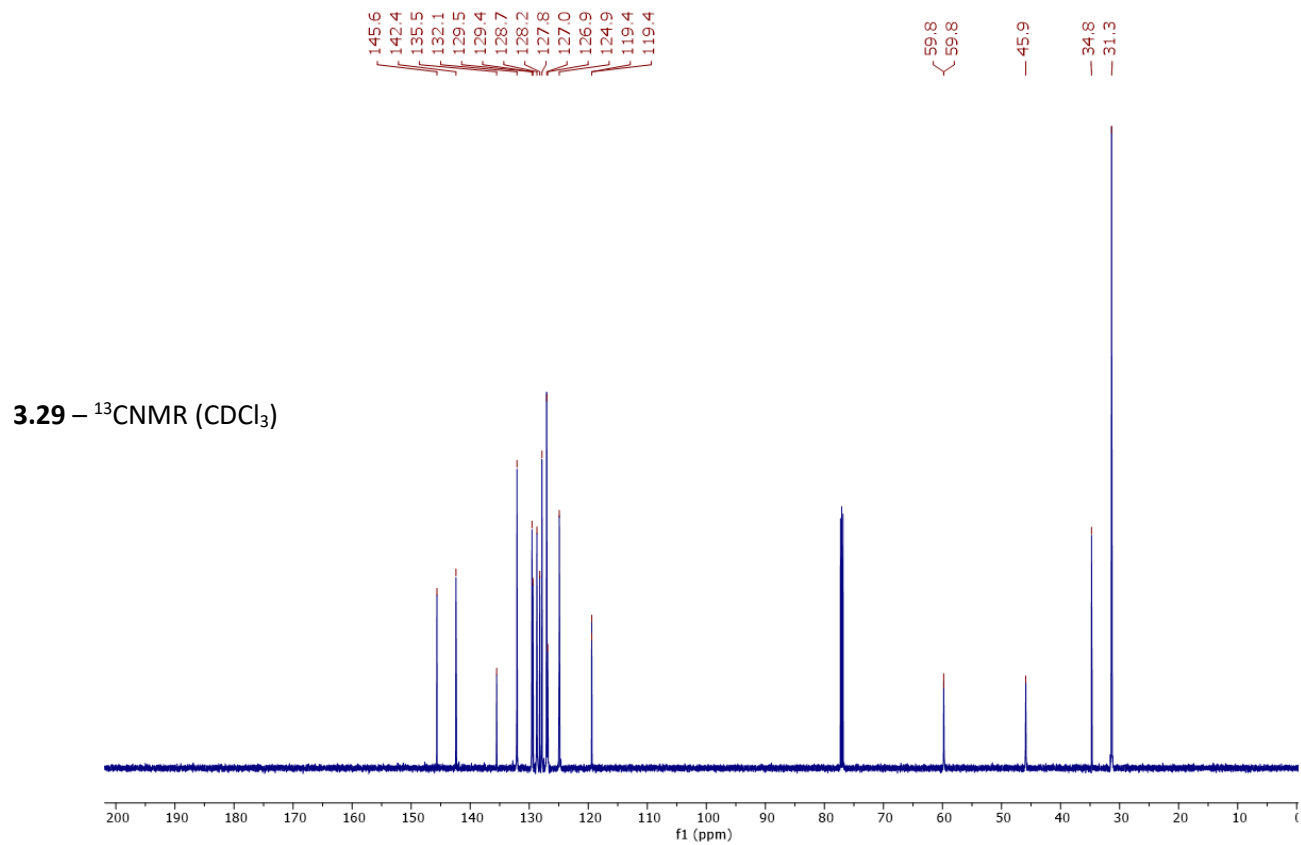
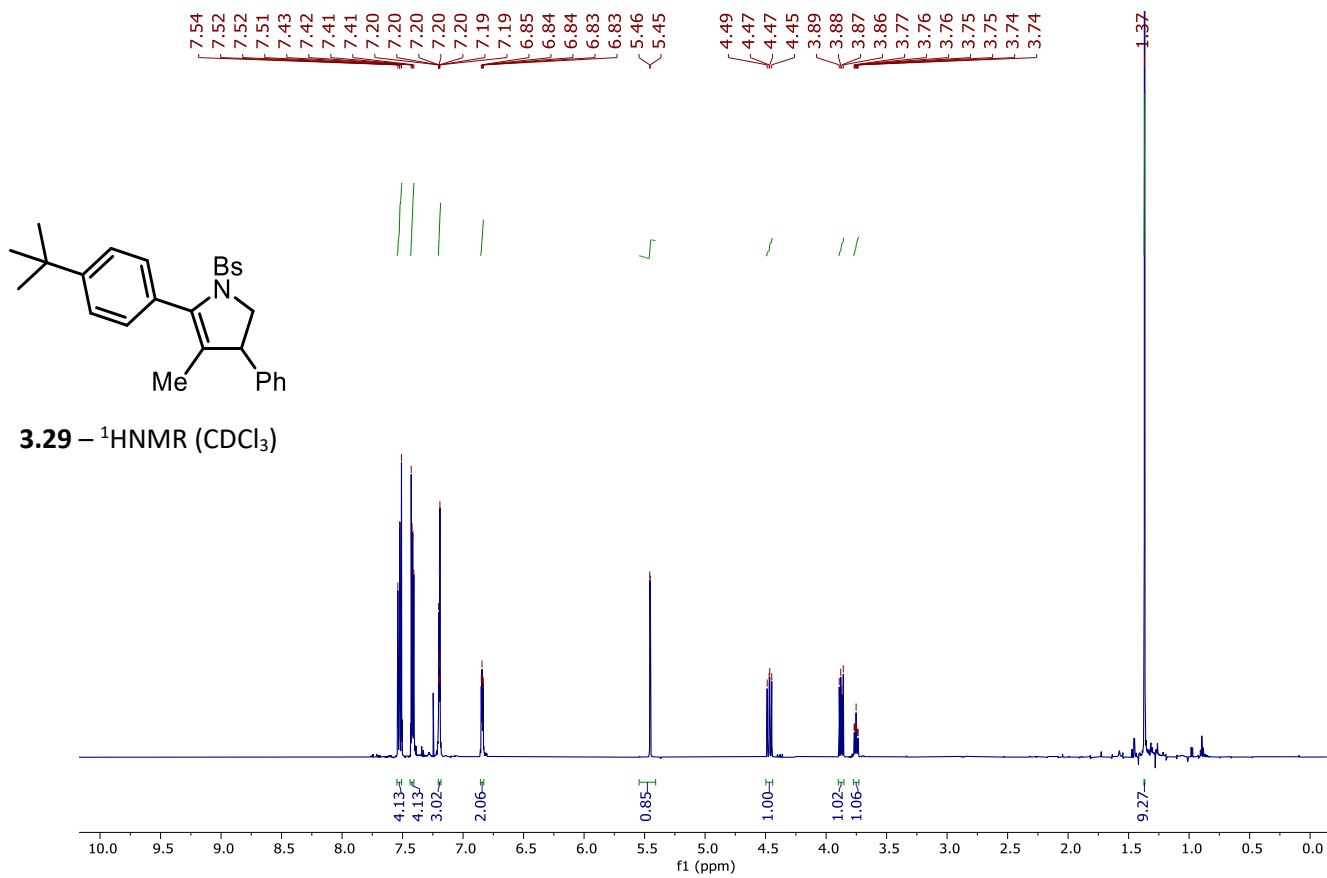


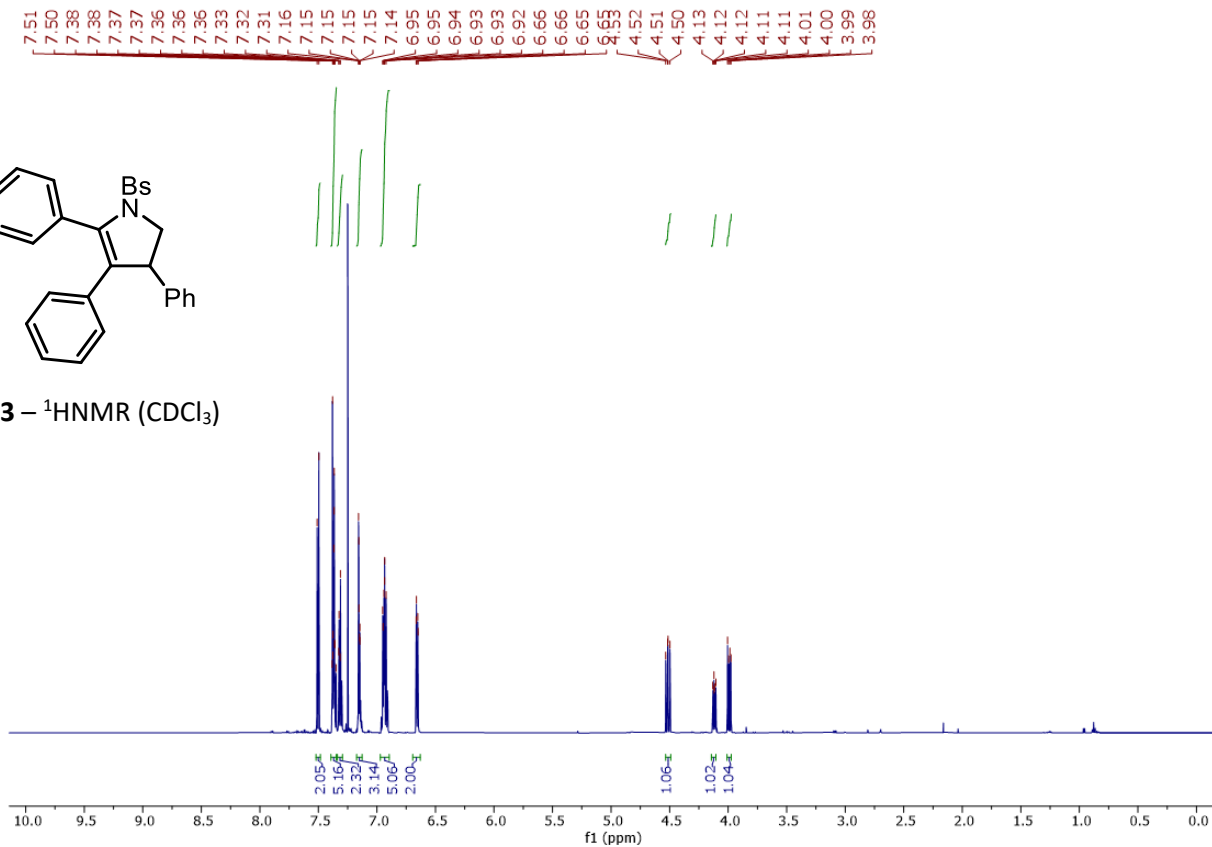
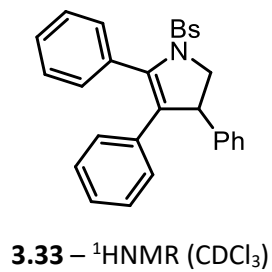
3.30 –  $^1\text{H}$ NMR ( $\text{CDCl}_3$ )



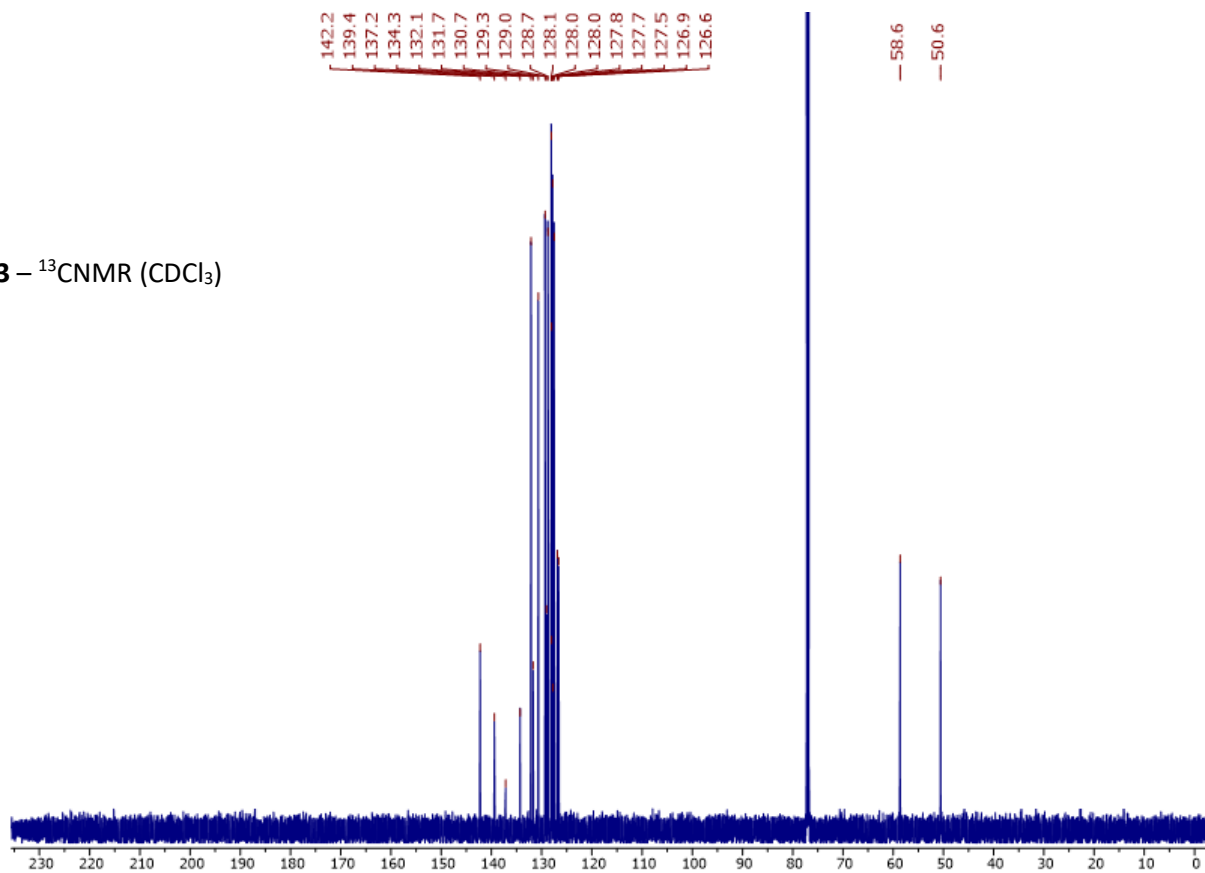
3.30 –  $^{13}\text{C}$ NMR ( $\text{CDCl}_3$ )

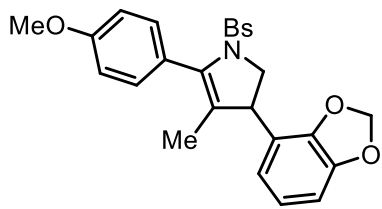




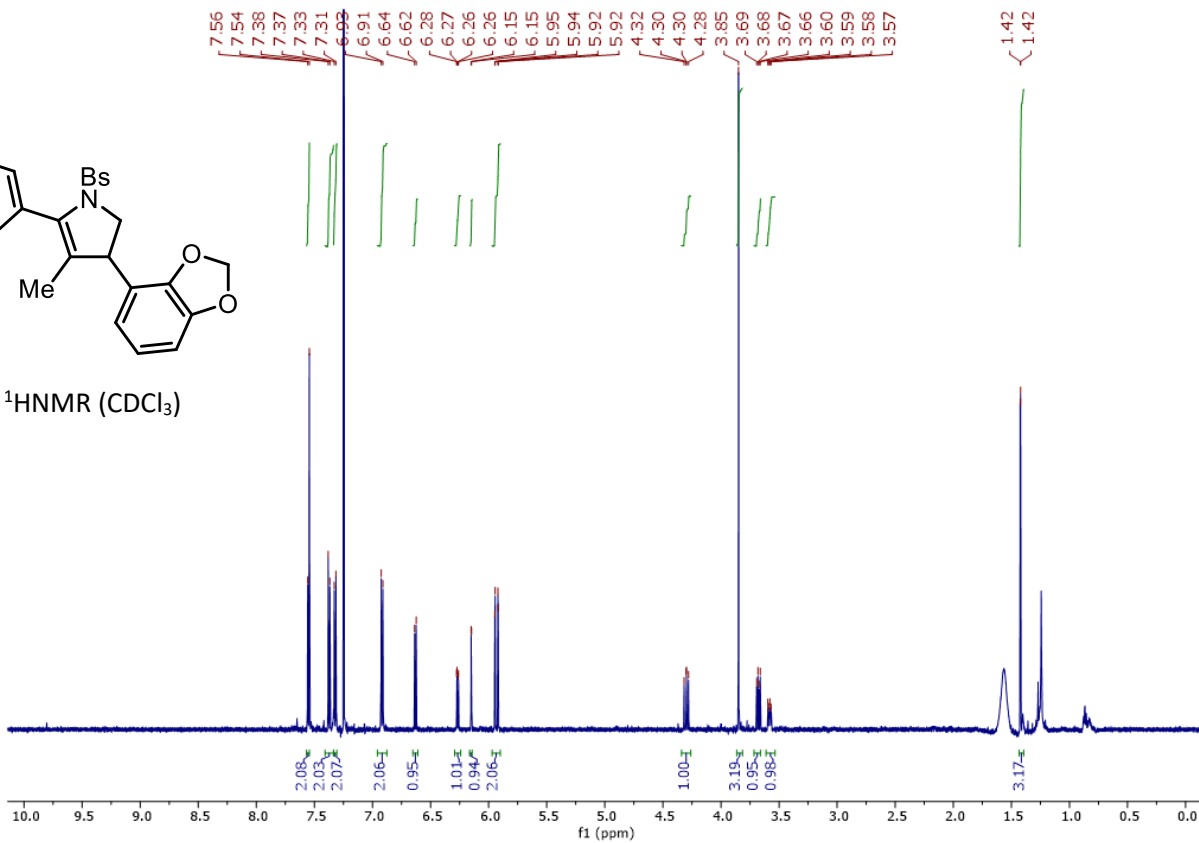


**3.33** –  $^{13}\text{C}$ NMR ( $\text{CDCl}_3$ )

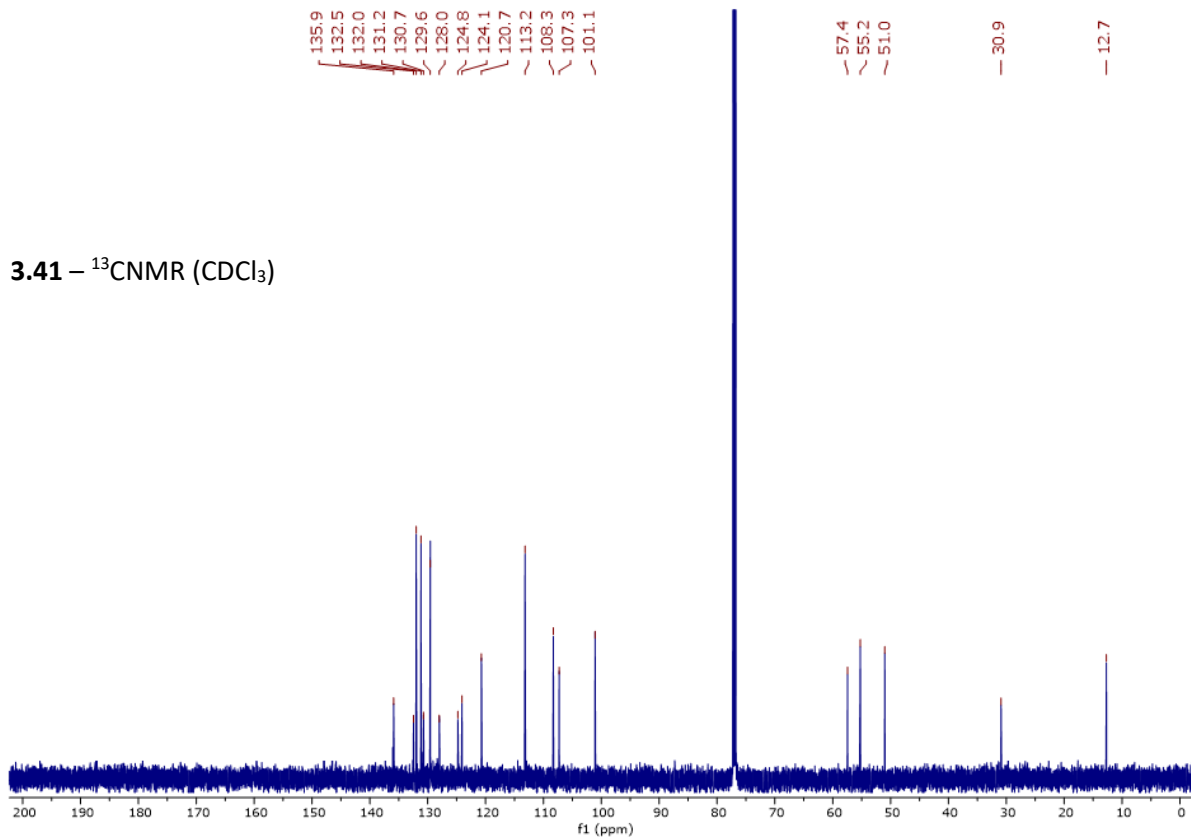


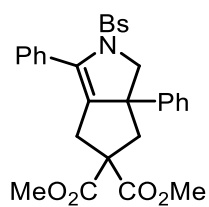


3.41 –  $^1\text{H}$ NMR ( $\text{CDCl}_3$ )

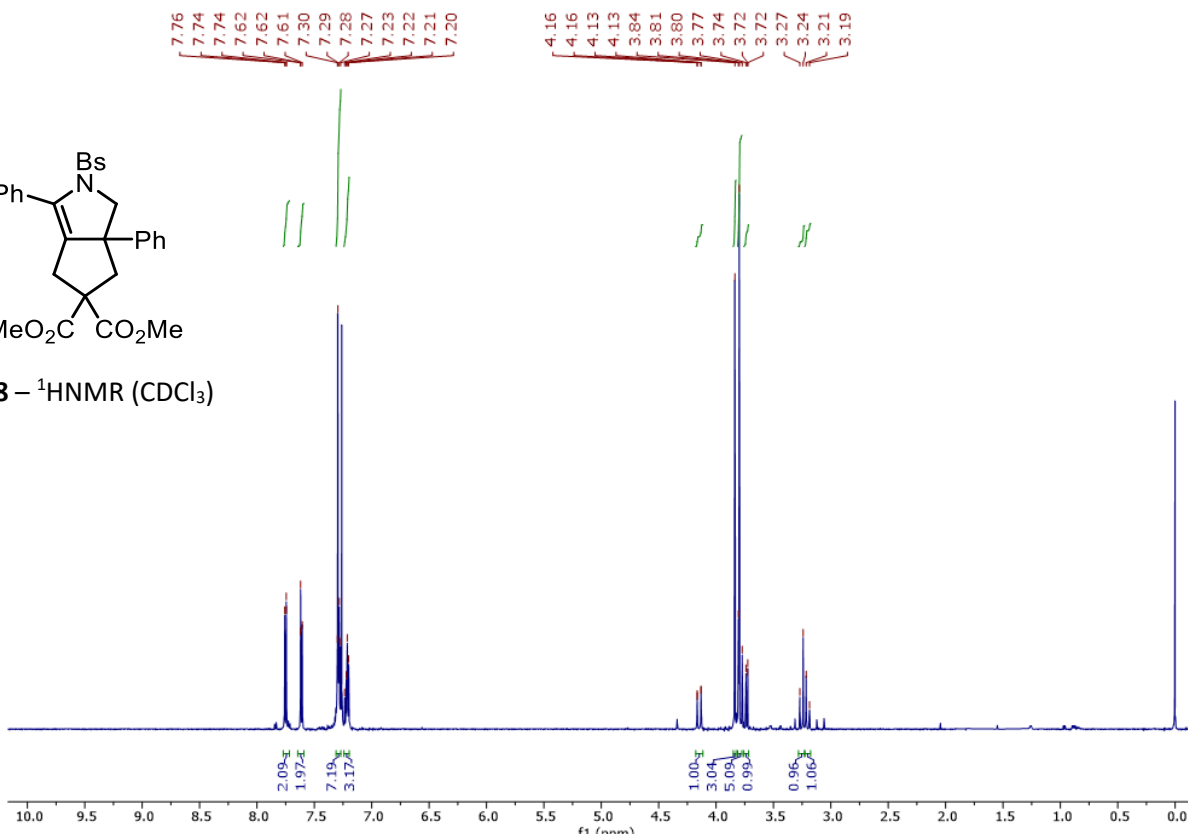


3.41 –  $^{13}\text{C}$ NMR ( $\text{CDCl}_3$ )

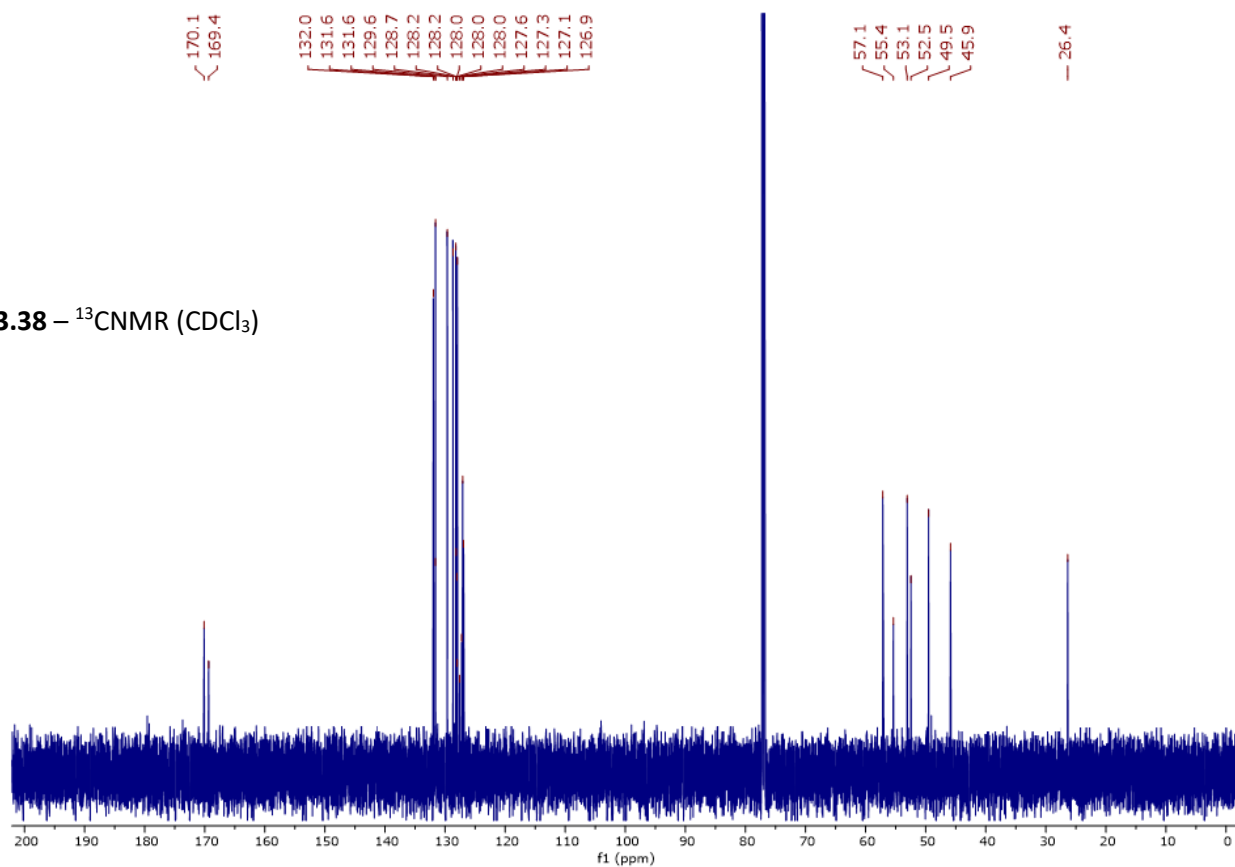


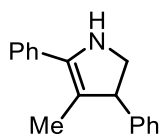


3.38 –  $^1\text{H}$ NMR ( $\text{CDCl}_3$ )

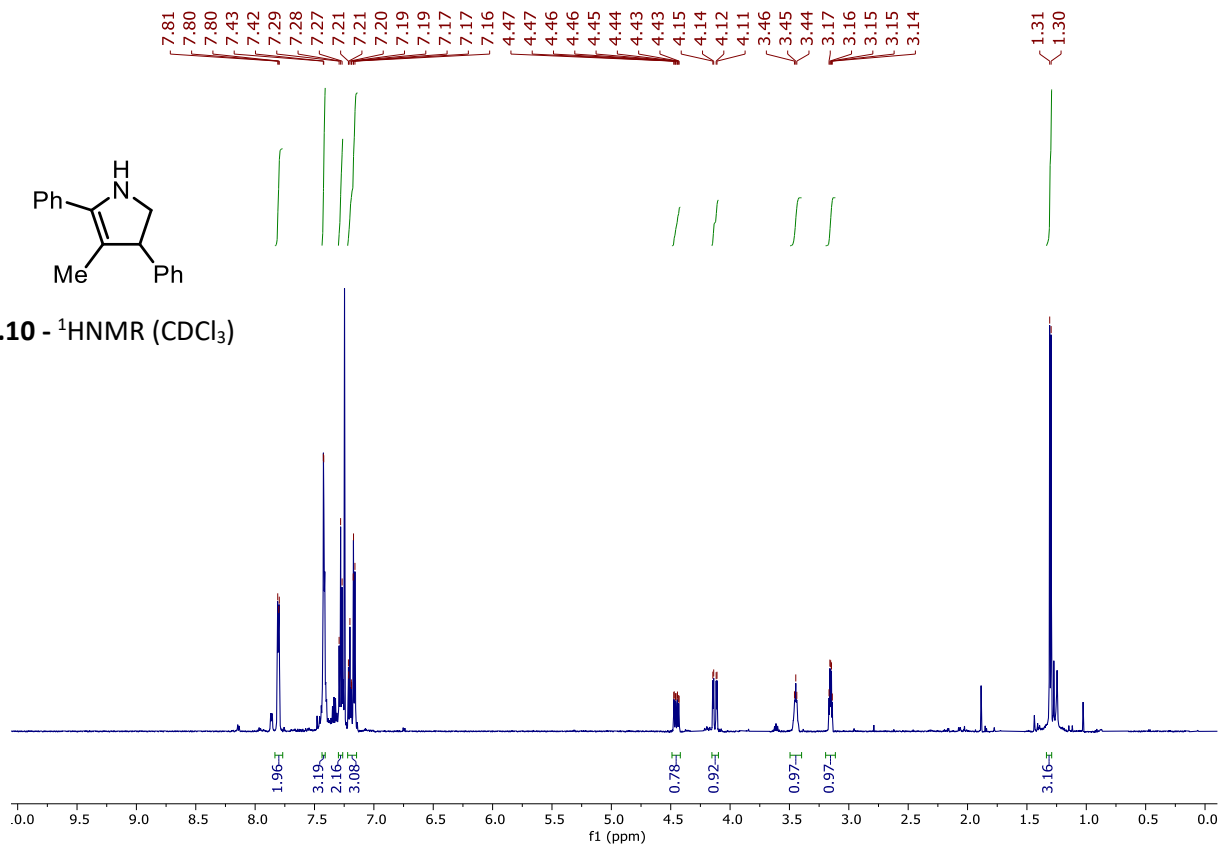


3.38 –  $^{13}\text{C}$ NMR ( $\text{CDCl}_3$ )

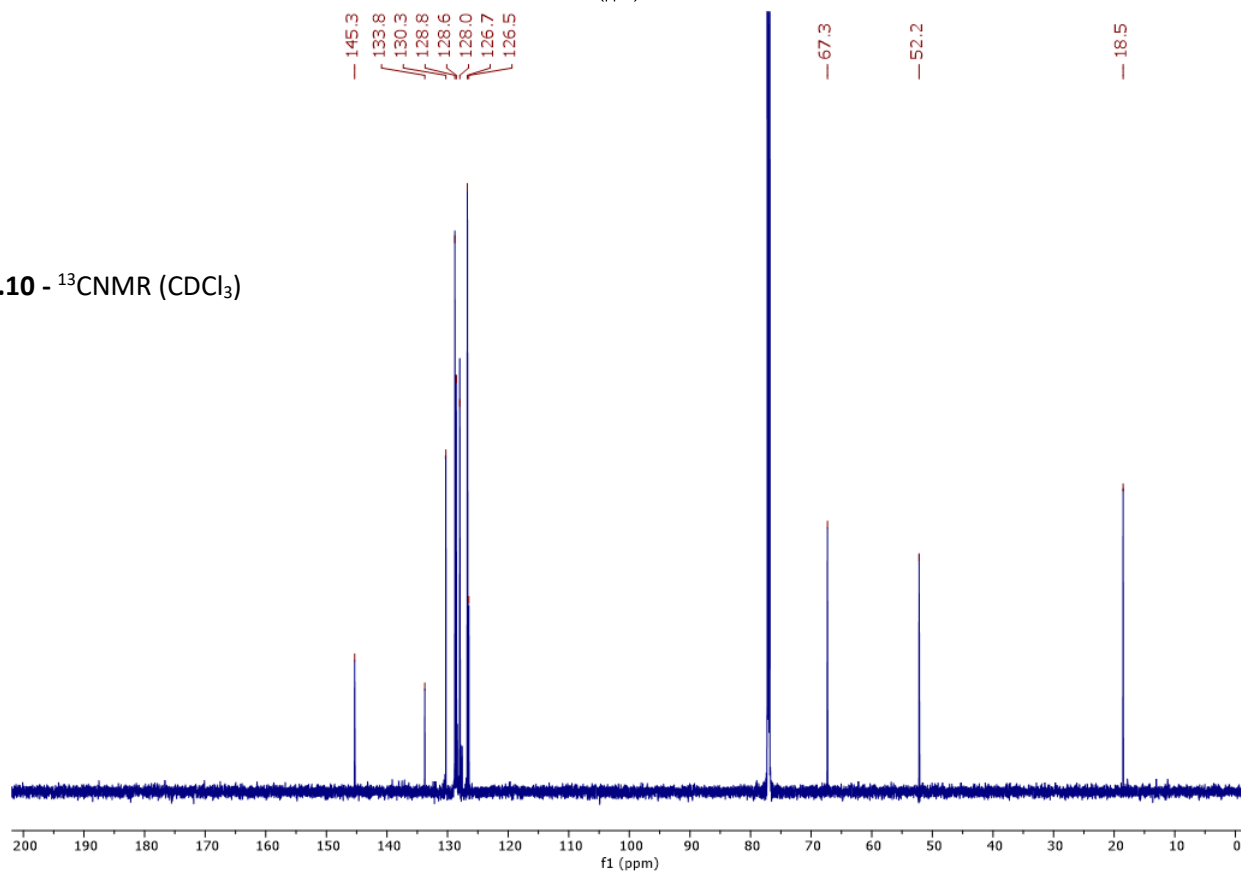


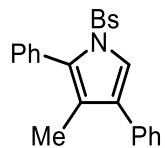


**B.10** -  $^1\text{H}$ NMR ( $\text{CDCl}_3$ )

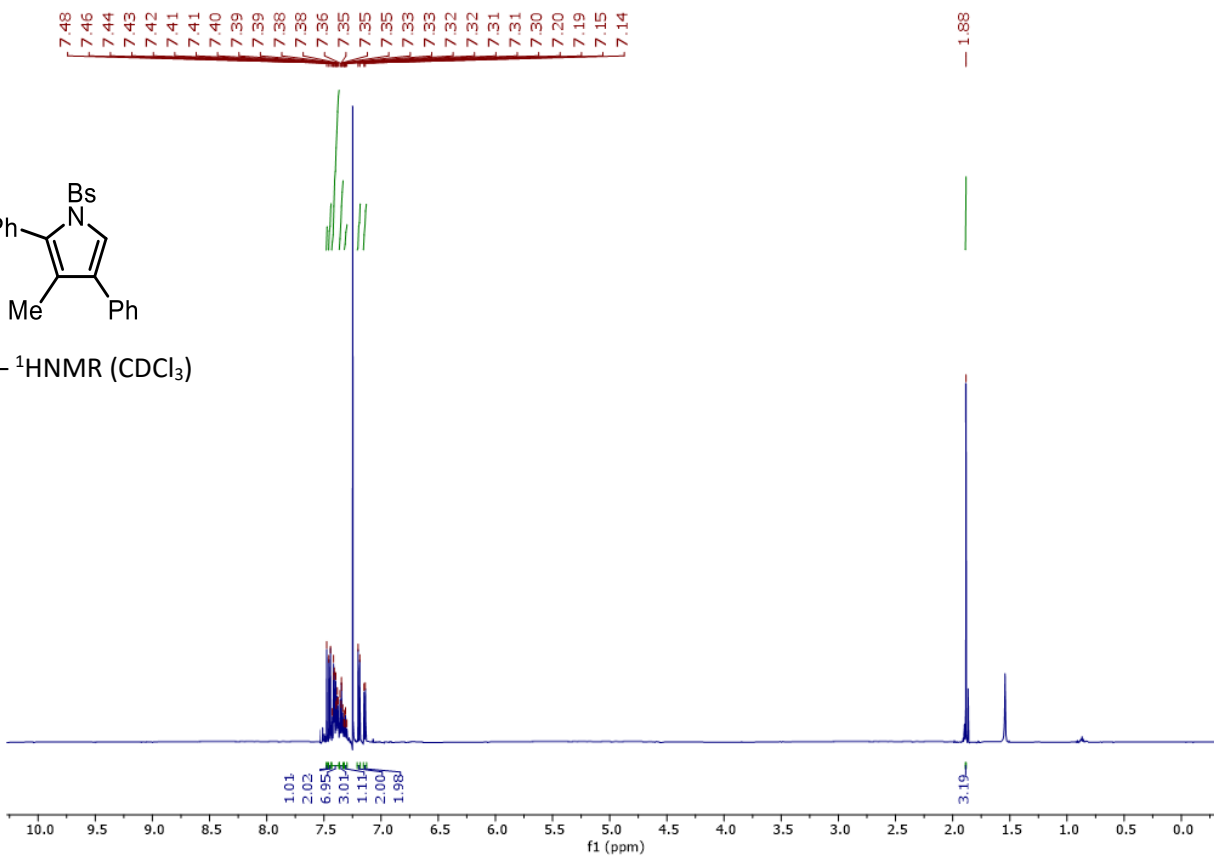


**B.10** -  $^{13}\text{C}$ NMR ( $\text{CDCl}_3$ )





**B.11** – <sup>1</sup>HNMR (CDCl<sub>3</sub>)



**B.11** – <sup>13</sup>CNMR (CDCl<sub>3</sub>)

